Ana Sofia dos Santos Fajardo

# Treatment of liquid effluents by electrochemical processes

PhD thesis in Chemical Engineering, supervised by Professor Doctor Rosa M. Quinta-Ferreira and co-supervised by Doctor Rui C. Martins,
submitted to the Department of Chemical Engineering, Faculty of Sciences and Technology, University of Coimbra

November 2016

· U C ·

Universidade de Coimbra

Ana Sofia dos Santos Fajardo

# Treatment of liquid effluents by electrochemical processes

PhD thesis in the scientific area of Chemical Engineering and submitted to the Department of Chemical Engineering,
Faculty of Sciences and Technology, University of Coimbra

**Supervisors**
Professor Doctor Rosa M. Quinta-Ferreira
Doctor Rui C. Martins

**Host institution**
CIEPQPF - Research Centre for Chemical Processes Engineering and Forest Products, Department of Chemical Engineering,
Faculty of Sciences and Technology of the University of Coimbra

**Financing**
FCT - Portuguese Foundation for Science and Technology
Doctoral degree grant: SFRH/BD/87318/2012

Coimbra
2016

· U C ·

UNIVERSIDADE DE COIMBRA

*“The value of things is not on the time they last,*
*but on the intensity with which they occur.*
*Because of that, there are unforgettable moments,*
*inexplicable things and incomparable people.”*
*Fernando Pessoa*

# AGRADECIMENTOS

*À Prof. Doutora Rosa M. Quinta-Ferreira, minha orientadora, por me permitir fazer parte do GERST (Group on Environment, Reaction, Separation and Thermodynamics) da Universidade de Coimbra (UC) e desenvolver trabalho com a finalidade de melhorar o nosso meio-ambiente. Reconhecendo com satisfação o seu apoio, confiança e disponibilidade ao guiar-me nesta "caminhada" evolutiva.*

*Ao Doutor Rui C. Martins, meu co-orientador, por me ter iniciado e mostrado o mundo da investigação científica através dos seus olhos! Premeio a sua dedicação, motivação e profissionalismo em tudo o que se propõe a realizar. Sendo grata a sua disponibilidade, paciência e incentivo.*

*A ambos os orientadores agradeço os conselhos, as sugestões e as críticas que me fizeram crescer quer a nível profissional quer pessoal.*

*Ao Prof. Doutor Carlos A. Martínez-Huitle, por ter sido meu tutor e me ter dado a oportunidade de trabalhar no seu grupo de investigação LEAA (Laboratório de Eletroquímica Ambiental e Aplicada) na Universidade Federal do Rio Grande do Norte (UFRN) em Natal no Brasil. Para além de adquirir novos conhecimentos de eletroquímica, cimentar os existentes e de termos riquíssimas trocas de ideias.*

*Ao Prof. Doutor Luís M. Castro, que contribuiu para o meu conhecimento académico durante o Bacharelato e Licenciatura no DEQB do Instituto Superior de Engenharia de Coimbra e que continuou através de parcerias e discussões científicas frutíferas e enriquecedoras durante o Doutoramento.*

*Ao Doutor Sergi Garcia-Segura, um colega da área dos Processos Eletroquímicos e grande amigo, capaz de me apontar uma direção nos momentos mais nublados, tranquilizando-me através das suas palavras simpáticas de incentivo.*

*Às alunas de mestrado de Engenharia Química (agora Mestres) Raquel F. Rodrigues e Helga F. Seca, por terem partilhado comigo o entusiasmo pelo trabalho na área dos Processos Eletroquímicos.*

*Aos colegas dos grupos de investigação GERST e LEAA, e ainda às colegas do DEQ da UC (Ana Lourenço, a Ana Vieira e a Carla Cotas), pela troca de conhecimentos e também pelos momentos de conversa e descontração necessários para continuar o trabalho diário. O GERST é um grupo com mobilidade de pessoas de diferentes nacionalidades que vão e vêm. Resultando em amizades profundas e duradouras: Angel Gonzalo, Dany Kramer, Flávia Batista, Maria Victor-Ortega, Marta Gmürek e Tales Abrantes. No LEAA, todos ajudaram para que me sentisse integrada, fazendo parte desta "família" académica. A aprendizagem com o intercâmbio não é só o desenvolvimento dos conhecimentos científicos e das capacidades intelectuais, mas também a troca das heranças cuturais, de costumes, de pensamentos, de ambiências que nos enquadram numa comunidade de pessoas diferentes, mas iguais.*

*Aos colaboradores do DEQ, Dr. Adamo Caetano, D. Dulce Pancas, D. Fernanda Ferreira, Sr. José Santos, Sr. Luís Santos, D. Mafalda Fernandes, Engª Maria João Bastos e D. Rosa Gaspar, agradeço a forma como contribuíram para o desenvolvimento do meu trabalho com a sua presença, disponibilidade e paciência.*

*Aos parceiros: Empresa-Universidade – por compreenderem a importância destas parcerias e disponibilizarem material essencial ao desenvolvimento do trabalho científico como as empresas Filzinc e Victor Monteiro; Universidade-Universidade – por existir espírito de cooperação e de entreajuda como nos casos do Prof. Doutor João F. Sousa do DEQ da UFRN colocando ao dispor o equipamento de HPLC, da Prof. Doutora Maria E. Quinta-Ferreira do DF da UC pelos testes de toxicidade neuronal em cérebros de rato e dos Prof. Doutores Lícino Gando-Ferreira e Margarida Quina do DEQ da UC pelo apoio e facilidades concedidas para a realização deste trabalho.*

*À Fundação para a Ciência e Tecnologia (FCT) no âmbito do projeto QREN – POPH – Tipologia 4.1 – Formação Avançada comparticipado pelo Fundo Social Europeu e por fundos nacionais do Ministério da Ciência, Tecnologia e Ensino Superior, pela bolsa de doutoramento SFRH/BD/87318/2012.*

*Como nem só de academia se faz a vida:*

*À Abi Gomez, ao Alexsandro Jhones, à Ana Santos, à Débora Escrafani, à Mariana Medeiros e ao Sergi Garcia-Segura, que apesar da distância sempre estiveram comigo em pensamento e coração.*

*Em especial, um muito obrigada aos meus pais, por terem estado sempre presentes durante as etapas mais importantes da minha vida, pelo seu amor incondicional, apoio moral e compreensão demonstrada. E por tudo o que fizeram de e por mim e continuam a fazer.*

***A todos o meu sincero agradecimento e gratidão…***

# ABSTRACT

Water quality and its exhaustion are topics of great importance in our daily life. The constant seeking for well-being and comfort is bringing the natural resources towards dangerous limits. Therefore, and as a result of social and political awareness, stricter legislation is being implemented regarding the wastewater discharge in natural water streams. The appearance of harmful organic pollutants recalcitrant to classical biological treatments stimulated the development of new depuration technologies operating at room conditions of pressure and temperature. Among them, the electrochemical processes have emerged as promising solutions with generally simple operations and inexpensive equipment. These techniques are versatile, robust and amenable to automation. In this regard, the aim of the present study consists in the use of electrocoagulation (ECG) and electrochemical oxidation (EO) processes to purify agro-industrial and dye wastewaters by reaching the operating conditions that lead to the best energy consumption/efficiency ratio.

The performance of the ECG process was evaluated by testing different sacrificial anode materials (Al, Cu, Fe, Pb and Zn) for the depuration of a simulated phenolic mixture containing six phenolic compounds typically found in olive mill wastewaters (OMW). The Zn material revealed to be an attractive option with the highest removal of total phenolic content (TPh) and chemical oxygen demand (COD), after 180 min of electrolysis. Subsequently several operating conditions were analysed and the optimal were $pH_0$ 3.2, current density (*j*) of 25 mA $cm^{-2}$, distance between electrodes of 1.0 cm, 1.5 g $L^{-1}$ of NaCl and stainless steel as cathode, promoting 84.2 % and 40.3 % for TPh and COD removal, respectively, with an energetic consumption of 40 kWh $m^{-3}$. Those parameters applied to a filtered real OMW without the NaCl addition led to 72.3 % of TPh and 20.9 % of COD abatements with a consumption of 34 kWh $m^{-3}$. Ecological impact was still detected by bio-luminescence analysis.

Aqueous solutions containing a Reactive Black 5 dye were treated by an ECG process using Al anodes in batch-stirred and recirculation flow reactor configurations. The best results for both systems were achieved at *j* of 16 mA $cm^{-2}$, $pH_0$ 6 and an initial concentration of the dye of 100 mg $L^{-1}$ (and 800 rpm for the batch-stirred reactor). In the batch-stirred, an actual textile effluent was also depurated using Al or Zn anode materials. Final satisfactory legal values of discharge were attained for both cases.

Regarding the EO process, it was applied to the treatment of a synthetic OMW in a batch-stirred reactor by testing the materials $Ti/RuO_2$ and the $Ti/IrO_2$ as anodes. After 180 min of reaction, each electrode allowed a total TPh abatement and 100 % or 84.8 % of COD removal for the ruthenium or iridium materials, respectively, with the following conditions, 10 g $L^{-1}$ of NaCl, 119 mA $cm^{-2}$ and initial pH 3.4. Although no morphological differences were observed between the fresh and used $Ti/RuO_2$ anode, the surface of $Ti/IrO_2$ evidenced some changes. The impact in neuronal activity of the untreated and treated phenolic effluents was evaluated through the formation of synaptic reactive oxygen species (ROS). The treated effluent caused a smaller depression and a larger potentiation upon its removal than the untreated

one, probably due to the formation of end products obtained. The depuration of real undiluted OMWs ($COD_0$=6.5 and 23 $gO_2$ $L^{-1}$) with both active anodes revealed a high ability to remove phenolic content, achieving only COD removal around 17 %. Conversely, when a diluted OMW ($COD_0$=1.1 $gO_2$ $L^{-1}$) was tested with $Ti/IrO_2$ material, there was an increase of the COD abatement to 62.8 %. The results ensure the applicability of these approaches as pre-treatment processes.

In another study, electrochemical measurements (cyclic voltammetry and polarisation curves) and bulk electrolysis with one or two flow cells in series were employed to evaluate the performance of $Ti/IrO_2$-$Ta_2O_5$ and Nb/BDD anode materials in the elimination of Amaranth dye from aqueous solutions. Nb/BDD showed a major oxidation power to remove the dye. Similarly, the best colour (98.5–100 %) and COD removals (43.2–49.1 %) were attained by both materials individually at different *j* (30 or 60 mA $cm^{-2}$) and reaction times (60 or 360 min). The energy consumptions varied from 14.3 to 33.8 kWh $m^{-3}$. The combination $Ti/IrO_2$-$Ta_2O_5$+Nb/BDD at 30+30 mA $cm^{-2}$ obtained the most interesting results, enhancing COD abatement to 75.1 %, after 60 min of treatment and consuming 25.4 kWh $m^{-3}$. This reveals that the efficiency of a serial configuration may be higher with less energy consumption than the sum of the individual cells. An analogous work was performed with Ti/Pt and Ti/Pt-SnSb materials in order to avoid dependence on the use of higher cost materials such as BDD. Polarisation curves demonstrated that Ti/Pt-SnSb has higher electroactivity to remove the dye when compared to Ti/Pt. Besides, after 360 min treatment, the experiment with the former anode at 30 mA $cm^{-2}$ led to 97.5 % and 70.3 % of colour and COD removal, respectively, consuming 72 kWh $m^{-3}$ of energy. The combination of the two active anodes in cells in series promoted a faster colour removal. Trials combining Ti/Pt-SnSb and Nb/BDD materials were also performed. Among them, the configuration Nb/BDD+Ti/Pt-SnSb at 30+30 mA $cm^{-2}$ provided the best results after 180 min of reaction, with 100 % and 69.9 % of colour and COD removals, respectively, as well as 78 kWh $m^{-3}$ of energy consumed. The most interesting strategy to purify a synthetic solution containing the Amaranth dye was endorsed by the $Ti/IrO_2$-$Ta_2O_5$+Nb/BDD at 30+30 mA $cm^{-2}$ arrangement.

ECG and EO are versatile processes able to be quickly adjustable to different effluents, final target parameters and required thresholds.

# RESUMO

A qualidade da água e a sua exaustão são tópicos de grande interesse nos dias de hoje. A procura constante pelo bem-estar e conforto tem dimínuido drasticamente a disponibilidade dos recursos naturais. Como resultado de uma tomada de consciência social e política tem-se vindo a aplicar legislação cada vez mais rígida relativamente à descarga de efluentes em meios aquáticos. O aparecimento de poluentes orgânicos recalcitrantes aos processos biológicos estimulou também o desenvolvimento de novas tecnologias de tratamento que operassem em condições normais de pressão e temperatura. Entre estes sistemas emergiram os processos eletroquímicos como soluções promissoras, geralmente com operações simples e equipamento pouco oneroso, sendo estas técnicas versáteis, robustas e adequadas à automação. Desta forma, o objetivo deste estudo centra-se na utilização de processos de eletrocoagulação (ECG) e oxidação eletroquímica (OE) para o tratamento de águas residuais da agroindústria e da indústria de corantes, de modo a atingir o melhor rácio entre consumo de energia e eficiência do sistema.

O desempenho do processo de ECG foi avaliado através de testes com diferentes ânodos sacrificiais (Al, Cu, Fe, Pb e Zn) na depuração de uma mistura fenólica simulando efluentes de lagares de azeite. O ânodo de Zn foi a solução mais atrativa, com as remoções mais elevadas de carência química de oxigénio (CQO) e conteúdo fenólico total (CFT), após 180 min de eletrólise. Em seguida, testaram-se várias condições de operação, tendo-se obtido a optimização dos parâmetros: $pH_0$ 3.2, densidade de corrente ($j$)=25 mA $cm^{-2}$, distância entre elétrodos=1.0 cm, 1.5 g $L^{-1}$ de NaCl e o aço inoxidável como cátodo, que envolveram a remoção de 84.2 % e 40.3 % de CFT e CQO, respetivamente, consumindo 40 kWh $m^{-3}$. Essas condições foram aplicadas a um efluente real de lagares de azeite sem a adição de NaCl permitindo remover 72.3 % de CFT e 20.9 % de CQO com um consumo de 34 kWh $m^{-3}$. Foi ainda avaliado o impacto ecológico do efluente depois do tratamento através de estudos de inibição de bioluminescência.

Foram tratadas soluções aquosas contendo o corante *Reactive Black 5* por ECG usando ânodos de Al em duas configurações reacionais: descontínuo-agitado e de fluxo com recirculação. Os melhores resultados para ambos os sistemas foram alcançados a $j$=16 mA $cm^{-2}$, $pH_0$ 6 e 100 mg $L^{-1}$ de corante (e 800 rpm para o reator descontínuo-agitado). No reator descontínuo-agitado, foi também tratado um efluente têxtil real utilizando ânodos de Al ou Zn. Nos dois casos foram obtidos valores de remoção satisfatórios para a descarga do efluente.

Em relação ao processo de OE, este foi aplicado à purificação de uma água residual simulada de lagares de azeite testando ânodos de $Ti/RuO_2$ e $Ti/IrO_2$. Após 180 min de reação, cada material permitiu a degradação total do CFT e 100 % ou 84.8 % de remoção de CQO para os ânodos de ruténio e irídio, respetivamente, com as seguintes condições de operação 10 g $L^{-1}$ de NaCl, 119 mA $cm^{-2}$ e $pH_0$ 3.4. Embora não tenham sido verificadas diferenças morfológicas no elétrodo de $Ti/RuO_2$ após tratamento,

no caso do $Ti/IrO_2$ foram detetadas algumas alterações na sua superfície. O impacto na atividade neuronal do efluente fenólico não-tratado e tratado foi testado pela formação de espécies reativas de oxigénio. O efluente tratado causou uma pequena depressão e uma maior potenciação após a sua remoção quando comparado com o efluente não-tratado, provavelmente devido à natureza dos produtos finais formados. Testou-se ainda o processo usando efluentes reais de lagares de azeite não diluídos (CQO=6.5 e 23 $gO_2$ $L^{-1}$) com os dois ânodos. Neste caso a remoção de CFT foi bastante eficiente embora a degradação de CQO tenha atingido apenas 17 %. Contudo, quando um efluente real diluído (CQO=1.1 $gO_2$ $L^{-1}$) foi tratado com $Ti/IrO_2$, a eficiência de remoção da CQO aumentou atingindo 62.8 %. Estes resultados demonstram a capacidade do processo de OE como pré-tratamento de efluentes com elevada carga orgânica.

Noutro estudo foram realizadas medições eletroquímicas (voltimetria cíclica e curvas de polarização) e de eletrólise em solução com uma ou duas células em série de modo a avaliar o desempenho dos materiais anódicos $Ti/IrO_2$-$Ta_2O_5$ e Nb/BDD na eliminação do corante *Amaranth* em soluções aquosas. O ânodo de Nb/BDD exibiu maior poder de oxidação para remover o corante. De forma similar, os melhores valores de remoção de cor (98.5–100 %) e CQO (43.2–49.1 %) foram obtidos por ambos os materiais individualmente a diferentes $j$ (30 ou 60 mA $cm^{-2}$) e tempos de reação (60 ou 360 min), com consumos de energia variando entre 14.3 e 33.8 kWh $m^{-3}$. A combinação $Ti/IrO_2$-$Ta_2O_5$+Nb/BDD a 30+30 mA $cm^{-2}$ em células duplas promoveu os resultados mais interessantes com o aumento da remoção da CQO para 75.1 %, após 60 min de tratamento e consumindo 25.4 kWh $m^{-3}$. Estes resultados revelam que a eficiência das células em série pode ser mais elevada e com menor consumo de energia, do que a soma das células individuais. Foi feito um trabalho análogo com ânodos de Ti/Pt e Ti/Pt-SnSb, de modo a evitar o recurso a materiais de elevado custo como o BDD. As curvas de polarização demonstraram que o ânodo de Ti/Pt-SnSb possui uma maior eletroatividade para remover o corante quando comparado com o de Ti/Pt. Além disso, após 360 min de tratamento, a experiência com Ti/Pt-SnSb a 30 mA $cm^{-2}$ promoveu 97.5 % e 70.3 % de remoções de cor e CQO, respetivamente, consumindo 72 kWh $m^{-3}$. A combinação destes dois ânodos ativos em células em série promoveram uma remoção de cor mais rápida. Foram também realizadas experiências combinando os materiais de Ti/Pt-SnSb e Nb/BDD, tendo-se concluído que a configuração Nb/BDD+Ti/Pt-SnSb a 30+30 mA $cm^{-2}$ providenciou os melhores resultados, após 180 min de reação, com 100 % e 69.9 % remoções de cor e CQO, respetivamente, assim como 78 kWh $m^{-3}$ de energia consumida. A estratégia mais interessante para purificar uma solução sintética com o corante *Amaranth* foi a configuração $Ti/IrO_2$-$Ta_2O_5$+Nb/BDD a 30+30 mA $cm^{-2}$.

A eletrocoagulação e a oxidação eletroquímica são processos versáteis que podem ser eficientemente ajustados a diferentes tipos de efluentes, parâmetros finais e limites legais de descarga.

# LIST OF CONTENTS

Page

LIST OF FIGURES ......XVII
LIST OF TABLES ......XXIII
LIST OF ABBREVIATIONS ......XXV
LIST OF SYMBOLS ......XXVII

PART A. THESIS SCOPE AND OUTLINE ...... 1

I. INTRODUCTION ...... 3

- I.1 WATER SCARCITY AND ITS POLLUTION ...... 3
- I.2 ORGANIC CONTAMINANTS ...... 3
  - I.2.1 Phenolic acids and Olive mill wastewaters (OMW) ...... 4
  - I.2.2 Dye wastewaters (DW) ...... 5
- I.3 WASTEWATER REMEDIATION STRATEGIES ...... 5
  - I.3.1 Traditional treatments ...... 6
  - I.3.2 Advanced oxidation processes ...... 7
  - I.3.3 Electrochemical advanced processes ...... 8
- I.4 MOTIVATION AND SCOPE OF THE WORK ...... 9
- I.5 STRUCTURE OF THE THESIS ...... 10
- REFERENCES ...... 12

II. ELECTROCHEMICAL PROCESSES: FUNDAMENTALS AND LITERATURE OVERVIEW ...... 15

- II.1 ELECTROCOAGULATION (ECG) PROCESS ...... 15
- II.2 ELECTROCHEMICAL OXIDATION (EO) PROCESS ...... 16
  - II.2.1 Electrogneration of reactive oxygen species (ROS) ...... 17
  - II.2.2 Electrogeneration of chlorine active species ...... 20
  - II.2.3 Other electrogenerated species ...... 21
- II.3 PROCESS PERFORMANCE INDICATORS AND ENERGETIC PARAMETERS ...... 21
- II.4 REACTOR DESIGN ...... 22
- II.5 LITERATURE OVERVIEW - OPERATING CONDITIONS ...... 24
  - II.5.1 Electrocoagulation (ECG) process ...... 24
  - II.5.2 Electrochemical oxidation (EO) process ...... 33
- II.6 CONCLUSIONS ...... 41
- REFERENCES ...... 43

PART B. ELECTROCOAGULATION PROCESS ...... 49

III. TREATMENT OF A SYNTHETIC PHENOLIC MIXTURE BY ELECTROCOAGULATION USING Al, Cu, Fe, Pb, AND Zn AS ANODE MATERIALS ...... 51

- ABSTRACT ...... 51

III.1 INTRODUCTION ........ 52
III.2 EXPERIMENTAL SECTION ........ 54
  III.2.1 Wastewater Preparation and ECG Procedure ........ 54
  III.2.2 Analytical Techniques. ........ 55
III.3 RESULTS AND DISCUSSION ........ 55
  III.3.1 Total phenolic content ........ 56
  III.3.2 Chemical oxygen demand ........ 57
  III.3.3 Electrodes dissolution ........ 61
  III.3.4 Biodegradability and toxicity assessment ........ 62
  III.3.5 Energetic analysis ........ 63
III.4 CONCLUSIONS ........ 64
ACKNOWLEDGMENTS ........ 64
REFERENCES ........ 65

**IV. PHENOLIC WASTEWATERS TREATMENT BY ELECTROCOAGULATION PROCESS USING Zn ANODE ........ 67**

ABSTRACT ........ 67
IV.1 INTRODUCTION ........ 68
IV.2 MATERIAL AND METHODS ........ 69
  IV.2.1 Synthetic and real effluent ........ 69
  IV.2.2 Electrocoagulation system and procedure ........ 69
  IV.2.3 Analytical techniques ........ 70
IV.3 RESULTS AND DISCUSSION ........ 71
  IV.3.1 Synthetic effluent ........ 71
    IV.3.1.1 Effect of pH ........ 72
    IV.3.1.2 Effect of current density ........ 74
    IV.3.1.3 Effect of the distance between electrodes ........ 76
    IV.3.1.4 Effect of the nature of the electrolyte ........ 77
    IV.3.1.5 Effect of different cathodes ........ 78
    IV.3.1.6 Analysis of the concentration of the different phenolic acids parents in the effluent ........ 79
    IV.3.1.7 Toxicity analysis ........ 80
    IV.3.1.8 Electrical energy consumption ........ 80
    IV.3.1.9 Electrodes stability and durability ........ 81
  IV.3.2 Application to a real effluent ........ 82
IV.4 CONCLUSIONS ........ 85
ACKNOWLEDGMENTS ........ 86
REFERENCES ........ 87

**V. REACTIVE BLACK 5 DYE ELIMINATION FROM AQUEOUS SOLUTIONS BY USING ALUMINIUM ANODES IN –BATCH AND –RECIRCULATION FLOW ELECTROCOAGULATION SYSTEMS ........ 91**

ABSTRACT ........ 91

V.1 INTRODUCTION ........ 92
V.2 EXPERIMENTAL ........ 93
  V.2.1 Synthetic and real effluent ........ 93
  V.2.2 Electrocoagulation systems and procedure ........ 94
  V.2.3 Analytical techniques ........ 95
V.3 RESULTS AND DISCUSSION ........ 95
  V.3.1 Batch stirred system ........ 95
    V.3.1.1 Effect of stirring rate ........ 95
    V.3.1.2 Effect of current density ........ 96
    V.3.1.3 Effect of initial pH ........ 97
    V.3.1.4 Effect of dye concentration ........ 99
    V.3.1.5 Effect of the nature of the anode material on the treatment of the synthetic and real effluent ........ 100
  V.3.2 Recirculation flow system ........ 102
    V.3.2.1 Effect of current density ........ 102
    V.3.2.2 Effect of initial pH ........ 103
    V.3.2.3 Effect of initial concentration of the dye ........ 104
    V.3.2.4 Energy consumption ........ 106
V.4 CONCLUSIONS ........ 107
ACKNOWLEDGMENTS ........ 107
REFERENCES ........ 108

**PART C. ELECTROCHEMICAL OXIDATION PROCESS ........ 111**

**VI. ELECTROCHEMICAL OXIDATION OF PHENOLIC WASTEWATERS USING A BATCH-STIRRED REACTOR WITH NaCl ELECTROLYTE AND Ti/RuO$_2$ ANODES ........ 113**

ABSTRACT ........ 113
VI.1 INTRODUCTION ........ 114
VI.2 EXPERIMENTAL ........ 116
  VI.2.1 Synthetic and real effluents ........ 116
  VI.2.2 Electrochemical oxidation procedure ........ 116
  VI.2.3 Analytical techniques ........ 117
  VI.2.4 SEM analysis ........ 118
  VI.2.5 Neuronal studies ........ 118
VI.3 RESULTS AND DISCUSSION ........ 119
  VI.3.1 Effect of the nature of the supporting electrolyte ........ 119
  VI.3.2 Effect of the concentration of the electrolyte ........ 120
  VI.3.3 Effect of the current density and kinetic study ........ 122
  VI.3.4 Effect of pH ........ 124
  VI.3.5 Morphological analysis of the Ti/RuO$_2$ anodes ........ 125
  VI.3.6 Energy consumption and current efficiency ........ 126

VI.3.7 Effect of the synthetic phenolic effluent in neuronal ROS signals 127
VI.3.8 Application to a real effluent 128
VI.4 CONCLUSIONS 130
ACKNOWLEDGMENTS 130
REFERENCES 132

**VII. PHENOLIC WASTEWATERS DEPURATION BY ELECTROCHEMICAL OXIDATION PROCESS USING Ti/IrO$_2$ ANODES 137**

ABSTRACT 137
VII.1 INTRODUCTION 138
VII.2 EXPERIMENTAL 140
VII.2.1 Synthetic and real effluent 140
VII.2.2 Electrochemical oxidation (EO) procedure 142
VII.2.3 Analytical techniques 142
VII.2.4 Morphological characterisation of the anode 143
VII.2.5 Detection of reactive oxygen species (ROS) signals from brain slices 143
VII.3 RESULTS AND DISCUSSION 144
VII.3.1 Effect of the nature and concentration of the supporting electrolytes 144
VII.3.2 Effect of current density 147
VII.3.3 Effect of initial pH 148
VII.3.4 Ti/IrO$_2$ anode morphology 150
VII.3.5 Impact of the phenolic effluents in neuronal ROS activity 151
VII.3.6 Application to a real effluent 152
VII.4 CONCLUSIONS 154
ACKNOWLEDGMENTS 154
REFERENCES 155

**VIII. TREATMENT OF AMARANTH DYE IN AQUEOUS SOLUTION BY USING ONE CELL OR TWO CELLS IN SERIES WITH ACTIVE AND NON-ACTIVE ANODES 159**

ABSTRACT 159
VIII.1 INTRODUCTION 160
VIII.2 EXPERIMENTAL 161
VIII.2.1 Synthetic effluent 161
VIII.2.2 Electrochemical measurement 162
VIII.2.3 Electrochemical system and procedure 162
VIII.2.4 Analytical techniques 163
VIII.3 RESULTS AND DISCUSSION 163
VIII.3.1 Cyclic voltammetry (CV) and polarisation curves 163
VIII.3.2 Single cell – Effect of the type of anode and current density 165
VIII.3.3 Two cells in series – Effect of the cell assembly and the current density 168
VIII.3.4 Energy consumption 171

VIII.4 CONCLUSIONS ........ 173
ACKNOWLEDGMENTS ........ 174
REFERENCES ........ 175

**IX. ELECTROCHEMICAL ABATEMENT OF AMARANTH DYE SOLUTIONS USING INDIVIDUAL OR AN ASSEMBLING OF FLOW CELLS WITH Ti/Pt AND Ti/Pt-SnSb ANODES ........ 179**

ABSTRACT ........ 179
IX.1 INTRODUCTION ........ 180
IX.2 MATERIAL AND METHODS ........ 182
  IX.2.1 Synthetic solution ........ 182
  IX.2.2 Electrochemical measurements ........ 182
  IX.2.3 Electrochemical system ........ 182
  IX.2.4 Analytical techniques ........ 183
IX.3 RESULTS AND DISCUSSION ........ 184
  IX.3.1 Cyclic voltammetry and polarisation curves ........ 184
  IX.3.2 Bulk electrolysis ........ 186
    IX.3.2.1 Single flow cells ........ 186
    IX.3.2.2 Electrochemical cells in series ........ 190
    IX.3.2.3 Effect of electrochemical arrangements (single or assembling of cells in series) in energy consumption ........ 192
  IX.3.3 Effect of the non-active anode in an assembling of flow cells in series ........ 193
IX.4 CONCLUSIONS ........ 197
ACKNOWLEDGMENTS ........ 197
REFERENCES ........ 198

**PART D. MAIN CONCLUSIONS AND FORTHCOMING WORK ........ 201**

**X. GENERAL OVERVIEW AND CONCLUDING REMARKS ........ 203**

**XI. SUGGESTIONS OF FORTHCOMING WORK ........ 207**

# LIST OF FIGURES

Page

Figure I.1. Classification of advanced oxidation processes. ........ 8

Figure II.1. Mechanism for the electrocoagulation process. ........ 16

Figure II.2. Scheme for a) direct and b) indirect electrochemical oxidation processes. ........ 17

Figure II.3. Representation of the mechanism of electrochemical oxidation of organic compounds on active and non-active anodes. ........ 18

Figure II.4. (a) Monopolar electrodes in (a) parallel and (b) serial configurations, and bipolar electrodes in a serial configuration........ 23

Figure II.5. Conceptual diagram of an electrochemical reactor. ........ 24

Figure III.1. EGC experimental setup. (1-Reactor of perspex, 2-Floater, 3-Electrodes, 4-Magnetic bar stirrer, 5-Double wall for water recirculation). ........ 55

Figure III.2. TPh removal over time (I=0.4 A, Electrode area=33.5 $cm^2$, Intergap=10 mm, [NaCl]=1.5 g $L^{-1}$)........ 56

Figure III.3. COD removal over time (I=0.4 A, Electrode area=33.5 $cm^2$, Intergap=10 mm, [NaCl]=1.5 g $L^{-1}$)........ 57

Figure III.4. pH medium followed over time (I=0.4 A, Electrode area=33.5 $cm^2$, Intergap=10 mm, [NaCl]=1.5 g $L^{-1}$). ........ 59

Figure III.5. Energy consumption value for each anode material regarding the optimum contact time. ........ 63

Figure IV.1. Effect of the initial pH medium on a) TPh removal, b) COD removal and c) pH over time (current density=120 A $m^{-2}$, distance between electrodes=1.0 cm, [NaCl]=1.5 g $L^{-1}$, Zn anode/SS cathode)........ 73

Figure IV.2. TPh/COD ratio over time (current density=120 A $m^{-2}$, distance between electrodes=1.0 cm, [NaCl]=1.5 g $L^{-1}$, Zn anode/SS cathode)........ 74

Figure IV.3. Effect of the current density effect on a) TPh removal, b) COD removal and c) pH over time (pH=3.2, distance between electrodes=1.0 cm, [NaCl]=1.5 g $L^{-1}$, Zn anode/SS cathode)........ 75

Figure IV.4. Effect of the distance between electrodes on a) TPh removal, b) COD removal and c) pH over time (pH=3.2, current density=250 A $m^{-2}$, [NaCl]=1.5 g $L^{-1}$, Zn anode/SS cathode). ........ 76

Figure IV.5. Effect of the type of electrolyte on a) TPh removal, b) COD removal and c) pH over time (pH=3.2, current density=250 A $m^{-2}$, distance between electrodes=1.0 cm, [NaCl]=1.5 g $L^{-1}$, Zn anode/SS cathode)........ 78

Figure IV.6. Effect of the pair of electrodes on a) TPh removal, b) COD removal and c) pH over time (pH=3.2, current density=250 A $m^{-2}$, distance between electrodes=1.0 cm, [NaCl]=1.5 g $L^{-1}$)........ 79

Figure IV.7. Removal of parent phenolic acids over time for the synthetic effluent (pH=3.2, current density=250 A $m^{-2}$, distance between electrodes=1.0 cm, [NaCl]=1.5 g $L^{-1}$, Zn anode/SS cathode)........ 80

Figure IV.8. Effect of electrodes reuse on a) TPh and b) COD removal by electrocoagulation process (pH=3.2, current density=250 A $m^{-2}$, distance between electrodes=1.0 cm, [NaCl]=1.5 g $L^{-1}$, Zn anode/SS cathode). 81

Figure IV.9. Scheme of the mass loss of the zinc anode along reuses (pH=3.2, current density=250 A $m^{-2}$, distance between electrodes=1.0 cm, [NaCl]=1.5 g $L^{-1}$, Zn anode/SS cathode). 82

Figure IV.10. a) TPh removal, b) COD removal and c) pH profiles for the synthetic and real effluent with the best operating conditions (pH=3.2, current density=250 A $m^{-2}$, distance between electrodes=1.0 cm, [NaCl]=1.5 g $L^{-1}$, Zn anode/SS cathode). 83

Figure IV.11. Zn concentration in solution over time for the synthetic and real effluent. 84

Figure V.1. (a) Batch and (b) flow cell electrocoagulation systems. (1-DC power supply, 2-Electrodes (2 anodes + 2 cathodes, 3-Floater, 4-Magnetic stirrer, 5-Stir plate, 6-Double wall for water recirculation, 7-Reservatory, 8-Pump, 9-Electrochemical flow cell). 94

Figure V.2. Effect of the stirring speed on colour removal over time. Inset: Effect of the stirring speed on COD removal over time. Operating conditions: batch system, current density=4 mA $cm^{-2}$, $pH_0$=6, 100 mg $L^{-1}$ of Reactive Black 5 and Al anode. 96

Figure V.3. Effect of the current density on colour removal over time. Inset: Effect of the current density on COD removal over time. Operating conditions: batch system, stirring speed=800 rpm, $pH_0$=6, 100 mg $L^{-1}$ of Reactive Black 5 and Al anode. 97

Figure V.4. Effect of the initial pH on (a) colour removal and (b) pH medium over time. Inset (a): Effect of the initial pH on COD removal over time. Operating conditions: batch system, stirring speed=800 rpm, current density=16 mA $cm^{-2}$, Al anode and 100 mg $L^{-1}$ of Reactive Black 5. 99

Figure V.5. (a) Effect of the initial concentration of Reactive Black 5 on colour removal over time. (b) Colour removal profile at different initial Reactive Black 5 concentrations at 90 min of reaction. (c) Effect of the initial concentration of Reactive Black 5 on pH medium over time. Inset (a): Effect of the initial concentration of the pollutant on COD removal over time. Operating conditions: batch system, stirring speed=800 rpm, current density=16 mA $cm^{-2}$, Al anode and $pH_0$=6. 100

Figure V.6. Effect of the nature of the anode material on (a) colour and (b) COD removal, as well as on pH medium over time, using a synthetic and a real effluents. Operating conditions: batch system, stirring speed=800 rpm, current density=16 mA $cm^{-2}$, $pH_0$=6 and 100 mg $L^{-1}$ of Reactive Black 5 (for synthetic effluent). 102

Figure V.7. Effect of the current density on colour removal over time, for batch and flow systems. Inset: Colour removal as a function of the applied charge at different current densities for the flow system. Operating conditions: $pH_0$=6, 100 mg $L^{-1}$ of Reactive Black 5, stirring speed=800 rpm (batch system) and flow rate=160 L $h^{-1}$ (flow system). 103

Figure V.8. Effect of the $pH_0$ at (a) 3, (b) 6 and (c) 9 on colour removal over time, for batch and flow systems. Insets: Evolution of pH medium over time. Operating conditions: current density=16 mA $cm^{-2}$, 100 mg $L^{-1}$ of Reactive Black 5, stirring speed=800 rpm (batch system) and flow rate=160 L $h^{-1}$ (flow system). 104

Figure V.9. Effect of the initial Reactive Black 5 concentrations, (a) 50, (b) 100 and (c) 200 mg $L^{-1}$, on colour removal over time, for batch and flow systems. Operating conditions: current density=16 mA $cm^{-2}$, $pH_0$=6, stirring speed=800 rpm (batch system) and flow rate=160 L $h^{-1}$ (flow system). 106

Figure V.10. Energy consumption as a function of colour removal for batch and flow systems, at their respective time of treatment. Operating conditions: current density=16 mA $cm^{-2}$, $pH_0$=6, 100 mg $L^{-1}$ of Reactive Black 5, stirring speed=800 rpm (batch system) and flow rate=160 L $h^{-1}$ (flow system). 106

Figure VI.1. Effect of the nature of the electrolyte on (a) TPh and (b) COD removal over time. Operating conditions: 100 mg $L^{-1}$ of synthetic phenolic solution, 10 g $L^{-1}$ of electrolyte, $pH_{initial}$=3.4, current density=57 mA $cm^{-2}$, distance between electrodes=1 cm, T=20 °C. ............... 120

Figure VI.2. Effect of the NaCl concentration on (a) TPh removal, (b) COD removal and (c) pH medium over time. Inset of Figure VI.2b: COD removal for the different NaCl concentrations after 120 min of treatment. Operating conditions: 100 mg $L^{-1}$ of synthetic phenolic solution, $pH_{initial}$=3.4, current density=57 mA $cm^{-2}$, distance between electrodes=1 cm, T=20 °C. ............... 122

Figure VI.3. Effect of the current density on (a) TPh removal and (b) COD removal over time. (c) Kinetic analysis assuming a pseudo-first-order reaction for COD removal at different current desnities.Operating conditions: 100 mg $L^{-1}$ of synthetic phenolic solution, [NaCl]=10 g $L^{-1}$, $pH_{initial}$=3.4, distance between electrodes=1 cm, T=20 °C............... 123

Figure VI.4. Effect of the initial pH medium on (a) TPh removal, (b) COD removal and (c) pH medium over time. Operating conditions: 100 mg $L^{-1}$ of synthetic phenolic solution, [NaCl]=10 g $L^{-1}$, current density=119 mA $cm^{-2}$, distance between electrodes=1 cm, T=20 °C........ 125

Figure VI.5. SEM photographs at 500× of the Ti/$RuO_2$ anode material, (a) before and (b) after EO treatment. Operating conditions: 100 mg $L^{-1}$ of synthetic phenolic solution, [NaCl]=10 g $L^{-1}$, $pH_{initial}$=3.4, current density=119 mA $cm^{-2}$, distance between electrodes=1 cm, T=20 °C. ............... 126

Figure VI.6. Analysis of the energy consumption (EC) and current efficient (CE) over COD removal. Operating conditions: 100 mg $L^{-1}$ of synthetic phenolic solution, [NaCl]=10 g $L^{-1}$, $pH_{initial}$=3.4, current density=119 mA $cm^{-2}$, distance between electrodes=1 cm, T=20 °C. ............... 127

Figure VI.7. ROS signals from brain slices evoked by the synthetic phenolic effluent. Effect of the phenolics mixture in ROS signals recorded in the normal and the pollutants media. The data were acquired using the fluorescent ROS indicator $H_2$DCFDA (20 µM) and were normalised by the average of the first 10 responses. (a) ROS changes in the presence of the phenolics mixture, applied during the period indicated by the bar (30 min). (b) The pollutants mixture containing NaCl (171 mM) was applied during the period represented by the bar............... 127

Figure VI.8. Timecourse of ROS changes induced by the treated phenolic effluent. Normalised fluorescence data obtained from slices incubated with the ROS indicator $H_2$DCFDA (20 µM). The bar indicates the period (30 min) of application of the treated medium, containing NaCl (171 mM), being the data represented as mean ± s.e.m (n=3).......... 128

Figure VI.9. (a) TPh removal, (b) COD removal and (c) pH medium over time for the synthetic and real effluent at the best operating conditions: 100 mg $L^{-1}$ of synthetic phenolic solution, conductivity=16.6 mS $cm^{-1}$, pHinitial=3.4, current density=119 mA $cm^{-2}$, distance between electrodes=1 cm, T=20 °C. ............... 129

Figure VI.10. Discoloration of the real OMW over time. Operating conditions: 100 mg $L^{-1}$ of synthetic phenolic solution, [NaCl]=5 g $L^{-1}$, $pH_{initial}$=3.4, current density=119 mA $cm^{-2}$, distance between electrodes=1 cm, T=20 °C. ............... 130

Figure VII.1. Effect of the nature of electrolytes on TPh and COD removal as a function of the applied charge. Operating conditions: 100 mg $L^{-1}$ of synthetic phenolic solution, 10 g $L^{-1}$ of electrolyte, $pH_{initial}$=3.4, current density=57 mA $cm^{-2}$, distance between electrodes=1 cm, T=20 °C............... 144

Figure VII.2. Effect of the NaCl concentration on (a) TPh removal, (b) COD removal, (c) energy consumption, (d) conductivity and (e) cell potential. (a), (b), (d) and (e) as a function of the applied charge and (c) over COD removal. Inset of Figure VII.2: Evolution of pH medium at different NaCl concentrations. Operating conditions: 100 mg $L^{-1}$ of synthetic phenolic solution, $pH_{initial}$=3.4, current density=57 mA $cm^{-2}$, distance between electrodes=1 cm, T=20 °C. 147

Figure VII.3. Effect of the current density on (a,b) TPh removal and (c,d) COD removal as a function of the applied charge (a,c) and over time (b,d). Operating conditions: 100 mg $L^{-1}$ of synthetic phenolic solution, [NaCl]=10 g $L^{-1}$, $pH_{initial}$=3.4, distance between electrodes=1 cm, T=20 °C. 148

Figure VII.4. Effect of the initial pH medium on (a) TPh removal, (b) COD removal and (c) pH medium evolution as function of the applied charge. Inset of Figure VII.4b: Current efficiency at 7.5 Ah $L^{-1}$ for the different initial pH mediums. Operating conditions: 100 mg $L^{-1}$ of synthetic phenolic solution, [NaCl]=10 g $L^{-1}$, current density=119 mA $cm^{-2}$, distance between electrodes=1 cm, T=20 °C. 150

Figure VII.5. SEM photographs at 500× of the Ti/$IrO_2$ anode material, (a) before and (b) after EO treatment. Operating conditions: 100 mg $L^{-1}$ of synthetic phenolic solution, [NaCl]=10 g $L^{-1}$, $pH_{initial}$=3.4, current density=119 mA $cm^{-2}$, distance between electrodes=1 cm, T=20 °C. 150

Figure VII.6. Neuronal ROS signals evoked by the synthetic effluent plus NaCl. The points indicate the normalised amplitude of fluorescence signals recorded with the ROS indicator $H_2$DCFDA (20 µM), in the absence and presence (period indicated by the bar) of the treated effluent. Inset: The white bars represent the normalised amplitude of the depression in the presence of the raw effluent (left bar) and of the signal at the end of the washout period (right bar). The grey bars represent the equivalent data obtained for the treated effluent. The data were acquired using the ROS indicator $H_2$DCFDA (20 µM) and are represented as the mean ± s.e.m (n=3) for the treated effluent. 152

Figure VII.7. (a) TPh removal and (b) COD removal as function of the applied charge. Inset of Fig. 7a: Evolution of pH medium over the applied charge. Operating conditions: 10 g $L^{-1}$ of NaCl, current density=119 mA $cm^{-2}$, raw pH, distance between electrodes=1 cm, T=20 °C. 153

Figure VII.8. Discolouration of the undiluted and diluted real effluents (RE) over time and as a function of the applied charge. Operating conditions: 10 g $L^{-1}$ of NaCl, current density=119 mA $cm^{-2}$, raw pH, distance between electrodes=1 cm, T=20 °C. 153

Figure VIII.1. Amaranth dye structure. 162

Figure VIII.2. Cyclic voltammograms of the (a) Ti/$IrO_2$-$Ta_2O_5$ and (b) Nb/BDD anodes in 20 g $L^{-1}$ of $Na_2SO_4$, without (full line) and with 100 mg $L^{-1}$ of Amaranth dye (dashed line); scan potential from 0.0 to 3.0 V and scan rate 100 mV $s^{-1}$ (10 voltammetric cycles). Insets: Zoom to the cyclic voltammograms (a) and (b), respectively. 164

Figure VIII.3. Polarisation curves in the presence of the supporting electrolyte (full line) and in the supporting electrolyte plus the Amaranth dye (dashed line) for the (a) Ti/$IrO_2$-$Ta_2O_5$ and (b) Nb/BDD anodes with a scan rate of 100 mV $s^{-1}$. 165

Figure VIII.4. Oxidation of the Amaranth dye using a single cell. Effect of the anode material and current density on (a) colour removal over time for Ti/$IrO_2$-$Ta_2O_5$ anode, inset: colour removal over time for Nb/BDD anode; (b) COD removal and (c) decay of the normalised dye concentration. Operating conditions: 100 mg $L^{-1}$ of Amaranth dye, 20 g $L^{-1}$ of $Na_2SO_4$, current density=30, 60 and 80 mA $cm^{-2}$, T=25 °C. 168

Figure VIII.5. Oxidation of the Amaranth dye using two cells in a serial mode. Effect of current density on colour removal and decay of the normalised dye concentration over time for Ti/$IrO_2$-$Ta_2O_5$+Nb/BDD (a and c) and Nb/BDD+Ti/$IrO_2$-$Ta_2O_5$ (b and d) arrangements. Operating conditions: 100 mg $L^{-1}$ of Amaranth dye, 20 g $L^{-1}$ of $Na_2SO_4$, current density=30 and 60 mA $cm^{-2}$, T=25 °C. 169

Figure VIII.6. Oxidation of the Amaranth dye using two cells in a serial mode. Effect of current density on COD removal after 60 min of treatment for (a) Ti/$IrO_2$-$Ta_2O_5$+Nb/BDD and (b) Nb/BDD+Ti/$IrO_2$-$Ta_2O_5$ arrangements. Operating conditions: 100 mg $L^{-1}$ of Amaranth dye, 20 g $L^{-1}$ of $Na_2SO_4$, current density=30 and 60 mA $cm^{-2}$, T=25 °C. .................... 170

Figure VIII.7. Effect of the current density and system configuration on COD abatement at single cells (Ti/$IrO_2$-$Ta_2O_5$ and Nb/BDD) and two cells in a serial mode (Ti/$IrO_2$-$Ta_2O_5$+Nb/BDD and Nb/BDD+Ti/$IrO_2$-$Ta_2O_5$) at a specific electric charge of 3.8 Ah $L^{-1}$. Operating conditions: 100 mg $L^{-1}$ of Amaranth dye, 20 g $L^{-1}$ of $Na_2SO_4$, current density=30 and 60 mA $cm^{-2}$, T=25 °C. .................... 171

Figure VIII.8. Effect of the arrangement of the cells on energy consumption (kWh $m^{-3}$) for the (a) single cell and the (b) two cells in a serial mode during 60 min of treatment. Operating conditions: 100 mg $L^{-1}$ of Amaranth dye, 20 g $L^{-1}$ of $Na_2SO_4$, current density=30, 60 and 80 mA $cm^{-2}$, T=25 °C. .................... 172

Figure IX.1. Cyclic voltammograms of the Ti/Pt (a) and Ti/Pt-SnSb (b) anodes in 20 g $L^{-1}$ de $Na_2SO_4$, without (full line) and with 100 mg $L^{-1}$ of amaranth dye (dashed line); scan potential from 0.0 to 3.0 V and scan rate 100 mV $s^{-1}$ (10 voltammetric cycles). Insets: Zoom to the cyclic voltammograms (a) and (b), respectively. .................... 185

Figure IX.2. Polarisation curves in the presence of the supporting electrolyte (full line) and in the supporting electrolyte plus the AM dye (dashed line) for the Ti/Pt (a) and Ti/Pt-SnSb (b) anodes with a scan rate of 100 mV $s^{-1}$. .................... 186

Figure IX.3. Effect of the current density on colour removal over time with Ti/Pt (a) and Ti/Pt-SnSb (b) anodes. Insets: Absorbance band evolution over time by employing Ti/Pt (a) and Ti/Pt-SnSb (b) electrodes at 30 mA $cm^{-2}$. Operating conditions: Individual flow cell, 100 mg $L^{-1}$ of amaranth dye, 20 g $L^{-1}$ of $Na_2SO_4$, flow rate=250 L $h^{-1}$, T=25 °C. .................... 187

Figure IX.4. Effect of the applied current density on COD removal over time with Ti/Pt (a) and Ti/Pt-SnSb (b) anodes. Insets: Comparison of the current efficiency in each current density for the Ti/Pt (a) and Ti/Pt-SnSb (b) electrodes. Operating conditions: Individual flow cell, 100 mg $L^{-1}$ of amaranth dye, 20 g $L^{-1}$ of $Na_2SO_4$, flow rate=250 L $h^{-1}$, T=25 °C, current densities=30, 60 and 80 mA $cm^{-2}$. .................... 189

Figure IX.5. Effect of the applied current density on colour removal over time with Ti/Pt+Ti/Pt-SnSb (a) and Ti/Pt-SnSb+Ti/Pt (b) anodes. Insets: Absorbance band evolution over time by employing Ti/Pt+Ti/Pt-SnSb (a) and Ti/Pt-SnSb+Ti/Pt (b) electrodes at 30+30 mA $cm^{-2}$. Operating conditions: Assembling of flow cells in series, 100 mg $L^{-1}$ of amaranth dye, 20 g $L^{-1}$ of $Na_2SO_4$, flow rate=250 L $h^{-1}$, T=25 °C. .................... 190

Figure IX.6. Effect of the applied current density on COD removal over time with Ti/Pt+Ti/Pt-SnSb (a) and Ti/Pt-SnSb+Ti/Pt (b) anodes. Inset: Effect of the combinations of current density in energy consumption at the final COD removal values (black circles) after 300 min of treatment time with Ti/Pt+Ti/Pt-SnSb (a) and Ti/Pt-SnSb+Ti/Pt (b) anodes. Operating conditions: Assembling of flow cells in series, 100 mg $L^{-1}$ of amaranth dye, 20 g $L^{-1}$ of $Na_2SO_4$, flow rate=250 L $h^{-1}$, T=25 °C, current densities=30+30, 60+60, 30+60 and 60+30 mA $cm^{-2}$. .................... 191

Figure IX.7. Energy consumption to achieve approximately 90 % of colour removal using single and an assembling of electrochemical flow cells in series, and respectively COD removal values (black circles). (a) Ti/Pt at 30 mA $cm^{-2}$ and Ti/Pt-SnSb at 30 mA $cm^{-2}$, (b) Ti/Pt at 60 mA $cm^{-2}$ and Ti/Pt-SnSb at 60 mA $cm^{-2}$, (c) Ti/Pt at 30 mA $cm^{-2}$ and Ti/Pt-SnSb at 60 mA $cm^{-2}$ and (c) Ti/Pt at 60 mA $cm^{-2}$ and Ti/Pt-SnSb at 30 mA $cm^{-2}$. SUM corresponds to the sum of energy consumption applying both single flow cells. Operating conditions: Individual flow cell and an assembling of flow cells in series, 100 mg $L^{-1}$ of amaranth dye, 20 g $L^{-1}$ of $Na_2SO_4$, flow rate=250 L $h^{-1}$, T=25 °C, current densities=30 and 60 mA $cm^{-2}$. .................... 193

Figure IX.8. Effect of the applied current density on colour removal over time with Ti/Pt-SnSb+Nb/BDD (a) and Nb/BDD+Ti/Pt-SnSb (b) anodes. Insets: Absorbance band evolution over time by employing Ti/Pt-SnSb+Nb/BDD (a) and Nb/BDD+Ti/Pt-SnSb (b) electrodes at 30+30 mA $cm^{-2}$. Operating conditions: Assembling of flow cells in series, 100 mg $L^{-1}$ of amaranth dye, 20 g $L^{-1}$ of $Na_2SO_4$, flow rate=250 L $h^{-1}$, T=25 °C. ....... 194

Figure IX.9. Energy consumption to achieve the maximum colour removal (black circles) using single and an assembling of electrochemical flow cells in series. (a) Ti/Pt-SnSb at 30 mA $cm^{-2}$ and Nb/BDD at 30 mA $cm^{-2}$, (b) Ti/Pt-SnSb at 60 mA $cm^{-2}$ and Nb/BDD at 60 mA $cm^{-2}$, (c) Ti/Pt-SnSb at 30 mA $cm^{-2}$ and Nb/BDD at 60 mA $cm^{-2}$ and (c) Ti/Pt-SnSb at 60 mA $cm^{-2}$ and Nb/BDD at 30 mA $cm^{-2}$. SUM corresponds to the sum of energy consumption applying both single flow cells. Operating conditions: Individual flow cell and an assembling of flow cells in series, 100 mg $L^{-1}$ of amaranth dye, 20 g $L^{-1}$ of $Na_2SO_4$, flow rate=250 L $h^{-1}$, T=25 °C, current densities=30 and 60 mA $cm^{-2}$. ................................. 195

# LIST OF TABLES

**Page**

Table I.1. Categories and main phenolic compounds present in olive mill wastewater. 4

Table II.1. Reactor design features in electrochemical processes. 23

Table II.2. ECG studies with phenolic mixtures and olive mill wastewaters: operating conditions and main results. 30

Table II.3. ECG studies with dye wastewaters: operating conditions and main results. 31

Table II.4. EO studies with phenolic mixtures and olive mill wastewaters: operating conditions and main results. 37

Table II.5. EO studies with dye wastewaters: operating conditions and main results. 39

Table III.1. Main characteristics of the synthetic effluent. 56

Table III.2. TPh and COD removal with electrocoagulation after 180 min of reaction for each anode material (I=0.4 A, Electrode area=33.5 cm$^2$, Intergap=10 mm, [NaCl]=1.5 g L$^{-1}$). 58

Table III.3. Theoretical and experimental values of anode materials dissolution, as well as leaching results for each metal after 180 min and their correspondent legal limit of discharge into aquatic environment. (I=0.4 A, Electrode area=33.5 cm$^2$, Intergap=10 mm, [NaCl]=1.5 g L$^{-1}$). 62

Table III.4. EC$_{20}$ and EC$_{50}$ values of the synthetic effluent treated by the electrocoagulation process for each anode. 63

Table IV.1. Main characteristics of the synthetic and real effluent. 71

Table IV.2. EC$_{20}$ and EC$_{50}$ values for the synthetic effluent before and after treatment. 80

Table IV.3. Zinc mass. 84

Table V.1. Characteristics and chemical structure and of the Reactive Black 5 dye. 93

Table V.2. Main characteristics of the synthetic (100 mg L$^{-1}$ of Reactive Black 5) and real effluents. 93

Table VI.1. Main characteristics of the synthetic and real effluents. 116

Table VII.1. Characteristics and chemical structure of phenolic acids. 141

Table VII.2. Main characteristics of the synthetic and real effluents. 142

Table VIII.1. Cell potentials and respective energy consumption for different applied current densities using one (cell 1) or two cells (cell 1 and 2) in a serial mode, after 60 min of treatment. Sum of the individual COD removals and energy consumptions of the single cells for 60 min of electrolysis time. 173

Table IX.1. Chemical structure and characteristics of the Amaranth dye. 182

Table IX.2. Energy consumption (kWh m$^{-3}$) for different applied current density ($j$) after 360 min of electrolysis using the single flow cells with Ti/Pt and Ti/Pt–SnSb. 189

Table IX.3. Summary of the best experiments of assembling of electrochemical flow cells in series according to electric power demand and COD removal. 196

# LIST OF ABBREVIATIONS

| | |
|---|---|
| ACSF | Artificial cerebrospinal fluid |
| AG | Agitation |
| AM | Amaranth dye |
| AO | Anodic oxidation |
| AOPs | Advanced oxidation processes |
| BDD | Boron doped diamond |
| BOD | Biochemical oxygen demand |
| BR | Batch reactor |
| BS | Batch system |
| CE | Current efficiency |
| CFR | Continuous flow reactor |
| COD | Chemical oxygen demand |
| DSA | Dimensional stable anode |
| DW | Dye wastewater |
| EAOPs | Electrochemical advanced oxidation processes |
| EC | Energy consumption |
| ECG | Electrocoagulation |
| Electr. | Electrode |
| ElectrC | Electrode consumption |
| Electr. mat. | Electrode material |
| EO | Electrochemical oxidation |
| FDR | Flow discontinuous reactor |
| FS | Flow system |
| GA | Gallic acid |
| HPLC | High performance liquid chromatography |
| LTP | Long term potentiation |
| OMW | Olive mill wastewater |
| Op.cost | Operation cost |
| ORP | Oxidation-reduction potential |
| PAC | Pre-polymerized $Al^{3+}$ chemical |
| PC | Parallel conection |
| RB5 | Reactive Black 5 dye |
| RE | Real effluent |
| Ref. | Reference |
| rem | Removal |
| ROS | Reactive oxygen species |
| SC | Serial connection |
| SE | Synthetic effluent |
| SEC | Specific energy consumption |

| | |
|---|---|
| SEM | Scanning electron microscopy |
| SHE | Standard hydrogen electrode |
| SS | Stainless steel |
| TDFW | Total dyeing and finishing wastewaters |
| TEA | Tetraethylammonium |
| TOC | Total organic carbon |
| TPh | Total phenolic content |
| TSS | Total suspended solids |
| TW | Textile wastewater |
| US | Ultrasound energy |
| UV | Ultraviolet radiation |
| VORW | Vegetable oil refinery wastewater |
| XRD | X-ray diffraction |
| $^{13}$C NMR | Carbon-13 nuclear magnetic resonance |

# LIST OF SYMBOLS

| | |
|---|---|
| A | Anode |
| Abs | Absorbance |
| C | Cathode |
| $COD_0$ | Chemical oxygen demand at initial electrolysis time |
| $COD_t$ | Chemical oxygen demand at time t |
| $e^-$ | Electron |
| $E^0$ | Standard electrode potential |
| [E] | Concentration of the electrolyte |
| $EC_{20}$ | Toxicity level - Concentration of a sample that inhibits 20 % of bacteria light emission. |
| $EC_{50}$ | Toxicity level - Concentration of a sample that inhibits 50 % of bacteria light emission. |
| $E_{cell}$ | Average of the potential diference of the cell |
| F | Faraday's constant |
| $H^+$ | Hydrogen ion |
| I | Current intensity |
| *j* | Current density |
| M | Anode surface |
| $m_{metal\ theoretical}$ | Theoretical anode consumption |
| MO | Superoxide |
| $M(^{\bullet}OH)$ | Physisorbed hydroxyl radical |
| $M_w$ | Molecular weight |
| $^{\bullet}OH$ | Hydroxyl radical |
| $OH^-$ | Hydroxide ion |
| $pH_0$ | Initial pH |
| R | Organic compound |
| RO | Conversion of the organic compound |
| t | Electrolysis time |
| T | Temperature |
| V | Volume of the solution |
| X | General analysis parameter |
| $X_0$ | General analysis parameter at initial electrolysis time |
| $X_t$ | General analysis parameter at time t |
| z | Electrons transferred per ion |
| $\Delta COD$ | Experimental abatement of the COD |
| $\Delta_{metal\ experimental}$ | Mass of the anode dissolved |
| $\lambda_{max.}$ | Maximum wavelength |

# PART A. THESIS SCOPE AND OUTLINE

# I. INTRODUCTION

In the second half of the 19th century and throughout the 20th century, industrial activities experienced an exponential expansion. This intensification enabled humanity to reach modern welfare, yet it caused the indiscriminate use of raw material resources and the unavoidable pollution of the environment with tragic effects to atmosphere, water systems and soil. When its foundations are not based on sustainable premises, industrial development represents a major threat to human wellbeing. Therefore, sustainability will be the suitable plan to a better future, where economic growth must be forced to coexist with social cohesion and environmental protection [1–3].

## I.1 WATER SCARCITY AND ITS POLLUTION

Water availability and its quality are two considerable problems that society faces today. In fact, these issues can be accentuated in the future by climate change that causes higher water temperatures, melting of glaciers and an intensification of the water cycle, with potentially more floods and droughts. Water is a fundamental substance in our world and essential in our lives. Only less than 1 % of the planet's water is available for human consumption and, according to the World Health Organisation [4], one quarter of the world's population does not have access to adequate sanitation facilities and proper hygienic practices, which are related to the lack of safe drinking water. While this occurs in developing countries, other dramatic factors that affect the environment arise from developed countries, such as the wide variety of harmful effluents that are directly discharged into natural water courses as a result of industrial and domestic activities. These actions not only threaten the supply of freshwater but also aquatic life and all the food chain.

Water pollution consists in any physical, chemical, or biological change in water quality that has a negative impact on living organisms. Thus, the purification of wastewaters becomes indispensable to achieve the ideal degree of quality. The sources and impacts of the common classical pollutants such as natural organic compounds are reasonably well understood, but designing sustainable treatment technologies for them remains a scientific challenge [1,5,6]. Fortunately, the European Parliament reflected a new awareness through the directive 2000/60/EC, accentuating the necessity to diminish the quantity of pollutants through the implementation of new processes to combat water pollution [5].

## I.2 ORGANIC CONTAMINANTS

There are several industrial effluents which incorrect disposal into water courses causes considerable effects on the environment. In this work, the focuses were on olive mill wastewaters (OMW) and dye-stuff effluents. The following sections describe the main features of each selected effluent.

### I.2.1 PHENOLIC ACIDS AND OLIVE MILL WASTEWATERS (OMW)

The seasonal olive oil extraction industry generates an excessive amount of wastewaters encompassing several organic compounds like sugars, lipids, phenols and polyphenols [7]. This kind of waste may contain high concentrations of phenolic compounds, including most importantly cinnamic acid derivatives, benzoic acid derivatives and compounds related to tyrosol (Table I.1). The resemblance between these compounds consists of an aromatic ring with one or more substituent hydroxyl groups and a functional side chain [8–10]. Phenolic mixtures are usually present in agro-industrial effluents and incorporate a significant contaminant load due to their high toxicity, refractory character and high stability in water [11–14].

**Table I.1. Categories and main phenolic compounds present in olive mill wastewater.**

| Cinnamic acid derivates | Benzoic acid derivates | Compounds related to tyrosol |
|---|---|---|
| Cinnamic | Benzoic | Tyrosol |
| *p*-Cumaric | p-Hydroxybenzoic | Hydroxytyrosol |
| Caffeic | Protocatechuic | p-Hydroxyphenylacetic |
| Ferulic | Vanillic | |
| | Veratric | |
| | Gallic | |
| | Syringic | |

Adapted from: [14].

The composition of the agro-effluents depends on the olive variety, olive seed maturity, cultivation parameters, geological-climatic conditions and extraction process [8,10,15]. These polluted streams are responsible for a significant contamination problem in Portugal and other Mediterranean countries, where a great number of small factories are engaged in the production and refining of olive oil, accounting for 97 % of the worldwide olive oil production [8,10,15,16].

The treatment of liquid wastes produced from olive oil production is still the most important challenge that this industry has to handle. Commonly, the ways of dealing with the olive mill wastewaters (OMW) entails their direct discharge into sewer networks and central lagoons or its storage in small ponds where it is left to evaporate until the next season. However, important environmental impacts may occur, like the colouring of natural waters, contamination of surface and ground waters, modifications in soil quality, phytotoxicity and bad odours [10,14,15,17]. Consequently, rigorous requirements have been imposed to effluents discharge into public aqueous streams. However, the treatment of OMW by conventional biological processes has proved to be inefficient due to their bio-refractory nature and seasonality character of the olive oil cycle production, impeding the needed microorganisms acclimatation. Thus, new suitable cost-effective treatment technologies to reduce recalcitrant and toxic phenolic contaminants are demanded [11,18,19].

### I.2.2 DYE WASTEWATERS (DW)

Dyes can have a natural or synthetic origin, being the latter more widely used not only because of its stability but also because of its low cost of production compared to the former one [20]. These substances have complex aromatic molecular structures that make them difficult to biodegrade [21]. More than 100 000 dyes are available in the world market leading to a production of approximately $7x10^5$ tons of dyestuffs per year, including for the textile, cosmetic, paper, leather, pharmaceutical and food industries [22]. The dyeing and finishing processes generate a large quantity of contaminated effluents which are oftenly discharged with poor or no treatment. Due to the high concentration of dyes and other components such as salts, acids, bases, surfactants, dispersants, humectants, oxidants and detergents, these effluents cause a great environmental problem [23]. One of the main concerns is the colourisation of the aquatic systems even with low concentrations of dyes, which obstructs the light penetration and the oxygen solubility, thus affecting the aquatic life [22,24]. Serious risks may also arise from the toxicity and the carcinogenicity character of the azo dyes (60–70 % of the colourants employed worldwide), as well as the potential mutagenicity of the breakdown products formed during the cleavage of chromophore groups, in particular the aromatic amines [22,25–28]. In addition, these dyes are very stable in environment and very resistant to natural processes of oxidation/reduction, biodegradability and photodecomposition [23,29].

Therefore, the treatment of these wastewaters becomes crucial to completely eliminate the initial contaminants and reduce the environmental impact of the intermediates generated during its degradation.

## I.3 WASTEWATER REMEDIATION STRATEGIES

Wastewater treatment systems must guarantee the elimination or recovery of pollutants in order to reach the strict authorised limits to discharge contaminated effluents in natural hydric resources. In general, the removal of organic substances in aqueous solution requires one or more basic purification techniques depending on the concentration, volume flow of the stream to be treated, and the cost of the process [11,18,30].

Traditional methods used for water and wastewater handling can be broadly categorised by the nature of the operation process as biological, thermal, physical or chemical methods. Nowadays, the combination of technologies is becoming more popular since it offers the possibility to combine both environmental and economic advantages of each process [10,13,18,30]. Among contemporaneous techniques, advanced oxidation processes (AOPs) are being increasingly applied to destroy organic compounds present in several wastewaters from different industrial plants [8,10,12,13,18].

### I.3.1 TRADITIONAL TREATMENTS

Biological processes are the most widespread because they are considered environmentally compatible, trustworthy and, in most cases, cost-effective [8,10,31]. Commonly, searched methods are the anaerobic and aerobic oxidation. Several studies have reported that anaerobic digestion is usually the main biological treatment process because it has many advantages when compared to aerobic treatment. For example, it has low energy demand and produces less waste sludge, while it also leads to energy generation in the form of biogas and potential re-use of the effluent in irrigation [8,10,19]. For DW, they are efficient in colour removal and require lower nutrients than the conventional activated sludge process [32]. However, both systems (anaerobic and aerobic) are not the most suitable to eliminate or reduce the high organic load of olive mill or dye wastewaters that are recalcitrant to biodegradation and inhibitory to microorganisms activity. In the case of OMW, it is compulsory to dilute numerous times the effluent before the biological treatment, which leads to relevant cost implications [3,8,10,14,22,31,33].

Thermal processes such as combustion, co-combustion and pyrolysis are known to destroy pollutants at high temperatures, reducing the waste volume and providing energy recovery. Nevertheless, these kinds of processes have low efficiency to remove phenolic compounds. Besides, expensive facilities are generally required with high fuel costs and can be responsible for emissions of dangerous substances into the atmosphere [3,10,34]. Moreover, for low organic charge wastewaters, the effluents concentration would be required with inherent high energetic costs.

The technologies that only separate the pollutants from the water either by means of a support system or by transferring it to another phase and do not involve chemical transformations of the pollutants are the so-called separation treatment techniques. In other words, these processes only give partial solution to the problem because afterwards a final destination still needs to be set for the separated contaminants. Filtration, coagulation/flocculation, adsorption and ion exchange are examples of these non-destructive methods. The main membrane filtration technologies applied to wastewater treatment are microfiltration, ultrafiltration, nanofiltration and reverse osmosis. This type of approach is widely used and interesting in water reuse, but the initial investment and maintenance costs associated to the membranes are very high [14,22,30,35,36]. Normally, coagulation/flocculation processes are employed as a pre or post-treatment stage because they are not very efficient when used alone since most of the organics found in OMW and DW are difficult to precipitate [10,14,22]. Adsorption techniques using activated carbon are successful in the treatment of wastewater contaminated with low concentrations of phenolic compounds and dyes. During long contact times and high concentrations of oxygen, the phenolic compounds tend to be irreversibly adsorbed on the coal surface. A similar behaviour occurs in the removal of dyes from effluents [22]. This process has the disadvantage of requiring a step of regeneration, during which the contaminant is concentrated in the vapour phase [3]. Ion exchange processes allow the replacement of ions in solution using chemical reagents and it may be used to remove phenols and polyphenols [14]. On the other hand, this technique is not usually used for the removal of dyes, since ion exchangers cannot accommodate a wide range of dyes [29].

None of these physical-chemical processes alone is able to reduce the organic load and the toxicity of OMW and DW to acceptable limits. They are too expensive and do not solve the problem of sludge disposal and/or the by-products that derive from their application [10,19,28]. Therefore, it is essential to seek and develop new types of treatments to deal with phenolic compounds and dyes.

### I.3.2 ADVANCED OXIDATION PROCESSES

Advanced oxidation processes (AOPs) are gaining popularity among the scientific community for wastewater remediation, since they involve the generation of hydroxyl radicals ($^{\bullet}OH$). These powerful non-selective species have high oxidation potential and are able to react very quickly with a wide variety of organic compounds. These processes often ensure the complete abatement and mineralisation of the pollutants leading to the end products: carbon dioxide, water and inorganic ions; or the conversion of the contaminants to less harmful compounds that may be further degraded in activated sludge systems [5,18,37].

The AOPs may be classified according to the reaction phases involved (homogeneous and heterogeneous) or depending on the source of the oxidising species (ozonation, Fenton-type reactions, photochemical oxidation, electrochemical oxidation and ultrasound degradation) (Figure I.1). Each of them offers different ways to generate hydroxyl radicals. Among these processes, it shall be given preference to those that perform oxidation reactions at ambient or close to ambient conditions, thereby limiting the investment costs [38]. In fact, these technologies show high efficiency in water and wastewater treatment, particularly for effluents containing refractory, toxic and non-biodegradable materials. Nevertheless, they often encompass high capital and operating costs when compared with conventional methodologies so that they do not replace the inexpensive bio-remediation whenever it is possible [5,18,37,39]. Therefore, the AOPs can be used to treat toxic and/or non-biodegradable effluents during a short time, optimising chemicals and energy consumption and generating an intermediate wastewater that can be fully biodegradable. This opens the possibility of a subsequent biological treatment for the complete removal of organic matter. An integrated plant combining the environmental and economic advantages of AOPs and biological treatments seems to be an interesting option from an economical point of view and a practical solution for the removal of toxic compounds from water [5,18,40].

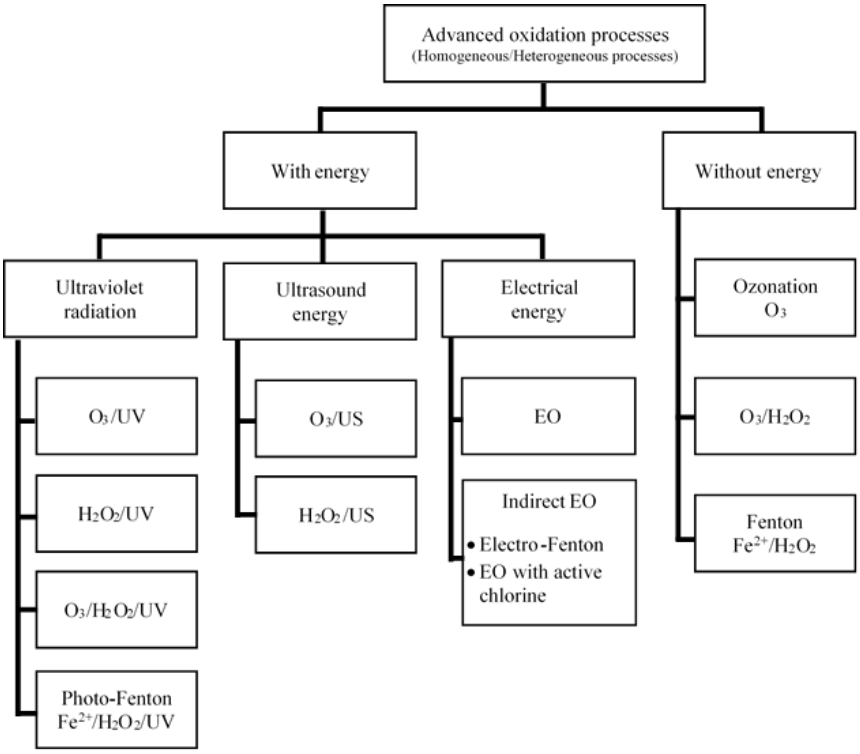
Advanced oxidation processes
(Homogeneous/Heterogeneous processes)
With energy
Without energy
Ultraviolet radiation
Ultrasound energy
Electrical energy
Ozonation O3
O3/UV
H2O2/UV
O3/H2O2/UV
Photo-Fenton Fe2+/H2O2/UV
O3/US
H2O2/US
EO
Indirect EO
• Electro-Fenton
• EO with active chlorine
O3/H2O2
Fenton Fe2+/H2O2

**Figure I.1. Classification of advanced oxidation processes.**
Abbreviations used: $O_3$ ozonation; $H_2O_2$ hydrogen peroxide; UV ultraviolet radiation; US ultrasound energy; $Fe^{2+}$ ferrous ion; EO electrochemical oxidation. Adapted from: [22,39].

### I.3.3 ELECTROCHEMICAL ADVANCED PROCESSES

The electrochemical oxidation (EO) is one of the electrochemical advanced oxidation processes (EAOPs) involving in-situ electro generation of strong oxidants, allowing a better efficiency in the removal of organic compounds when compared to analogous techniques, such as ozonation and Fenton's processes [2,41,42]. Other distinctive electrochemical method is the electrocoagulation (ECG), which is based on the generation of coagulants in-situ by the dissolution of sacrificial anodes to the liquid. The generated metal ions are hydrolysed to produce metal hydroxide ions leading to the entrapment of the pollutants. Electrocoagulation is more effective and yields more rapid contaminants separation with smaller amount of produced sludge and lower operating costs than the traditional coagulation systems [43,44].

The required equipment and operations for these types of electrochemical processes are generally simple and inexpensive; nonetheless various considerations must be taken into account to optimise efficiency, such as nature of the electrode material, reactor configuration and experimental conditions. These techniques are versatile and robust because allow dealing with several pollutants, treating diverse volumes of wastewaters, completing the reaction easily in short periods of time by cutting the power off, and having a rapid reset when operation problems occur [2,41]. In addition, their potential can be easily controlled and the operational parameters can be designed to minimise power losses. These processes are amenable to automation since the electrical variables are simple enough to use for data acquisition, process automation and control. However, the main disadvantage of these systems consists on their high operating cost due to high energy consumption [2,41,45].

## I.4 MOTIVATION AND SCOPE OF THE WORK

A long time ago, water was considered an unlimited low cost resource. However, that paradigm changed in the latest years due to the continuous increase of worldwide over consumption and contamination of the natural water courses. These factors brought risks to ecosystems since water is essential to life in general. The gap between its supply and demand is raising concern among society and governments; thus, the intense use of water is being limited and the recycle and reuse of this precious natural resource is being emphasised. The imposition of ever-stricter discharge regulations has driven up effluent treatment costs, requiring capital expenditures with little or no productive return. Additionally, there are wastewaters which cannot reach the present standards by conventional treatment techniques. In this regard, efforts should be made to develop and implement new efficient and economical treatment methods.

Electrochemical processes are the chosen advanced treatments to be studied and developed in this work, since they can operate at ambient conditions of pressure and temperature and are more efficient and compact when compared to other technologies.

The effluents obtained from olive mills and dye industries are particularly difficult to be biologically degraded and are the ones that are intended to be studied in the manuscript. In Portugal, a large number of these industrial units are responsible for most of water pollution. Thus, the demand of alternative treatment proves to be crucial for the environmental preservation of our ecosystems.

In this context, the main goals of this thesis can be summarised as follows:

- Study of the purification of synthetic wastewaters simulating olive mill effluents and dye effluents with further application to real wastewaters.
- Application of two electrochemical processes, electrocoagulation and electrochemical oxidation, to treat olive mill and dye wastewaters by evaluating the effect of the following parameters:
    - Initial pH;
    - Pollutant concentration;
    - Current density;
    - Nature and concentration of the electrolyte;
    - Nature of the electrode material;
    - Distance between electrodes;
    - Stability and durability of the electrodes;
    - Reactor configuration (batch-stirred and batch-recirculation flow).

- Assess of the contaminants degradation through the chemical oxygen demand (COD). In the case of OMW, the depletion of the phenolic content was also determined (TPh), while for the dyes, the decolourisation rate was determined from the decrease of the UV-vis absorbance.
- Monitoring the concentration of pollutants over time using chromatography of high efficiency (HPLC).
- Calculation of the energy efficiency and energy consumption.
- Optimisation of the operating conditions with the synthetic wastewaters, moving later to real effluents.
- Fulfil the legislate standards for discharge into aquatic streams or even to achieve the parameters to apply a final biological treatment process.
- Assess of the effect of the electrochemical treatment over the effluents toxicity and human health impact.

## I.5 STRUCTURE OF THE THESIS

This thesis is divided into four main parts. In Part A, chapter I intends to contextualise the reader with the specific liquid effluents situation, containing an introductory role on the environmental problems associated to olive mill and dye wastewaters, as well as the kind of treatments that can be used in their purification. Also, the motivations to perform this work are identified and a description of the strategy followed to achieve those goals is made. Chapter II presents an updated overview about the electrochemical processes used in this work, namely electrocoagulation and electrochemical oxidation, to depurate phenolic and dye wastewaters. Fundamentals of each technology are presented to better understand their basic theory related to mechanisms, reactor design and operating conditions.

Parts B and C are composed by chapters mainly based on the publication of peer-reviewed articles. Part B is devoted to the electrocoagulation process experiments and covers chapter III to V. In chapter III, anodes materials are screened in order to select the most promising to enhance the ECG technology action over a mixture comprising six major phenolic pollutants usually presents in OMW (3,4,5-trimethoxybenzoic, 4-hydroxybenzoic, gallic, protocatechuic, trans-cinnamic and veratric acids), regarding COD and TPh enhancement. In Chapter V, a special interest was given to the use of the Zn anode material applied to the previous phenolic mixture and the effect of several operating conditions were tested for the purpose of improving the ECG process. The electrode stability and durability is also addressed. After the optimisation of those conditions, the remediation of a real OMW was accomplished. Chapter V studies the Reactive Black 5 dye elimination from aqueous solutions by using aluminium anodes in batch-stirred and flow discontinuous ECG systems. The treatment of an actual DW has also been considered.

Part C is dedicated to the electrochemical oxidation process assays and comprises the chapters from VI to IX. In chapters VI and VII, two active anodes, Ti/$RuO_2$ and Ti/$IrO_2$ were evaluated, respectively. Both materials were analysed taking into account the reduction of COD and TPh parameters from the synthetic phenolic mixture and real OMW, as well as the impact of these contaminants on neuronal studies, before and after the EO treatment. Chapter VIII focus on the anodic oxidation of the Amaranth dye in aqueous solution by electrochemical measurements (cyclic voltammetry and polarisation curves) and bulk electrolysis using one cell or two cells in series with active (Ti/$IrO_2$-$Ta_2O_5$) and non-active (Nb/BDD) anodes. Chapter IX refers to the comparison of two active anodes (Ti/Pt and Ti/Pt-SnSb) using the same EO systems as in the previous chapter. Enclosing the study, the performance of flow cells in a serial mode with Ti/Pt-SnSb and Nb/BDD anodes was addressed, aiming to assess the effect of the BDD material on the system.

Part D finally summarises the main conclusions of the work and encompasses the future work perspectives as well (chapters X and XI, respectively).

## REFERENCES

[1] Inglezakis V, Poulopoulos S (2006) Adsorption, Ion Exchange and Catalysis Design of Operations and Environmental Applications, Elsevier Science, 1–28.

[2] Martínez-Huitle C, Ferro S (2006) Electrochemical oxidation of organic pollutants for the wastewater treatment: direct and indirect processes. Chem. Soc. Rev. 35(12): 1324–1340.

[3] Britto J, Rangel M (2008) Revisão. Quim. Nova, 31, 114–122.

[4] World Health Organization and United Nations Children Fund (2000) Global Water Supply and Sanitation Assessment Report – WHO/UNICEF Joint Monitoring Programme for Water Supply and Sanitation.

[5] Pera-Titus M, García-Molina V, Baños M, Giménez J, Esplugas S (2004) Degradation of chlorophenols by means of advanced oxidation processes: a general review. Appl. Catal. B: Environ. 47: 219–256.

[6] Schwarzenbach R, Egli T, Hofstetter T, von Gunten U, Wehrli B (2010) Global water pollution and human health. Annu. Rev. Environ. Resour. 35: 109–136.

[7] Fezzani B, Cheikh RB (2010), Two-phase anaerobic co-digestion of olive mill wastes in semi-continuous digesters at mesophilic temperature, Bioresour. Technol. 101: 1628–1634.

[8] Mantzavinos D, Kalogerakis N (2005) Treatment of olive mill effluents Part I. Organic matter degradation by chemical and biological processes-an overview. Environ. Int. 31: 289–295.

[9] Ahmadi M, Vahabzadeh F, Bonakdarpour B, Mehranian M, Mofarrah E (2006) Phenolic removal in olive oil mill wastewater using loofah-immobilized Phanerochaete chrysosporium. World J. Microb. Biotechol. 22: 119–127.

[10] Paraskeva P, Diamadopoulos E (2006) Technologies for olive mill wastewater (OMW) treatment: a review. J. Chem. Technol. Biotechnol. 81: 1475–1485.

[11] Beltran-Heredia J, Torregrosa J, Dominguez J, Peres J (2001) Comparison of the degradation of p-hydroxybenzoic acid in aqueous solution by several oxidation processes. Chemosphere 42: 351–359.

[12] Beltran-Heredia J, Torregrosa J, Dominguez J, Peres J (2001) Kinetics of the reaction between ozone and phenolic acids present in agro-industrial wastewaters. Water Res. 35: 1077–1085.

[13] Carbajo M, Beltrán F, Gimeno O, Acedo B, Rivas F (2007) Ozonation of phenolic wastewaters in the presence of a perovskite type catalyst. Appl. Catal. B: Environ. 74: 203–210.

[14] Kapellakis I, Tsagarakis K, Crowther J. (2008) Olive oil history, production and by-product management. Rev. Environ. Sci. Biotechnol. 7: 1–26.

[15] Mert B, Yonar T, Kiliç M, Kestioğlu K (2010) Pre-treatment studies on olive oil mill effluent using physicochemical, Fenton and Fenton-like oxidations processes. J. Hazard. Mater. 174: 122–128.

[16] Benitez F, Beltran-Heredia J, Peres J, Dominguez J (2000) Kinetics of p-hydroxybenzoic acid photodecomposition and ozonation in a batch reactor. J. Hazard. Mater. 73: 161–178.

[17] El-Gohary F, Badawy M, El-Khateeb M, El-Kalliny A (2009) Integrated treatment of olive mill wastewater (OMW) by the combination of Fenton's reaction and anaerobic treatment. J. Hazard. Mater. 162: 1536–1541.

[18] Azabou S, Najjar W, Bouaziz M, Ghorbel A, Sayadi S. (2010) A compact process for the treatment of olive mill wastewater by combining wet hydrogen peroxide catalytic oxidation and biological techniques. J. Hazard. Mater. 183: 62–69.

[19] Duarte J, Pires S, Paixão S, Sàágua M (2010) Olive mill wastewater bioremediation by Bjerkandera paranensis: A sustainability and technological evalutation in Procedings of the 2nd International Conference of IAMAW, 79–85.

[20] Yamjala K, Nainar MS, Ramisetti NR (2016) Methods for the analysis of azo dyes employed in food industry – A review. Food Chem. 192: 813–824.

[21] Nguyen TA, Juang R-S (2013) Treatment of waters and wastewaters containing sulfur dyes: A review. Chem. Eng. J. 219: 109–117.

[22] Brillas E, Martínez-Huitle CA (2015) Decontamination of wastewaters containing synthetic organic dyes by electrochemical methods. An up dated review, Appl. Catal. B: Environ. 166–167: 603–643.

[23] Solís M, Solís A, Pérez HI, Manjarrez N, Flores M (2012) Microbial decolouration of azo dyes: A review. Process Biochem. 47: 1723–1748.

[24] Oturan MA, Aaron JJ (2014) Advanced oxidation processes in water/wastewater treatment: principles and applications. A review. Crit. Rev. Environ. Sci. Technol. 44: 2577–2641.

[25] Forgacs E, Cserháti T, Oros G (2004) Removal of synthetic dyes from wastewaters: a review. Environ. Int. 30: 953–971.

[26] Garcia-Segura S, Centellas F, Arias C, Garrido JA, Rodríguez RM, Cabot PL, Brillas E (2011) Comparative decolorization of monoazo, diazo and triazo dyes by electro-Fenton Process, Electrochim. Acta 58: 303–311.

[27] Solanki K, Subramanian S, Basu S (2013), Microbial fuel cells for azo dye treatment with electricity generation: A review, Bioresour. Technol. 131: 564–571.

[28] Khandare RV, Govindwar SP (2015) Phytoremediation of textile dyes and effluents: Current scenario and future prospects. Biotechnol. Adv. 33 (2015) 1697–1714.

[29] Robinson T, McMullan G, Marchant R, Nigam P (2001) Remediation of dyes in textile effluent: a critical review on current treatment technologies with a proposed alternative. Bioresour. Technol. 77: 247–255.

[30] Azabou S, Najjar W, Gargoubi A, Ghorbel A, Sayadi S (2007) Catalytic wet peroxide photo-oxidation of phenolic olive oil mill wastewater contaminants. Appl. Catal. B: Environ. 77: 166–174.

[31] Rivas F, Beltrán F, Gimeno O (2000) Joint treatment of wastewater from table olive processing and urban wastewater. Integrated ozonation–aerobic oxidation. Chem. Eng. Technol. 23: 177–181.

[32] Punzi M, Anbalagan A, Börner RA, Svensson B-M, Jonstrup M, Mattiasson B (2015) Degradation of a textile azo dye using biological treatment followed by photo-Fenton oxidation: Evaluation of toxicity and microbial community structure. Chem. Eng. J. 270: 290–299.

[33] Bianco B, De Michelis I, Vegliò F (2011) Fenton treatment of complex industrial wastewater: optimization of process conditions by surface response method. J. Hazard. Mater. 186: 1733–1738.

[34] Caputo A, Scacchia F, Pelagagge P (2003) Disposal of by-products in olive oil industry: waste-to-energy solutions. Appl. Therm. Eng. 23: 197–214.

[35] Curinha J. (2008) Adição de Produtos Químicos e Ensaios de Electro-Coagulação e Electro-Oxidação para o (Pré) Tratamento das Águas Residuais Provenientes dos Lagares de Produção de Azeite. Universidade Nova de Lisboa, 1–172.

[36] Vijayaraghavan K, Ahmad D, Lesa R (2006) Electrolytic treatment of beer brewery wastewater. Ind. Eng. Chem. Res. 45: 6854–6859.

[37] Andreozzi R, Caprio V, Insola A, Marotta R, Sanchirico S (2000) Advanced oxidation processes for the treatment of mineral oil - contaminated wastewaters. Water Res. 34: 620–628.

[38] Peñarroya, J. (2007) Coupled Photochemical-Biological System to Treat Biorecalcitrant Wastewaters. Universitat de Barcelona, 1–202.

[39] Poyatos J, Muñio M, Almecija M, Torres J, Hontoria E, Osorio F (2010) Advanced oxidation processes for wastewater treatment: state of the art. Water, Air, Soil Pollut. 205: 187–204.

[40] Mantzavinos D, Psillakis E (2004) Enhancement of biodegradability of industrial wastewaters by chemical oxidation pre-treatment. J. Chem. Technol. Biotechnol. 79: 431–454.

[41] Anglada Á, Urtiaga A, Ortiz I (2009) Contributions of electrochemical oxidation to waste-water treatment: fundamentals and review of applications. J. Chem. Technol. Biotechnol. 84: 1747–1755.

[42] Cañizares P, Paz R, Sáez C, Rodrigo M (2009) Costs of the electrochemical oxidation of wastewaters: a comparison with ozonation and Fenton oxidation processes. J. Environ. Manage. 90: 410–420.

[43] Chen G. (2004) Electrochemical technologies in wastewater treatment. Sep. Purif. Technol. 38: 11–41.

[44] Mollah MYA, Pathak SR, Patil PK, Vayuvegula M, Agrawal TS, Gomes JAG, Kesmez M, Cocke DL (2004) Treatment of orange II azo-dye by electrocoagulation (EC) technique in a continuous flow cell using sacrificial iron electrodes. J. Harzard. Mater. B109: 165–171.

[45] Panizza M, Cerisola G (2009) Direct and mediated anodic oxidation of organic pollutants. Chem. Rev. 109: 6541–6569.

# II. ELECTROCHEMICAL PROCESSES: FUNDAMENTALS AND LITERATURE OVERVIEW

Electrochemical processes are considered environmentally friendly since they use the electron as a clean and efficient reagent, without demanding the addition of further chemicals [1,2]. The application of electrochemical technologies in wastewater treatment has shown high effectiveness in the elimination of organic contaminants [1,3,4]. Before beginning to examine how electrochemistry can play a useful role in environmental science through literature overview, some fundamental concepts about electrocoagulation and electrochemical oxidation technologies will be first addressed and used as buildings blocks for later chapters in this thesis.

## II.1 ELECTROCOAGULATION (ECG) PROCESS

The electrocoagulation (ECG) is a phase separation technology that has been known for more than a century. However, it had not been extensively applied to the treatment of water and wastewaters because of its high initial investment and energy costs. Nevertheless, in the 21st century, the prices of electricity as well as power sources have substantially lowered, turning the ECG into a viable alternative for environmental purposes [5,6]. This technology involves the electro dissolution of sacrificial anodes into aqueous medium yielding metallic ions. Subsequently, metal hydroxides are formed by the reaction of the yielded metal ions at the anode and the hydroxide released during the water reduction to hydrogen at the cathode. It should be noticed that the distribution and solubility of the metallic ions and their hydroxocomplexes are dependent on pH and ionic strength. These metal ionic species and hydroxocomplexes react with negatively charged particles in the water to form flocs, which will have the power to destabilise and aggregate the suspended particles in order to precipitate, trap or adsorb dissolved contaminants. Moreover, the phenomenon of electroflotation can also take place when the hydrogen bubbles evolve at the cathode, attaching the coagulated particles and transporting them to the surface of the solution where they can be separated [4,5,7]. Figure II.1 represents a scheme of the electrocoagulation process.

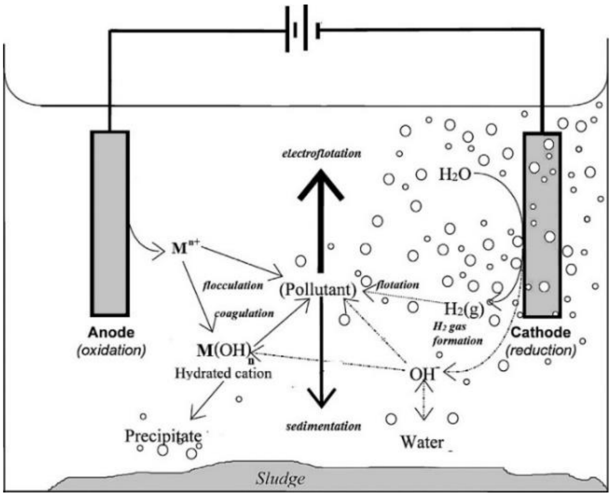

**Figure II.1. Mechanism for the electrocoagulation process.**
Source: [4].

Therefore, it is possible to state that the ECG is based on the interaction of three conventional technologies combining their mechanisms and advantages: chemical coagulation, flotation and electrochemistry. All of these are well-known processes with a long period of research and development. However, the deep knowledge about the relation between these technologies in an ECG system, is still somehow misty. More studies on the core basis of electrocoagulation are required to develop a better understanding of this process as a whole [6].

## II.2 ELECTROCHEMICAL OXIDATION (EO) PROCESS

The first studies on electrochemical oxidation (EO) for wastewater remediation were reported in the 19th century, although its extensive investigation started in the 20th century focused on the electrochemical conversion/destruction of organics. During the past two decades, many research groups all over the world have been devoted and are still involved in the discovery of the potentials of this process due to the evident relevance in developing new technologies to preserve water resources and environment [1,2,4,5,8–11].

The EO is the most popular treatment of contaminants among the electrochemical processes and it can occur through two different mechanisms:

- Direct oxidation, where the pollutants are diffused from the bulk solution to the surface of the anode, being oxidised there by direct charge transfer processes (Figure II.2a);
- Indirect oxidation, where the pollutants are indirectly oxidised by electrochemically generated oxidants. These species are generated by the oxidation of a mediator on the surface of the anode that will react with the contaminants in the bulk (Figure II.2b).

In addition, both mechanisms may coexist during oxidation [2].

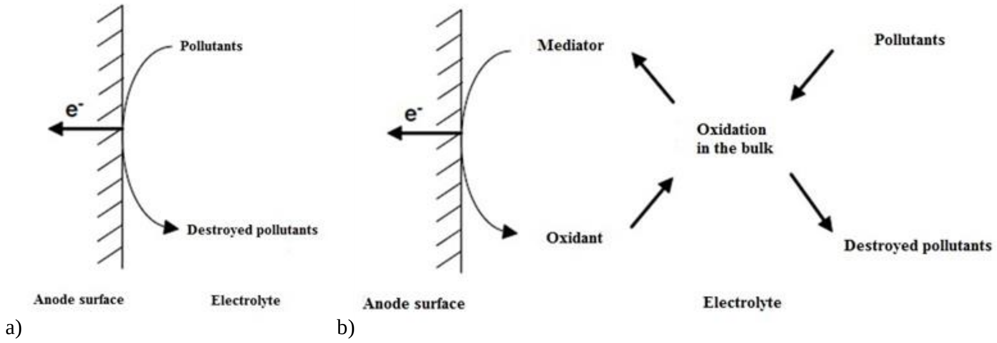

**Figure II.2. Scheme for a) direct and b) indirect electrochemical oxidation processes.**
Adapted from: [2].

The main disadvantage of direct oxidation is its catalytic activity decrease due to the poisoning effect caused by the development of a polymeric film on the electrode's surface. The adsorption properties of the anode surface, as well as the concentration and the nature of organic compounds and even their degradation intermediates are factors that influence the electrodes deactivation. This problem can be avoided if oxidation is accomplished in the potential region of water discharge, with simultaneous oxygen evolution, or by indirect electrochemical oxidation [11].

In the indirect oxidation process, the most common oxidants electrogenerated are the reactive oxygen species (ROS) such as hydroxyl radicals, ozone and hydrogen peroxide, as well as different active species that depend on the electrolyte used. For example if NaCl is applied active chlorine species like $Cl_2$, HClO and $ClO^-$ are produced.

### II.2.1 ELECTROGNERATION OF REACTIVE OXYGEN SPECIES (ROS)

In 1994, Comninellis [12] established a comprehensive model of the oxidation of organics in an acidic medium comprising the competition with the $O_2$ evolution reaction. This scheme was slightly modified over time and the different behaviour of the anodes in EO was explained by considering two limiting cases as in the schematic model of Figure II.3. The anode materials were classified in two big groups depending on the species which were mainly electrogenerated: active anodes (Pt, $IrO_2$ and $RuO_2$) with low $O_2$ overpotentials where chemisorbed radicals are preferentially formed, and non-active anodes ($PbO_2$, $SnO_2$ and BDD) with high $O_2$ overpotentials where the hydroxyl radical remains physisorbed.

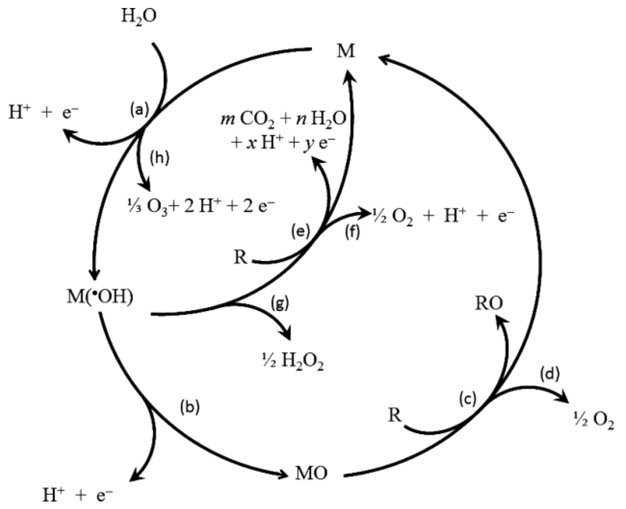

**Figure II.3. Representation of the mechanism of electrochemical oxidation of organic compounds on active and non-active anodes. Active anodes - reactions (a), (b), (c) and (d) and non-active anodes - reactions (a), (e) and (f).**
**(a) Formation of M(•OH); (b) Formation of the higher metal oxide, MO; (c) Electrochemical conversion of the organic compound, R, via the MO; (d) Oxygen evolution by the chemical decomposition of the MO; (e) Electrochemical combustion of the organic compound, R, via •OH radicals; (f) Oxygen evolution by EO of •OH radicals; (g) Hydrogen peroxide production via •OH radicals and (h) Ozone production.**
Source: [4].

According to the proposed model, the first step, which is common for both types of anodes (generically denoted as M), consists in the oxidation of the water molecules electrogenerating physisorbed M(•OH) radicals as represented in Equation (II.1).

$$\mathrm{M + H_2O \rightarrow M(\,^{\bullet}OH) + H^+ + e^-} \qquad \textbf{(II.1)}$$

After the hydroxyl radicals formation and depending on the electrode nature (active or non-active), two limiting behaviours can occur. In the case of the active anodes, their surface strongly interacts with •OH radicals leading to the formation of the superoxide (MO), Equation (II.2).

$$\mathrm{M(\,^{\bullet}OH) \rightarrow MO + H^+ + e^-} \qquad \textbf{(II.2)}$$

The redox couple MO/M will act as a mediator in the oxidation of the organic compounds (Equation (II.3)) and at the same time will compete with the parasitic reaction of the $O_2$ evolution through the decomposition of the MO (Equation (II.4)).

$$\mathrm{MO + R \rightarrow M + RO} \qquad \textbf{(II.3)}$$

$$\mathrm{MO \rightarrow M + \frac{1}{2} O_2} \qquad \textbf{(II.4)}$$

In its turn, the surface of the non-active anodes has a weak interaction with the •OH radicals, allowing the oxidation of the organics by M(•OH), leading to their complete mineralisation to carbon dioxide and water (Equation (II.5)).During this process, the competition of the side reaction of the $O_2$ evolution (Equation (II.6)) may also occur or even the dimerization of the M(•OH) to $H_2O_2$ ((II.7)).

$$aM(^{\bullet}OH) + R \rightarrow aM + mCO_2 + nH_2O + (a-2n)\ H^+ + (a-2n)\ e^- \tag{II.5}$$

$$M(^{\bullet}OH) \rightarrow M + \frac{1}{2}O_2 + H^+ + e^- \tag{II.6}$$

$$2M(^{\bullet}OH) \rightarrow 2M + H_2O_2 \tag{II.7}$$

As can be realised through this mechanism, anodes with low oxygen evolution overpotential have an active behaviour, allowing only partial oxidation of organics. On the contrary, anodes with high oxygen evolution overpotential like the non-active ones privileges complete oxidation of organic compounds. As a result, these last electrodes are regarded as the most suitable for wastewater treatment [1,11–13].

Ozone is another electrochemically generated oxidant, being recognised as a powerful oxidising agent ($E^0$=2.07 V *vs* SHE), which is able to participate in a high number of reactions. The synthesis of this substance occurs from the anodic oxidation of water in an acidic media, requiring low voltage (E°=1.51 V *vs* SHE) and it is represented by Equation (II.8).

$$3H_2O \rightarrow O_3 + 6H^+ + 6e^- \tag{II.8}$$

Ozone generation efficiency can be limited by the $O_2$ evolution reaction (Equation (II.9)) that takes place at a lower potential ($E^0$=1.23 V *vs* SHE), being certainly thermodynamically preferred than Equation (II.8). Therefore, the parasitic reaction should be minimised in order to get ozone at significant current efficiencies [11,14].

$$2H_2O \rightarrow O_2 + 4H^+ + 4e^- \tag{II.9}$$

Moreover, in order to improve the electrogeneration efficiency of ozone, anodes with high $O_2$ overpotential which are stable in highly acidic media and electrolytes whose composition do not participate in competitive reactions are required [14].

Beyond the anodic formation of ROS (reactive oxygen species), there is also the cathodic generation of oxidants like the hydrogen peroxide (Equation (II.10)) through the reduction of the oxygen gas which can be directly injected as pure oxygen or bubbled air at the cathode [15].

$$O_2 + 2H_2O + 2e^- \rightarrow H_2O_2 + 2OH^- \tag{II.10}$$

This oxidant is considered as “green” since it just decomposes itself into water and oxygen (Equation (II.11)). However, this spontaneous decomposition decreases peroxide activity, as well as the electrochemical reduction of hydrogen peroxide at the cathode (Equation (II.12)) that diminishes the current efficiency reducing the degradation achieved by the process [14,15].

$$2H_2O_2 \rightarrow H_2O + O_2 \tag{II.11}$$

$$H_2O_2 + 2H^+ + 2e^- \rightarrow 2H_2O \tag{II.12}$$

Although hydrogen peroxide is widely used in wastewater treatments, it is considered a weak oxidant when applied alone. Nonetheless, its oxidation power can be highly improved owing to its combination with ozone, UV-light and transition metal catalysts such as iron ions that break the hydroxide peroxide bond and produce hydroxyl radicals, known as Fenton's process (Equation (II.13)).

$$\mathrm{Fe^{2+} + H_2O_2 \rightarrow Fe^{3+} + {}^{\bullet}OH + OH^-} \quad \textbf{(II.13)}$$

This know-how was adjusted to the indirect electrochemical treatment, being called electro-Fenton's process, wherein the hydrogen peroxide, continuously produced in-situ, is mixed with iron catalyst in the aqueous solution promoting the formation of $^{\bullet}OH$ radicals in the bulk via Fenton's process. The major advantages of this method over the classic Fenton's process is the higher organic compounds removal rate due to continuous regeneration of the iron ($Fe^{2+}$) at the cathode and the on-site production of H2O$_2$ avoiding the risks related to its transport, storage and handling [15].

### II.2.2 ELECTROGENERATION OF CHLORINE ACTIVE SPECIES

Chlorine active species ($Cl_2$, HClO and $ClO^-$) are probably the most usual electrochemically produced oxidants during wastewaters treatment due to the ubiquitous presence of chloride in effluents, and because of their effective performance. Furthermore, in electro-based processes, NaCl is the most common electrolyte applied to improve the conductivity of the effluent.

The direct oxidation of chloride ions at the surface of the anode allows the generation of soluble chlorine, as observed in Equation (II.14). Additionally, this species can be rapidly hydrolysed to hypochlorous acid (HClO) and chloride ion, after being diffused from anode towards the bulk solution (Equation (II.15)). At this medium, the HClO is in equilibrium with $ClO^-$ ion with $pK_a=7.55$ (Equation (II.16)) [5,11].

$$\mathrm{2Cl^- \rightarrow Cl_{2\,(aq)} + 2e^-} \quad \textbf{(II.14)}$$

$$\mathrm{Cl_{2\,(aq)} + H_2O \rightleftarrows HClO + Cl^- + H^+} \quad \textbf{(II.15)}$$

$$\mathrm{HClO \rightleftarrows ClO^- + H^+} \quad \textbf{(II.16)}$$

The pH of the solution is an essential parameter in indirect electrochemical oxidation, since the electrogeneration of certain oxidising species is dependent on the medium pH [4]. In the case of the formation of the active chlorine species, until pH 3.0, the main species is $Cl_{2\,(aq)}$, while the predominant one in the pH range 3–8 is HClO and for pH > 8 is $ClO^-$. It is theoretically expected that the $Cl^-$ mediated oxidation of the pollutants with the active chlorine species is more extended in acidic than in alkaline media due to the higher standard potentials of $Cl_{2\,(aq)}$ ($E^0$=1.36 V *vs* SHE) and HClO ($E^0$=1.49 V *vs* SHE) than $ClO^-$ ($E^0$=0.89 V *vs* SHE).

### II.2.3 OTHER ELECTROGENERATED SPECIES

In addition, when anodes with high $O_2$ overpotential are used, other weaker oxidising agents like peroxodisulfate (Equation (II.17)), peroxodicarbonate (Equation (II.18)) and peroxodiphosphate (Equation (II.19)) are generated by anodic oxidation [11].

$$2SO_4^{2-} \rightarrow S_2O_8^{2-} + 2e^- \tag{II.17}$$

$$2CO_3^{2-} \rightarrow C_2O_6^{2-} + 2e^- \tag{II.18}$$

$$2PO_4^{3-} \rightarrow P_2O_8^{4-} + 2e^- \tag{II.19}$$

## II.3 PROCESS PERFORMANCE INDICATORS AND ENERGETIC PARAMETERS

Regardless the electrochemical process used for the treatment of wastewaters, its efficiency is assessed in terms of performance indicators, while the economic viability is set by energetic parameters.

The depuration process of organic compounds is commonly monitored bearing in mind environmental legislation by following the abatement of chemical oxygen demand (COD) and biochemical oxygen demand ($BOD_5$). From these data, the removal percentages are calculated by generic Equation (II.20).

$$\mathrm{X\ removal\ (\%)} = \frac{\mathrm{X_0 - X_t}}{\mathrm{X_0}} \times 100 \tag{II.20}$$

Where X corresponds to the parameter in analysis, $X_0$ (mg $L^{-1}$) and $X_t$ (mg $L^{-1}$) to the values of the parameter before the electrolysis and at an electrolysis time t, respectively. The removal of the phenolic content, in the case of the phenolic mixtures, and the decolourisation efficiency for dyes are also parameters studied. In the first case, TPh will be expressed as milligrams of gallic acid equivalents (mgGA $L^{-1}$) since the calibration curve is prepared based on the Folin-Ciocalteau method using different concentrations of this compound to relate the absorbance with the concentration of the phenolic compounds, while in the second case the parameter is measured at the wavelength of maximum absorbance ($\lambda_{max}$) of the substance determined from UV–vis spectrophotometry.

In the electrocoagulation process, normally, the dissolution of the anode is theoretically calculated based on Faraday’s law (Equation (II.21)).

$$\mathrm{m_{metal\ theoretical}\ (g)} = \frac{\mathrm{I\ t\ M}_w}{\mathrm{z\ F}} \tag{II.21}$$

where I refers to current intensity (A), t to the time of the electrocoagulation process (s), $M_w$ to the molecular weight of the metal (g $mol^{-1}$), z to the electrons transferred per ion and F to the Faraday’s constant (96485 C $mol^{-1}$).

The current efficiency (CE) is also an important parameter and can be determined by different ways for electrocoagulation (ECG) and electrochemical oxidation (EO) processes. For ECG, it can be calculated based on the comparison of the experimental weight loss of the anode, which will correspond to the anode mass dissolved in solution ($\Delta_{\text{metal experimental}}$), with the theoretical anode consumption ($m_{\text{metal theoretical}}$), as presented by Equation (II.22). Whereas for EO, the current efficiency is defined as the ratio of the charge used for the oxidation of each compound to the total charge passed during electrolysis (Equation (II.23)) [11].

$$\mathrm{CE}_{\mathrm{ECG}}(\%) = \frac{\Delta_{\text{metal experimental}}}{m_{\text{metal theoretical}}} \times 100 \tag{II.22}$$

$$\mathrm{CE}_{\mathrm{EO}}(\%) = \frac{(\mathrm{COD}_0 - \mathrm{COD}_t)\ F\ V}{8It} \times 100 \tag{II.23}$$

where $COD_0$ and $COD_t$ corresponds to chemical oxygen demands at time t=0 and time t, respectively in $gO_2\ L^{-1}$. I is the current intensity (A), F is the Faraday's constant (96485 C $mol^{-1}$), V is the electrolyte volume (L), 8 is the oxygen equivalent mass (32 $gO_2\ mol^{-1}$ per 4 $e^{-}$) and t is the electrolysis time (s).

Key specific energetic parameters such as energy consumption per volume of treated effluent, in kWh $m^{-3}$ or per consumed mass of anode, in kWh $kg_{metal}^{-1}$ or per unit mass of organic load removed, in kWh $kgCOD^{-1}$ can be obtained through Equation (II.24), Equation (II.25) and Equation (II.26), respectively

$$\mathrm{EC}(\mathrm{kWh\ m^{-3}}) = \frac{E_{\text{cell}}\ I\ t}{V} \tag{II.24}$$

$$\mathrm{EC}(\mathrm{kWh\ kg\ metal^{-1}}) = \frac{E_{\text{cell}}\ I\ t}{\Delta_{\text{metal experimental}}} \tag{II.25}$$

$$\mathrm{EC}(\mathrm{kWh\ kgCOD^{-1}}) = \frac{E_{\text{cell}}\ I\ t}{\Delta \mathrm{COD}\ V} \tag{II.26}$$

where $E_{cell}$ corresponds to the average potential difference of the cell (V), I to the current intensity (A), t to the electrolysis time (h), $\Delta_{\text{metal experimental}}$ to the anode mass dissolved (g), ΔCOD to the experimental abatement of COD ($gO_2\ L^{-1}$) and V to the solution volume (L).

## II.4 REACTOR DESIGN

The electrochemical reactors design lies on the specific needs of the depuration process, involving economic, technological, safety and environmental issues [3]. In Table II.1 are summarised the main characteristics of the posible arrangements.

**Table II.1. Reactor design features in electrochemical processes.**

| | | |
|---|---|---|
| **Mode of operation** | Batch | Continuous |
| **Number of electrode pairs** | Single | Multiple |
| **Electrode geometry** | Two-dimensional | Three-dimensional |
| **Electrode motion** | Static | Moving |
| **Electrode connections** | Monopolar | Bipolar |
| **Interelectrode gap** | Moderate | Capillary |
| **Electrolyte manifolding** | External | Internal |
| **Cell division** | Undivided | Divided |
| **Reactor sealing** | Open | Closed |

Adapted from: [3].

Electrochemical reactors may be categorised under their operation mode as batch or continuous. The reactor design encompasses electrodes configuration which can have two or three dimensions, being static or dynamic. Three dimensional electrodes have the advantage of a higher value of electrode surface to cell volume ratio and moving electrodes hint greater values of mass-transport coefficient caused by turbulence. Nevertheless, two dimensional electrodes are most commonly used because it is easier to scale them up [3]. In electrochemical cells, monopolar or bipolar electrodes may be connected in parallel or in a serial mode. Monopolar electrodes require contact with the power supply and their two faces are active with the same polarity. On the other hand, bipolar electrodes do not have electrical connections and are located between two end monopolar electrodes, i.e. the voltage applied between the outer electrodes by the power supply causes the polarisation of the inner electrodes, acquiring different polarities in the opposite faces [3,16,17]. The schematic diagram of monopolar and bipolar electrodes in parallel and in series connections is shown in Figure II.4.

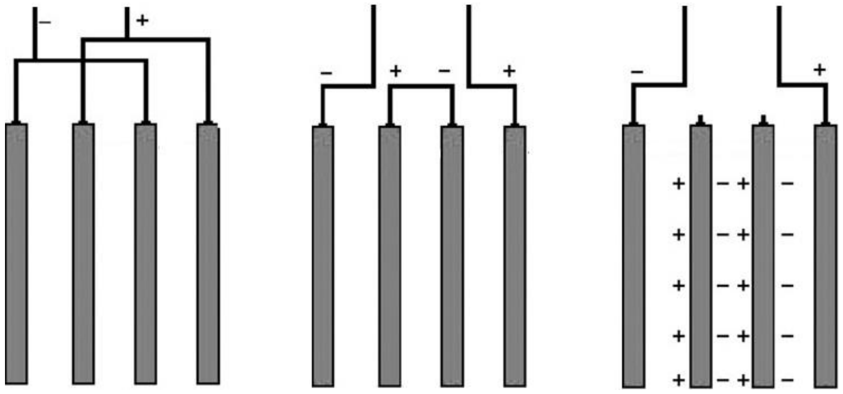

**Figure II.4. (a) Monopolar electrodes in (a) parallel and (b) serial configurations, and bipolar electrodes in a serial configuration.**
Adapted from: [16].

In addition, the cells can be divided or undivided. When the cell is divided by a porous diaphragm or an ion conducting membrane, both the anolyte and catholyte are separated. However, the use of these apparatuses must be avoided whenever possible, because separators are expensive and may lead to mechanical and corrosion problems [18–20]. Moreover, in an electrochemical reactor, heat can be produced due to the reaction itself (exothermic reaction), being, therefore, important to take into account changes in heat capacities of reagents and products when the reactor is being designed [2,3].

Figure II.5 represents a typical batch reactor, which includes a power supply and two monopolar electrodes. In this scheme, the anode and the cathode are displayed in a parallel connection linked by a power supply and are submerged in the solution to treat (with or without the addition of electrolyte). Since electrons are not able to move freely in solutions, a charge has to be passed in the electrochemical cell to promote redox reactions of the chemical species besides enhancing the movement of ions and molecules [21]. Normally, the solution is continuously stirred (magnetically or mechanically) in order to guarantee the homogeneity in the reactor. This kind of reactor is widely used as a first approach to determine the influencing parameters and their experimental domains.

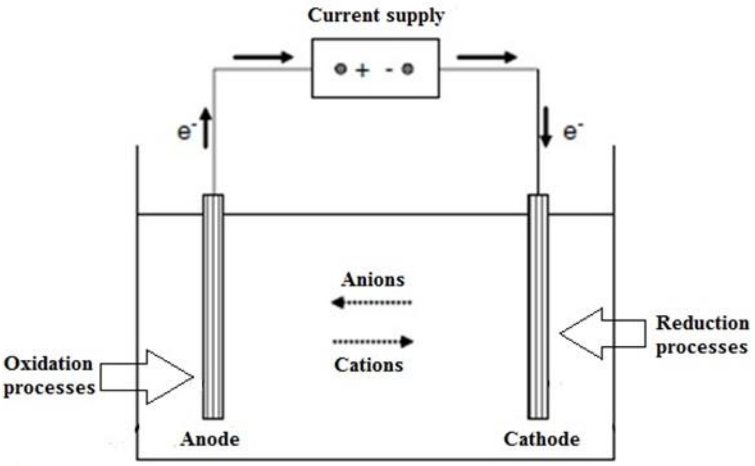

**Figure II.5. Conceptual diagram of an electrochemical reactor.**
Adapted from: [2].

## II.5 LITERATURE OVERVIEW - OPERATING CONDITIONS

The main goal of an electrochemical system is to achieve the maximum efficiency of the process through the combination of several variables, such as reactor design, electrode material, current density (intensity per unit area of the electrode), pH, conductivity, temperature, effluent characteristics and operation time. In this subsection, the action of these parameters will be discussed based on the literature overview dedicated to the treatment of olive mill and dye wastewaters by electrocoagulation and electrochemical processes.

### II.5.1 ELECTROCOAGULATION (ECG) PROCESS

In what concerns the studies published in the literature involving the electrocoagulation (ECG) process, a review is summarised in Table II.2 for the phenolic compounds and olive mill wastewaters (OMW) and in Table II.3 for dye wastewaters (DW). These tables are presented later at the end of this section in pages 30 and 31. Some highlights of those researches are now addressed. As observed from the analysis of the tables for most of the ECG experiments performed with those two types of effluents, the batch reactor has been used with monopolar electrodes in parallel connection, containing either one or multiple anode-cathode pairs, varying the number of electrodes between 2 and 16 (OMW – [7,22–26] and DW – [16,27–41]. Kobya *et al.* [7] evaluated the performance of the monopolar and bipolar electrodes in the two possible connections, in parallel and in a serial mode for DW degradation. The results showed that the monopolar electrode in parallel connection was the most cost-effective configuration. Sengil and Özacar 2009 [32] used a bipolar serial arrangement to decolourise the Reactive Black 5 dye in aqueous solution. In these batch ECG systems, stirring rate of the solution causes the increase of contact between the flocs and their agglomeration during the process. Conversely, the intensive stirring can break the flocs, which means that the speed rate is a parameter that must be optimised [35].

Essadki *et al.* [42] employed a 20 L external-loop airlift ECG reactor in order to depollute a red dye from the Moroccan textile industry and validate this innovative application of airlift reactors. The mixture of the solution and the complete flotation of the pollutants were achieved using only the overall liquid recirculation induced by $H_2$ microbubbles generated by water electrolysis. Experimental outcomes exhibited that the axial position of the electrodes and the residence time in the separator section were considered the strategic parameters to attain good mixing conditions, to avoid bubbles/particles recirculation in the downcomer and to prevent floc break-up/erosion by hydrodynamic shear forces. This arrangement without mechanical agitation, pumping requirements or air injection allowed to achieve lower specific energy and electrode consumptions than the conventional gas–liquid contacting devices. El-Ashtoukhy and Amin [43] presented a new batch self gas stirred electrochemical cell to remove the Acid Green 50 dye. Naje *et al.* [44], built a batch-stirred tank with a cylindrical form and inside of it a rotating shaft was attached to an adjustable speed motor in order to hold the impeller structure and also to maintain the electrode rotations. The rotating anode consisted of 10 impellers and each one had four main rods, with 10 rings used as a cathodes. The experimental results indicated that the optimum conditions for the treatment of the textile wastewater were achieved at current density of 4 mA cm$^{-2}$, rotational speed of 150 rpm, interelectrode gap of 1 cm, retention time of 10 min, pH of 4.6 and temperature of 25 °C. The removal efficiencies of COD, TSS and colour were all higher than 96 %, with an energy consumption of 4.7 kWh m$^{-3}$.

Phalakornkule *et al.* [31] and Ardhan *et al.* [39] attempted to develop continuous flow reactors from the data gathered with the experiments performed with batch systems to remove Direct Red 23 and Reactive Blue 21 dyes from an aqueous solutions, respectively. Similar batch configurations were employed to optimise the design parameters. Different continuous flow reactors were described in both works, in the former one, the ECG reactor was a 10 L acrylic column with a set of 25 pairs of electrodes made of Fe with a total area of 5235 cm$^2$. Each electrode had the same configuration as those employed in the batch experiments, being connected vertically with a gap distance of 0.8 cm. In the second one, the reactor was composed by 2 hollow Fe tubes put together in a concentric configuration with an effective electrode area of 1500 $cm^2$. For these two studies, the application of the set of optimal parameters was successfully implemented to an up scaled continuous flow reactor with > 90 % of colour removal and energy consumptions in the order of 0.7–0.9 kWh $m^{-3}$. Other experimental setup of continuous ECG cell was provided by Merzouk *et al.* [45], in which the reactor consists of a rectangular tank divided into two compartments. The first compartment has the electrodes and the second compartment was designed to favour the floc removal by electroflotation. This scheme was performed to enhance the mixing in the first compartment, using both the liquid flow and $H_2$ microbubbles and the position of the outlet tube in the second section was considered to avoid the presence of solid particles in the effluent stream.

Aluminium (Al) and iron (Fe) are the sacrificial electrode materials usually employed in ECG [5,46]. The popularity of these metals is due to their availability, inexpensive price, non-toxicity, and proven effectiveness [47]. Occasionally, other metals, such as stainless steel (SS) may also be used [35,37]. When Al is applied as the anode in the process, it occurs its dissolution to the liquid in the form of $Al^{3+}$ species (Equation (II.27)) and at the cathode takes place the cathodic reduction of $H_2O$ to $OH^-$ ion and $H_2$ (Equantion (II.28)).

$$\mathrm{Al} \rightarrow \mathrm{Al}^{3+} + 3\mathrm{e}^- \qquad \textbf{(II.27)}$$

$$3\mathrm{H_2O} + 3\mathrm{e}^- \rightarrow 3\mathrm{OH}^- + \frac{3}{2}\mathrm{H}_{2\,(g)} \qquad \textbf{(II.28)}$$

The $Al^{3+}$ and $OH^-$ ions generated at the electrodes surface react in the liquid bulk to form soluble monomeric species such as $Al(OH)^{2+}$, $Al(OH)_2^+$ and $Al(OH)_3$ in acidic medium, as well as $Al(OH)_4^-$ in an alkaline medium. Polymeric species like $Al_2(OH)_2^{4+}$, $Al_6(OH)_{15}^{4+}$, $Al_7(OH)_{17}^{4+}$ can evolve from the two former cations. All these ions can be converted to the insoluble $Al(OH)_3$, as shown in Equation (II.29).

$$\mathrm{Al}^{3+} + 3\mathrm{H_2O} \rightarrow \mathrm{Al(OH)}_{3\,(s)} + 3\mathrm{H}^+ \qquad \textbf{(II.29)}$$

In the case of Fe anodes, the dissolution of $Fe^{2+}$ is prometed to the liquid (Equation (II.30)), whereas in the cathode occurs the generation of hydroxyl ions and hydrogen gas by the reduction of water (Equation (II.31)).

$$\mathrm{Fe} \rightarrow \mathrm{Fe}^{2+} + 2\mathrm{e}^- \qquad \textbf{(II.30)}$$

$$2\mathrm{H_2O} + 2\mathrm{e}^- \rightarrow 2\mathrm{OH}^- + \mathrm{H}_{2\,(g)} \qquad \textbf{(II.31)}$$

At pH higher than 5.5, the $Fe(OH)_2$ precipitates (Equation (II.32)) being in equilibrium with $Fe^{2+}$ up to pH 9.5 or with monomeric species such as $Fe(OH)^+$ or $Fe(OH)_3^-$ at higher pH values.

$$\mathrm{Fe}^{2+} + 2\mathrm{OH}^- \rightarrow \mathrm{Fe(OH)}_{2\,(s)} \qquad \textbf{(II.32)}$$

The $Fe^{2+}$ ion can also be further oxidised to $Fe^{3+}$ if the oxidation-reduction potential (ORP) and pH conditions are suitable (Equation (II.33)). Oxygen has to be present and pH has to be neutral or alkaline to a reasonable reaction rate be achieved.

$$4Fe^{+} + \ 10H_2O + O_{2\,(g)} \rightarrow 4Fe(OH)_{3\,(s)} + 8H^{+} \tag{II.33}$$

The released $H^+$ can be directly reduced to $H_2$ gas at the cathode (Equation (II.34)) giving the total reaction (Equation (II.35)) in the electrolytic cell.

$$8H^{+} + 8e^{-} \rightarrow 4H_{2\,(g)} \tag{II.34}$$

$$4Fe^{+} + \ 10H_2O + O_{2\,(g)} \rightarrow 4Fe(OH)_{3\,(s)} + 4H_{2\,(g)} \tag{II.35}$$

There are several studies discussing the effect of the electrode material, Al or Fe, on the ECG depuration efficiency of OMW and DW (Table II.2 and Table II.3). Satisfactory treatment efficiencies in terms of COD, TPh and colour were attained by both anode materials, depending on the characteristics of the effluents and on the operating conditions applied.

In alkaline pH solutions, the best indices are representative of Fe anodes, whereas in neutral and weak acidic solutions the most effective purification takes place in the presence of Al anodes [22,23,27,38]. This behaviour is in accordance with the amphoteric character of $Al(OH)_3$ that does not precipitate at pH < 2, and at pH > 10 its solubility increases, leading to the formation of the soluble $AlO_2^-$ which is not useful for wastewater treatment. Normally, the pH of the medium changes during the process. This variation is influenced by the type of the electrode material and the initial pH. In the case of Al, the final pH is higher for initial pH < 8, and above this value the final pH is lower. For experiments with Fe anodes, the final pH is always higher than the initial one and the difference between them diminishes for initial pH > 8. These results suggest that ECG displays pH buffering capacity, particularly in an alkaline medium [27].

In most of studies, Fe is superior to Al as sacrificial electrode material, from the point of view of COD removal efficiency and energy consumption for the depuration of both types of wastewaters (OMW and DW), while the electrode consumption per kgCOD removed is lower generally with Al [24,27]. Combining these two electrode materials (Al – Fe or Fe – Al) good efficiencies for colour removal may also be obtained, for OMW and DW [23,34].

However, in removing dark colour of OMW, Al anode was found to be more effective than Fe, since the effluent treated with the latter sacrificial anode turns yellow first and then brownish. This behaviour may be due to the excess of $Fe^{2+}$ and $Fe^{3+}$ species generated during the electrolysis and characterised by their characteristic colour, yellow-brown. This colour may also result from the formation of brown soluble compounds by the complexing reaction between Fe ions and polyphenol molecules [22,23].

In the experiments relating the efficiency of the process with SS and Fe anodes in parallel connection, the former material led to interesting results for treatment of a dye and textile wastewater. For example, by applying SS electrodes to the system, a textile wastewater was successfully electrocoagulated with 90 % of COD, 91 % of TOC, 90 % of turbidity, and 94 % of TSS removals as well as 2.4 kWh $m^{-3}$ of energy and 0.05 kg $m^{-3}$ of electrode consumptions [37].

The number of electrodes was also found to influence removal efficiencies. Ahlawat *et al.* [30] stated that increasing the number of electrodes from 4 to 10, the Cotton Blue dye removal efficiency increased from 92 to 97 %. The electrodes being in a parallel connection, a higher number of them leads to a higher dissolution of the metal to the liquid, allowing a higher removal of the pollutant. Beyond the number of electrodes, the space between them (interelectrode gap distance) is also important, since it affects the amount of energy which is necessary to be supplied to the system in order to generate an electric field and induce the movement of ions [48]. When the interelectrode spacing increases, there is the decrease of the amount of the metal dissolved to the liquid, weakening the interactions between the pollutant molecules and the flocs, leading to the diminution of the removal efficiency [30,33].

Parsa *et al.* [35] studied the effect of covering one face of the anodes with a resistant resin on the depuration of the Acid Brown 14 dye. These covered anodes were located in the electrolysis cell in two different positions, the active surface of the anodes were turned to the cathode or back to it. It seems that the colour conversion rate is dependent on the anode surface and its position to cathode. When the active surface of the anode is turned to the cathode, the solution resistance is lower than in the other case due to the inferior distance between electrodes. Regarding the energy consumption, this parameter is lower for both covered anodes rather than uncovered ones. For the back to cathode configuration, it may be due to a lower generated current in the electrolysis cell, and for the face to the cathode, a lower ECG time is needed to achieve the total colour removal. Therefore, the covered anode with face to cathode position can be preferred to others due to low energy consumption and to its higher ECG rate [35].

One of the most crucial variables in the ECG process is the current density ($j$), because it determines the coagulant dosage rate, the bubble production rate, the size and growth of the flocs. At high $j$, the amount of metal dissolved to the solution increases, resulting in a greater quantity of precipitate to remove the pollutants. Furthermore, it was demonstrated that bubbles density increases and their size decreases with increasing $j$, resulting in a greater upwards flux and a faster removal of contaminants and sludge flotation. As the $j$ decreases, the time needed to achieve similar efficiencies rises [7,24]. The current density and the electrolysis time must be optimised to be attained a cost effective operation [26,29].

In the electrochemical processes, the supporting electrolyte is used to increase the conductivity of the solution. When the conductivity is increased, the total resistance in the solution decreases, thus the necessary voltage to reach on optimum current density will diminish, and consequently the consumed electrical energy will decrease [7]. The most common electrolytes employed to increase the conductivity are NaCl, $Na_2SO_4$, $Na_2CO_3$ and $NaNO_3$. NaCl plays a significant role to the depuration of wastewaters, due to the formation of active chlorine yielding higher removal rates compared to the other salts [25]. Moreover, $Cl^-$ does not present the adverse impact of adding $CO_3^{-2}$ or $SO_4^{2-}$ anions. The presence of $CO_3^{-2}$ may lead to the precipitation of $Ca^{2+}$ or $Mg^{2+}$ ions, that can form a passivating layer on the surface of the electrodes. This layer would sharply increase the ohmic resistance of the electrochemical cell and result in a significant decrease in the current efficiency and treatment conversion [33,35]. Aoudj *et al.* [33] also suggests the decline in dye removal in the presence of $CO_3^{-2}$ is due to competition for adsorption sites on $Al(OH)_3$ of this anion and dye molecules. Khosravi *et al.* [40] tested four types of electrolytes (NaCl, KCl, $Na_2SO_4$ and $KNO_3$) on the decoulorisation efficiency of Acid Red 18 dye with Al electrodes and showed that $CO_3^{-2}$ had almost similar behaviour as the $Cl^-$ ions. The removal efficiency only declined with $KNO_3$ and this can be own to the variation in the final pH in different electrolytes.

There are some studies in literature about the use of conventional coagulant to aid ECG. For example, $Al^{3+}$ salts or the PAC, a pre-polymerized $Al^{3+}$ chemical are used. PAC encompasses a range of hydrolysis and polymeric species, being relatively large and carrying a high cationic charge. Its enhanced surface activity and improved charge neutralising capacity may make it more effective at a comparatively lower dose than $Al^{3+}$ salts. This substance lowers and stabilises the pH near the optimum value during the process, being supplied more coagulant to the wastewater. The initial presence of Al in the wastewater, induced and accelerated the formation of more sweep $Al(OH)_3$ flocs which adsorb particulate and soluble organic matter. The advantages of PAC are the following: rapid aggregation velocity, larger and heavier flocs, and lower required dosage. PAC was found to significantly enhance the COD removal rate and efficiency, depending on the amount of the total aluminium supplied, by initial addition and electrochemical generation and the electrical energy consumption was also lowered with a significant decrease in the operating cost [7,24,28].

As aforementioned the characteristics of the wastewaters also affect the treatment process that is why, normally, the first step was to optimise the method by removing individual pollutants from aqueous solutions, like a specific phenolic acid or dye. Nowadays, some authors are using directly an actual effluent [7,16,22–28,36–38,44,49] or trying to test the effect of a contaminant dissolved in a real wastewater matrix [41] or even to mix two or more pollutants in an aqueous solution [34,42,45].

**Table II.2. ECG studies with phenolic mixtures and olive mill wastewaters: operating conditions and main results.**

| Wastewater | Reactor design | Electr. mater. A – C | Operation conditions | Initial pollutant characteristics | Main conclusions | Ref. |
|---|---|---|---|---|---|---|
| Fresh and stored OMW | BR with 7 electr. in PC (3 A + 4 C) | Al – Al<br>Fe – Fe | IG=1 cm<br>*j*=10–120 mA cm$^{-2}$<br>[E]=NA<br>pH$_0$=2–10<br>V=0.5 L<br>Stirring=200 rpm<br>t=60 min | COD$_0$=58–75 gO$_2$ L$^{-1}$<br>TPh$_0$=2.4 g L$^{-1}$ | Al – Al<br>COD$_{rem}$=59–81 %<br>TPh$_{rem}$=78–91 %<br>Colour$_{rem}$=92–96 %<br><br>Fe – Fe<br>COD$_{rem}$=60 %<br>TPh$_{rem}$=80 %<br>Colour$_{rem}$=45 % | [22] |
| OMW | BR with 16 electr. in PC (8 A + 8 C) | Al – Fe<br>Fe – Al | IG=0.3 cm<br>*j*=10 – 40 mA cm$^{-2}$<br>[E]=NA<br>pH$_0$=4–9<br>Stirring=ND<br>V=ND<br>t=2–30 min | COD$_0$=5 gO$_2$ L$^{-1}$<br>SS$_0$=0.2 g L$^{-1}$ | Al – Fe<br>COD$_{rem}$=30–52 %<br>Colour$_{rem}$=92–97 %<br>SS$_{rem}$=50–68 %<br><br>Fe – Al<br>COD$_{rem}$=35–47 %<br>Colour$_{rem}$=90–96 %<br>SS$_{rem}$=48–68 % | [23] |
| OMW | BR (cathode) with a metallic stirrer (anode) | Al – Al<br>Fe – Fe | IG=ND<br>*j*=10–40 mA cm$^{-2}$<br>[E]=NA<br>pH$_0$=5.5 (Al) or 6.5 (Fe)<br>V=0.3 L<br>Stirring=60 rpm<br>t=180 min<br>[H$_2$O$_2$]=0–2.3 %<br>[PAC]=0–0.5 g L$^{-1}$ | COD$_0$=45 gO$_2$ L$^{-1}$ | Al – Al<br>COD$_{rem}$=76 %<br>EC=302 kWh m$^{-3}$<br><br>Fe – Fe<br>COD$_{rem}$=56–86 %<br>EC=29–188 kWh m$^{-3}$ | [24] |
| OMW | Semi-pilot scale reactor, divided in four compartments. Each compartment contains 4 plates (2 A + 2 C) | Fe – Fe | IG=2 cm<br>*j*=13 mA cm$^{-2}$<br>[E]=NA<br>pH$_0$=5.2<br>V=ND<br>Stirring=ND<br>t=120 min | COD$_0$=37 gO$_2$ L$^{-1}$<br>TPh$_{0\ monomers}$=4 g L$^{-1}$<br>TPh$_{0\ o\text{-}diphols}$=2 g L$^{-1}$<br>BOD$_5$/COD=0.3 | COD$_{rem}$=34 %<br>Colour$_{rem}$=75 %<br>TPh$_{rem\ monomers}$=92 %<br>TPh$_{rem\ o\text{-}diphols}$=48 %<br>BOD$_5$/COD=0.6 | [49] |
| VORW | BR with 6 electr. in PC (3 A + 3 C) | Al – Al | IG=0.8 cm<br>*j*=25–35 mA cm$^{-2}$<br>[Na$_2$SO$_4$]=0–71 g L$^{-1}$<br>pH$_0$=1.4–9<br>V=0.3 L<br>Stirring=ND<br>t=120 min<br>[PAC]=0–0.5 g L$^{-1}$ | COD$_0$=15 gO$_2$ L$^{-1}$ | COD$_{rem}$=70–99 %<br>EC=42–131 kWh kgCOD$^{-1}$ | [7] |
| OMW | BR with 2 electr. in PC | Al – Al | IG=2.8 cm<br>*j*=2.5–38 mA cm$^{-2}$<br>[NaCl]=0.5–3 g L$^{-1}$<br>pH$_0$=2–10<br>V=0.1 L<br>Stirring=200 rpm<br>t=15 min$^{-}$ | COD$_0$=20 gO$_2$ L$^{-1}$<br>TPh$_0$=0.3 g L$^{-1}$ | COD$_{rem}$=42–84 %<br>TPh$_{rem}$=33–87 %<br>Colour$_{rem}$=55–92 %<br>EC=0.1–4 kWh kgCOD$^{-1}$ | [25] |
| OMW | BR with 2 electr. in PC | Al – Al<br>Fe – Fe | IG=5.5 cm<br>*j*=12–58 mA cm$^{-2}$<br>[E]=NA<br>pH$_0$=4.3<br>V=0.25 L<br>AG=ND<br>t=120 min | COD$_0$=57 gO$_2$ L$^{-1}$ | COD$_{rem}$=48–64 %<br>EC=5–6 kWh kgCOD$^{-1}$ | [26] |

NA – Parameter not applied to the system.
ND – Parameter not defined in the article.

**Table II.3. ECG studies with dye wastewaters: operating conditions and main results.**

| **Pollutant/ wastewater** | **Reactor design** | **Electr. mater. A – C** | **Operating conditions** | **Initial pollutant characteristics** | **Main conclusions** | **Ref.** |
|---|---|---|---|---|---|---|
| TW | BR with 4 electr. in PC (2 A + 2 C) | Al – Al<br>Fe – Fe | IG=1.1 cm<br>*j*=5–20 mA cm$^{-2}$<br>Conductivity=1–4 mS cm$^{-1}$<br>pH$_0$=3–11<br>V=0.25 L<br>Stirring=200 rpm<br>t=15 or 30 min | COD$_0$=3 gO$_2$ L$^{-1}$ | COD$_{rem}$=26–77 %<br>EC=0.6–3 kWh kgCOD$^{-1}$<br>ElectrC=0.1–0.35 kgAl kgCOD$^{-1}$<br>ElectrC=0.1–0.65 kgFe kgCOD$^{-1}$ | [27] |
| TW | BR with 4 electr. in PC (2 A + 2 C) | Al – Al | IG=1.1 cm<br>*j*=10 mA cm$^{-2}$<br>[E]=NA<br>pH$_0$=7<br>V=0.25 L<br>Stirring=200 rpm<br>t=10 or 30 min$^1$<br>[PAC]=0–1 g L$^{-1}$<br>[Al]= 0–1 g L$^{-1}$ | COD$_0$=3 gO$_2$ L$^{-1}$ | COD$_{rem}$=50–80 %<br>EC=0.3–3 kWh kgCOD$^{-1}$ | [28] |
| Levafix orange dye | BR with 4 electr. in PC (2 A + 2 C) | Al – Al | IG=1.1 cm<br>*j*=2.5–25 mA cm$^{-2}$<br>Conductivity=0.25–4 mS cm$^{-1}$<br>pH$_0$=3–11<br>V=0.25 L<br>Stirring=200 rpm<br>t=15 or 20 min | [Dye]$_0$=0.1–0.5 g L$^{-1}$ | Colour$_{rem}$=77–100 %<br>EC=6–199 kWh kgDye$^{-1}$<br>ElectrC=0.2–5 kgAl kgDye$^{-1}$ | [29] |
| TW | BR with 4 electr. (2 A + 2 C) in PC (monopolar) and SC (monopolar and bipolar) | Al – Al<br>Fe – Fe | IG=2 cm<br>*j*=3–6 mA cm$^{-2}$<br>[E]=NA<br>pH$_0$=5–10<br>V=0.75 L<br>Stirring=250 rpm<br>t=15 or 25 min | COD$_0$=2 gO$_2$ L$^{-1}$<br>Turbidity=671 NTU | COD$_{rem}$=20–70 %<br>Turbidity$_{rem}$=0–92 %<br>EC=0.6–0.7 kWh m$^{-3}$<br>ElectrC=0.1–0.6 kg m$^{-3}$<br>Op.cost=0.2–1.5 $ m$^{-3}$ | [16] |
| Aniline Blue WS dye | BR with 4 or 10 electr. in PC (2 or 5 A + 2 or 5 C) | Al – Al | IG=0.5–1.3 cm<br>Appl.voltage=11–20 V<br>[E]=NA<br>pH$_0$=3–11<br>V=1.5 L<br>Stirring=ND<br>t=5 or 15 or 30 min | [Dye]$_0$=0.1–1 g L$^{-1}$ | Dye$_{rem}$=70–98 %<br>ElectrC=0.09–0.14 g Al | [30] |
| Mixture of 2-naphthoic acid and 2-naphtol | Semi-batch airlift reactor | Al – Al | IG=2 cm<br>*j*=5.1–51 mA cm$^{-2}$<br>Conductivity=2–28 mS cm$^{-1}$<br>pH$_0$=5–10<br>V=14–20 L<br>Stirring=ND<br>t=50 min | [Dye]$_0$=0.02 g L$^{-1}$<br>COD$_0$=2.5 gO$_2$ L$^{-1}$ | COD$_{rem}$=35–100 %<br>Colour$_{rem}$=71–100 %<br>Turbidity$_{rem}$=45–95 %<br>EC=5–160 kWh kgDye$^{-1}$<br>EC=125 kWh kgCOD$^{-1}$<br>ElectrC=0.5–1.6 kgAl kgDye$^{-1}$ | [42] |
| Mixture of 2-naphthoic acid and 2-naphtol | Flow reactor with 2 electr. in PC | Al – Al | IG=1 cm<br>*j*=21–63 mA cm$^{-2}$<br>[NaCl]=0–5 g L$^{-1}$<br>pH$_0$=3–9<br>V=ND<br>Flow rate=0.4–1.3 L min$^{-1}$<br>t=32 min | [Dye]$_0$=0.025–0.20 g L$^{-1}$<br>COD$_0$=2.5 gO$_2$ L$^{-1}$ | COD$_{rem}$>80 %<br>Colour$_{rem}$>80 %<br>EC=0–14 kWh kgDye$^{-1}$ | [45] |
| Direct red 23 dye | BR with 10 electr. in PC (5 A + 5 C) | Al – Al<br>Fe – Fe | IG=0.5–1.2 cm<br>*j*=1–4 mA cm$^{-2}$<br>[E]=NA<br>pH$_0$=4–10<br>V=1.8 L<br>Stirring=ND<br>T=28–60 °C<br>t=2, 5, 10 and 15 min | [Dye]$_0$=0.1 gO$_2$ L$^{-1}$ | Colour$_{rem}$=100 %<br>EC=1–2.5 kWh m$^{-3}$ | [31] |
| Direct red 23 dye<br>TW | Continuous reactor with 50 electr. | Fe – Fe | IG=0.8 cm<br>*j*=30–40 mA cm$^{-2}$<br>[E]=NA<br>pH$_0$=10<br>V=ND<br>Flow rate=0.02–0.08 L min$^{-1}$<br>T=28 °C<br>t=5 and 10 min | [Dye]$_0$=0.1 gO$_2$ L$^{-1}$<br>COD$_{0\ TW}$=0.3–0.7 gO$_2$ L$^{-1}$ | Colour$_{rem}$=100 %<br>EC=0.5–2.5 kWh m$^{-3}$<br>ElectroC=1–4 gFe<br>Colour$_{rem\ TW}$=70–90 %<br>EC$_{TW}$=0.2–0.9 kWh m$^{-3}$ | |
| Reactive Black 5 dye | BR with 4 electr. in SC (2 A + 2 C) | Fe – Fe | IG=2.5 cm<br>*j*=2–9 mA cm$^{-2}$<br>[NaCl]=0.2–3 mS cm$^{-1}$<br>pH$_0$=3–9<br>V=0.5 L<br>Stirring=120 rpm<br>t=10 min | [Dye]$_0$=0.04–0.2 g L$^{-1}$ | Colour$_{rem}$=40–100 %<br>EC=2–80 kWh kgDye$^{-1}$ | [32] |

**Table II.3. ECG studies with dye wastewaters: operating conditions and main results. (cont.)**

| Pollutant/ wastewater | Reactor design | Electr. mater. A – C | Operating conditions | Initial pollutant characteristics | Main conclusions | Ref. |
|---|---|---|---|---|---|---|
| Direct red 81 dye | BR with 2 electr. in PC | Al – Al | IG=0.5–5 cm<br>$j$=0.1–5 mA cm$^{-2}$<br>[NaCl] or [Na$_2$SO$_4$] or [NaNO$_3$] or [Na$_2$CO$_3$]=2 g L$^{-1}$<br>pH$_0$=3–11<br>V=0.5 L<br>Stirring=200 rpm<br>t=60 min | [Dye]$_0$=0.025–0.2 g L$^{-1}$ | Colour$_{rem}$=20–100 % | [33] |
| Acid Green 50 dye | BR with 2 electr. in PC | Al – Al | IG=1 cm<br>$j$=1–3 mA cm$^{-2}$<br>[NaCl]=0.5–2 g L$^{-1}$<br>pH$_0$=2–11<br>V=3 L<br>AG–gas H$_2$ bubbles<br>t=21 min | [Dye]$_0$=0.1–0.3 g L$^{-1}$ | COD$_{rem}$=87 %<br>Colour$_{rem}$>70 %<br>EC=3–13 kWh kgDye$^{-1}$<br>EC=4 kWh kgCOD$^{-1}$ | [43] |
| Reactive Blue 140 dye (RB140)<br>Disperse Red 1 dye (DR1)<br>TW | BR with 10 electr. in PC (5 A + 5 C) | Al – Al<br>Fe – Fe<br>Al – Fe | IG=0.5–1.2 cm<br>$j$=1–4 mA cm$^{-2}$<br>[E]=ND<br>pH$_0$=4–10<br>V=1.8 L<br>Stirring=150 rpm<br>T=28–60 °C<br>t=1, 2, 3, 4, 5, 10, and 15 min | [RB140]$_0$=0.1 g L$^{-1}$<br>[DR1]$_0$=0.1 g L$^{-1}$<br>COD$_{0\ TW}$=0.3–0.7 gO$_2$ L$^{-1}$ | Colour$_{rem\ RB140}$=80–100 %<br>EC$_{RB140}$=0.5–4 kWh m$^{-3}$<br>Colour$_{rem\ DR1}$=95–100 %<br>EC$_{DR1}$=0.1–4 kWh m$^{-3}$<br>COD$_{rem\ RB140+DR1}$=90 %<br>Colour$_{rem\ RB140+DR1}$=100 %<br>Colour$_{rem\ TW}$=58–97 %<br>EC$_{TW}$=0.4–1.6 kWh m$^{-3}$ | [34] |
| Acid Brown 14 dye | BR with 3 electr. in PC (2 A + 1 C) | Al – SS | IG=1 cm<br>$j$=0.1–1.6 mA cm$^{-2}$<br>[NaCl]=0.25–0.5 g L$^{-1}$<br>pH$_0$=2–10<br>V=0.5 L<br>Stirring=Slow, medium, high<br>t=25 min | [Dye]$_0$=0.03–0.1 g L$^{-1}$ | COD$_{rem}$=80–90 %<br>Colour$_{rem}$=10–100 %<br>EC=0.05 kWh m$^{-3}$<br>CE=91 % | [35] |
| | Flow discontinous reactor with 2 electr. in PC | Al – SS | IG=3 cm<br>$j$=0.3 mA cm$^{-2}$<br>[NaCl]=0.5 g L$^{-1}$<br>pH$_0$=6.4<br>V=9 L<br>Flow rate=ND<br>t=198 min | [Dye]$_0$=0.05 g L$^{-1}$ | COD$_{rem}$=64 %<br>Colour$_{rem}$=80 %<br>EC=0.04 kWh m$^{-3}$<br>CE=85 % | |
| Acid Black 52 dye (AB52)<br>Acid Yellow 220 dye (AY220)<br>TW | BR with 2 electr. in PC | Al – Al | IG=1 cm<br>$j$=1–12 mA cm$^{-2}$<br>[NaCl]=2–8 g L$^{-1}$<br>pH$_0$=2.5–10<br>V=0.25 L<br>Stirring=200 rpm<br>t=7.5 min | [Dye]$_0$=0.2–0.6 g L$^{-1}$ | Dye$_{rem\ AB52\ and\ AY220}$=46–98 %<br>Dye$_{rem\ TW}$>80 %<br>EC$_{TW}$=95–6509 kWh m$^{-3}$ | [36] |
| Reactive Orange 84 dye<br>TW | BR with 2 electr. in PC | SS – SS<br>Fe – Fe | IG=1 cm<br>$j$=7–15 mA cm$^{-2}$<br>[NaCl]=ND<br>pH$_0$=4–9<br>V=1.5 L<br>Stirring=250 rpm<br>t=10, 20, 30, 40 and 50 min | [Dye]$_0$=0.2–0.6 g L$^{-1}$<br>COD$_{0\ TW}$=0.9 gO$_2$ L$^{-1}$<br>TOC$_{0\ TW}$=0.15 g L$^{-1}$ | Dye$_{rem\ RO84}$=10–100 %<br>TOC$_{rem\ RO84}$=30–92 %<br>EC$_{RO84}$=10–60 kWh kgDye$^{-1}$<br>ElectrC$_{RO84}$=0.5–5 kg kgDye$^{-1}$<br>Op.cost$_{RO84}$=1.4–3.4 $ kg kgDye$^{-1}$<br>Op.cost$_{RO84}$=4.7–11.1 $ kg TOC$^{-1}$<br>COD$_{rem\ TW}$=80–90 %<br>TOC$_{rem\ TW}$=85–91 %<br>EC$_{TW}$=2.4 kWh m$^{-3}$<br>ElectrC$_{TW}$=0.05–0.28 kg m$^{-3}$<br>Op.cost$_{TW}$=0.8–1 $ kg COD$^{-1}$ | [37] |
| TW | BR with 4 electr. in PC (2 A + 2 C) | Al – Al<br>Fe – Fe | IG=4.5 cm<br>$j$=3–10 mA cm$^{-2}$<br>[E]=NA<br>pH$_0$=4–8<br>V=4 L<br>Stirring=250 rpm<br>t=10–40 min | COD$_0$=2 gO$_2$ L$^{-1}$<br>TOC$_0$=0.5 g L$^{-1}$ | COD$_{rem}$=69–82 %<br>TOC$_{rem}$=68–77 %<br>Op.cost=2.1–2.4 € m$^{-3}$ | [38] |
| Reactive Blue 21 dye | BR with 10 electr. in PC (5 A + 5 C) | Fe – Fe | IG=0.8 cm<br>$j$=1–4 mA cm$^{-2}$<br>[E]=NA<br>pH$_0$=8.3<br>V=1.8 L<br>Stirring=150 rpm<br>t=2, 3, 4, 5, 7, 9, 10, 12 and 15 min | [Dye]$_0$=0.5 g L$^{-1}$ | Dye$_{rem}$=83–99 %<br>COD$_{rem}$=38–90 %<br>EC=0.3–1 kWh m$^{-3}$ | [39] |
| | CFR with 2 electr. in PC | | IG=0.75 cm<br>$j$=3 mA cm$^{-2}$<br>[E]=NA<br>pH$_0$=8.3<br>V=1000 L<br>Flow rate=0.10 – 0.75 L min$^{-1}$<br>t=2, 3, 4, 5, 7, 9, 10, 12 and 15 min | [Dye]$_0$=0.5 g L$^{-1}$ | Dye$_{rem}$=99 %<br>COD$_{rem}$=90 %<br>EC=0.9 kWh m$^{-3}$ | |

**Table II.3. ECG studies with dye wastewaters: operating conditions and main results. (cont.)**

| Pollutant/ wastewater | Reactor design | Electr. mater. A – C | Operating conditions | Initial pollutant characteristics | Main conclusions | Ref. |
|---|---|---|---|---|---|---|
| Acid Red 18 dye | BR with 2 electr. in PC | Al – Al | IG=1–4 cm<br>$j$=3.5–42 mA cm$^{-2}$<br>[NaCl] or [KCl] or [$Na_2CO_3$] or [$KNO_3$]=1 g L$^{-1}$<br>$pH_0$=4–11<br>V=0.25 L<br>Stirring=ND<br>t=2–80 min | $[Dye]_0$=0.025–0.4 g L$^{-1}$ | $Dye_{rem}$=47–95 %<br>EC=7–52 kWh m$^{-3}$ | [40] |
| TW | Batch<br>(4 A + 10 C) | Al – Al | IG=1–2 cm<br>$j$ = 4–8 mA cm$^{-2}$<br>[NaCl] or [$Na_2SO_4$]=0–10 g L$^{-1}$<br>$pH_0$=5–10<br>V=10 L<br>Rotation speed=75–250 rpm<br>T=25–45 °C<br>t=10–30 min | $COD_0$=1 g$O_2$ L$^{-1}$<br>$TSS_0$=3 g L$^{-1}$ | $COD_{rem}$=91–97 %<br>$Colour_{rem}$=90–97 %<br>$TSS_{rem}$=93–98 %<br>EC=0.03–6.0 kWh m$^{-3}$<br>CE=339–349 % | [44] |
| Acid Black 194 dye (AB194)<br>TW + AB194 | BR with 2 electr. in PC | Al – Al | IG=2 cm<br>$j$=0.5–10 mA cm$^{-2}$<br>[NaCl]=3 g L$^{-1}$<br>$pH_0$=4–8.5<br>V=1 L<br>Stirring=ND<br>t=60, 120 and 300 min | $[Dye]_0$=0.05–0.2 g L$^{-1}$<br>$[TW+Dye]_0$=0.13 g L$^{-1}$<br>$COD_{0\ TW+AB194}$=1.5 g$O_2$ L$^{-1}$<br>$TOC_{0\ TW+AB194}$=0.6 g L$^{-1}$ | $COD_{rem\ AB194}$=80–90 %<br>$TOC_{rem\ AB194}$>90 %<br>$Colour_{rem\ AB194}$=100 %<br>$COD_{rem\ TW+AB194}$=60 %<br>$TOC_{rem\ TW+AB194}$=85 %<br>$Colour_{rem\ TW+AB194}$=100 %<br>$EC_{\ TW+AB194}$=0.3 kWh kgTOC$^{-1}$ | [41] |

NA – Parameter not applied to the system.
ND – Parameter not defined in the article.

### II.5.2 ELECTROCHEMICAL OXIDATION (EO) PROCESS

The application of the electrochemical oxidation (EO) process to the treatment of olive mill and dye wastewaters has been reported by numerous authors. A summary of some studies performed, the main operating conditions used and respective key conclusions are presented in Table II.4 and Table II.5 for OMW and DW, respectively in pages 37 and 39.As it can be observed, there are different anode materials investigated for the depuration of these effluents. The choice of the electrode material is guided by some properties like: high physical and chemical stability to prevent its erosion and/or corrosion or even fouling; high electrical conductivity; catalytic activity and selectivity; and low cost/life ratio wherein less costly and more durable should be preferred [2,4]. In some papers found in specialised literature, it is indicated that the way in which the electrodes are obtained will influence the efficiency of the process. Electrodes preparation techniques are like an art, aiming to improve their properties. Electrocatalytic electrodes are usually composed by metals, noble metals or substrates covered with an active layer which facilitates the transportation of electrical charge between the base metal and the electrode/electrolyte interface, turning the electrodes stable and extending their lifetime [8,50,51].

Titanium (Ti) is the mostly used inert substrate in electrochemical oxidation, due to its features: light, cheap and resistant to corrosion. This material is commonly covered by noble metals (Pt) or oxide-metals ($IrO_2$, $RuO_2$). The Ti/Pt anode was applied by Vlyssides *et al.* [52] (Table II.5) and satisfactory results were attained for the reduction of the organic load and the effluent colour of a textile dye wastewater in relatively short treatment times (COD removal=77–90 %, $BOD_5$ removal=72–89 %; Decolourisation ≈ 100 %). The colour reduction is very important for this kind of effluent. Differences in the treatment behaviour of the wastewater from total dyeing and finishing stages (TDFW) and the one coming only from the dyeing stage (DW) were explained by the different concentrations of the pollutants and the quantity of electrolyte used. In the case of olive mill wastewaters a similar pattern is followed. Belaid *et al.* [53] and Kotta *et al.* [54] (Table II.4) verified the effect of some parameters such as applied current, initial electrolyte concentration, initial effluent concentration and anode area on COD, phenolic content and colour removal. These authors reported that although moderate aromatics and colour removal values could be rapidly accomplished, complete mineralisation would require more tough conditions. OMW, normally, have solids in their composition. Its presence had practically no effect on phenols removal, but their oxidation promotes a substantial solid fraction dissolution, increasing the colour of the samples and the soluble COD, partially inhibiting the EO treatment. The evolution of the OMW and the disappearance of the polyphenols using this anode material were for the first time controlled by the cyclic voltammetry and the $^{13}$C NMR techniques by Belaid *et al* [55], confirming the total removal of phenolic compounds and the cleavage of the benzene ring.

Regarding the Ti/IrO$_2$, it is considered an active anode. The stability and activity of this electrode is based on the adequate *j* for O$_2$ evolution and on the type of molecules to be oxidised. For example, the phenolic compounds during oxidation may go through oxidative polymerisation, producing polymeric deposits which can obstruct active sites on the anode leading to its deactivation, being recommended the use of low values of *j*. The degradation of these compounds and real olive mill wastewaters occurs via partial oxidation reaction to intermediates and it seems to follow zero-order kinetics with respect to lumped organic concentration. Ecotoxicity elimination and low to moderate COD removal values were achieved to the depuration of OMW, as well as substantial decolourization and phenolic content removal. These two last parameters may be enhanced by the addition of NaCl, which stimulates the indirect bulk electrolysis beyond the direct one that already exists [56]. Comparing the previous electrode with Ti/RuO$_2$ anode material [57,58], also for the oxidation of OMW, it was observed that ruthenium was considerably more active than iridium in terms of COD, TPh, and colour removal. Despite the inferior activity of Ti/IrO$_2$, this material appears to be more stable than Ti/RuO$_2$ since, upon prolonged utilisation of pure ruthenium anodes, corrosion phenomena took place. A way to enhance ruthenium stability and surpass the previous problem can be through the use of metal oxide alloys. Ti/TiRuO$_2$ [59], Ti/RuOx-TiOx [60], Ti/RuO$_2$-Pt [61] and Sb$_2$O$_5$-doped Ti/RuOx-ZrOx [62] are examples of metal alloys using ruthenium with coated titanium substrate. Among these cases, the electrode stability has been investigated for the last two materials and the activity for longer operation times only for the Ti/RuO$_2$-Pt anode. Interesting results were attained with these modifications, being yielded greater oxidising performances and relatively long service life for DW treatments.

The EO of OMW using a Ti anode covered by a thin film of Ta-Pt-Ir alloy led to a complete decolourisation and phenol degradation for treatment times up to 60 min. Nevertheless, COD removal never exceeded 40 % even after 240 min of electrolytic treatment [63]. On the other hand, when the electrodes were composed of the same metals arranged differently, i.e. the metallic base was consisted of Ti-Ta coated with Pt-Ir, it was attained 71 % of COD removal after 480 min of electrolysis with 30 g L$^{-1}$ of NaCl and 16 V, while colour and turbidity were completely removed after short periods of time.

The simultaneous use of $FeCl_3$ (20 g $L^{-1}$) and NaCl (1 g $L^{-1}$) may contribute to the phenomenon of ECG of the phenolic wastewaters, although 86 % of COD removal efficiency is reached [64]. Along with these results, it was verified that the ecotoxicity of OMW, using luminescence marine bacteria *Vibrio fischeri* and microorganisms *Daphnia magna*, remained or increased probably because of the formation of organochlorinated by-products during the treatment.

So far, it has been discussed the application of the active anodes. These electrodes are known not to have the sufficient $O_2$ evolution overpotential to the depuration of pollutants from wastewaters. Therefore, other materials that have high $O_2$ evolution overpotential, and mainly limited to $PbO_2$, $SnO_2$ and diamond, will also be addressed in this literature overview.

$PbO_2$ and $SnO_2$ materials are relatively cheap and easy to manufacture, but a common drawback of these electrodes is their poor electrochemical stability [65]. The Ta/$PbO_2$ [66], Ti/$PbO_2$ [67] anodes achieved COD removals ranging from 67 % to 100 % (OMW and DW, respectively). Contrary to what was expected the Ti/$Sb_2O_5$-$SnO_2$ electrode only attained a maximum COD depletion of 27 % from a dye contaminant [65]. The performance of these three electrodes was compared to the boron-doped diamond (BDD) material, being revealed that a higher oxidation rate and a higher current efficiency is accomplished by it. This behaviour can be explained by the physisorbed $^{\bullet}OH$ radicals electrogenerated on the surface of the electrodes that can be more ($PbO_2$ or $Sb_2O_5$-$SnO_2$) or less (BDD) linked to it [66]. BDD is a promising anode material that can be deposited on Nb, Ti, Ta and Si substrates and that already have demonstrated good stability [68]. The large scale utilisation of Nb and Ta as substrates is not still a practical action due to their high acquisition cost. That is why most of the works are performed with Ti/BDD [65,69] and Si/BDD electrodes [67,70–78].

The BDD thin films deposited on Si substrate have shown interesting results for COD and TOC removals (> 90 % – 100 %), when applied to the purification of phenolic [70,71,78] and dye wastewaters [67,72–77,79]. The total or almost complete mineralisation of the contaminants is obtained with high current efficiencies limited only by mass transport processes [70,71,74]. Bogdanowicz *et al.* [74] presented the preparation, characterisation and use of the Si/BDD electrode with different boron doping levels to the process of EO of the Rubin F-2B dye. The different boron doping levels will influence the quantity of crystallites with a small diameter and the density of active sites on the surface, as well as the oxidation rate of the dye. Regardless the electrolyte (NaCl or $Na_2SO_4$) applied to the system, the highest doped BDD electrode was more efficient for dye removal than the less doped. Besides this difference is more pronounced for the experiments with NaCl, suggesting a dependence between the efficiency of oxidants generation and the doping level of diamond electrode.

This same anode material was studied by Abdessamad *et al.* [73] as a monopolar or bipolar electrode in two different cells to treat a solution containing Alizarin Blue Black B dye. The degradation efficiency with bipolar electrodes was 1.2 times when compared to the monopolar system, and the accumulation of large amounts of intermediates was not detected, being achieved a non toxic solution using seed germination of alfalfa (*M. sativa*) after the EO treatment.

Even though it has an expensive cost, the Nb/BDD anode has been mainly applied to the treatment of DW. For example, Zhang *et al.* [80] investigated the EO of an acrylic fiber manufacturing wastewater, employing a factorial design methodology to evaluate the statistically importance of some operating conditions, such as treatment time, flow rate, current intensity and initial COD load on the treatment efficiency. The experimental results demonstrated the suitability of the Nb/BDD anode for COD removal and also its superiority when related to a Ti/$IrO_2$-$RuO_2$ material (an active anode) either in COD depuration rate or in energy consumption. Aquino *et al.* [81] also compared the Nb/BDD with other electrode, in this case with Ti-Pt/β-$PbO_2$, in the absence or presence of chloride ions. Once again the BDD yielded much higher decolourisation and COD removal rates, at all experimental conditions. The best results were attained applying a current density of 5 mA $cm^{-2}$, at 55 °C, without NaCl addition. On the other hand, the colour removal rate increased when NaCl was added to the system, due to the greater ability of active chlorine to degrade the chromophore group of the dyes present in the effluent. This non-active anode could be an excellent option for the remediation of textile effluents [82], especially if its cost is diminished. However, if the final objective is simply to decolourise the textile effluent, the Ti-Pt/β-$PbO_2$ may still be an adequate choice taking into account the cost of BDD anodes and the possible instability of diamond films in the presence of chloride ions.

Cañizares *et al.* [71] compared the treatment of an OMW by three different AOPs: EO, ozonation and Fenton's process (Table II.4). The EO with a Si/BDD anode was highly efficient in the complete mineralisation of wastewater with less energy consumption, while with the ozonation and Fenton's processes, a great concentration of intermediates was formed and could not be further oxidised by $^{\bullet}OH$ radicals.

The literature survey demonstrates that the EO experiments with OMW and DW have been conducted in electrochemical cells at batch mode with stirring [53,56,58,61,65,66,72,74,76] or recirculation systems [52,54,55,62–64,67–71,73,75,77,79–82]. The hydrodynamics of the cell plays a fundamental role in the mass transport towards the electrodes to efficiently oxidise the organics pollutants [83]. The recircurlation configuration or flow cell is being the most widely applied arrangement to EO treatments. In this system, parallel plate/cylindrical electrodes are used, and the solution (inlet effluent) may be stored in a separated thermoregulated reservoir which will circulate through the cell by means of a pump. The reservoir temperature can be maintained by the use of a cooling jacket [59,84] or a spiral coil immersed in the liquid and connected to tap water supply to remove the heat liberated from the reaction [54,63,64]. There are cases where the cooling water jacket system is applied to the electrochemical cell [52], or even both to the feeding tank and to the cell [57]. In Cañizares *et al.* [70,71] studies, a heat exchanger was used to maintain the temperature at the desired set-point. This experimental configuration also contains a cyclone for gas-liquid separation, and a gas absorber to collect the $CO_2$ contained in the gases evolved from the reactor into sodium hydroxide.

Belaid *et al.* [53,55] carried out electrochemical experiments in a cell, which comprises two compartments separated by a cation-exchange membrane, to treat OMW. The difference between these two works is based on the way how the mixture of the solution is done. In the first situation a mechanical stirrer is used and in the second one a pump. All experiments were performed at room temperature, in order to minimise the energy consumption and no effort was made to thermoregulate the reactor.

Basha *et al.* [60] evaluated the EO of organic pollutants present in the dye-bath and wash water effluents from the textile industry in batch-stirred, batch recirculation and recycle reactor configurations. Batch recirculation provided better pollutant and COD removal results than batch-stirred system, probably due to the enhancement of ionic conductivity by bulk movement and mass transfer resistances reduction on the electrode surface. In addition, continuous systems were superior to the batch ones in energy utilization with comparable COD removal. The recycle reactor was found to be a better configuration, due to its flexibility operation. On the other hand, a single pass operation did not show relevant COD removal results among the configurations covered, probably because of the lower residence time.

**Table II.4. EO studies with phenolic mixtures and olive mill wastewaters: operating conditions and main results.**

| Pollutant/ wastewater | Reactor design | Electr. mater. A and C | Operating conditions | Initial pollutant characteristics | Main conclusions | Ref. |
|---|---|---|---|---|---|---|
| OMW | FDR with 2 electr. in PC | Ti/Ta-Pt-Ir and SS | IG=1–2 cm<br>Volt appl.=5–9V<br>[NaCl]=10–40 g $L^{-1}$<br>$pH_0$=5<br>V =10 L<br>Flow rate=24–37 L $min^{-1}$<br>t=120 min | $COD_0$=1.5–6.5 g$O_2$ $L^{-1}$<br>$TPh_0$=0.08–0.3 g $L^{-1}$ | $COD_{rem}$=5–35 %<br>$TPh_{rem}$=100 %<br>$Colour_{rem}$=100 %<br>EC=32–191 kWh kgCOD$^{-1}$ | [63] |
| OMW | Modified Grignard reactor, two compartments separated by a cation-exchange membrane | Ti/Pt | IG=0.5 cm<br>*j*=25–98 mA $cm^{-2}$<br>[E]=NA<br>$pH_0$=5.2<br>V=0.3 L<br>Stirring=ND<br>t=300 min | $COD_0$=0.8–42 g$O_2$ $L^{-1}$<br>$TOC_0$=13 g $L^{-1}$<br>$TPh_0$=0.1–6 g $L^{-1}$ | $COD_{rem}$=40–65 %<br>$TOC_{rem}$=25–45 %<br>$TPh_{rem}$=80–98 %<br>$Colour_{rem}$=90–100 %<br>EC=32–191 kWh kgCOD$^{-1}$ | [53] |
| OMW | FDR with 2 electr. in PC | Si/BDD and SS | IG=0.9 cm<br>*j*=30 mA $cm^{-2}$<br>[NaCl]=0–6 g $L^{-1}$ or<br>[$Na_2SO_4$]=0–8 g $L^{-1}$<br>$pH_0$=7<br>V=ND<br>Flow rate=2.5 L $min^{-1}$<br>Q=0–25 Ah $L^{-1}$<br>t=ND | $COD_0$=0.7 g$O_2$ $L^{-1}$ | $COD_{rem}$=100 %<br>$TOC_{rem}$=100 %<br>EC=100–300 kWh $m^{-3}$ | [70] |
| OMW | FDR with 2 electr. in PC | Ti/Ti$RuO_2$ and SS | IG=0.5 cm<br>*j*=37–62 mA $cm^{-2}$<br>[NaCl]=1–8 g $L^{-1}$<br>$pH_0$=5<br>V=ND<br>Flow rate=3 L $min^{-1}$<br>t=900–1950 min | $COD_0$=27 g$O_2$ $L^{-1}$ | $COD_{rem}$>90 %<br>$TPh_{rem}$=100 %<br>$Colour_{rem}$=100 %<br>EC=180–800 kWh $m^{-3}$<br>CE=5–70 % | [59] |
| OMW | FDR with 2 electr. in PC | Si/BDD and SS | IG=0.9 cm<br>*j*=30 mA $cm^{-2}$<br>[E]=NA<br>$pH_0$=6<br>V=ND<br>Flow rate=2.5 L $min^{-1}$<br>Q=0–80 Ah $L^{-1}$<br>t=ND | $COD_0$=3 g$O_2$ $L^{-1}$ | $COD_{rem}$=100 %<br>$TOC_{rem}$=100 %<br>EC=1200 kWh $m^{-3}$<br>CE=0–100 % | [71] |

**Table II.4. EO studies with phenolic mixtures and olive mill wastewaters: operating conditions and main results. (cont.)**

| Pollutant/ wastewater | Reactor design | Electr. mater. A and C | Operating conditions | Initial pollutant characteristics | Main conclusions | Ref. |
|---|---|---|---|---|---|---|
| OMW | FDR with 2 electr. in PC | Ti-Ta/Pt-Ir and SS | IG=ND<br>Volage appl.=14–24 V<br>[NaCl]=15–30 g L$^{-1}$ or<br>[Na$_2$SO$_4$]=20–30 g L$^{-1}$ or<br>[Na$_2$SO$_4$]=20 g L$^{-1}$ +<br>[FeCl$_3$]=1 g L$^{-1}$<br>pH$_0$=5 and 9<br>V$_{\text{water}}$=10–30 L<br>V$_{\text{OMW}}$=10–15 L<br>Flow rate=0.25 L min$^{-1}$<br>t=300 and 480 min | COD$_0$=16–38 gO$_2$ L$^{-1}$ | COD$_{\text{rem}}$=7–86 %<br>Colour$_{\text{rem}}$=98 %<br>EC=10–150 kWh kgCOD$^{-1}$ | [64] |
| OMW | FDR with 2 electr. in PC | Ti/Pt and SS | IG=ND<br>*j*=78–313 mA cm$^{-2}$<br>Salinity= 1–4%<br>pH$_0$=5<br>V=10 L<br>Flow rate=60 L min$^{-1}$<br>t=180 min | COD$_0$=12–47 gO$_2$ L$^{-1}$<br>TPh$_0$=0.2–0.7 g L$^{-1}$ | COD$_{\text{rem}}$=0–60 %<br>TPh$_{\text{rem}}$=30–100 %<br>Colour$_{\text{rem}}$=0–100 %<br>EC=61–514 kWh kgTPh$^{-1}$ | [54] |
| OMW | FDR with 8 electr. in PC (4 A + 4 C) | Ti/RuO$_2$ and Ti/RuO$_2$ | IG=0.8 cm<br>*j*=25–135 mA cm$^{-2}$<br>[NaCl]=58–292 g L$^{-1}$<br>pH$_0$=5<br>V=0.4 L<br>Flow rate=0.07–0.47 L min$^{-1}$<br>T=7–40 °C<br>t=480 min | COD$_0$=41 gO$_2$ L$^{-1}$<br>TPh$_0$=0.2 g L$^{-1}$ | COD$_{\text{rem}}$=63–99 %<br>TPh$_{\text{rem}}$=100 %<br>EC=5–27 kWh kgCOD$^{-1}$ | [57] |
| p-Coumaric acid<br>caffeic acid<br>cinnamic acid<br>phenol<br>OMW | BR with 2 electr. in PC | Ti/IrO$_2$ and SS | IG–ND<br>*j*=50 mA cm$^{-2}$<br>[HClO$_4$]=100 g L$^{-1}$ or<br>[NaCl]=0–1.5 g L$^{-1}$<br>pH$_0$=4<br>V=0.1 L<br>Stirring=ND<br>T=60–80 °C<br>Q=6–120 Ah L$^{-1}$<br>t=ND | COD$_0$=1.3 gO$_2$ L$^{-1}$<br>TPh$_0$=0.1 g L$^{-1}$ | COD$_{\text{rem phenolic acids}}$=5–60 %<br>TOC$_{\text{rem phenolic acids}}$=18–50 %<br>TPh$_{\text{rem phenolic acids}}$=60–93 %<br>CE$_{\text{phenolic acids}}$=1–11 %<br>COD$_{\text{rem OMW}}$=20–60 %<br>TPh$_{\text{rem OMW}}$=10–100 %<br>Colour$_{\text{rem OMW}}$=5–100 %<br>EC=72 kWh kgCOD$^{-1}$ | [56] |
| OMW- | BR with 2 electr. in PC | Ti/RuO$_2$ and SS | IG=ND<br>*j*=15–30 mA cm$^{-2}$<br>[NaCl]=0–1.2 g L$^{-1}$ or<br>[Na$_2$SO$_4$]=0–2.8 g L$^{-1}$ or<br>[FeCl$_3$]=0–0.3 g L$^{-1}$<br>pH$_0$=4<br>V=0.1 L<br>Stirring=ND<br>T=80 °C<br>t=360–1440 min | COD$_0$=0.3–1.2 gO$_2$ L$^{-1}$<br>TOC$_0$=0.07–0.60 g L$^{-1}$ | COD$_{\text{rem}}$=7–71 %<br>TOC$_{\text{rem}}$=20–67 %<br>TPh$_{\text{rem}}$=81–96 %<br>Colour$_{\text{rem}}$>91 %<br>EC=4–39 kWh kgCOD$^{-1}$<br>CE=5–52 % | [58] |
| OMW | Modified Grignard reactor, 2 compartments separated by a cation-exchange membrane | Ti/Pt | IG=0.5 cm<br>*j*=25–35 mA cm$^{-2}$<br>[E]=NA<br>pH$_0$=5.2<br>V=0.5 L<br>Flow rate=0.002 L min$^{-1}$<br>t=120, 240 and 600 min | COD$_0$=65 gO$_2$ L$^{-1}$<br>TOC$_0$=25 g L$^{-1}$ | COD$_{\text{rem}}$=40–55 %<br>TOC$_{\text{rem}}$=40–50 %<br>Colour$_{\text{rem}}$=70–90 %<br>CE=81–95 % | [55] |
| Ferulic acid (FA) | FDR with 2 electr. in PC | Si/BDD and SS | IG=1 cm<br>*j*=4–30 mA cm$^{-2}$<br>[Na$_2$SO$_4$]=7 g L$^{-1}$ or<br>[Na$_2$SO$_4$]=7 g L$^{-1}$ +<br>[NaCl]=1 g L$^{-1}$ or<br>[Na$_2$SO$_4$]=7 g L$^{-1}$ +<br>[NaCl]=2 g L$^{-1}$<br>pH$_0$=2–8<br>V=ND<br>Flow rate=5 L min$^{-1}$<br>T=20–50 °C<br>t=210 min | [FA]$_0$=0.1–0.3 gO$_2$ L$^{-1}$ | FA$_{\text{rem}}$=100 %<br>COD$_{\text{rem}}$>90 %<br>TOC$_{\text{rem}}$=100 %<br>EC=9.5–97 kWh kgCOD$^{-1}$<br>CE=81–95 % | [78] |
| TOW | BR with 2 electr. in PC | Ta/PbO$_2$ or BDD and SS | IG=ND<br>*j*=20–100 mA cm$^{-2}$<br>[Na$_2$SO$_4$]=14 g L$^{-1}$<br>pH$_0$=10.5<br>V=ND<br>Stirring=ND<br>t=360–480 min | COD$_0$=6 gO$_2$ L$^{-1}$ | Ta/PbO$_2$<br>COD$_{\text{rem}}$>67 %<br>EC=5–70 kWh m$^{-3}$<br><br>BDD<br>COD$_{\text{rem}}$=100 %<br>EC=5–45 kWh m$^{-3}$ | [66] |

NA – Parameter not applied to the system.
ND – Parameter not defined in the article.

**Table II.5. EO studies with dye wastewaters: operating conditions and main results.**

| Pollutant/ Wastewater | Reactor design | Electr. mater. A and C | Operating conditions | Initial pollutant characteristics | Main conclusions | Ref. |
|---|---|---|---|---|---|---|
| Total dyeing and finishing stages (TDFW)<br>Wastewater only from dyeing stage (DW) | FDR with 2 electr. in PC | Ti/Pt and SS | IG=ND<br>$j$=ND<br>$[NaCl]=10–40\ g\ L^{-1}$<br>$pH_0=5$<br>V=ND<br>Flow rate=10 L min$^{-1}$<br>t=18 min | $COD_{0\ TDFW}=1.3\ gO_2\ L^{-1}$<br>$COD_{0\ DW}=3.3\ gO_2\ L^{-1}$ | $COD_{rem}=77–90$ %<br>$BOD_{5\ rem}=72–89$ %<br>$Colour_{rem}=100$ % | [52] |
| Orange II (O. II)<br>Reactive Red HE-3B (RRHE-3B) | BR with 2 electr. in PC | Ti/BDD or $Ti/Sb_2O_5-SnO_2$ and SS | IG=ND<br>$j=20\ mA\ cm^{-2}$<br>$[Na_2SO_4]=2\ g\ L^{-1}$<br>$pH_0=1–12$<br>V=0.025 L<br>Flow rate=10 L min$^{-1}$<br>T=10–50 °C<br>$Q=0–6\ Ah\ L^{-1}$<br>t=ND | $[O.\ II]_0 = 1.12\ g\ L^{-1}$<br>$[RRHE\text{-}3B]_0=0.75\ g\ L^{-1}$ | Ti/BDD<br>$COD_{rem\ O.\ II}=91\%$<br>$COD_{rem\ RRHE\text{-}3B}=95$ %<br>$CE_{O.\ II}=100$ %<br>$CE_{\ RRHE\text{-}3B}=90$ %<br>$Ti/Sb_2O_5-SnO_2$<br>$COD_{rem\ O.\ II}=27$ %<br>$COD_{rem\ RRHE\text{-}3B}=22$ % | [65] |
| Cibacron Yellow HW200<br>Cycafiw Yellow FLN250<br>Cycafiw Navy-blue F2B<br>Monozol Black SGRN<br>Monozol Blue BRF-150<br>Monozol RedF3B150<br>Monozol T-blue HFG<br>Monozol Yellow F3R150<br>Procion Blue HE-RD<br>Reactive Blue R<br>Reactive Red HE-7B<br>Samafix Red S-3B<br>Samafix Yellow S-3R<br>Unicion Green S6B<br>Unicion Red S-3BF80 | BR with 2 electr. in PC | Ti/BDD and SS | IG=ND<br>$j=10\ mA\ cm^{-2}$<br>$[Na_2SO_4]=2\ g\ L^{-1}$<br>$pH_0=5–7$<br>V=0.025 L<br>Flow rate=10 L min$^{-1}$<br>T=30 °C<br>$Q=0–4\ Ah\ L^{-1}$<br>t=ND | $[Dye]_0 =1.0\ g\ L^{-1}$ | $COD_{rem}=89–96$ %<br>$EC=9–18\ kWh\ m^{-3}$<br>CE=51–90 % | |
| Methyl Red | FDR with 2 electr. in PC | $Ti/PbO_2$ or Si/BDD and SS | IG=0.5 cm<br>$j=10–40\ mA\ cm^{-2}$<br>$[NaClO_4]=61\ g\ L^{-1}$<br>$pH_0=3–7$<br>V=ND<br>Flow rate=1.7–4.0 L min$^{-1}$<br>t=210–780 min | $[Dye]_0=0.1\ g\ L^{-1}$ | $Dye_{rem\ Ti/PbO2}=100$ %<br>$COD_{rem\ Ti/PbO2}=100$ %<br>$EC_{Ti/PbO2}=48–204\ kWh\ m^{-3}$<br>$CE_{Ti/PbO2}=1–25$ %<br>$COD_{rem\ Si/BDD}=100$ %<br>$EC_{Si/BDD}=30\ kWh\ m^{-3}$<br>$CE_{\ Si/BDD}=1–60$ % | [67] |
| Alphazurine A dye | BR with 2 electr. in PC | Si/BDD and Zr | IG=ND<br>$j=30–90\ mA\ cm^{-2}$<br>$[Na_2SO_4]=71\ g\ L^{-1}$<br>$pH_0$=ND<br>V=ND<br>Stirring=100–400 rpm<br>T=25–60 °C<br>t=240–600 min | $[Dye]_0=0.50–0.76\ g\ L^{-1}$ | $COD_{rem}>90$ %<br>$Colour_{rem}=100$ %<br>$EC=29–141\ kWh\ kgCOD^{-1}$<br>CE=5–45 % | [72] |
| Acrylic fiber manufacturing wastewater (AFMW) | FDR with 2 electr. in PC | Nb/BDD or $Ti/IrO_2-RuO_2$ and Nb/Pt | IG=1 cm<br>$j=6–13\ mA\ cm^{-2}$<br>[E]=NA<br>$pH_0=6$<br>V=0.2 L<br>Flow rate=0.4–0.6 L min$^{-1}$<br>t=60–120 min | $COD_0=0.4–0.7\ gO_2\ L^{-1}$ | $COD_{rem\ Nb/BDD}=39–80$ %<br>$EC_{Nb/BDD}=79\ kWh\ m^{-3}$<br>$CE_{Nb/BDD}=100$ %<br>$COD_{rem\ Ti/IrO2\text{-}RuO2}=18$ %<br>$EC_{Ti/IrO2\text{-}RuO2}=65\ kWh\ m^{-3}$ | [80] |
| TW | FDR with 2 electr. in PC | Nb/BDD or Ti-Ta/β-$PbO_2$ | IG=ND<br>$j_{Nb/BDD}=5–20\ mA\ cm^{-2}$<br>$j_{Ti\text{-}Ta/\beta\text{-}PbO2}=15–45\ mA\ cm^{-2}$<br>$[Na_2SO_4]=14\ g\ L^{-1}$ +<br>$[NaCl]=0–1.5\ g\ L^{-1}$<br>$pH_0=8$<br>V=0.4 L<br>Flow rate=6 L min$^{-1}$<br>$Q=0–9\ Ah\ L^{-1}$<br>t=ND | $COD_0=0.3\ gO_2\ L^{-1}$ | $COD_{rem\ Nb/BDD}=80–100$ %<br>$Colour_{rem\ Nb/BDD}>90$ %<br>$EC_{Nb/BDD}=30\ kWh\ m^{-3}$<br>$COD_{rem\ Ti\text{-}Ta/\beta\text{-}PbO2}=20–70$ %<br>$Colour_{rem\ Ti\text{-}Ta/\beta\text{-}PbO2}=20–70$ %<br>$EC_{Ti\text{-}Ta/\beta\text{-}PbO2}>30\ kWh\ m^{-3}$ | [81] |

**Table II.5. EO studies with dye wastewaters: operating conditions and main results. (cont.)**

| Pollutant/ wastewater | Reactor design | Electr. mater. A and C | Operating conditions | Initial pollutant characteristics | Main conclusions | Ref. |
|---|---|---|---|---|---|---|
| Dye-bath wastewater (DBW) | BR with 2 electr. in PC | Ti/RuOx-TiOx and SS | IG=ND<br>*j*=10–50 mA cm$^{-2}$<br>[E]=NA<br>pH$_0$=9<br>V=0.3–0.5 L<br>Stiring=ND<br>t=480 min | COD$_{0\ DBW}$=5.8 gO$_2$ L$^{-1}$<br>BOD$_{0\ DBW}$=0.18 g L$^{-1}$ | COD$_{rem\ DBW}$=47–100 %<br>EC$_{DBW}$=8–50 kWh kgCOD$^{-1}$<br>CE$_{DBW}$=29 – 89 % | [60] |
| Dye-bath wastewater (DBW)<br>Wash water (WW) | FDR with 3 electr. in PC (1 A + 2 C) | | IG=1.3 cm<br>*j*=25–50 mA cm$^{-2}$<br>[E]=NA<br>pH$_0$=8–9<br>V=1.5 L<br>Flow rate=0.3–1.7 L min$^{-1}$<br>t=360 min | COD$_{0\ DBW}$=5.8 gO$_2$ L$^{-1}$<br>BOD$_{0\ DBW}$=0.18 g L$^{-1}$ | COD$_{rem\ DBW}$=80–94 %<br>EC$_{DBW}$=2–5 kWh kgCOD$^{-1}$<br>COD$_{rem\ WW}$=80–91 %<br>EC$_{DBW}$=84–97 kWh kgCOD$^{-1}$ | |
| Wash water (WW) | FDR with 3 electr. in PC (1 A + 2 C) | | IG=1.3 cm<br>*j*=50 mA cm$^{-2}$<br>[E]=NA<br>pH$_0$=8<br>V=2 L<br>Flow rate=1.3 L min$^{-1}$<br>t=30 min | COD$_{0\ WW}$=0.56 gO$_2$ L$^{-1}$<br>BOD$_{0\ WW}$=0.03 g L$^{-1}$ | COD$_{rem\ WW}$=53–76 %<br>EC$_{DBW}$=12–40 kWh kgCOD$^{-1}$ | |
| TW | FDR with 2 electr. in PC | Si/BDD and Ti | IG=1 cm<br>*j*=20–60 mA cm$^{-2}$<br>[Na$_2$SO$_4$]=0 or 5 g L$^{-1}$<br>pH$_0$=10<br>V=1 L<br>Flow rate=3–7 L min$^{-1}$<br>T=25–60 °C<br>t=240–1380 min | COD$_0$=0.65 gO$_2$ L$^{-1}$ | COD$_{rem}$>90 %<br>Colour$_{rem}$=50–100 %<br>EC=75–500 kWh m$^{-3}$<br>CE=5–90% | [79] |
| Alizarin Blue Black B | FDR with 2 electr. in PC (Cell 1)<br><br>FDR with 3 compartments and 4 electr. (2 bipolar Si/BDD and 2 monopolar Si/BDD) (Cell 2) | Si/BDD and SS | IG=0.1 (Cell 2) or 0.3 (Cell 1) cm<br>*j*=20–80 mA cm$^{-2}$<br>[Na$_2$SO$_4$]=14 g L$^{-1}$<br>pH$_0$=2–8<br>V=ND<br>Flow rate=ND<br>t=180 min | [Dye]$_0$= 0.0024 g L$^{-1}$cm$^{-2}$ | COD$_{rem\ Cell\ 1}$=65 %<br>Colour$_{rem\ Cell\ 1}$=88–94 %<br>CE$_{Cell\ 1}$=0–38 %<br>COD$_{rem\ Cell\ 2}$=100 %<br>Colour$_{rem\ Cell\ 2}$=77–100 %<br>EC$_{Cell\ 2}$=83 kWh kgCOD$^{-1}$<br>CE$_{Cell\ 2}$=10–100 % | [73] |
| Rubin F-2B dye | BR with 2 electr. in PC | Si/BDD$_2$ or Si/BDD$_{10}$ and SS | IG=1 cm<br>*j*=2.5 or 5 mA cm$^{-2}$<br>[Na$_2$SO$_4$]=7 g L$^{-1}$ or [NaCl]=7 g L$^{-1}$<br>pH$_0$=6<br>V=0.1 L<br>Stirring=ND<br>Q=0–0.6 Ah L$^{-1}$<br>t=ND | [Dye]$_0$=0.02 g L$^{-1}$ | Colour$_{rem\ Si/BDD\ 2}$=31–75 %<br>Colour$_{rem\ Si/BDD\ 10}$=36–95 % | [74] |
| Malachite green oxalate | FDR with 2 electr. in PC | Si/BDD and SS | IG=0.3 cm<br>*j*=16–48 mA cm$^{-2}$<br>[NaNO$_3$]=8 g L$^{-1}$ or [NaCl]=6 g L$^{-1}$ or [Na$_2$SO$_4$]=14 g L$^{-1}$<br>pH$_0$=3–7<br>V=1 L<br>Flow rate=1.8–2.6 L min$^{-1}$<br>t=180 min | [Dye]$_0$=0.02 g L$^{-1}$ | Dye$_{rem}$=100 %<br>COD$_{rem}$=40–90 %<br>Colour$_{rem}$=100 %<br>EC=7.5–25 kWh m$^{-3}$<br>CE=2.5–60 % | [75] |
| Novacron Yellow C-RG | BR with 2 electr. in PC | BDD or Ti/Pt and Ti | IG=ND<br>*j*=10–50 mA cm$^{-2}$<br>[Na$_2$SO$_4$]=36 g L$^{-1}$ + [NaCl]=0–2.3 g L$^{-1}$<br>pH$_0$=ND<br>V=0.35 L<br>Stirring=400 rpm<br>t=30–540 min | [Dye]$_0$=0.2–0.6 g L$^{-1}$ | TOC$_{rem\ BDD}$=71–90 %<br>Colour$_{rem\ BDD}$=90–100 %<br>EC$_{BDD}$=0.95–45 kWh m$^{-3}$<br>TOC$_{rem\ Ti/Pt}$=17–34 %<br>Colour$_{rem\ Ti/Pt}$=90–100 %<br>EC$_{Ti/Pt}$=1.6–35 kWh m$^{-3}$ | [76] |
| Acid Orange 7 | BR with 2 electr. in PC | Ti/RuO$_2$-Pt and SS | IG=1 cm<br>*j*=10–30 mA cm$^{-2}$<br>[Na$_2$SO$_4$]=0.7–7 g L$^{-1}$ or [NaCl]=0.06–0.58 g L$^{-1}$<br>pH$_0$=2.1–11<br>V=ND<br>AG=ND<br>t=90–450 min | [Dye]$_0$=0.03–0.10 g L$^{-1}$ | Dye$_{rem}$=10–100 %<br>TOC$_{rem}$=80 %<br>EC$_{BDD}$=71–89 kWh kgDye$^{-1}$ | [61] |

**Table II.5. EO studies with dye wastewaters: operating conditions and main results. (cont.)**

| **Pollutant/ wastewater** | **Reactor design** | **Electr. mater. A and C** | **Operating conditions** | **Initial pollutant characteristics** | **Main conclusions** | **Ref.** |
|---|---|---|---|---|---|---|
| Rhodamine B | FDR with 2 electr. in PC | Si/BDD and SS | IG=0.9 cm<br>$j$=15–120 mA $cm^{-2}$<br>[$Na_2SO_4$] or [$HClO_4$] or [$H_3PO_4$] or [NaCl]=1 g $L^{-1}$<br>$pH_0$=ND<br>V=1 L<br>Flow rate=0.4 L $min^{-1}$<br>Q=0–150 Ah $L^{-1}$<br>t=ND | $[Dye]_0$=0.1 g $L^{-1}$ | $TOC_{rem}$=100 % | [77] |
| Indigo carmine | FDR with 2 electr. in PC | $Sb_2O_5$-doped Ti/$RuO_x$-$ZrO_x$ | IG=ND<br>$j$=5–20 mA $cm^{-2}$<br>[NaCl]=3 g $L^{-1}$<br>$pH_0$=ND<br>V=ND<br>Flow rate=1–5 L $min^{-1}$<br>t=60–480 min | $[Dye]_0$=0.3 g $L^{-1}$ | $Dye_{rem}$=90–100 %<br>$COD_{rem}$=20–90 %<br>EC=38–79 kWh $m^{-3}$ | [62] |
| Acid Red 211 | FDR with 2 electr. in PC | Nb/BDD and SS | IG=0.5 cm<br>$j$=4–16 mA $cm^{-2}$<br>[$HClO_4$]=10 g $L^{-1}$ or<br>[$H_2SO_4$]=10 g $L^{-1}$ or<br>[$Na_2SO_4$]=7 g $L^{-1}$<br>$pH_0$=ND<br>V=0.5 L<br>Flow rate=0.2 L $min^{-1}$<br>t=60 min | $[Dye]_0$=0.1 g $L^{-1}$ | $TOC_{rem\ HClO4}$=32–47 %<br>$EC_{HClO4}$=2.1–12.1 kWh $m^{-3}$<br>$CE_{HClO4}$=10–40 %<br>$TOC_{rem\ H2SO4}$=31–53 %<br>$EC_{H2SO4}$=2.2–11.1 kWh $m^{-3}$<br>$CE_{H2SO4}$=10–40 %<br>$TOC_{rem\ Na2SO4}$=43–70 %<br>$EC_{Na2SO4}$=2.0–13.1 kWh $m^{-3}$<br>$CE_{Na2SO4}$=5–40 % | [82] |
| Reactive Black 5 | BR with 2 electr. in PC | Ti/BDD | IG=ND<br>$j$=10–100 mA $cm^{-2}$<br>[$K_2SO_4$]=17 g $L^{-1}$ or<br>$pH_0$=2.5<br>V=0.43 L<br>Stirring=250 rpm<br>t=120 and 480 min | $[Dye]_0$=0.05 g $L^{-1}$ | $Dye_{rem}$=30–100 %<br>$TOC_{rem}$=2–100 %<br>$Colour_{rem}$=100 %<br>CE=2.5–22.5 % | [69] |

NA – Parameter not applied to the system.
ND – Parameter not defined in the article.

## II.6 CONCLUSIONS

The electrocoagulation (ECG) and electrochemical oxidation (EO) processes seem to be adequate solutions to treat OMW and DW. Even if some operating conditions do not lead to the results needed to comply with the legislation with respect to direct discharge in a determined receptor medium, these pre-treated effluents are generally already in position to move to biological depuration, since the non-biodegradable and toxic compounds can be partially degraded in those technologies. For this reason, seeking for the best way to improve treatment efficiency regarding both mineralisation and biodegradability enhancement is a matter of particular industrial and academic concern.

As aforementioned, several works have been published in the ECG field for the depuration of olive mill wastewaters (OMW) and dye wastewaters (DW) using mainly Al and Fe electrodes. However, literature is still scarce in what regards this process using other sacrificial anodes to depurate complex synthetic mixtures and real wastewaters. In the case of the EO, different less costly anodes should be tested in order to avoid the dependence on the expensive BDD electrodes. The study of other reactor configurations able to improve efficiency while reducing the energy consumtpion is also missing for both electrochemical processes.

Definitely, it is very challenging to predict the success of an electrode material or to define its lifetime without extended studies under realistic process conditions. In this ambit, in the present thesis, preliminary ECG and EO batch experiments were mainly undertaken with simulated effluents (phenolic or dyeing solutions) aiming to screen new suitable anode materials to depurate the contaminants. The influence of the key operating parameters was investigated in what concerns the process performance at different levels as follows: total phenol content (TPh), colour, chemical oxygen demand (COD), biochemical oxygen demand ($BOD_5$) and high performance liquid chromatography (HPLC). The toxic effect of the treated effluents is also an important concern since the initial contaminant degradation by-products may present higher impact. Thus, traditional acute toxicity bioassays based on *Vibrio fischeri* luminescence were applied. However, to infer about human health impact innovative methodologies were addressed based on neuronal studies by determining the formation of neuronal reactive oxygen species (ROS) due to the contact with both raw and treated effluents. Furthermore, two reactor configurations were also explored, batch-stirred and flow discontinuous reactors. This last arrangement was tested using one cell or two cells in series. In a final stage, real wastewaters (olive mill and dye) were treated by these two electrochemical technologies.

The selection of the best depuration approach for each effluent had into account not only the amount of organic compounds reduced, but also the biodegradability and toxicity achieved, attempting to reach a cost-effective method that probably go through the integration of the electrochemical techniques with the biological ones.

## REFERENCES

[1] Martínez-Huitle C, Ferro S (2006) Electrochemical oxidation of organic pollutants for the wastewater treatment: direct and indirect processes. Chem. Soc. Rev. 35(12): 1324–1340.

[2] Anglada Á, Urtiaga A, Ortiz I (2009) Contributions of electrochemical oxidation to waste-water treatment: fundamentals and review of applications. J. Chem. Technol. Biotechnol. 84: 1747–1755.

[3] Rajeshwar K, Ibanez JG (1997) Environmental Electrochemistry: Fundamentals and Applications in Pollution Sensors, Elsevier Science & Technology Books, 1–776.

[4] Brillas E, Martínez-Huitle CA (2015) Decontamination of wastewaters containing synthetic organic dyes by electrochemical methods. An up dated review. Appl. Catal. B: Environ. 166–167: 603–643.

[5] Chen G. (2004) Electrochemical technologies in wastewater treatment. Sep. Purif. Technol. 38: 11–41.

[6] Holt PK, Barton GW, Mitchell CA (2005) The future for electrocoagulation as a localised water treatment technology. Chemosphere 59: 355–367.

[7] Un UT, Koparal AS, Ogutveren UB (2009) Electrocoagulation of vegetable oil refinery wastewater using aluminum electrodes. J. Environ. Manage. 90: 428–433.

[8] Comninellis C (1994) Electrochemical oxidation of organic pollutants for wastewater treatment. Stud. Environ. Sci. 59: 77–102.

[9] Rajeshwar K, Ibanez J, Swain G (1994) Electrochemistry and the environment. J. Appl. Electrochem. 24: 1077–1091.

[10] Jüttner K, Galla U, Schmieder H (2000) Electrochemical approaches to environmental problems in the process industry. Electrochim. Acta 45: 2575–2594.

[11] Panizza M, Cerisola G (2009) Direct and mediated anodic oxidation of organic pollutants. Chem. Rev. 109: 6541–6569.

[12] Comninellis C (1994) Electrocatalysis in the electrochemical conversion/combustion of organic pollutants. Electrochim. Acta 39: 1857–1862.

[13] Cañizares P, Domínguez J, Rodrigo M, Villaseñor J, Rodríguez J (1999) Effect of the current intensity in the electrochemical oxidation of aqueous phenol wastes at an activated carbon and steel anode. Ind. Eng.Chem. Res. 38: 3779–3785.

[14] Brillas E, Cabot P, Casado J (2003) Electrochemical Methods for Degradation of Organic Pollutants in Aqueous Media in M. A. Tarr (ed.). Chemical Degradation Methods for Wastes and Pollutants: Environmental and Industrial Applications, 210–273.

[15] Brillas E, Sirés I, Oturan M (2009) Electro-Fenton process and related electrochemical technologies based on Fenton’s reaction chemistry. Chem. Rev. 109(12): 6570–6631.

[16] Kobya M, Bayramoglu M, Eyvaz M (2007) Techno-economical evaluation of electrocoagulation for the textile wastewater using different electrode connections. J. Hazard. Mater. 148: 311–318.

[17] Martínez-Huitle CA, Brillas E (2009) Decontamination of wastewaters containing synthetic organic dyes by electrochemical methods: A general review. Appl. Catal. B: Environ. 87: 105–145.

[18] Comninellis C, Pulgarin C (1993) Electrochemical oxidation of phenol for wastewater treatment using $SnO_2$ anodes. J. Appl. Electrochem. 23: 108–112.

[19] Chen G, Betterton E, Arnold R (1999) Electrolytic oxidation of trichloroethylene using a ceramic anode. J. Appl. Electrochem. 29: 961–970.

[20] Tahar N, Savall A (1999) A comparison of different lead dioxide coated electrodes for the electrochemical destruction of phenol. J. New Mater. Electrochem. Syst. 2: 19–26.

[21] Muff J (2010) Applications of Electrochemical Oxidation for Degradation of Aqueous Organic Pollutants. Aalborg University, 1–99.

[22] Adhoum N, Monser L (2004) Decolourization and removal of phenolic compounds from olive mill wastewater by electrocoagulation. Chem. Eng. Process. 43: 1281−1287.

[23] Inan H, Dimoglo A, Şimşek H, Karpuzcu M (2004) Olive oil mill wastewater treatment by means of electro-coagulation. Sep. Purif. Technol. 36: 23−31.

[24] Ün UT, Uğur S, Koparal AS, Öğütveren ÜB (2006) Electrocoagulation of olive mill wastewaters. Sep. Purif. Technol. 52: 136−141.

[25] Hanafi F, Assobhei O, Mountadar M (2010) Detoxification and discoloration of Moroccan olive mill wastewater by electrocoagulation. J. Hazard. Mater. 174: 807−812.

[26] Coskun T, İlhan F, Demir NM, Debik E, Kurt U (2012) Optimization of energy costs in the pretreatment of olive mill wastewaters by electrocoagulation. Environ. Technol. 33: 801−807.

[27] Kobya M, Can OT, Bayramoglu M (2003) Treatment of textile wastewaters by electrocoagulation using iron and aluminum electrodes. J. Hazard. Mater. B100: 163–178.

[28] Can OT, Kobya M, Demirbas E, Bayramoglu M (2006) Treatment of the textile wastewater by combined electrocoagulation. Chemosphere 62: 181–187.

[29] Kobya M, Demirbas E, Can OT, Bayramoglu M (2006) Treatment of levafix orange textile dye solution by electrocoagulation. J. Hazard. Mater. B132: 183–188.

[30] Ahlawat R, Srivastava VC, Mall ID, Sinha S (2008) Investigation of the Electrocoagulation Treatment of Cotton Blue Dye Solution using Aluminium Electrodes. Clean 36 (10–11): 863–869.

[31] Phalakornkule C, Polgumhang S, Tongdaung W (2009) Performance of an Electrocoagulation Process in Treating Direct Dye: Batch and Continuous Upflow Processes. Int. Sch. Sci. Res. Innov. 3(9): 494–499.

[32] Şengil İA, Özacar M (2009) The decolorization of C.I. Reactive Black 5 in aqueous solution by electrocoagulation using sacrificial iron electrodes J. Hazard. Mater. 161: 1369–1376.

[33] Aoudj S, Khelifa A, Drouiche N, Hecinia M, Hamitouche H (2010) Electrocoagulation process applied to wastewater containing dyes from textile industry. Chem. Eng. Process. 49: 1176–1182.

[34] Phalakornkule C, Polgumhang S, Tongdaung W, Karakat B, Nuyut T (2010) Electrocoagulation of blue reactive, red disperse and mixed dyes, and application in treating textile effluent. J. Environ. Manage. 91: 918–926.

[35] Parsa JB, Vahidian HR, Soleymani AR, Abbasi M (2011) Removal of Acid Brown 14 in aqueous media by electrocoagulation: Optimization parameters and minimizing of energy consumption. Desalination 278: 295–302.

[36] Pajootan E, Arami M, Mahmoodi NM (2012) Binary system dye removal by electrocoagulation from synthetic and real colored wastewaters. J. Taiwan Inst. Chem. Eng. 43 (2012) 282–290.

[37] Yuksel E, Eyvaz M, Gurbulak E (2013) Electrochemical Treatment of Colour Index Reactive Orange 84 and Textile Wastewater by Using Stainless Steel and Iron Electrodes. Environ. Prog. Sustain. Energy 32(1): 60–68.

[38] Kobya M, Gengec E, Sensoya MT, Demirbasc E (2014) Treatment of textile dyeing wastewater by electrocoagulation using Fe and Al electrodes: optimisation of operating parameters using central composite design. Color. Technol. 130: 226–235.

[39] Ardhan N, Ruttithiwapanich T, Songkasiri W, Phalakornkule C (2015) Comparison of performance of continuous-flow and batch electrocoagulators: A case study for eliminating reactive blue 21 using iron electrodes. Sep. Purif. Technol.146: 75–84.

[40] Khosravi R, Hazrati S, Fazlzadeh M (2016) Decolorization of AR18 dye solution by electrocoagulation: sludge production and electrode loss in different current densities, Desalination Water Treat. 57(31): 14656–14664.

[41] Vidal J, Villegas L, Peralta-Hernández JM, González RS (2016) Removal of Acid Black 194 dye from water by electrocoagulation with aluminum anode, J. Environ. Sci. Health A 51(4): 289–296.

[42] Essadki AH, Bennajah M, Gourich B, Vial Ch, Azzi M, Delmas H (2008) Electrocoagulation/ electroflotation in an external-loop airlift reactor—Application to the decolorization of textile dye wastewater: A case study. Chem. Eng. Process 47: 1211–1223.

[43] El-Ashtoukhy E-SZ, Amin NK (2010) Removal of acid green dye 50 from wastewater by anodic oxidation and electrocoagulation—A comparative study. J. Hazard. Mater. 179: 113–119.

[44] Naje AS, Chelliapan S, Zakaria Z, Abbas SA (2016) Electrocoagulation using a rotated anode: A novel reactor design for textile wastewater treatment. J. Environ. Manage. 176: 34–44.

[45] Merzouk B, Gourich B, Sekkic A, Madanid K, Vial Ch, Barkaoui M (2009) Studies on the decolorization of textile dye wastewater by continuous electrocoagulation process. Chem. Eng. J. 149: 207–214.

[46] Mollah MYA, Schennach R, Parga JR, Cocke DL (2001) Electrocoagulation (EC)—science and applications. J. Hazard. Mater. B84: 29–41.

[47] Chen X, Chen G, Yue PL (2000) Separation of pollutants from restaurant wastewater by electrocoagulation. Sep. Purif. Technol. 19: 65–76.

[48] Vasudevan S, Lakshmi J, Sozhan G (2013) Electrochemically assisted coagulation for the removal of boron from water using zinc anode. Desalination 310: 122−129.

[49] Khoufi S, Feki F, Sayadi S (2007) Detoxification of olive mill wastewater by electrocoagulation and sedimentation processes. J. Hazard. Mater. 142: 58–67.

[50] Klamklang S, Vergnes H, Senocq F, Pruksathorn K, Duverneuil P, Damronglerd S. (2006) Restaurant Wastewater Treatment by Electrochemical Oxidation: Preparation and Characterization of $SnO_2$ Electrode by MOCVD in Technology and Innovation for Sustainable Development Conference. Khon Kaen University, 455–460.

[51] Klamklang S (2007) Restaurant Wastewater Treatment by Electrochemical Oxidation in Continuous Process. Institut National Polytechnique de Toulouse, 1–205.

[52] Vlyssides AG, Papaioannou D, Loizidoy M, Karlis PK, Zorpas AA (2000) Testing an electrochemical method for treatment of textile dye wastewater. Waste Manage. 20: 569–574.

[53] Belaid C, Kallel M, Khadhraou M, Lalleve G, Elleuch B, Fauvarque JF (2006) Electrochemical treatment of olive mill wastewaters: Removal of phenolic compounds and decolourization. J. App. Electrochem. 36: 1175–1182.

[54] Kotta E, Kalogerakis N, Mantzavinos D (2007) The effect of solids on the electrochemical treatment of olive mill effluents. J. Chem. Technol. Biotechnol. 82: 504–511.

[55] Belaid C, Khadraoui M, Mseddi S, Kallel M, Elleuch B, Fauvarque JF (2013) Electrochemical treatment of olive mill wastewater: Treatment extent and effluent phenolic compounds monitoring using some uncommon analytical tools J. Environ. Sci. 25(1): 220–230.

[56] Chatzisymeon E, Dimou A, Mantzavinos D, Katsaounis A (2009) Electrochemical oxidation of model compounds and olive mill wastewater over DSA electrodes: 1. The case of Ti/$IrO_2$ anode. J. Hazard. Mater. 167: 268–274.

[57] Un UU, Altay U, Koparal AS, Ogutveren UB (2008) Complete treatment of olive mill wastewaters by electrooxidation. Chem. Eng. J. 2008, 139: 445−452.

[58] Papastefanakis N, Mantzavinos D, Katsaounis A (2010) DSA electrochemical treatment of olive mill wastewater on Ti/$RuO_2$ anode. J. Appl. Electrochem. 40: 729–737.

[59] Panizza M, Cerisola G (2006) Olive mill wastewater treatment by anodic oxidation with parallel plate electrodes. Water Res. 40: 1179–1184.

[60] Basha CA, Sendhil J, Selvakumar KV, Muniswaran PKA, Lee CW (2012) Electrochemical degradation of textile dyeing industry effluent in batch and flow reactor systems. Desalination 285: 188–197.

[61] Zhang C, Liu L, Li W, Wua J, Rong F, Fu D (2014) Electrochemical degradation of Acid Orange II dye with boron-doped diamond electrode: Role of operating parameters in the absence and in the presence of NaCl. J. Electroanal. Chem. 726: 77–83.

[62] Palma-Goyes RE, Vazquez-Arenas J, Torres-Palma RA, Ostos C, Ferraro F, González I (2015) The abatement of indigo carmine using active chlorine electrogenerated on ternary $Sb_2O_5$-doped Ti/$RuO_2$-$ZrO_2$ anodes in a filter-press FM01-LC reactor. Electrochim. Acta 174: 735–744.

[63] Gotsi M, Kalogerakis N, Psillakis E, Samaras P, Mantzavinos D (2005) Electrochemical oxidation of olive oil mill wastewaters. Water Res. 39: 4177–4187.

[64] Giannis A, Kalaitzakis M, Diamadopoulos E (2007) Electrochemical treatment of olive mill wastewater. J. Chem. Technol. Biothecnol. 671: 663−671.

[65] Chen X, Chen G, Gao F, Yue PL (2003) High-Performance Ti/BDD Electrodes for Pollutant Oxidation. Environ. Sci. Technol. 37: 5021–5026.

[66] Gargouri B, Gargouri OD, Khmakhem I, Ammar S, Abdelhèdi R, Bouaziz M (2017) Chemical composition and direct electrochemical oxidation of table olive processing wastewater using high oxidation power anodes. Chemosphere 166: 363–371.

[67] Panizza M, Cerisola G (2008) Removal of colour and COD from wastewater containing acid blue 22 by electrochemical oxidation. J Hazard Mater 153: 83–88.

[68] Fryda M, Herrmann D, Schafer L, Klages CP, Perret A, Haenni W, Comninellis C, Gandini, D. (1999) Properties of diamond electrodes for wastewater treatment. New Diam. Front C Technol. 9: 229–240.

[69] Vasconcelos VM, Ponce-de-León C, Nava JL, Lanza MRV (2015) Electrochemical degradation of RB-5 dye by anodic oxidation, electro-Fenton and by combining anodic oxidation-electro-Fenton in a filter-press flow cell. J. Electroanal. Chem. 765: 179–187.

[70] Cañizares P, Martínez L, Paz R, Sáez C, Lobato J, Rodrigo MA. (2006) Treatment of Fenton-refractory olive oil mill wastes by electrochemical oxidation with boron-doped diamond anodes. J. Chem. Technol. Biotechnol. 81: 1331–1337.

[71] Cañizares P, Lobato J, Paz R, Rodrigo MA, Sáez C (2007) Advanced oxidation processes for the treatment of olive-oil mills wastewater. Chemosphere 67: 832–838.

[72] Bensalah N, Alfaro MAQ, Martínez-Huitle CA (2009) Electrochemical treatment of synthetic wastewaters containing Alphazurine A dye. Chem. Eng. J. 149: 348–352.

[73] Abdessamad N, Akrout H, Hamdaoui G, K Elghniji, Ksibi M, Bousselm L (2013) Evaluation of the efficiency of monopolar and bipolar BDD electrodes for electrochemical oxidation of anthraquinone textile synthetic effluent for reuse. Chemosphere 93: 1309–1316.

[74] Bogdanowicz R, Fabiańska A, Golunski L, Sobaszek M, Gnyba M, Ryl J, Darowicki K, Ossowski T, Janssens SD, Haenen K, Siedlecka EM (2013) Influence of the boron doping level on the electrochemical oxidation of the azo dyes at Si/BDD thin film electrodes. Diam. Relat. Mat. 39: 82–88.

[75] Guenfoud F, Mokhtari M, Akrout H (2014) Electrochemical degradation of malachite green with BDD electrodes: Effect of electrochemical parameters. Diam. Relat. Mater. 46: 8–14.

[76] Rocha JHB, Gomes MMS, Santos EV, Moura ECM, Silva DR, Quiroz MA, Martínez-Huitle CA (2014) Electrochemical degradation of Novacron Yellow C-RG using boron-doped diamond and platinum anodes: Direct and Indirect oxidation. Electrochim. Acta 140: 419–426.

[77] Araújo DM, Sáez C, Martínez-Huitle CA, Cañizares P, Rodrigo MA (2015) Influence of mediated processes on the removal of Rhodamine with conductive-diamond electrochemical oxidation. Appl. Catal. B: Environ. 166–167: 454–459.

[78] Ellouze S, Panizza M, Barbucci A, Cerisola G, Mhiri T, Elaoud SC (2016) Ferulic acid treatment by electrochemical oxidation using a BDD anode. J. Taiwan Inst. Chem. Eng. 59: 132–137.

[79] Martínez-Huitle C.A, Santos EV, DM Araújo, Panizza M (2012) Applicability of diamond electrode/anode to the electrochemical treatment of a real textile effluent. J. Electroanal. Chem. 674: 103–107.

[80] Zhang C, Wang J, Murakami T, Fujishima A, Fu D, Gu Z (2010) Influence of cations during Orange-II degradation on boron-doped diamond electrode. J. Electroanal. Chem. 638: 91–98.

[81] Aquino JM, Pereira GF, Rocha-Filho RC, Bocchi N, Biaggio SR (2011) Electrochemical degradation of a real textile effluent using boron-doped diamond or b-$PbO_2$ as anode. J. Hazard. Mater. 192: 1275–1282.

[82] Uranga-Flores A, Rosa-Júarez C, Gutierrez-Granados S, Moura DC, Martínez-Huitle CA, Peralta Hernández JM (2015) Electrochemical promotion of strong oxidants to degrade Acid Red 211: Effect of supporting electrolytes. J. Electroanal. Chem. 738: 84–91.

[83] Ferreira MB, Rocha JHB, Melo JV, Martinez-Huitle CA, Alfaro MAQ (2013) Use of a Dual Arrangement of Flow Cells for Electrochemical Decontamination of Aqueous Solutions Containing Synthetic Dyes. Electrocatal. 4: 274–282.

[84] Panizza M, Cerisola G (2007) Electrocatalytic materials for the electrochemical oxidation of synthetic dyes. Appl. Catal. B: Environ. 75: 95–101.

# PART B. ELECTROCOAGULATION PROCESS

# III. TREATMENT OF A SYNTHETIC PHENOLIC MIXTURE BY ELECTROCOAGULATION USING Al, Cu, Fe, Pb, AND Zn AS ANODE MATERIALS

AS Fajardo, RC Martins and RM Quinta-Ferreira

CIEPQPF−Centro de Investigação em Engenharia dos Processos Químicos e Produtos da Floresta; GERST−Group on Environment, Reaction, Separation and Thermodynamics; Department of Chemical Engineering, Faculty of Sciences and Technology, University of Coimbra, Pólo II, Rua Sílvio Lima, 3030-790 Coimbra, Portugal.

*Industrial & Engineering Chemistry Research 53 (2014) 18339–18345*

## ABSTRACT

Phenolic compounds constitute an important source of pollution causing severe environmental threats in countries that produce olive oil. The efficiency of five metal anodes (Al, Cu, Fe, Pb and Zn) was tested in an electrocoagulation system, in order to purify a phenolic-simulated effluent. Among them, Zn anode was found to be promising, because 86 % of the total phenolic content and 49 % of chemical oxygen demand was removed after 180 min of treatment within the operational conditions used (pH=3.0, current intensity=0.4 A, [NaCl]=1.5 g $L^{-1}$, intergap distance=1.0 cm, effective anodic area=33.5 $cm^2$). The biodegradability of the mixture was assessed by measuring the ratio $BOD_5$/COD before and after each treatment, as well as the ecological impact through *Vibrio fischeri* bacteria. The electrical energy consumption varied between 8−14 kWh $m^{-3}$. The results also point out that during the treatment process, beyond the electrocoagulation route, the electrooxidation of organic compounds is also expected to occur.

## III.1 INTRODUCTION

Olive mill wastewaters (OMW) are mainly produced in Mediterranean countries and contain phenolic mixtures in their composition. These compounds incorporate a significant contaminant load due to their high toxicity, refractory character, and high stability in water. These factors do not allow an efficient application of biological treatments so that the recourse for chemical purification methods is requested before the effluents' discharge into the aquatic environment [1]. Electrochemical processes appear as interesting alternatives to conventional systems to treat wastewaters, allowing a great efficacy in the removal of organic compounds. Among these technologies is electrocoagulation (ECG), an easy system to operate, requiring low equipment costs, not needing high temperature and pressure such as incineration and supercritical oxidation systems [2–4]. In the ECG system, sacrificial anodes dissolve into the aquatic medium leading to the generation of metal ions which are hydrolysed to produce metal hydroxide ions. The solubility of the complexes formed is dependent on pH and ionic strength. The cationic metallic species are responsible for particles destabilisation (charge neutralisation), leading to the formation of flocs particles, which will have the power to precipitate or enmesh (sweep coagulation) dissolved contaminants. The in situ generation of coagulants has the advantage of reducing the quantity of chemical reagents introduced to the system, or even avoiding the addition of those substances [3,5−7].

The ECG process has begun to be successfully applied to the treatment of olive mill wastewaters with the aid of anodes of aluminium or iron material. Through the common use of these material electrodes, two mechanisms (acid and alkaline conditions) have been suggested for the production of metal hydroxide for each anode (Equations (III.1)–(III.6)) [2,3,5−10].

Al anode:

$$\mathrm{Al} \rightarrow \mathrm{Al}^{3+} + 3\mathrm{e}^- \tag{III.1}$$

In solution:

with alkaline conditions

$$\mathrm{Al}^{3+} + 3\mathrm{OH}^- \rightarrow \mathrm{Al(OH)}_3 \tag{III.2}$$

with acidic conditions

$$\mathrm{Al}^{3+} + 3\mathrm{H_2O} \rightarrow \mathrm{Al(OH)}_3 + 3\mathrm{H}^+ \tag{III.3}$$

Fe anode:

$$\mathrm{Fe} \rightarrow \mathrm{Fe}^{2+} + 2\mathrm{e}^- \tag{III.4}$$

In solution:

with alkaline conditions

$$\mathrm{Fe^{2+} + 2OH^- \rightarrow Fe(OH)_2} \quad \textbf{(III.5)}$$

with acidic conditions

$$\mathrm{4Fe^{2+} + O_2 + 2H_2O \rightarrow 4Fe^{3+} + 4OH^-} \quad \textbf{(III.6)}$$

At the cathode occurs the production of hydrogen gas which allows the formed flocks to float (Equation (III.7), Al material and Equation (III.8), Fe material) [2,3,5].

$$\mathrm{3H_2O + 3e^- \rightarrow \frac{3}{2}H_2 + 3OH^-} \quad \textbf{(III.7)}$$

$$\mathrm{2H_2O + 2e^- \rightarrow H_2 + OH^-} \quad \textbf{(III.8)}$$

The performed experiments revealed that the ECG usage is a viable solution that could be combined with biologic processes to achieve a high quality effluent and become a cost-effective pretreatment. In addition, ECG is a faster and more effective process when compared to biological methods alone [2,5].

The removal capacity of the ECG systems ranges between 59−76 % for COD, 70−91 % for polyphenols, and 70−95 % for dark colour, after 20−45 min. The specific energy consumption (SEC) was found to be around 2−3 kWh kg COD$^{-1}$ removed [2,3,5−9]. Additionally, if the OMW is treated without adjusting its initial pH, the final pH may be almost neutral which allows it to be directly treated by biological methods [2,5,7]. The main parameters evaluated and taken into consideration in the ECG process are the pH, type, and concentration of the pollutant, and kind and concentration of the electrolyte, as well as current density. This last parameter regulates the coagulant dosage rate, the bubble production rate and size, flock stability, and agglomerate size [2−5].

Un *et al.*[3] studied the effect of the introduction and concentration of a coagulant-aid (polyalminum chloride, PAC) as well as the application of $Na_2SO_4$ as supporting electrolyte. The addition of the PAC had the objective of achieving particle instability, rapid aggregation velocity, and growth in the particle size (larger and heavier flocks). When $Na_2SO_4$ was used, more coagulant was delivered to the medium. The increasing concentration of these two substances led to the improvement of COD removal efficiency and consequently the decrease of the energy consumption. Ün *et al.* [9] tested the application of different concentrations of $H_2O_2$ and PAC and verified that the ECG without the oxidant and coagulant-aid is not too efficient to the treatment of OMW. The best results were achieved using 2.3 % $H_2O_2$ and 0.5 g L$^{-1}$ PAC.

García−García *et al.* [6] examined different electrode materials position [Al(+)/Fe(−), Al(−)/Fe(+), Al(+)/Al(−), or Fe(+)/Fe(−)] and operational conditions. The electrode set Al(−)/Fe(+) with an intergap distance of 0.6 cm and a current density of 250 A m$^{-2}$ led to the greatest depuration rate. Coskun *et al.*

[7] identified a cost-effective operation for the ECG process, pointing out that parameters such as current density and contact time must be optimised.

The ECG process used in the previous works is considered a primary method, since the organic content of the resulting effluent is not low enough to meet discharge standards for receiving bodies. Therefore, a synergetic combination of ECG and electrooxidation (EO) has been tried by Linares-Hernández *et al.* [10], where the ECG quickly removed colloidal and suspended particles, as well as many charged species after 30‒45 min. Then, EO oxidised the remaining organics, because it is very effective in eliminating stable organic compounds as reflected in a higher removal of COD and $BOD_5$. EO alone requires at least 21 h to achieve optimal removal values, which is not feasible on a practical level. The integration of these two processes can eliminate the COD, $BOD_5$, colour, and turbidity parameters within a practicable time of 120 min.

The main objective of this research was to compare the effect of Al, Fe, Cu, Pb, and Zn anode materials on the treatment of a mixture of six phenolic acids usually present in olive mill wastewaters. To the best of our knowledge, this is the first time that a comparison of these electrodes is reported in literature to the depuration of this kind of wastewater. The assessment of their activity is given in terms of total phenolic content (TPh), chemical oxygen demand (COD) and biochemical oxygen demand ($BOD_5$) removal as well as effluent toxicity parameters. Furthermore, the dissolution of electrodes into the aquatic medium and the process electrical energy consumption will also be discussed.

## III.2 EXPERIMENTAL SECTION

### III.2.1 WASTEWATER PREPARATION AND ECG PROCEDURE

The synthetic effluent encompasses 100 mg $L^{-1}$ of each one of the following phenolic acids to simulate real olive mill wastewaters: 3,4,5-trimethoxybenzoic, 4-hydroxybenzoic, gallic, protocatechuic, trans-cinnamic, and veratric acids. No further purification was applied to them before use. The conductivity of the mother-solution was evaluated using a Consort C863 measurer, and 1.5 g of NaCl was added in order to promote a higher conductivity to the solution (±3.0 mS $cm^{-1}$). The electrochemical oxidation process was performed in a Perspex batch stirred reactor (Figure III.1) at 300 rpm, under controlled temperature (20 °C), and at atmospheric pressure, during 180 min. In each experiment, the reactor was filled with 1000 mL of the model solution and the flat anode and cathode were placed parallel with a distance of 10 mm, linked to a DC power supply HY3010 Kaise (I=0.4 A) [11,12]. Al, Cu, Fe, Pb, and Zn anodes, as well as a stainless steel cathode were used with an effective area of 33.5 $cm^2$ (6.4 cm × 2.5 cm × 0.1 cm). Samples were periodically withdrawn and immediately filtered for further analysis. The pH was measured using a HANNA pH meter and adjusted using NaOH at 3 M or $H_2SO_4$ at 2 M whenever necessary.

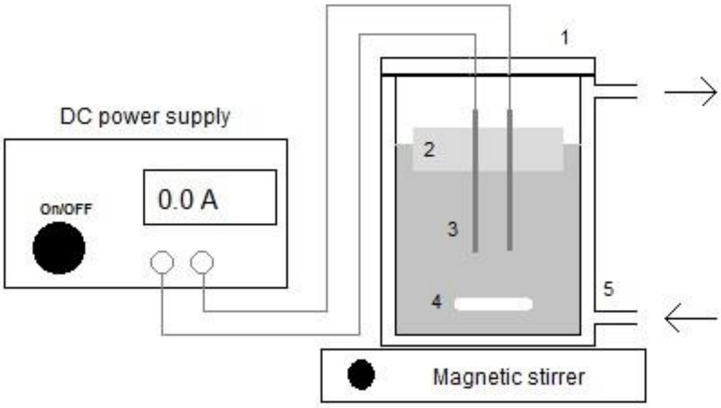

**Figure III.1. EGC experimental setup. (1-Reactor of perspex, 2-Floater, 3-Electrodes, 4-Magnetic bar stirrer, 5-Double wall for water recirculation).**

### III.2.2 ANALYTICAL TECHNIQUES.

Total phenol content (TPh) was measured in terms of gallic acid (GA) by the Folin−Ciocalteau method, which is described elsewhere [13]. COD and $BOD_5$ were determined according to the Standard Methods [14]. COD was analysed with the closed reflux procedure using potassium dichromate as oxidant, and $BOD_5$ was obtained by the difference between the dissolved oxygen before and after a microorganism population from garden soil being in contact with the pollutants samples during 5 days. The toxicity of the effluent was assessed through the LUMIStox equipment (Dr. Lange, Germany) according to the standard method DIN/EN/ISO 11348-2, which is based on light inhibition of the *Vibrio fischeri* bacteria. The ecotoxicity levels were expressed as EC values which represent the concentration of a sample that inhibits 20 % ($EC_{20}$) and 50 % ($EC_{50}$) of bacteria light emission.

Some experiments were randomly run in duplicate or triplicate and the samples withdrawn were analysed in duplicate in order to minimise the experimental error. The deviations between runs were always lower than 10 %, 8 %, 20 %, and 2 % for TPh, COD, $BOD_5$, and toxicity determinations, respectively.

## III.3 RESULTS AND DISCUSSION

The synthetic effluent which tends to simulate the real olive mill wastewaters encompasses a high organic charge and has an acidic character (pH 3), as depicted in Table III.1.

**Table III.1. Main characteristics of the synthetic effluent.**

| Characteristics | Values |
|---|---|
| TPh (mgGA/L) | 365±13 |
| COD (mgO2 L-1) | 1065±20 |
| BOD5 (mgO2 L-1) | 353±20 |
| BOD5/COD | 0.33 |
| EC20 (%) | 10±2 |
| EC50 (%) | 35±2 |
| pH | 3.0 |

According to Portuguese environmental laws (Decree Law Nº 236/98, 1st of August), an effluent should not have COD and $BOD_5$ values higher than 150 and 40 $mgO_2$ $L^{-1}$, respectively. Normally, a wastewater is considered as totally biodegradable when the $BOD_5$/COD ratio is higher than 0.4 [15]. This model solution shows a ratio of 0.3, which is closer to that limit. However, OMW presents a seasonal character with flow and composition varying during the year which would demand for constant biomass acclimation. The toxicity of the effluent was evaluated by testing the inhibition of luminescent bacteria, enabling the estimation of the $EC_{20}$ and $EC_{50}$ values. The model solution displayed a high toxicity as a dilution involving only 10 % and 36 % of the pollutants sample led to 20 % and 50 % of the *Vibrio Fischeri*'s population light production decay respectively, demonstrating its high negative impact over life forms. Therefore, to treat this solution, five different kinds of metals (Al, Cu, Fe, Pb and Zn) were used as anodes in the ECG process.

### III.3.1 TOTAL PHENOLIC CONTENT

Wastewaters containing high phenolic content have low biodegradability, justifying the assessment of the TPh removal parameter over time (Figure III.2) by the Folin-Ciocalteau method.

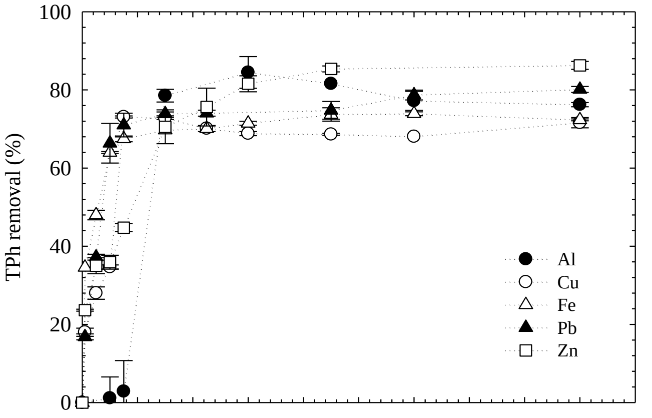

**Figure III.2. TPh removal over time (I=0.4 A, Electrode area=33.5 cm$^2$, Intergap=10 mm, [NaCl]=1.5 g L$^{-1}$).**

As can be observed there was a quick phenolic depletion in the first 15 min for the experiments with Cu, Fe and Pb anodes, stabilising thereafter. In the case of the Al and the Zn anode, such stabilisation was achieved after 30 min. This latter achievement could be due to the capacity of the aluminium to create stable oxide films around the anode. Moreover, zinc material has a low corrosion rate and a good resistance to corrosion what will take more time to allow the dissolution of metals to the liquid [16]. At the end of 180 min of reaction, the Zn anode removed 86 % of TPh, followed by Pb (80 %), Al (76 %) and Fe (72 %) ≈ Cu (72 %).

### III.3.2 CHEMICAL OXYGEN DEMAND

COD removal along the depuration time is displayed in Figure III.3. The degradation rates for this parameter were not so marked as those for the TPh removal.

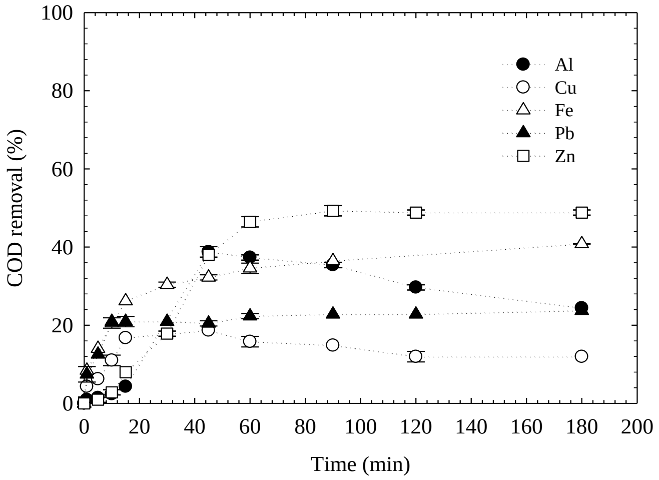

**Figure III.3. COD removal over time (I=0.4 A, Electrode area=33.5 cm$^2$, Intergap=10 mm, [NaCl]=1.5 g L$^{-1}$).**

These COD depletion results suggest that there might be the formation of by-products contributing to the still significant final COD values. Table III.2 supports what was aforementioned once, although a relatively high TPh removal (72–86 %) could be achieved after 180 min of reaction, only a maximum of 49 % of COD was abated within this time. If just the phenomenon of ECG occurred the COD removal should be similar to the depletion of the initial-phenolic compounds, since this process is based on the precipitation and/or adsorption of pollutants.

**Table III.2. TPh and COD removal with electrocoagulation after 180 min of reaction for each anode material (I=0.4 A, Electrode area=33.5 cm$^2$, Intergap=10 mm, [NaCl]=1.5 g L$^{-1}$).**

| Experiment (Metal) | TPh Removal (%) | COD removal (%) |
|---|---|---|
| Al | 76.2 | 24.4 |
| Cu | 71.6 | 12.0 |
| Fe | 72.3 | 40.8 |
| Pb | 80.1 | 23.7 |
| Zn | 86.3 | 48.8 |

In ECG, NaCl, besides working as electrolyte, may be involved in chemical reactions such as the oxidation of the $\mathrm{Cl}^-$ (Equation (III.9)) [2,17,18].

$$2\mathrm{Cl}^- + 2\mathrm{e}^- \rightarrow \mathrm{Cl}_2 \qquad \textbf{(III.9)}$$

For pHs higher than 3–4, the chlorine produced may suffer a dismutation reaction (Equation (III.10)–(III.11)) [2,18].

$$\mathrm{Cl}_2 + \mathrm{H}_2\mathrm{O} \rightarrow \mathrm{HOCl} + \mathrm{H}^+ + \mathrm{Cl}^- \qquad \textbf{(III.10)}$$

$$\mathrm{HOCl} \rightarrow \mathrm{ClO}^- + \mathrm{H}^+ \qquad \textbf{(III.11)}$$

The hypochlorous acid (HOCl) and hypochlorite ion ($\mathrm{ClO}^-$) can decompose organic matter because of their high oxidative potentials, leading to complete mineralisation of pollutants, or as in this particular case the formation of intermediary compounds [18].

The highest COD depletion obtained, after 180 min of reaction, was about 49 % with the Zn anode, which was closely followed by the Fe electrode with a final value of around 41 %. Lower COD degradations were attained for Pb (24 %) and Cu anodes (12 %). During the Al and Cu anode experiments, a maximum efficacy of the COD removal value was achieved after 45 min of reaction, with 39 % and 19 %, respectively. These values decreased until the end of the reaction time to 24 % and 12 %. This reduction could be possible due to the depletion of chlorine in-situ generation in the reactor and thus the availability of the hypochlorite to oxidise organic compounds [18]. On other hand, the COD removal results may also be sustained by the pH of the medium, since the formation of the metal hydroxide depends on this parameter and the kind of the metal that it is used. Figure III.4 shows the changes in the pH medium during the reaction time.

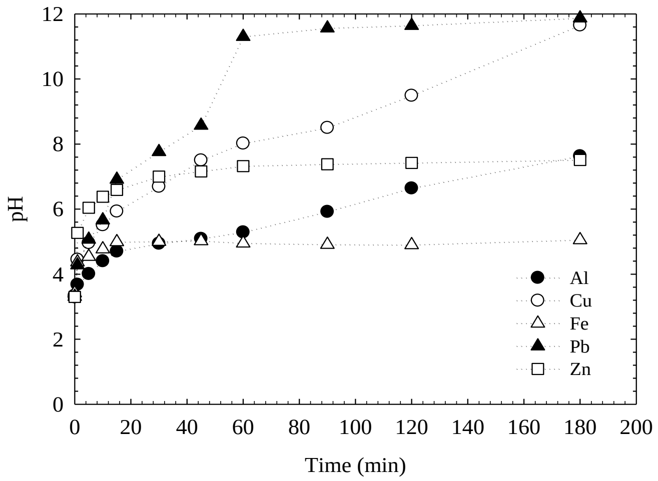

**Figure III.4. pH medium followed over time (I=0.4 A, Electrode area=33.5 cm$^2$, Intergap=10 mm, [NaCl]=1.5 g L$^{-1}$).**

As it can be observed, pH increased for all studied anode materials, as a consequence of the generation of the hydroxyl anions from the water reduction at the surface of the cathode. Different profiles for the pH mixture were obtained due to the diverse anodic and cathodic reactions that take place in the reactor for each anode analysed. During the wastewater treatment with the Zn anode, the pH medium increased from 3.0 to around 7.0, after 15 min of operation. The reactions when zinc is used as anode are presented in Equations (III.12)–(III.14) [19].

At the anode $$\mathrm{Zn} \rightarrow \mathrm{Zn}^{2+} + 2\mathrm{e}^- \quad \textbf{(III.12)}$$

At the cathode $$2\mathrm{H_2O} + 2\mathrm{e}^- \rightarrow \mathrm{H_2} + 2\mathrm{OH}^- \quad \textbf{(III.13)}$$

In the solution $$\mathrm{Zn}^{2+} + 2\mathrm{OH}^- \rightarrow \mathrm{Zn(OH)_2} \quad \textbf{(III.14)}$$

Thermodynamically and according to the Zn-$H_2O$ *Pourbaix* diagram provided by Pourbaix [19], the precipitation of zinc hydroxide would only be substantial at pH ≥ 8.6 [20]. Nevertheless, the interfacial pH-increase during the ECG process favoured the $Zn(OH)_2$ formation resulting in higher removal efficiency at pH 7 [19]. This diagram provides thermodynamic information that occurs on the surface of the metals in a given environment under specific conditions of pH and potential in equilibrium becoming fundamental the knowledge of the characteristics of the electrolyte.

The experiment with the Al anode had its best removal value (39 %) after 45 min of treatment and the medium pH was 5.1. pH and temperature directly contribute to the type of hydrolysed Al species found in solution. At 25 °C and in high acidic solutions (pH ≈ 3), the monomeric Al predominates and there is the possibility that the aluminium electrode may be covered by a layer of $Al(OH)_3$ [3,22]. Khemis et al. [23] stated that this substance is amphoteric, slightly soluble between pH 6–7 and its predominance occurs at the pH near 6.5. In the present work when pH is very acidic the COD removal is not perceived, then it increased to 39 % and after pH 6 is reached, the removal efficacy decreased suggesting that the precipitated hydroxide metal may tend to dissolve in liquid affecting adversely the performance of the process. Generally, this fact takes place as the medium turns extremely acidic or alkaline as observed by Inan *et al.* [8] and Ün *et al.* [9].

In the Al and Zn experiments, after 5 min of oxidation, the colour of the effluent began to turn cloudy and 10 min later, a white layer of foam (the respective metal hydroxides) appeared at the water surface. This situation may be due to an electroflotation process, in which bubbles can be formed by the release of gases produced at the cathode ($H_2$) or at the anode ($O_2$ and $Cl_2$) that will promote solids suspension [24].

For Cu experiments, the pH medium arose over time to pH ≈ 12. It seems that the release of $Cu^{2+}$ to the liquid occurred until pH 7; after this point the $Cu(OH)_2$ was the predominant substance (pH 8–10) which corresponds to the pH of the highest COD removal, at 45 min of reaction. After this time, the pH continues to increase, but on the other hand the COD removal decreases which suggests that at high pHs it is possible to occur the dissolution of some metal species ($\mathrm{HCuO_2^-}$ and $\mathrm{CuO_2^{2-}}$) to the liquid, revealing that these chemical species are not being favourable to the removal of organic compounds [20]. Another explanation to the COD abatement can be due to the formation of a green layer on the surface of the anode that may promote a greater resistance to the passage of electric current and thus making it difficult the dissolution of metal ions into the bulk medium, decreasing the degradation of organic compounds. Comparing the Cu anode to the others, this experiment was the only one where the potential between the electrodes greatly increased, reaching the maximum value of the equipment for the same current supply (I=0.4 A), meaning that the resistance to the current flow was very high. In accordance to the previous anode materials, the pH medium also increased over time with Pb. Lead in acidic solutions and atmospheric pressure is apt to decompose water through hydrogen evolution. This reaction is very slow due to the large hydrogen overpotential of lead. In these conditions, metallic lead is dissolved by acidic medium and $Pb^{2+}$ ions are formed. These ions when linked to with the $\mathrm{OH^-}$ ions from water decomposition generate insoluble $Pb(OH)_2$. According to literature [21], the minimum solubility of this hydroxide is within pH 10.3–11.2. As can be seen in Figure III.3, the highest COD removal was obtained after 10 min of treatment with 21 %, remaining almost constant thereafter. Contrary to what was expected, through Figure III.4, it is possible to realise that at that time pH was only 5.7. This may be supported by the presence of other species in solution that promote a higher pollutants removal with lower pHs [20, 21]. The reactions for Pb system are presented in Equations (III.15) – (III.17).

At the anode
$$\mathrm{Pb \rightarrow Pb^{2+} + 2e^-} \qquad \textbf{(III.15)}$$

At the cathode
$$\mathrm{2H_2O + 2e^- \rightarrow H_2 + 2OH^-} \qquad \textbf{(III.16)}$$

In the solution
$$\mathrm{Pb^{2+} + 2H_2O \rightarrow Pb(OH)_2 + 2H^+} \qquad \textbf{(III.17)}$$

Regarding the Fe experiment, after 10 min of treatment, 21 % of COD was removed at pH 4.8 which is in agreement with the value obtained by Inan *et al.* [8] when a pH medium of 4.6 was used with this anode material. These authors refer that under this pH the formation of $Fe(OH)_2$ is relatively low giving poorer COD removals. In the present work, during the process the formation of foam at the surface of the solution near the cathode (due to $H_2$ production) was observed and the colour of the solution turned to a green-black colour. This last phenomena may be due to the decomposition of a dark deposit (iron oxide) formed on the surface of the cathode, which leads to the production of green-black flocs ($Fe(OH)_2$). At the end of the process, there was the settling down of the iron oxide and the final COD decrease was 41 %.

### III.3.3 ELECTRODES DISSOLUTION

Metals content in the effluent plays an important role since their concentration and pH define possible chemical species present in the aqueous solution. The Faradays's law (Equation (III.18)) makes possible to calculate the maximum amount of metals electrochemically produced [4,25].

$$\mathrm{m}_{\text{metal theoretical}}\ (\mathrm{g}) = \frac{\mathrm{I\ t\ M}_w}{\mathrm{z\ F}} \qquad \textbf{(III.18)}$$

where I is the applied current (A), t is the treatment time (s), $M_w$ is the molar mass of the electrode material ($M_{w\,Al}$=26.98 g $mol^{-1}$, $M_{w\,Cu}$=63.55 g $mol^{-1}$, $M_{w\,Fe}$=55.85 g $mol^{-1}$, $M_{w\,Pb}$=207.20 g $mol^{-1}$ and $M_{w\,Zn}$=65.38 g $mol^{-1}$), z is the valency of ions of the electrode material ($z_{Al}$=3, $z_{Cu}$=2, $z_{Fe}$=2, $z_{Pb}$=3 and $z_{Zn}$=2), and F is Faraday's constant (96485 C $mol^{-1}$).

Theoretically, according to Faraday's law, the following values were obtained for metals dissolution: Al–0.4 g, Cu–1.4 g, Fe–1.3 g, Pb–4.6 g and Zn–1.5 g. Indeed, our experimental results confirm these values (Table III.3), with a greater difference for Al, where the theoretical amount of anodic dissolution was 68 % higher than for the real ECG application. This phenomenon is thought to be attributed to pitting corrosion, especially in the presence of chlorine ions [25]. The dissolution rate affects the life of the electrodes and the effective electrode consumption may be reduced or increased from this theoretical value depending on the wastewater characteristics and operational conditions [6].

The ions concentration in solution was determined in the final sample of each experiment by atomic absorption and these values were afterwards compared to the legal limits of discharge into aquatic medium (Table III.3). Among the experiments performed, just the concentration of the Al ion was below the reference values. The Cu and Zn ions detected after the treatment were 3 times above the established legal limit. In addition, there was a relatively high release of metal ions from the other metals proposed as anodes (Fe and Pb ions). For those materials, concentrations 14 and 79 times higher than the legal limit were detected. In order to prevent a second source of pollution, due to the dissolution of hazardous metal ions, an integration of technologies to recover and remove these substances is suggested to be accomplished before the depurated effluent is discharged into aquatic environment. As can be observed the removal of the metal ions from the system was by solid form, solid precipitation or foam formed.

**Table III.3. Theoretical and experimental values of anode materials dissolution, as well as leaching results for each metal after 180 min and their correspondent legal limit of discharge into aquatic environment. (I=0.4 A, Electrode area=33.5 cm$^2$, Intergap=10 mm, [NaCl]=1.5 g L$^{-1}$).**

| Experiment (Metal) | Theoretical dissolution (g) | Experimental dissolution (g) | mg of metal L$^{-1}$ leached (Obtained) | mg of metal L$^{-1}$ leached (Legal limit)[a] |
|---|---|---|---|---|
| Al | 0.5 | 0.7 | ≤0.2 | 10.0 |
| Cu | 1.4 | 1.3 | 3.4 | 1.0 |
| Fe | 1.3 | 1.4 | 27.8 | 2.0 |
| Pb | 4.6 | 4.5 | 78.9 | 1.0 |
| Zn | 1.5 | 1.4 | 16.4 | 5.0 |

[a] Portuguese Decree Law Nº 236/98, 1st of August.

### III.3.4 BIODEGRADABILITY AND TOXICITY ASSESSMENT

Biodegradability was assessed for all the experiments, starting from a value of 0.3 for the model solution. According to the results obtained for the TPh removal, it was expected that the ECG process would increase the biodegradability of the effluent over time, since it has reached a removal of phenolic content above 72 % at the end of the treatment. However, the biodegradability was reduced for all the experiments when comparing with the initial values suggesting that some bio refractory by-products were formed during the process. In fact, some chlorinated organics may have been produced. Moreover, this low biodegradability may also be related to the high metal leaching which misrepresents the biological action.

The toxicity of the effluent is displayed in Table III.4. For the Al experiment, the $EC_{20}$ and $EC_{50}$ values are approximately the same as the initial ones. The experiment with Cu anode led to the highest toxicity abatement within these anodes ($EC_{20}$–13 % and $EC_{50}$–43 %). Although the Fe electrode also exhibited the highest $EC_{20}$ value, 13 %, the $EC_{50}$ value was equal to that of the mother solution. In addition, the $EC_{20}$ and $EC_{50}$ values attained for Pb and Zn anodes were both lower than those of the starting mixture. The results demonstrated that the effluent still presents a significant ecological impact and the wastewater treated with Pb and Zn electrodes acquired a more toxic character, probably due to the formation of more toxic intermediate compounds and to the negative influence that the leached metals may have over the bacteria behaviour. Also according to Un *et al.* [26], it is possible that the ecotoxicity of the final effluent may be higher than that of the original solution because of the presence of the chloride ions which will lead to the production of chlorinated organic compounds during the process, through the chlorine that is formed, especially in acidic media.

**Table III.4. $EC_{20}$ and $EC_{50}$ values of the synthetic effluent treated by the electrocoagulation process for each anode.**

| Experiment | EC20 (%) | EC50 (%) |
|---|---|---|
| Al | 10.5 | 34.5 |
| Cu | 13.1 | 43.4 |
| Fe | 12.6 | 35.5 |
| Pb | 3.7 | 8.3 |
| Zn | 7.0 | 22.0 |

### III.3.5 ENERGETIC ANALYSIS

The system performance is greatly related to the current intensity, salinity, initial effluent concentration, type/size of the electrodes and contact time. The economic feasibility is determined by the sacrificial electrode loss and the electrical energy consumption (Equation (III.19)) in terms of kilowatt hour per $m^3$ of effluent treated ($kWh\ m^{-3}$) [25].

$$\mathrm{EC(kWh\ m^{-3})} = \frac{\mathrm{E_{cell}\ I\ t}}{\mathrm{V}} \qquad \text{(III.19)}$$

where $E_{cell}$ corresponds to voltage (V), I is current intensity (A), t is time (h) and V is the volume of effluent treated (L).

The energy consumption results presented in Figure III.5 are based on optimal contact times determined for each anode material. For example, for the Zn experiment, the COD removal efficiency increased 9 % from the 45th min to 60th min and just 2 % from 60 to 180 min (Figure III.3). Furthermore, after 60 min, the COD removal was not significantly affected, being this time considered the optimum contact time. In the case of the tests with Al and Fe is enough 30 min, while 15 min are required for the Cu anode and 10 min for the Pb experiment.

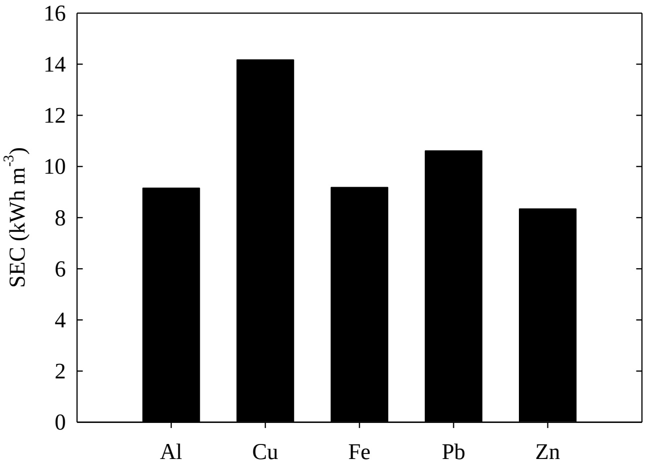

**Figure III.5. Energy consumption value for each anode material regarding the optimum contact time.**

As can be observed, the Zn anode material led to the lowest energy consumption value, 8 kWh $m^{-3}$, followed by the experiments with Al and Fe anodes with 9 kWh $m^{-3}$. Pb and Cu anode materials achieved the highest energy consumptions, around 11 and 14 kWh $m^{-3}$, respectively. These values are in accordance to those referred in literature by Kuokkanen *et al.* [25], 0.002–58 kWh $m^{-3}$. According to industrial sources, the energy cost is 0.12 € $kWh^{-1}$. Therefore, the treatment cost varies between 0.96–1.68 € $m^{-3}$.

## III.4 CONCLUSIONS

The performance of the electrocoagulation (ECG) process has been evaluated with different types of metal anode materials (Al, Cu, Fe, Pb and Zn) for the treatment of a phenolic simulated effluent. The main conclusions that can be obtained from this study can be resumed as follows:

- The operating conditions that were used were: pH=3.0, current intensity=0.4 A, [NaCl]=1.5 g $L^{-1}$, intergap distance=1.0 cm and effective anodic area=33.5 $cm^2$.
- The Zn anode promoted the highest removal of phenolic compounds (86 %) and organic load (49 %). Energy consumption=8 kWh $m^{-3}$.
- The treated effluent had low biodegradability and still high ecological impact, probably related with the formation of some chlorinated organic by-products and metal leaching content.
- This electrocoagulation process can be applied as a primary treatment method.

Among the anodes used, zinc seems an interesting material to be applied in a pretreatment of this kind of effluents. Another advanced oxidation process could be added after this treatment, since it is still not suitable to be handled directly by biological processes.

## ACKNOWLEDGMENTS

The authors, AS Fajardo and RC Martins gratefully acknowledge the Fundação para a Ciência e Tecnologia, for financial support under Ph.D. Grant (SFRH/BD/87318/2012) and post-Ph.D. Grant (SFRH/BPD/72200/2010), respectively.

## REFERENCES

[1] S'Habou, R, Zairi, Dhia HB (2005) Characterisation and environmental impacts of olive oil wastewater disposal. Environ. Technol. 26: 35−45.

[2] Adhoum N, Monser L (2004) Decolourization and removal of phenolic compounds from olive mill wastewater by electrocoagulation. Chem. Eng. Process. 43: 1281−1287.

[3] Un UT, Koparal AS, Ogutveren UB (2009) Electrocoagulation of vegetable oil refinery wastewater using aluminum electrodes. J. Environ. Manage. 90: 428−433.

[4] Barrera-Díaz C, Bilyeu B, Roa G, Bernal-Martinez L (2011) Physicochemical aspects of electrocoagulation. Sep. Purif. Rev. 40: 1−24.

[5] Hanafi F, Assobhei O, Mountadar M (2010) Detoxification and discoloration of Moroccan olive mill wastewater by electrocoagulation. J. Hazard. Mater. 174: 807−812.

[6] García-García P, López-López A, Moreno-Baquero JM, Garrido-Fernández A (2011) Treatment of wastewaters from the green table olive packaging industry using electro-coagulation. Chem. Eng. J. 170: 59−66.

[7] Coskun T, İlhan F, Demir NM, Debik E, Kurt U (2012) Optimization of energy costs in the pretreatment of olive mill wastewaters by electrocoagulation. Environ. Technol. 33: 801−807.

[8] Inan H, Dimoglo A, Şimşek H, Karpuzcu M (2004) Olive oil mill wastewater treatment by means of electro-coagulation. Sep. Purif. Technol. 36: 23−31.

[9] Ün UT, Uğur S, Koparal AS, Öğütveren ÜB (2006) Electrocoagulation of olive mill wastewaters. Sep. Purif. Technol. 52: 136−141.

[10] Linares-Hernández I, Barrera-Díaz C, Bilyeu B, Juárez-GarcíaRojas P, Campos-Medina E (2010) A combined electrocoagulation−electrooxidation treatment for industrial wastewater. J. Hazard. Mater. 175: 688−694.

[11] Soloman PA, Basha CA, Velan M, Balasubramanian N (2009) Electrochemical degradation of pulp and paper industry wastewater. J. Chem. Technol. Biotechnol. 84: 1303−1313.

[12] Basha CA, Soloman PA, Velan M, Miranda LR, Balasubramanian N, Siva R (2010) Electrochemical degradation of specialty chemical industry effluent. J. Hazard. Mater. 176: 154−164.

[13] Silva AMT, Nouli E, Xekoukoulotakis NP, Mantzavinos D (2007) Effect of key operating parameters on phenols degradation during $H_2O_2$-assisted $TiO_2$ photocatalytic treatment of simulated and actual olive mill wastewaters. Appl. Catal. B 73: 11−22.

[14] Greenberg A, Clesceri L, Eaton A (1992) Standard Methods for the Examination of Water and Wastewater, 18th ed.; American Public Health Association: Washington DC.

[15] Esplugas S, Contreras S, Ollis D (2004) Engineering aspects of the integration of chemical and biological oxidation: Simple mechanistic models for the oxidation treatment. J. Environ. Eng. 130: 967−974.

[16] Zhang XG (1996) Corrosion and Electrochemistry of Zinc; Springer: New York.

[17] Arslan-Alaton İ, Kabdaşlı I, Vardar B, Tünay O (2009) Electrocoagulation of simulated reactive dyebath effluent with aluminum and stainless steel electrodes. J. Hazard. Mater. 164: 1586−1594.

[18] Krishna BM, Murthy UN, Kumar BM, Lokesh KS (2010) Electrochemical pretreatment of distillery wastewater using an aluminum electrode. J. Appl. Electrochem. 40: 663−673.

[19] Pourbaix M (1966) Atlas of Electrochemical Equilibria in Aqueous Solutions, 1st ed.; Pergamon Press: Oxford.

[20] Vasudevan S, Lakshmi J, Sozhan G (2013) Electrochemically assisted coagulation for the removal of boron from water using zinc anode. Desalination 310: 122−129.

[21] Wang Y-y, Chai L-y, Chang H (2009) Equilibrium of hydroxyl complex ions in $Pb^{2+}$−$H_2O$ system. Trans. Nonferrous Met. Soc. China 19: 458−462.

[22] Xiao F, Zhang B, Lee C (2008) Effects of low temperature on aluminium(III) hydrolysis: Theoretical and experimental studies. J. Environ. Sci. 20: 907−914.

[23] Khemis M, Leclerc J-P, Tanguy G, Valentin G, Lapicque F (2006) Treatment of industrial liquid wastes by electrocoagulation: Experimental investigations and an overall interpretation model. Chem. Eng. Sci. 61: 3602−3609.

[24] Giannis A, Kalaitzakis M, Diamadopoulos E (2007) Electrochemical treatment of olive mill wastewater. J. Chem. Technol. Biothecnol. 671: 663−671.

[25] Kuokkanen V, Kuokkanen T, Rämö J, Lassi U (2013) Recent applications of electrocoagulation in treatment of water and wastewater - A review. Green Sus. Chem. 3: 89−121.

[26] Un UU, Altay U, Koparal AS, Ogutveren UB (2008) Complete treatment of olive mill wastewaters by electrooxidation. Chem. Eng. J. 139: 445−452.

# IV. PHENOLIC WASTEWATERS TREATMENT BY ELECTROCOAGULATION PROCESS USING Zn ANODE

AS Fajardo[a], RF Rodrigues[a], RC Martins[a], LM Castro[b] and RM Quinta-Ferreira[a]

[a] CIEPQPF – Centro de Investigação em Engenharia dos Processos Químicos e Produtos da Floresta, GERST – Group on Environment, Reaction, Separation and Thermodynamics, Department of Chemical Engineering, Faculty of Sciences and Technology, University of Coimbra, Pólo II, Rua Sílvio Lima, 3030-790 Coimbra, Portugal.

[b] Polytechnic Institute of Coimbra, Department of Chemical and Biological Engineering, Rua Pedro Nunes, Quinta da Nora, 3030-199 Coimbra, Portugal.

*Chemical Engineering Journal 275 (2015) 331–341*

## ABSTRACT

Electrocoagulation using a Zn anode was applied for the first time to remove the organic load of a liquid effluent. Different operating conditions (pH, current density, distance between electrodes, nature of electrolyte and kind of cathode) were tested with synthetic phenolic wastewater, in order to optimise the process. Both the medium pH and the type of electrolyte that were used greatly affected the efficiency of the system, followed by the influence of the current density and the cathode material, in a lesser extent. The effect of the distance between electrodes was quite negligible. Furthermore, a sequence of fed-batch trials involving the electrodes reuse showed almost constant activity during the operation time. The optimum operating conditions achieved were initial pH of the effluent equal to 3.2, current density of 250 A $m^{-2}$, distance between electrodes of 1.0 cm and 1.5 g $L^{-1}$ of NaCl. Moreover, the Zn anode/stainless steel cathode pair revealed the most interesting results. These parameters led to 84.2 % and 40.3 % of total phenolic (TPh) content and chemical oxygen demand (COD) removal, respectively. In addition, the depuration of a filtered real olive mill effluent without NaCl addition achieved the abatement of up to 72.3 % of TPh and 20.9 % of COD. An energy consumption of 40 kWh $m^{-3}$ and 34 kWh $m^{-3}$ was observed for the treatment of the simulated and the real wastewater, respectively. Furthermore, the ecological impact of the treated effluent was detected by bio-luminescence techniques.

This study shows the potentiality of the electrocoagulation process as a pre-treatment of other methods, namely the electrochemical oxidation, to ensure the legal limits values of the wastewater to be discharged into the aquatic environment regarding their organic load.

## IV.1 INTRODUCTION

Olive production is a common agro-industry in Mediterranean countries such as Spain (2.4 million ha), followed by Italy (1.4 million ha), Greece (1.0 million ha), Portugal (0.5 million ha) and France (40 thousand ha), with significant economic, social and environmental impact [1]. Olive mill wastewater represents an important ecological problem, due to its seasonal production, high pollution load and toxicity [2–4]. These properties hinder the use of biological treatments since the presence of phenolic compounds, which are recalcitrant substances, inhibit microorganisms' action. Therefore, the development of more effective processes emerges as an alternative to this environmental threat. Even though novel approaches on advanced oxidation processes appear to be promising and attractive options. However, handicaps, for example as high cost, formation of a second source of pollution and its experimental level, are still holding them back from widespread application in industry [5]. On the other hand, the electrocoagulation (ECG) process is an easy system to operate, requiring low equipment costs, maintenance and chemical consumption, as well as low quantity of sludge is produced when compared to the traditional chemical coagulation/flocculation process [6–8]. In the ECG system, sacrificial anodes dissolve into the liquid medium and metal hydroxides are formed by the reaction of metal ions generated at the anode with hydroxide anions released by water hydrolysis at the cathode. The solubility of the complexes formed is dependent on pH and ionic strength. The metal species react with negatively charged particles in the water to form flocs, which will have the power to destabilise and aggregate the suspended particles in order to precipitate or adsorb dissolved contaminants [9]. The ECG process has already been applied to the treatment of olive mill wastewaters, using aluminium or iron electrodes. In most studies, the same type of material served as both anode and cathode. However, some researchers, like García-García *et al.* [10] used a combination between aluminium and iron electrodes. These materials led to promising removal values of organic load (59–76 %), phenol content (70–91 %) and colour (70–95 %), after 25–45 min of treatment time [9–14]. According to the reported results, ECG can be considered as an effective solution for the treatment of OMW or even be combined with conventional biological processes to attain the environmental legal limits, before being discharged into natural aquatic streams. Moreover, ECG is pointed out to be faster and more effective than biological processes alone [11]. In later studies, the introduction of a coagulant aid and hydrogen peroxide was also considered and the efficiency of the process increased with their addition [15]. Although aluminium and iron are the most used electrodes in the electrocoagulation of OMW, other kind of electrode materials is employed in the treatment of different types of wastewaters. For example, copper to remove phosphorus from a simulated effluent [16], stainless steel to depurate a textile dye wastewater [17], and a combination of aluminium (anode)/stainless steel (cathode) to eliminate heavy metal species found in industrial polluted streams [18]. Zinc has also been used for the removal of a wide range of metals (cadmium, cesium, copper, iron, strontium) from water, demonstrating high removal efficiency (96.6–99.6 %) with 5–20 A $m^{-2}$ at pH 7 [19–22]. When applied to a dairy industry effluent, the best operating conditions achieved with this anode material were current density of 86 A $m^{-2}$, electrolysis time of 43 min and initial sample pH of 7. The reduction of chemical oxygen demand was about 58 % and turbidity 91 % [23].

Based on the existing literature, several electrocoagulation studies have been frequently performed by using Al or Fe electrodes. However, the cost and formation of higher quantities of sludge are the disadvantages of the use of these sacrificial electrodes; [24] therefore, the search for new materials to promote the electrochemical formation of coagulants is encouraged. In this regard, the novelty of this work focuses on the use of Zn material to treat organic polluted liquid effluents. Indeed, it shall be highlighted that to the best of our knowledge this is the first time that Zn is used as anode to depurate water streams contaminated with organic compounds. This hypothesis was based upon the interesting results recently addressed in literature works [19–21] for the removal of metals from water. Emphasis was given to phenolic contaminants due to their impact over the ecosystems. These substances are characteristic of the effluents coming from olive mills that are mostly located in Mediterranean area countries. Nonetheless, it should be highlighted that the results obtained with this work may be generalised for other agro-effluents. In fact, one of the common features of these wastewaters is their high load in such phenolic compounds, which are responsible for their biorefractory character. The effect of different operating conditions, such as initial pH, current density, distance between electrodes, kind of cathode and type of electrolyte were discussed and the best operating conditions were applied to an actual OMW in order to verify the possible real application of such technology.

## IV.2 MATERIAL AND METHODS

### IV.2.1 SYNTHETIC AND REAL EFFLUENT

A phenolic mixture composed of six acids (100 mg $L^{-1}$ of each) normally present in real olive mill wastewaters (3,4,5-trimethoxybenzoic, 4-hydroxybenzoic, gallic, protocatechuic, trans-cinnamic and veratric acids) was prepared to mimic the actual OMW [24]. No further purification was applied to them before use. The real wastewater was collected from a mill located in the Extremadura region of Spain and part of the experiments were performed with previously filtered effluent.

### IV.2.2 ELECTROCOAGULATION SYSTEM AND PROCEDURE

The electrocoagulation process was performed in a Perspex batch-stirred reactor, under controlled temperature (20 °C) and atmospheric pressure, during 180 min. In each experiment, the reactor was filled with 1000 mL of the model solution or real effluent. The flat anode and cathode were placed parallel at a specific distance (5–20 mm) and linked to a DC Power Supply HY3010 Kaise (I=0.4–1.7 A) [25,26]. Zn (Filzinc company, Oiã – Portugal) and stainless steel (SS) electrodes were used with an effective initial area of 33.5 $cm^2$. Samples were periodically withdrawn and immediately centrifuged at

3500 rpm (Nahita 2655) for further analysis. The conductivity of the electrolyte was measured using a Consort C863 measurer. 1.5 g $L^{-1}$ of NaCl or $Na_2SO_4$ salts were added to the system in order to promote higher conductivity to the solution. When the real effluent was tested, some experiments were also executed without salt addition. The initial pH of the medium was varied between 3 and 9, using NaOH at 3 M or $H_2SO_4$ at 2 M whenever necessary. This parameter was followed (HANNA pH meter) but not adjusted during the treatment time.

### IV.2.3 ANALYTICAL TECHNIQUES

In order to assess the progress of the treatment over time, some analytical techniques were performed, such as total phenolic content (TPh), chemical oxygen demand (COD), biochemical oxygen demand ($BOD_5$), eco-toxicity (LUMIStox), analysis of the concentration of each phenolic acid and the dissolution of the metal into the solution.

TPh was measured as gallic acid equivalents (GA) by the Folin–Ciocalteau method, as described elsewhere [27], using a T60 PG Instruments spectrophotometer. COD (closed reflux procedure) and $BOD_5$ were determined according to Standard Methods (5250D and 5210B, respectively) [28]. Eco-toxicity tests were based on the measurement of the light production before and after the luminescent marine bacteria *Vibrio fischeri* be incubated for 15 min at 15 °C with different dilutions of the pollutants. Toxicity levels were assessed through LUMIStox equipment (Dr. Lange) and were expressed as EC values, which represent the concentration of a sample that inhibits 20 % ($EC_{20}$) and 50 % ($EC_{50}$) of bacteria light emission. Some experiments were randomly run in duplicate to ensure the reproducibility of the results and the samples withdraw were measured in duplicate to minimise experimental errors. Deviations between runs were always lower than 10 %, 8 %, 20 % and 2 % for TPh, COD, $BOD_5$ and eco-toxicity determinations, respectively. The results displayed in the manuscript's figures correspond to the average of those measurements, including the respective standard deviations. The concentration of individual compounds of the synthetic effluent was followed by a Knauer high-performance liquid chromatography (HPLC) system. 20 µl of samples were injected via an autosampler (Knauer, Smartline 3800). The mobile phase, consisting of 20 % of methanol in water slightly acidified with phosphoric acid, was pumped using a Knauer WellChrom K-1001 pump at a flow rate of 1 mL $min^{-1}$ through a C18 column at 85 °C, and detection was performed at 280 nm in an ultraviolet (UV) detector. This technique was also applied to the real effluent. Furthermore, the concentration of zinc in solution was evaluated by atomic absorption using Perkin-Elmer 3300, Waltham, MA equipment.

# IV.3 RESULTS AND DISCUSSION

## IV.3.1 SYNTHETIC EFFLUENT

The synthetic wastewater was prepared according to the common composition of effluents from olive oil mills [24], and its main characteristics are displayed in Table IV.1.

**Table IV.1. Main characteristics of the synthetic and real effluent.**

| **Characteristics** | **Synthetic effluent** | **Real effluent** |
|---|---|---|
| pH | 3.2±0.3 | 4.0±0.4 |
| Conductivity (mS/cm) | 0.14±0.01 | 5.94±0.03 |
| TPh (mgGA/L) | 327±7 | 740±9 |
| COD (mg$O_2$/L) | 1118±20 | 22650±1302 |
| $BOD_5$ (mg$O_2$/L) | 372±20 | - |
| $BOD_5$/COD | 0.3 | - |
| $EC_{20}$ (%) | 10±2 | - |
| $EC_{50}$ (%) | 36±2 | 4±2 |

This effluent is an acidic solution (pH 3.2) with low conductivity, 0.14 mS cm$^{-1}$, since solutions are considered conductive of electrical current for values higher than 2.50 mS cm$^{-1}$ [29]. The high concentration of phenolic acids, determined as TPh (323 mgGA L$^{-1}$), is characteristic of this kind of wastewaters, being one of the key parameters to be reduced by the treatment, as well as the amount of organic matter expressed by COD (1118 mg$O_2$ L$^{-1}$) and $BOD_5$ (372 mg$O_2$ L$^{-1}$). According to the Portuguese Decree-Law 236/98 of 1st August, an effluent just can be directly discharged into an aquatic medium if COD and $BOD_5$ values are lower than 150 and 40 mg$O_2$ L$^{-1}$, respectively. Regarding the effluent's biodegradability $BOD_5$/COD=0.3, this value is below the threshold ratio of which the wastewaters are considered as totally biodegradable, 0.4 [30]. In addition, the toxicity of the mixture was also tested in order to infer about its effect on ecosystems, being evidenced that a solution involving only 10 and 36 % of the pollutant sample led to 20 and 50 % of the *Vibrio Fischeri*'s population light production inhibition, respectively, revealing its high negative impact over life forms. Therefore, the effluent is unfit for biological treatment due to its high organic load hard to biodegrade, seasonal production and varied composition which would require constant biomass acclimation, supporting the necessity of the application of another type of treatment, such as the electrocoagulation process.

In the following sections the effect of the key parameters ruling ECG efficiency were analysed using this simulated solution.

### IV.3.1.1 Effect of pH

The pH of the effluent is one of the most important parameters in the electrocoagulation process, since the solubility of the metal complexes formed is dependent on pH and ionic strength [9-10,13-14]. Moreover, phenolic acids are very sensitive to changes in pH. The system efficiency was evaluated for three different medium initial pH values, the raw effluent pH 3.2, followed by pHs 7 and 9, which were adjusted with NaOH or $H_2SO_4$, whenever necessary. During these experiments the other operating conditions were kept constant: current density=120 A $m^{-2}$, distance between electrodes=1.0 cm, [NaCl] =1.5 g $L^{-1}$ and Zn anode/SS cathode pair [9-15]. Figure IV.1a shows the wastewater phenolic content depletion over time and as can be observed a similar removal was achieved for pH 3.2 (49.4 %) and pH 7 (48.0 %), after 30 min of treatment. While for the experiment at pH 9, this time corresponds to the induction period from which begins a low removal evolution that actually ends up exceeding the values for pH 7 at 120 min of treatment. At the end of the process, the highest TPh removal (86.7 %) was attained for pH 3.2, followed by pH 9 (66.0 %) and at last pH 7 (50.7 %). Figure IV.1b revealed that the organic load decreased for all pHs studied and was only slightly affected by pH 7 and 9. In fact, the test with pH 3.2 led to a steadily COD removal (40.2 %) up to 60 min, remaining almost constant thereafter. At pH 9, there was a change in the initial solution’s colour from transparent to green, probably a result of the formation of quinones, which are not detected as phenols but are still accounted as organic matter.

These results are in agreement with the *Pourbaix* diagram for zinc material [31]. When the pH medium of the effluent is acidic, the dissolution of the electrode may occur to the solution in the form of $Zn^{2+}$, that subsequently reacts with the hydroxyl anion formed in the cathode and precipitates in the form of hydroxides, $Zn(OH)_2$. The possible reactions that may occur when zinc is used as anode are presented in Equation (IV.1) – (IV.4).

At the anode $$\mathrm{Zn \rightarrow Zn^{2+} + 2e^-} \qquad \textbf{(IV.1)}$$

At the cathode $$\mathrm{2H_2O + 2e^- \rightarrow H_2 + 2OH^-} \qquad \textbf{(IV.2)}$$

In the solution $$\mathrm{Zn^{2+} + 2OH^- \rightarrow Zn(OH)_2} \qquad \textbf{(IV.3)}$$

Global reaction $$\mathrm{Zn + 2H_2O \rightarrow H_2 + Zn(OH)_2} \qquad \textbf{(IV.4)}$$

This process promotes the coagulation with the aggregation of the pollutants, reducing the organic load and the concentration of pollutants in the liquid phase [21].

For pH 7 and 9, the initial phase corresponds to the lower dissolution of the electrode with $Zn^{2+}$ formation. For this reason, the process of formation of hydroxide flocs in solution to aggregate pollutants is reduced, leading to a low efficacy of the electrocoagulation process in what regards COD.

Figure IV.1c depicts the pH medium for all experiments followed over time. As can be observed, the pH increased for all tests. This increase may be explained by the reactions occurring at the cathode:

during the process, at this electrode, water molecules receive electrons and dissociate into hydrogen bubbles and hydroxyl ions, causing the pH medium increase. During the process with pH 3.2, the solution rose to neutral pH, which is in the ideal range, not needing pH adjustment, to be directly discharged or even to be used in biological processes.

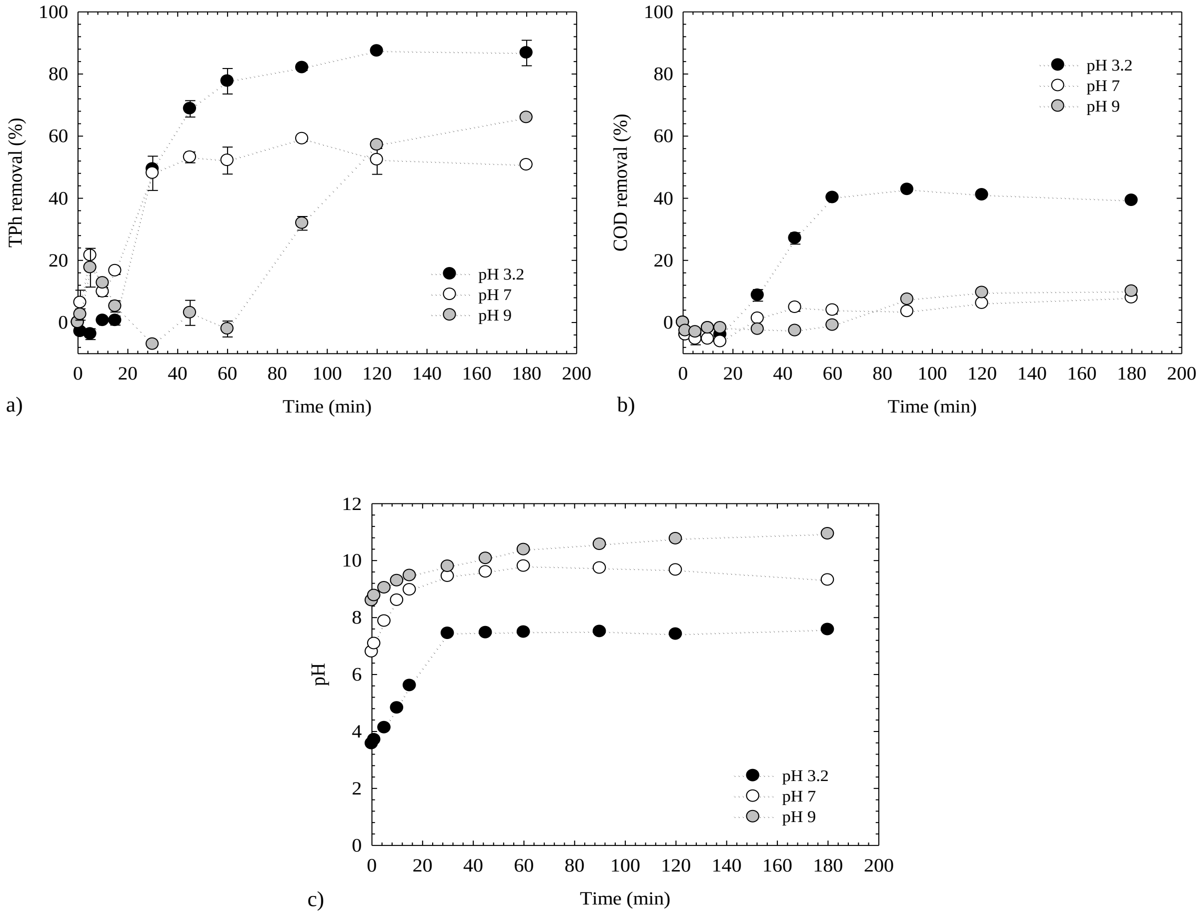

**Figure IV.1. Effect of the initial pH medium on a) TPh removal, b) COD removal and c) pH over time (current density=120 A $m^{-2}$, distance between electrodes=1.0 cm, [NaCl]=1.5 g $L^{-1}$, Zn anode/SS cathode).**

In order to verify the mechanisms that exist in this ECG process, the ratio TPh/COD is illustrated in Figure IV.2. As can be seen, this ratio is not constant over time, suggesting that the precipitation and adsorption of pollutants are not the only phenomena present once, if that would be the case, TPh and COD removal should follow the same trend. In fact, one can infer that it may also occur the oxidation of organic compounds into intermediates which are accounted for as COD but no longer have phenolic character.

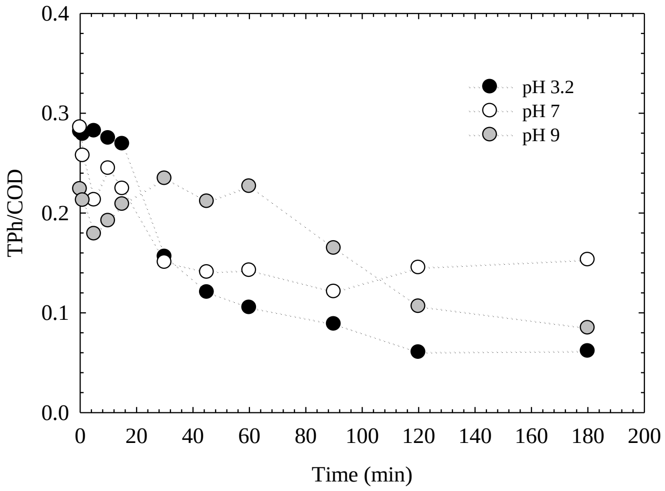

**Figure IV.2. TPh/COD ratio over time (current density=120 A m$^{-2}$, distance between electrodes=1.0 cm, [NaCl]=1.5 g L$^{-1}$, Zn anode/SS cathode).**

### IV.3.1.2 Effect of current density

In the ECG process, a current intensity is applied between the metallic electrodes immersed in the effluent, which promotes the dissolution of the electrodes being responsible for the formation of coagulant species that destabilise and aggregate the contaminants present in the effluent. Furthermore, this parameter determines the rate of hydrogen bubbles formation and the growth of flocs that may influence the efficiency of the process [21].

The effect of the current density (ratio current intensity/anodic area) was analysed between 120–500 A m$^{-2}$ and the studies were performed at pH 3.2, with a distance between electrodes of 1.0 cm and NaCl concentration of 1.5 g L$^{-1}$. Figure IV.3a displays the removal of phenolic content over time. As can be observed, there is a significant decrease of TPh (84.0–87.3 % of removal) during the first 30 min of reaction with 250 and 500 A m$^{-2}$. In the case of the experiment with 120 A m$^{-2}$ more time (120 min) was needed to achieve a similar removal value. Regarding COD decrease (Figure IV.3b), the test with 500 A m$^{-2}$ has a sharply depuration of 38.5 % during the first 15 min, followed by the experiment with 250 A m$^{-2}$ (15–30 min), whereas the assay using 120 A m$^{-2}$ continues to be the one that takes longer time (60 min) to get removals similar to the other experiments; this because at the beginning of the process the COD depletion is practically null. The current density applied to the system determines the amount of ions released as $Zn^{2+}$ and therefore the amount of the resulting coagulant. Thus, the higher the amount of dissolved $Zn^{2+}$ ions in solution the greater is the rate of $Zn(OH)_2$ formation and consequently a higher COD and TPh removal efficiency is achieved [21,32]. Additionally, the increase of current density promotes the generation of hydrogen bubbles and decreases its size, resulting in an intensification of the upward flow and a superior removal of pollutants by flotation. Consequently, it seems to be advantageous to use high current densities which enable high electrocoagulation efficiencies in short running times. However, at the end of 180 min of treatment time, the experiment with 500 A m$^{-2}$ led to the worst COD removal value. This might be due to the fact that higher current values lead to a high turbulence in the system and consequently the particles responsible for coagulation do not have enough time to agglomerate themselves and remove the pollutants. Important factors such as energy cost and durability of the electrodes must be taken into account in the process optimisation. Therefore, the current density of 250 A $m^{-2}$ was chosen to continue the experiments, because after 30 min the highest COD removal (51 %) was attained and if the higher current density would be used, it would cause higher consumption of the anode material

It was still observed that using different density current conditions no significant effect over pH evolution was detected and the final value for all cases was neutral (Figure IV.3c). However, for the initial times the quickest experiment was for 500 A $m^{-2}$ (5 min), followed by 250 (10 min) and 120 A $m^{-2}$ (30 min).

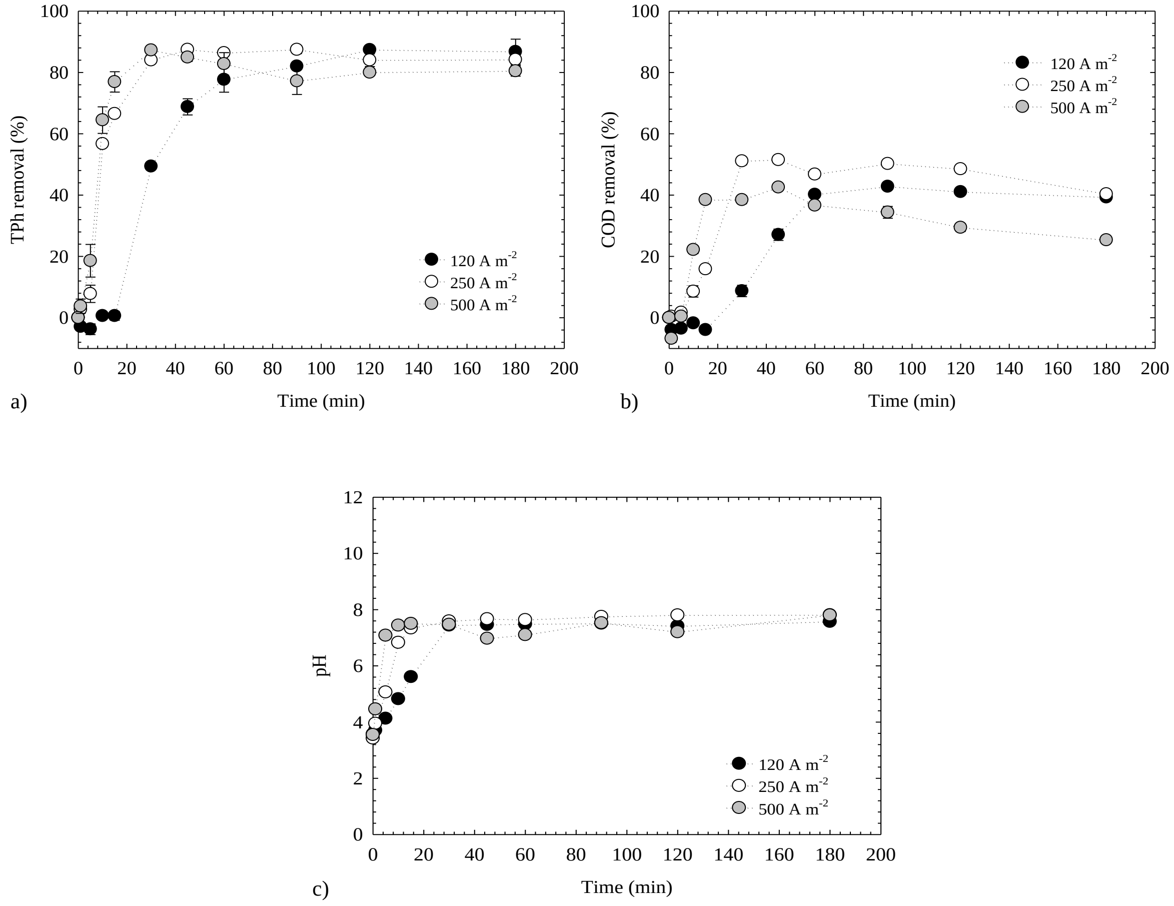

**Figure IV.3. Effect of the current density effect on a) TPh removal, b) COD removal and c) pH over time (pH=3.2, distance between electrodes=1.0 cm, [NaCl]=1.5 g $L^{-1}$, Zn anode/SS cathode).**

### IV.3.1.3 Effect of the distance between electrodes

The distance between electrodes influences the amount of energy which is necessary to be supplied to the system in order to generate an electric field and induce the movement of ions [21].

In the present work, this study was carried out at three different values (0.5, 1.0 and 2.0 cm), while the other operating conditions were kept constant (initial pH effluent=3.2, current density=250 A $m^{-2}$ and [NaCl]=1.5 g $L^{-1}$). The corresponding removal efficiencies over time for TPh and COD are depicted in Figure IV.4a and Figure IV.4b, respectively. The decrease of the electrode gap distance to 0.5 cm led to a TPh reduction around 93.7 % after 30 min of treatment, and slightly lower values were achieved for highest intergap distances (84.0 and 81.8 % for 1.0 and 2.0 cm, respectively). Considering the removal of organic matter and the pH profile (Figure IV.4c), no significant differences were obtained between the three distances applied (after 30 min: COD removal=42.8–51.1 % and pH=7.7). In fact, even if a low space between electrodes corresponds to a decrease in the resistance of the medium, which implies a low amount of energy to move ions, since the path they have to cover is smaller [21], it should be referred that the inter-electrode distance of 0.5 cm was difficult to maintain over time. Moreover, the final results for the three cases were quite similar; therefore, the subsequent experiments were carried out with 1.0 cm distance.

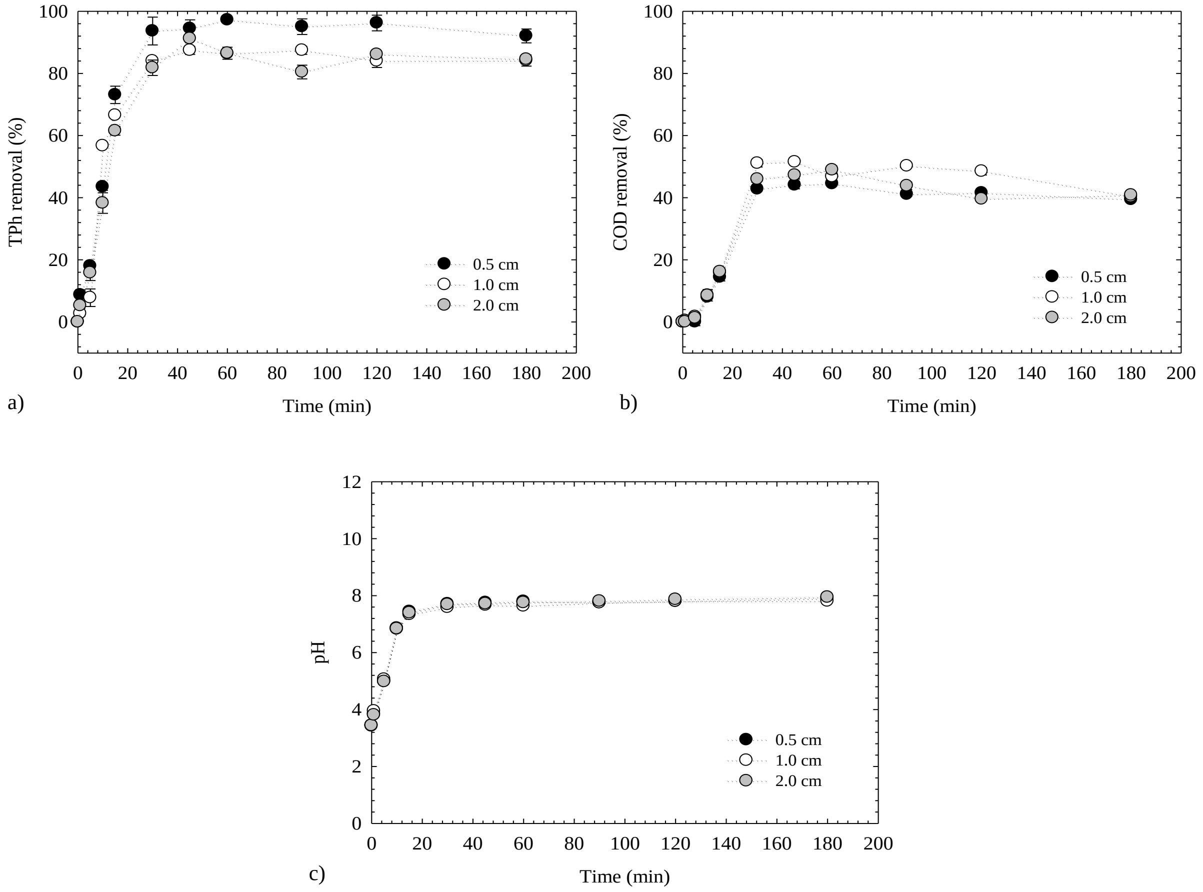

**Figure IV.4. Effect of the distance between electrodes on a) TPh removal, b) COD removal and c) pH over time (pH=3.2, current density=250 A $m^{-2}$, [NaCl]=1.5 g $L^{-1}$, Zn anode/SS cathode).**

### IV.3.1.4 Effect of the nature of the electrolyte

As aforementioned, the synthetic solution had not the required conductivity to perform the electrochemical experiments; hence two electrolytes were tested, NaCl and $Na_2SO_4$ at a concentration of 1.5 g $L^{-1}$, in order to increase the effluent's conductivity and decrease the energy consumption. This way, the initial conductivity of the effluent became 3.0 and 2.5 mS $cm^{-1}$ after the introduction of chlorine and sulphate salts, respectively. From the results (Figure IV.5a and Figure IV.5b) it was found out that at the end of 30 min NaCl, led to better degradation values (TPh removal=84.0 % and COD removal=51.1 %) than the ones achieved with $Na_2SO_4$ (TPh removal=62.1 % and COD removal=15.4 %).

In the presence of both salts it occurs the generation of oxidising species ($Cl_2$, HClO, $ClO^-$ and $S_2O_8^{2-}$) which are able to react with organic compounds during electrolysis [33]. The difference between the two electrolytes may be explained by the fact that the NaCl solution provides higher conductivity to the effluent and the chemical species that are formed are good oxidant reagents to decompose organic compounds, thereby improving the process efficiency. Moreover, moderate levels of chloride ions in solution decrease the passivation layer on the surface of the sacrificial anodes, increasing the removal efficiency of contaminants in the ECG process [34]. In addition, through the analysis of the evolution of the pH in the medium (Figure IV.5c) and according to the *Pourbaix* diagram, one can foresee that in the experiment with $Na_2SO_4$, the short time in neutral pH may have reduced the dose of coagulants and, on the other hand, the alkaline medium may have led to the formation of an oxide layer on the surface of the zinc electrode which prevents the dissolution of the metal, limiting also, this way, the coagulant generation. Thus the efficiency of the electrocoagulation process is inhibited [35].

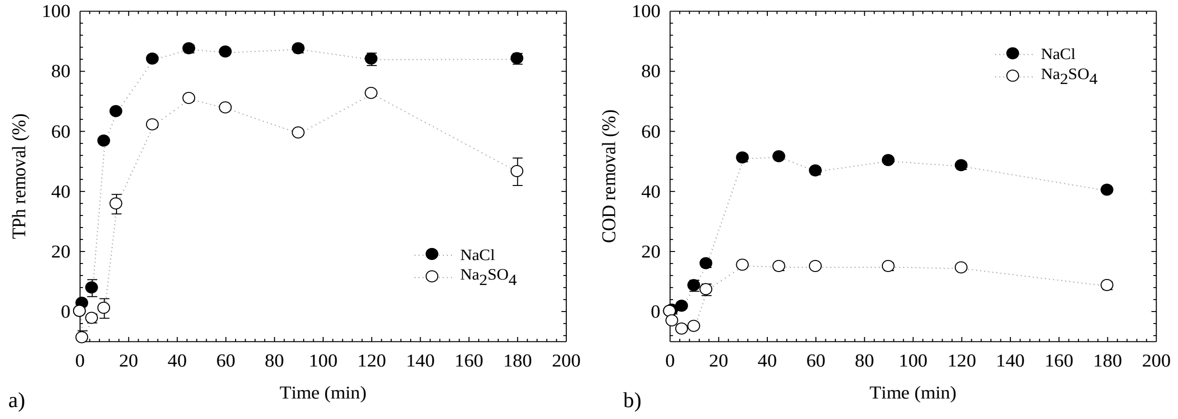

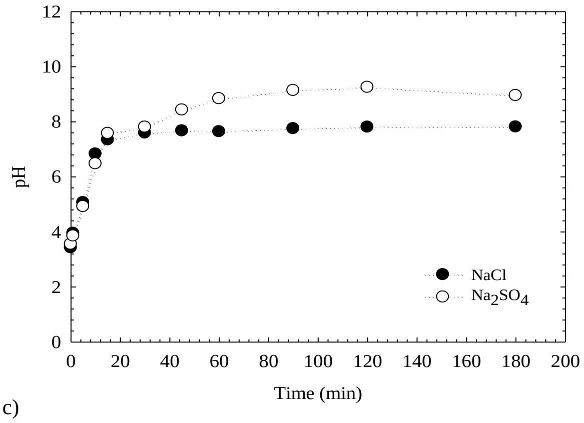

**Figure IV.5. Effect of the type of electrolyte on a) TPh removal, b) COD removal and c) pH over time (pH=3.2, current density=250 A $m^{-2}$, distance between electrodes=1.0 cm, [NaCl]=1.5 g $L^{-1}$, Zn anode/SS cathode).**

### IV.3.1.5 Effect of different cathodes

So far, the experiments have been performed with a Zn anode/SS cathode pair. Now, the Zn anode/Zn cathode set will be used in order to analyse its influence on TPh (Figure IV.6a) and COD (Figure IV.6b). Figure IV.6a evidences that the trend of the phenolic content removal for the two pairs of electrodes is similar. There is a rapid TPh depletion in the first 30 min of reaction (TPh removal=84.0 %), remaining practically constant thereafter. Nevertheless, in Figure IV.6b there is a significant difference in COD abatement for the two pairs of electrodes. Although, in the first 15 min, they follow the same tendency, achieving a removal of 15.0 %, afterwards, the set Zn anode/Zn cathode had a slower evolution attaining its major efficiency after 45 min with 39.4 %, whereas the Zn anode/SS cathode pair had its highest removal after 30 min with 51.1 %. These results may be explained by the pH medium evolution over time (Figure IV.6c). As can be observed, the experiment with Zn anode/Zn cathode had a slow transition from an acidic pH to neutral, taking longer time than the other set of electrodes to dissolve metal ions to the aquatic medium and subsequent formation of metal hydroxides necessary to remove pollutants.

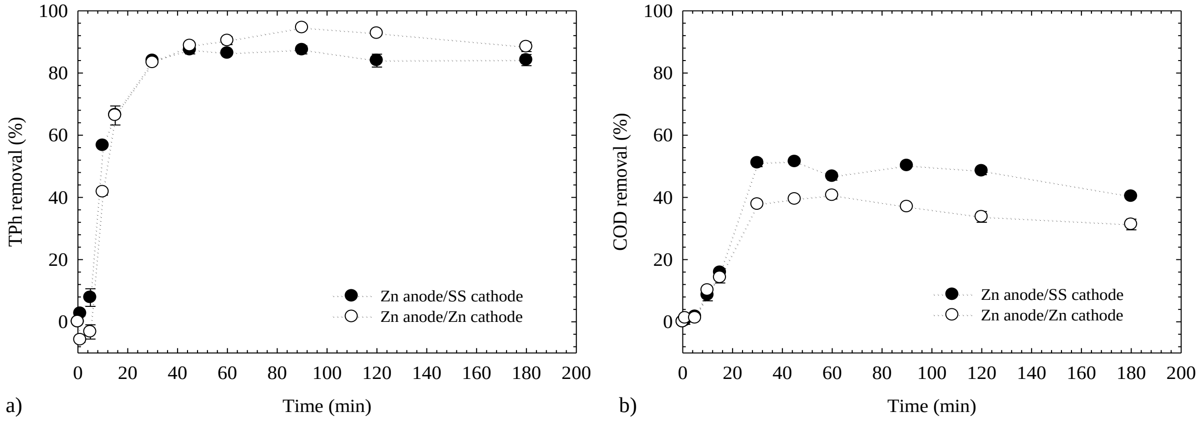

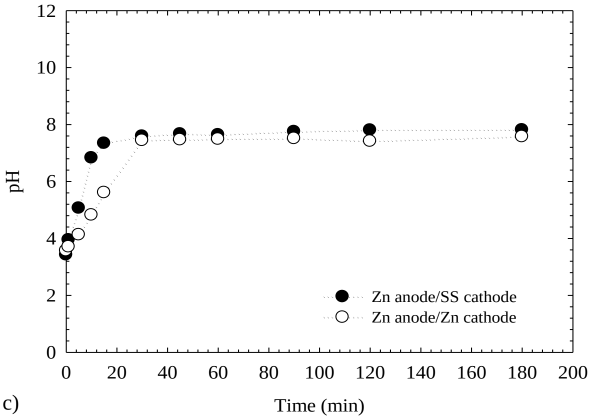

**Figure IV.6. Effect of the pair of electrodes on a) TPh removal, b) COD removal and c) pH over time (pH=3.2, current density=250 A m$^{-2}$, distance between electrodes=1.0 cm, [NaCl]=1.5 g L$^{-1}$).**

Our results point out that the operating conditions that have led to the greatest removal efficiency of phenolic content and organic matter of the simulated effluent by ECG were: raw pH (3.2), a current density of 250 A m$^{-2}$, a distance between electrodes of 1.0 cm, 1.5 g L$^{-1}$ of NaCl and the set Zn anode/SS cathode.

### IV.3.1.6 Analysis of the concentration of the different phenolic acids parents in the effluent

The individual concentration of the six parent phenolic acids was monitored by HPLC for the experiment involving the best operating conditions referred before. Figure IV.7 represents the removal profile for all compounds over time. After 15 min of treatment, it was noticeable the high efficiency of the process for the practically total degradation of gallic (96.4 %) and 3,4-dihidroxybenzoic (98.4 %) acid. In the case of 3,4-dimethoxybenzoic, 3,4,5-trimethoxybenzoic and 4-hydroxybenzoic acids, their removal had a sharp increase between 15 and 30 min, achieving their higher degradation (86.8–91.8 %) at this time, while 4-hydroxybenzoic acid had a smooth depletion between 30 and 60 min, keeping constant from there on (69.1 %). Regarding 3,4-dimethoxybenzoic, 3,4,5-trimethoxybenzoic and 4-hydroxybenzoic acids, after 60 min of treatment, their concentration in the liquid starts to increase again (their removal decreases), stabilising after 120 min.

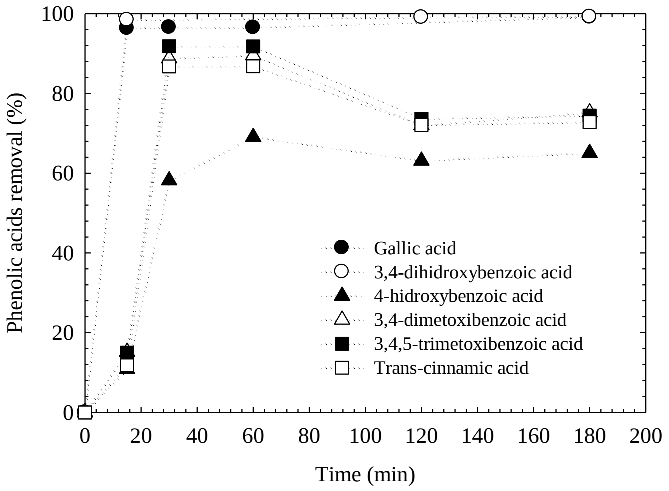

**Figure IV.7. Removal of parent phenolic acids over time for the synthetic effluent (pH=3.2, current density=250 A m$^{-2}$, distance between electrodes=1.0 cm, [NaCl]=1.5 g L$^{-1}$, Zn anode/SS cathode).**

### IV.3.1.7 Toxicity analysis

The eco-toxicity test was applied to the effluent before and after the electrocoagulation process for the best operating conditions referred before. The results obtained for $EC_{20}$ and $EC_{50}$ indicators are shown in Table IV.2. One can observe that the addition of the electrolyte NaCl increased the toxicity of the effluent by itself, reducing $EC_{20}$ from 10 % to 9 % and $EC_{50}$ from 36 % to 18 %. After treatment, even if the effluent remains toxic for bacteria a decrease on this parameter is detected subsequently to the ECG with $EC_{20}$=20 % and $EC_{50}$=38 %. Fulladosa *et al.* [36-37] determined $EC_{20}$ and $EC_{50}$ threshold values for $Zn^{2+}$ for *Vibrio fischeri* bacteria, which corresponded to 0.46±0.02 mg L$^{-1}$ and 0.86±0.11 mg L$^{-1}$, respectively. The concentration of $Zn^{2+}$ obtained in this work was 36 mg L$^{-1}$, value that is above $EC_{50}$ reported in literature. This aspect can be an important contribution to the toxicity present in the effluent at the end of the treatment.

**Table IV.2. $EC_{20}$ and $EC_{50}$ values for the synthetic effluent before and after treatment.**

| | | **$EC_{20}$ (%)** | **$EC_{50}$ (%)** |
|---|---|---|---|
| Initial effluent | | 10±2 | 36±2 |
| ECG | t=0min (electrolyte addition) | 9±2 | 18±2 |
| | t=180min | 20±2 | 38±2 |

### IV.3.1.8 Electrical energy consumption

The electrical energy consumption is the major operating cost associated with ECG process. Therefore, it is important to optimise this parameter in order to reduce economic and environmental impacts. The electrical energy consumption (EC) was determined in terms of kWh $m^{-3}$ according to Equation (IV.5) [38].

$$\mathrm{EC(kWh\ m^{-3})} = \frac{\mathrm{E_{cell}\ I\ t}}{\mathrm{V}} \tag{IV.5}$$

where $E_{cell}$ is the potential difference (V), I is the current intensity applied to the process (A), t is the reaction time (h) and V is the volume of treated effluent (L). A result of 40 kWh $m^{-3}$ was obtained for this process that is within the range of values referred in the literature for the energy consumption with electrocoagulation systems, lying between 0.002 and 58 kWh $m^{-3}$ [38].

### IV.3.1.9 Electrodes stability and durability

In order to test the electrodes stability and durability over time, a sequential fed batch trial was performed. The reactor was filled with fresh synthetic effluent, at each 180 min, to guarantee the same initial pollutants concentration during four consecutive tests. Figure IV.8a and Figure IV.8b represent TPh and COD removal, respectively. Even though COD removal remained practically unchanged (38.5–41.5 %), a slight difference was obtained in TPh removal efficiency (86.3–77.7 %).

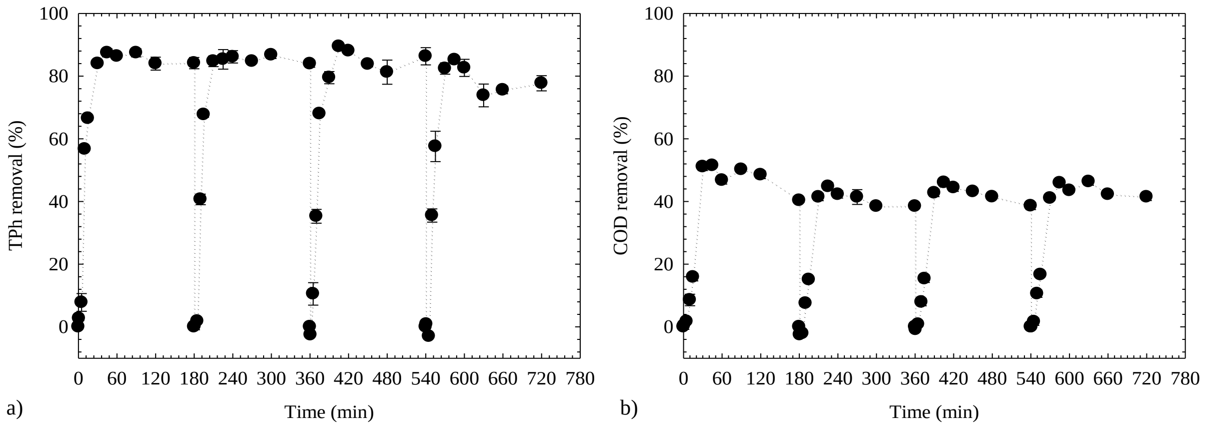

**Figure IV.8. Effect of electrodes reuse on a) TPh and b) COD removal by electrocoagulation process (pH=3.2, current density=250 A $m^{-2}$, distance between electrodes=1.0 cm, [NaCl]=1.5 g $L^{-1}$, Zn anode/SS cathode).**

Figure IV.9 represents the zinc anode loss, as well as the respective mass loss over time, during the sequential fed batch trials. It was found that after four trials, although the EG process has almost spent all the anode zinc (remaining the stainless steel intact) the efficiency of the process has remained practically unchanged. The dissolution of the anode material can be theoretically calculated based on Faraday's law (Equation (IV.6)) [21].

$$m_{\text{metal theoretical}}\ (\text{g}) = \frac{\text{I t M}_w}{\text{z F}} \qquad \textbf{(IV.6)}$$

Where I corresponds to current intensity (A), t to the time of ECG process (s), $M_w$ to the molar ratio of the metal (g $mol^{-1}$), $z$ to the valence electrons of the metal and $F$ to the Faraday's constant (96485 C $mol^{-1}$). The experimental dissolution value was determined by the difference between the initial and final mass of the zinc electrode, i.e. before and after the treatment process. In theory, the zinc mass loss would be 3.07 g. The values experimentally obtained support the theoretical with the exception of the last reuse, in which the anode would not have much material to dissolve into solution.

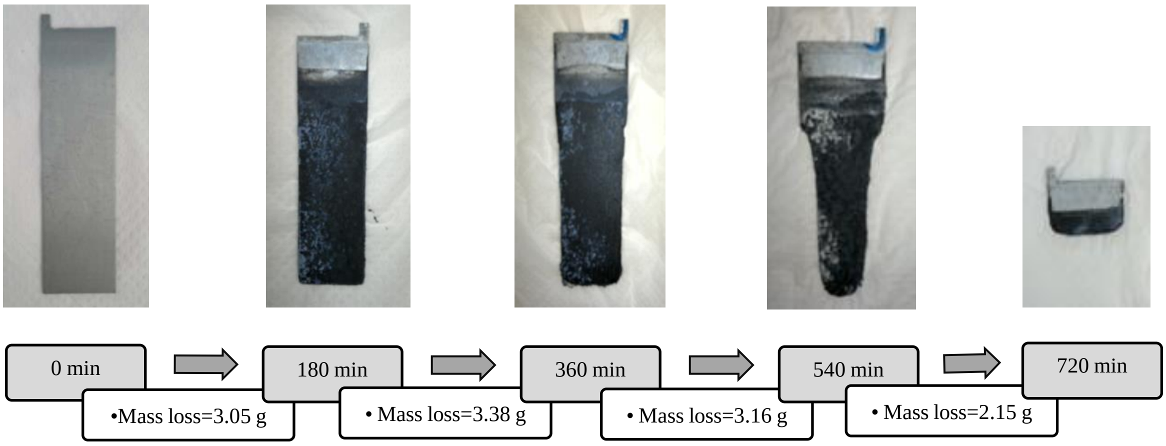

**Figure IV.9. Scheme of the mass loss of the zinc anode along reuses (pH=3.2, current density=250 A $m^{-2}$, distance between electrodes=1.0 cm, [NaCl]=1.5 g $L^{-1}$, Zn anode/SS cathode).**

### IV.3.2 APPLICATION TO A REAL EFFLUENT

After optimising the operating parameters, those conditions were applied to the treatment of a real olive mill effluent. The main features of the wastewater are displayed in Table IV.1. As can be seen, this wastewater has an acidic character (pH 4), good conductivity, high phenolic content (740 mg GA $L^{-1}$) and organic matter (22650 mg$O_2$ $L^{-1}$). The values obtained are within the characteristic range for this type of effluent [10,13,39]. High eco-toxicological impact with Vibrio Fisheri bacteria was also detected. The $EC_{20}$ value could not be measured which leads to the conclusion that the most dilute solution (6.3 %) has the ability to inhibit more than 20 % of bacteria, indicating that the olive mill effluent has a high toxicity.

Three treatments were performed with the real effluent in different conditions: filtered without NaCl addition (1), filtered with NaCl addition (2) and without filtration and NaCl addition (3). Even though final results seem quite similar, Figure IV.10a shows that experiments 1 and 2 led to the highest TPh removal values in less reaction time; for example at 90 min these two experiments achieved TPh removal values around 55.5–59.9 %, whereas for experiment 3 only 45.7 % was obtained. Nonetheless, at the same time and as before for the synthetic effluent, for COD removal (Figure IV.10b), the values for all assays were lower when compared to the phenolic content removal. There is no significant difference between trials, besides a slightly higher removal for the experiment 1 (19.5 %). Probably, during the treatment process, the initial phenolic acids are transformed into more refractory intermediates, which already had no phenolic character, but they may be accounted as organic matter. The obtained values are still far from the limits of discharge to the environment. Comparing the trend of the simulated effluent to the real one without NaCl, it appears that the evolution of pH of the medium in the latter case (Figure IV.10c) was too slow (at 15 min: simulated effluent–pH=7.3, real effluent without NaCl–pH=3.8–4.3), inhibiting the achievement of the required values to allow the dissolved metal ions ($Zn^{2+}$) to form metal hydroxides, leading to a high removal of pollutants.

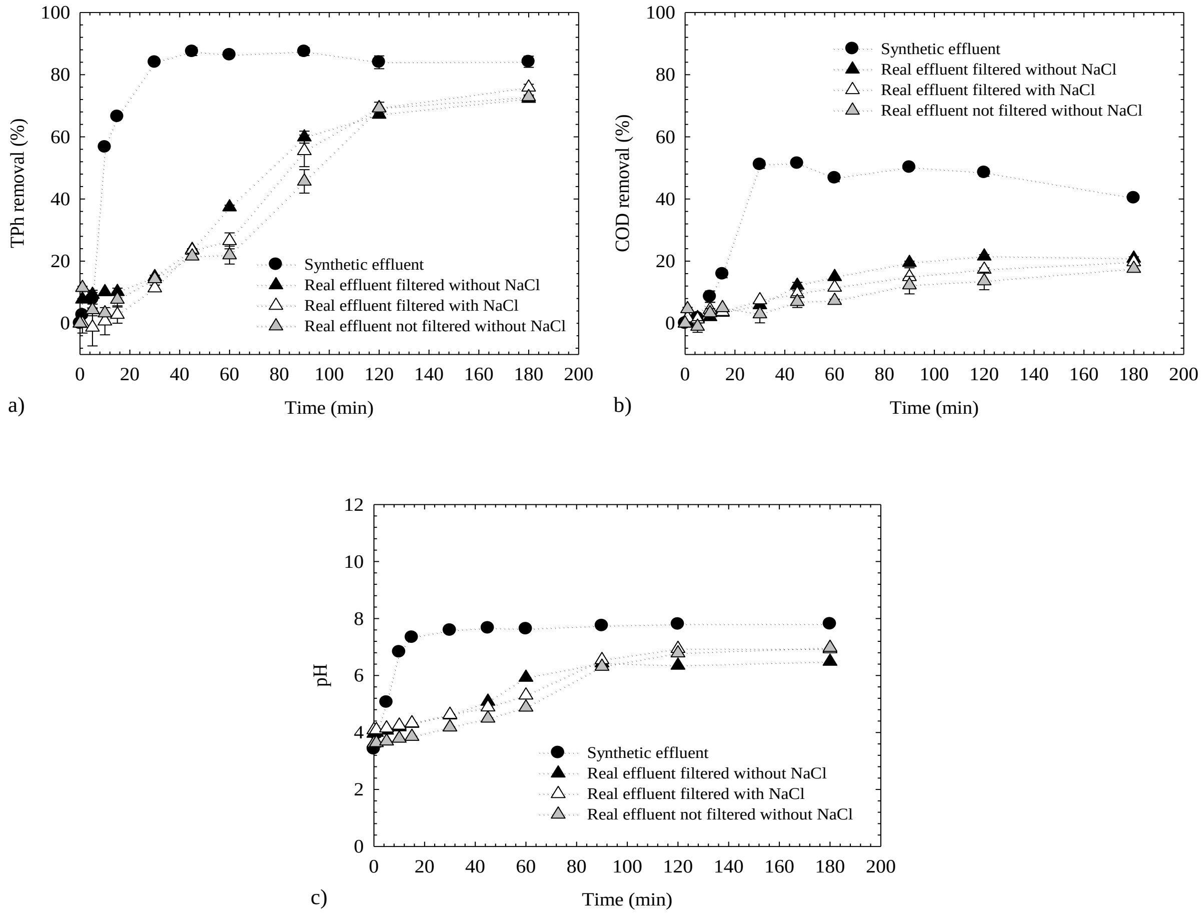

**Figure IV.10. a) TPh removal, b) COD removal and c) pH profiles for the synthetic and real effluent with the best operating conditions (pH=3.2, current density=250 A $m^{-2}$, distance between electrodes=1.0 cm, [NaCl]=1.5 g $L^{-1}$, Zn anode/SS cathode).**

The experiment 1 was the chosen to continue the tests with the real effluent, firstly because it leads to the slightly higher COD efficiency and secondly because it does not need the introduction of reagents (NaCl), which would make the process more costly.

As aforementioned, during the process of ECG, electrodes are subjected to electrochemical reactions that promote their dissolution, mainly for the anode where there is a great loss of mass to solution. In the test with the real effluent, the experimental mass loss of the zinc electrode was 3.11 g, very closely to the theoretical one (3.07 g).

Figure IV.11 shows the concentration of zinc ion over time for the simulated and real effluent depuration, which is above the commonly industrial limit used for discharge in the sewer (5 mg Zn $L^{-1}$).

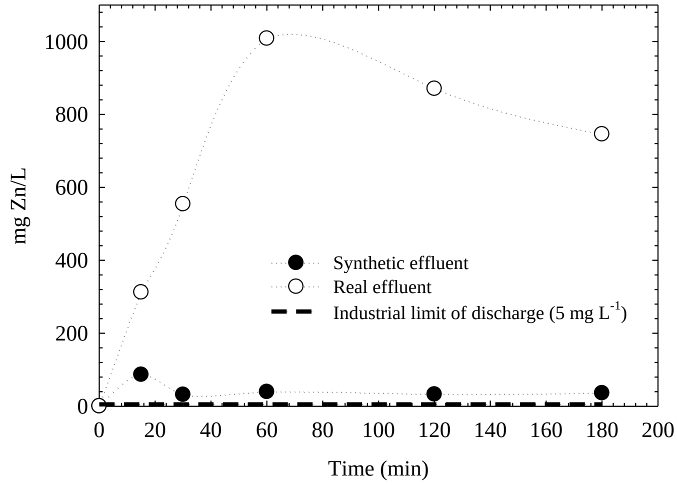

**Figure IV.11. Zn concentration in solution over time for the synthetic and real effluent.**

The dissolution of the zinc electrode is mainly due to the pH medium and the major dissolution of zinc occurs when pH is acidic. Once pH medium reaches neutral or basic values, the dissolved metals tend to form $Zn(OH)_2$ and as a result zinc concentration in the solution decrease. This analysis also indicates that most of the dissolved zinc was removed by precipitation and/or flotation of the pollutants and only one portion stayed dissolved in the effluent (Table IV.3).

**Table IV.3. Zinc mass.**

| Masses | Synthetic effluent (g) | Real effluent (g) |
|---|---|---|
| Zn anode ($t$=0 min) | 14.26 | 14.24 |
| Zn anode ($t$=180 min) | 11.20 | 11.13 |
| Mass loss | 3.06 | 3.11 |
| Zn ions in solution ($t$=180 min) | 0.036 | 0.75 |
| Zn removed by precipitation or flotation | 3.02 | 2.36 |

Regarding eco-toxicity, the $EC_{20}$ value, at the beginning and after the treatment, was not measured by the equipment, because the most dilute solution of the method has still the ability to inhibit more than 20 % of bacteria, and the $EC_{50}$ value decreased from 4 to 3 % after the application of the ECG process, which means that the treatment failed to remove the toxicity of the effluent.

Moreover, the obtained electrical energy consumption result for the real wastewater was 34 kWh $m^{-3}$. This value is somehow lower than the one achieved for the synthetic effluent (40 kWh $m^{-3}$) possibly due to its higher conductivity for the electrical current of 5.94 mS $cm^{-1}$ (Table IV.1), resulting then in a lower resistance of the medium and a lower power consumption by the process.

## IV.4 CONCLUSIONS

The depuration of a simulated and a real olive mill effluent was investigated in an electrocoagulation process using a Zn anode.

The treatment of the simulated effluent was strongly affected by the initial pH, since this parameter determines the quantity of ions that are released to the liquid medium and the formation of metal hydroxides necessary to remove pollutants from the system. In addition, depending on the type of the salt added, the process efficacy is also greatly affected. In its turn, current density had a sparingly impact, as well as the type of the cathode used. Moreover, the effect of the distance between electrodes was quite negligible and a sequence of fed batch trails involving the electrodes reutilisation showed almost constant activity during the operation time for four experiments. The operating conditions that led to the optimum results were: initial pH of the effluent equal to 3.2, current density of 250 A $m^{-2}$, space between electrodes equal to 1.0 cm, 1.5 g $L^{-1}$ of NaCl and set of Zn anode/SS cathode. According to these parameters, it was achieved a phenolic content and organic load removal (measured as COD), around 84.2 % and 40.3 %, respectively. Regarding the real effluent filtered without the addition of NaCl, the treatment attained 72.3 % for TPh removal and 20.9 % for COD removal. The depuration system, for both simulated and real wastewater, allowed the reduction of the initial concentration of pollutants. However, eco-toxicological tests revealed a still ecological impact for the treated effluents. The energy consumption obtained for the treatment of the simulated and the real wastewater was 40 kWh $m^{-3}$ and 34 kWh $m^{-3}$, respectively.

In short, the electrocoagulation process was optimised. Although, none of the treatments would allow the wastewater to be able to be directly discharged into the aquatic medium within environmental legislation thresholds, this study can support that the electrocoagulation process may be used as a pre-treatment of another method, as for instance being previously applied for further electrochemical oxidation technology. The results attained for the degradation of the phenolic content of the olive mill wastewater may be most likely generalised for other agro-effluents.

## ACKNOWLEDGMENTS

The authors, AS Fajardo and RC Martins gratefully acknowledge the Fundação para a Ciência e Tecnologia, for financial support under the Doc grant (SFRH/BD/87318/2012) and Post-Doc grant (SFRH/BPD/72200/2010), respectively.

Filzinc company, Oiã – Potugal, is also acknowledged for providing zinc electrodes.

# REFERENCES

[1] G. Beaufoy, The environmental impact of olive oil production in the European Union: Practical options for improving the environmental impact, Report produced by European Forum on Nature, http://ec.europa.eu/environment/agriculture/pdf/oliveoil.pdf, 4 February 2014. Conservation and Pastoralism and the Asociación para el Análisis y Reforma de la Política Agro-rural.

[2] Roig A, Cayuela ML, Sánchez-Monedero MA (2006) An overview on olive mill wastes and their valorisation methods. Waste Manage. 26: 960–969.

[3] de-la-Fuente C, Clemente R, Martınez-Alcal I, Tortosa G, Bernal MP (2011) Impact of fresh and composted solid olive husk and their water-soluble fractions on soil heavy metal fractionation; microbial biomass and plant uptake. J. Hazard. Mater. 186: 1283–1289.

[4] El-Abbassi A, Kiai H, Hafidi A (2012) Phenolic profile and antioxidant activities of olive mill wastewater. Food Chem. 132: 406–412.

[5] Arvanitoyannis IS, Kassaveti A, Stefanatos S (2007) Olive oil waste treatment: a comparative and critical presentation of methods, advantages & disadvantages. Crit. Rev. Food Sci. Nutr. 47 (3): 187–229.

[6] Mollah MYA, Schennach R, Parga JR, Cocke DL (2001) Electrocoagulation (EC)—science and applications. J. Hazard. Mater. B84: 29–41.

[7] Mollah MYA, Morkovsky P, Gomesc JAG, Kesmezc M, Pargad J, Cocke DL (2004) Fundamentals, present and future perspectives of electrocoagulation. J. Hazard. Mater. B114: 199–210.

[8] Barrera-Díaz C, Bilyeu B, Roa G, Bernal-Martinez L (2011)Physicochemical aspects of electrocoagulation. Sep. Purif. Rev. 40 (1): 1–24.

[9] Un UT, Koparal AS, Ogutveren UB (2009) Electrocoagulation of vegetable oil refinery wastewater using aluminum electrodes. J. Environ. Manage. 90: 428–433.

[10] García-García P, López-López A, Moreno-Baquero JM, Garrido-Fernández A (2011) Treatment of wastewaters from the green table olive packaging industry using electro-coagulation. Chem. Eng. J. 170: 59–66.

[11] Adhoum N, Monser L (2004) Decolourization and removal of phenolic compounds from olive mill wastewater by electrocoagulation. Chem. Eng. Process. 43: 1281–1287.

[12] Inan H, Dimoglo A, Simsek H, Karpuzcu M (2004) Olive oil mill wastewater treatment by means of electro-coagulation. Sep. Purif. Technol. 36: 23–31.

[13] Hanafi F, Assobhei O, Mountadar M (2010) Detoxification and discoloration of Moroccan olive mill wastewater by electrocoagulation. J. Hazard. Mater. 174: 807–812.

[14] Coskun T, Ilhan F, Demir NM, Debik E, Kurt U (2012) Optimization of energy costs in the pretreatment of olive mill wastewaters by electrocoagulation. Environ. Technol. 33 (7): 801–807.

[15] Ün ÜT, Uğur S, Koparal AS, Öğütveren UB (2006) Electrocoagulation of olive mill wastewaters. Sep. Purif. Technol. 52: 136–141.

[16] Hong K, Chang D, Bae H, Sunwoo Y, Kim J, Kim D (2013) Electrolytic removal of phosphorus in wastewater with noble electrode under the conditions of low current and constant voltage. Int. J. Electrochem. Sci. 8: 8557–8571.

[17] Murthy UN, Rekha HB, Bhavya (2011) Performance of electrochemical oxidation in treating textile dye wastewater by stainless steel anode. Int. J. Environ. Sci. Dev. 2 (6): 484–487.

[18] Shakir IK, Husein BI (2009) LEAD removal from industrial wastewater by electrocoagulation process. Iraqi J. Chem. Petrol. Eng. 10 (2): 35–42.

[19] Vasudevan S, Lakshmi J (2011) Effects of alternating and direct current in electrocoagulation process on the removal of cadmium from water – a novel approach. Sep. Purif. Technol. 80: 643–651.

[20] Vasudevan S (2012) Effects of alternating current (AC) and direct current (DC) in electrocoagulation process for the removal of iron from water. Can. J. Chem. Eng. 90: 1160–1169.

[21] Vasudevan S, Lakshmi J, Kamaraj R, Sozhan G (2013) A critical study on the removal of copper by an electrochemically assisted coagulation: equilibrium, kinetics, and thermodynamics. Asia-Pac. J. Chem. Eng. 8: 162–171.

[22] Kamaraj R, Vasudevan S (2015) Evaluation of electrocoagulation process for the removal of strontium and cesium from aqueous solution. Chem. Eng. Res. Des. 93: 522–530.

[23] Valente GFS, Mendonça RCS, Pereira JAM, Felix LB (2013) Aplicação eletrodos de zinco para tratamento de efluentes de indústria de lacticínios por electrocoagulação, III Simpósio Internacional sobre gerenciamento de resíduos agro-pecuários e agro-industriais, São Pedro.

[24] Balice V, Cera O (1984) Acid phenolic fraction of the olive vegetation water determined by a gas chromatographic method. Grasas y Aceites 35 (5): 178–180.

[25] Soloman PA, Basha CA, Velan M, Balasubramanian N (2009) Electrochemical degradation of pulp and paper industry waste-water. J. Chem. Technol. Biotechnol. 84: 1303–1313.

[26] Basha CA, Soloman PA, Velan M, Miranda LR, Balasubramanian N, Siva R (2010) Electrochemical degradation of specialty chemical industry effluent. J. Hazard. Mater. 176: 154–164.

[27] Silva AMT, Nouli E, Xekoukoulotakis NP, Mantzavinos D (2007) Effect of key operating parameters on phenols degradation during $H_2O_2$-assisted $TiO_2$ photocatalytic treatment of simulated and actual olive mill wastewaters. Appl. Catal. B Environ. 73: 11–22.

[28] Greenberg A, Clesceri L, Eaton A (1992) Standard Methods for the Examination of Water and Wastewater, 18th ed., American Public Health Association, Washington DC.

[29] Esplugas S, Contreras S, Ollis D (2004) Engineering aspects of the integration of chemical and biological oxidation: simple mechanistic models for the oxidation treatment. J. Environ. Eng. 130: 967–974.

[30] Cañizares P, Martínez L, Paz R, Sáez C, Lobato J, Rodrigo MA (2006) Treatment of Fenton-refractory olive oil mill wastes by electrochemical oxidation with boron-doped diamond anodes. J. Chem. Technol. Biotechnol. 81: 1331–1337.

[31] Pourbaix M (1966) Atlas of electrochemical equilibria in aqueous solutions, first ed., Pergamon Press, Oxford.

[32] Chithra K, Thilakavathi R, Murugan AA, Marimuthu C, Balasubramanian N (2008) Treatment of textile effluent using sacrificial electrode. Mod. Appl. Sci. 2 (4): 38–43.

[33] Turro E, Giannis A, Cossu R, Gidarakos E, Mantzavinos D, Katsaounis A (2011) Electrochemical oxidation of stabilized landfill leachate on DSA electrodes. J. Hazard. Mater. 190: 460–465.

[34] A-Mohammed A (2007) Electrocoagulation of phenol for wastewater treatment. Iraqi J. Chem. Petrol. Eng. 9: 37–41.

[35] Bonfatti F, De Battisti A, Ferro S, Lodi G, Osti S (2000) Anodic mineralization of organic substrates in chloride-containing aqueous media. Electrochim. Acta 46: 305–314.

[36] Fulladosa E, Murat JC, Villaescusa I (2005) Study on the toxicity of binary equitoxic mixtures of metals using the luminescent bacteria *Vibrio fischeri* as a biological target. Chemosphere 58: 551–557.

[37] Fulladosa E, Murat JC, Martínez M, Villaescusa I (2005) Patterns of metals and arsenic poisoning in *Vibrio fischeri* bacteria. Chemosphere 60: 43–48.

[38] Kuokkanen V, Kuokkanen T, Rämö J, Lassi U (2013) Recent applications of electrocoagulation in treatment of water and wastewater—a review. Green Sustain. Chem. 03: 89–121.

[39] Panizza M, Cerisola G (2006) Olive mill wastewater treatment by anodic oxidation with parallel plate electrodes. Water Res. 40: 1179–1184.

# V. REACTIVE BLACK 5 DYE ELIMINATION FROM AQUEOUS SOLUTIONS BY USING ALUMINIUM ANODES IN –BATCH AND –RECIRCULATION FLOW ELECTROCOAGULATION SYSTEMS

AS Fajardo[a], RC Martins[a], DR Silva[b], CA Martínez-Huitle[b] and RM Quinta-Ferreira[a]

[a] CIEPQPF – Centro de Investigação em Engenharia dos Processos Químicos e dos Produtos da Floresta; GERST – Group on Environment, Reaction, Separation and Thermodynamics; Department of Chemical Engineering, Faculty of Sciences and Technology, University of Coimbra, Pólo II, Rua Sílvio Lima, 3030-790 Coimbra, Portugal.

[b] LEAA – Laboratório de Eletroquímica Ambiental e Aplicada; Institute of Chemistry, Federal University of Rio Grande do Norte, Lagoa Nova, CEP 59078-970 Natal, RN, Brazil.

*Submitted to Industrial & Engineering Chemistry Research*

## ABSTRACT

An electrocoagulation (EC) process was employed to remove the Reactive Black 5 (RB5) from aqueous solutions by using batch-stirred and recirculation flow reactor configurations. Different operating conditions, such as current density, initial pH value, initial dye concentration, sacrificial anode materials and stirring rate were tested with the synthetic wastewater in order to optimise the treatment. The optimal operating conditions achieved for both systems were: current density of 16 mA $cm^{-2}$, $pH_0$ of 6, 100 mg $L^{-1}$ of RB5 and Al anodes (and 800 rpm for the batch-stirred setting). These parameters at the batch-stirred EC system led to 76 % and 97 % of decolourisation after 45 and 120 min of operation, with an energy consumption of 5 and 14 kWh $m^{-3}$, respectively. For recirculation flow system, complete colour removal was attained in 10 and 120 min requiring 2 kWh $m^{-3}$ and 22 kWh $m^{-3}$ of energy consumed, respectively. The behaviours observed at each one of the EC systems (–batch and –recirculation flow) are related to the way how the liquid was mixed and the location where samples were taken. In the batch-stirred system, a real textile wastewater was also treated applying Al or Zn anodes. Results clearly showed that the EC process is a promising alternative to depurate effluents containing dyes, since it guarantees the legal limits values of the wastewater to be discharged into the aquatic medium.

## V.1 INTRODUCTION

The large worldwide production of dye-containing wastewaters remains an important ecological issue due to the stability of the compounds, their low biodegradability and carcinogenic character. The natural streams contamination and aesthetic problems motivate the scientific community to search novel effective and inexpensive strategies for treating these industrial effluents [1]. Electrocoagulation (EC) is a widely accepted technology, since it is an easy system to operate, requires low equipment costs, maintenance and chemical consumption. Moreover, low quantity of sludge is produced when compared to the traditional chemical coagulation/flocculation processes [2–4]. EC uses sacrificial metal electrodes immersed in polluted water by applying electric current, promoting their dissolution. The metal ions formed in solution at an appropriate pH favour the generation of different coagulant species and metal hydroxides that destabilise and aggregate suspended particles or precipitate and adsorb dissolved contaminants [5]. Several studies highlight the high efficiency of EC to remove colour from dye effluents. However, this process efficiency depends on the operating parameters, such as initial pH, dye concentration, applied current density as well as reactor design [1]. Based on the existing literature, many works about EC approach have been performed by using batch systems with magnetic stirring to treat specific dyes, e.g. Acid Black 1, Acid Black 52, Acid Black 172, Acid Black 194, Acid Blue 19, Acid Red 2, Acid Red 14, Acid Red 87, Acid Yellow 23, Acid Yellow 220, Basic Violet 3, Basic Blue 9, Direct Brown 2, Disperse Blue 3, Reactive Black 5, Reactive Blue 4, Reactive Red 43 [6–19] or even real effluents [20,21]. Also, few studies have been developed with a batch recirculation flow configuration to depurate this kind of wastewaters [22–24]. Nonetheless, to the best of our knowledge, no enough attempts were reported comparing the performance of a batch stirred and a recirculation flow electrocoagulation systems for removing organic pollutants [25]. Therefore, this work is focused on the comparison of these two arrangements to remove the Reactive Black 5 (RB5) dye from aqueous solutions by applying EC approach. The effect of the current density, initial pH and initial concentration of the pollutant was evaluated on the colour and chemical oxygen demand (COD) removals, using sacrificial Al anodes. In order to extend the study, batch-stirred experiments were carried out with Zn anodes in order to compare their efficiency to the Al electrodes, in the treatment of the RB5 dye solutions and a real textile wastewater. The energy consumption was also estimated for both systems, batch and recirculation flow.

# V.2 EXPERIMENTAL

## V.2.1 SYNTHETIC AND REAL EFFLUENT

An aqueous solution with 100 mg $L^{-1}$ of Reactive Black 5 dye (RB5) was used as the model synthetic effluent. No purification was applied to the reagent before use. The characteristics and the chemical structure of the dye are presented in Table V.1.

**Table V.1. Characteristics and chemical structure and of the Reactive Black 5 dye.**

| Colour Index name | M (g $mol^{-1}$) | $\lambda_{max}$ (nm) | Chemical structure |
|---|---|---|---|
| Reactive Black 5 dye | 991.82 | 597 | 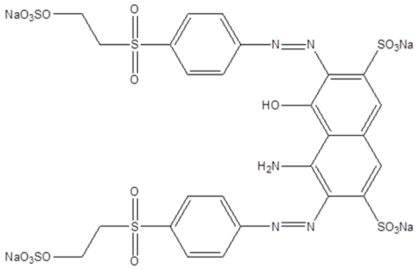 |

Some experiments were also performed with a previously filtered real textile effluent that was collect from a textile industry located in Portugal. The main features of the simulated and the actual wastewaters are displayed in Table V.2. As can be seen, both effluents have very similar pH conditions (pH=5.99–6.51). The synthetic effluent has low conductivity and low chemical oxygen demand (COD) (91.3 mS $cm^{-1}$ and 52 $mgO_2$ $L^{-1}$) when compared to the real wastewater (302.5 mS $cm^{-1}$ and 196 $mgO_2$ $L^{-1}$). Conversely, its absorbance is 9 times higher than the actual wastewater. According to the Portuguese Decree-Law 236/98 of 1st August, an effluent to be directly discharge into natural streams, its COD must be under 150 $mgO_2$ $L^{-1}$. Furthermore, colour must not be detected when diluted 20 times. Therefore, in order to attend the environmental legislations, the COD and colour removals were chosen as the main parameters to be monitored during the treatment of the effluent.

**Table V.2. Main characteristics of the synthetic (100 mg $L^{-1}$ of Reactive Black 5) and real effluents.**

| Characteristics | Synthetic effluent | Real effluent |
|---|---|---|
| pH | 6.00±0.36 | 6.51±0.04 |
| Conductivity (mS $cm^{-1}$) | 91.3±0.1 | 302.5±0.7 |
| Abs (a.u.) | 2.289±0.009 | 0.238±0.001 |
| COD (mgO2 $L^{-1}$) | 52±1 | 196±2 |

### V.2.2 ELECTROCOAGULATION SYSTEMS AND PROCEDURE

The EC process was accomplished using two different electrochemical reactor arrangements. One of them consisted in a Perspex batch-stirred reactor under controlled temperature (25±5 °C) and atmospheric pressure [26]. In each experiment, the reactor was filled with 1 L of the model solution or real effluent and, it was stirred with a magnetic stirrer at 300 or 800 rpm during 360 min by employing a stir plate Nahita Blue 692. Monopolar electrodes in parallel connections were tested. Two-flat anodes (Al material) and cathodes (stainless steel material), with an electrode gap of 0.5 cm, were linked to a DC Power Supply HY3010 Kaise (I=0.25–1.0 A) (Figure V.1a). These electrodes had an effective individual area of 31.8 cm$^2$, i.e. the anodic and cathodic areas were in total equal to 63.6 cm$^2$ in each case. Before each experiment, the electrodes were washed with a diluted HCl solution to clean the impurities on their surface.

The second configuration arrangement was based on a flow cell system working with a MINIPA MPL-3305M power supply (I=0.25–1.0 A) (Figure V.1b). Disk format electrodes were employed (Al as anode and stainless steel as cathode) with an electroactive area of 63.6 cm$^2$ and were placed in parallel with an inter-electrode gap of 1.2 cm. In each experiment, the reservoir was filled with 1 L of synthetic solution and recirculated through the system by a centrifugal pump working at 160 L h$^{-1}$, during 240 min. The experiments were conducted at mild conditions of pressure and temperature (30±5 °C).

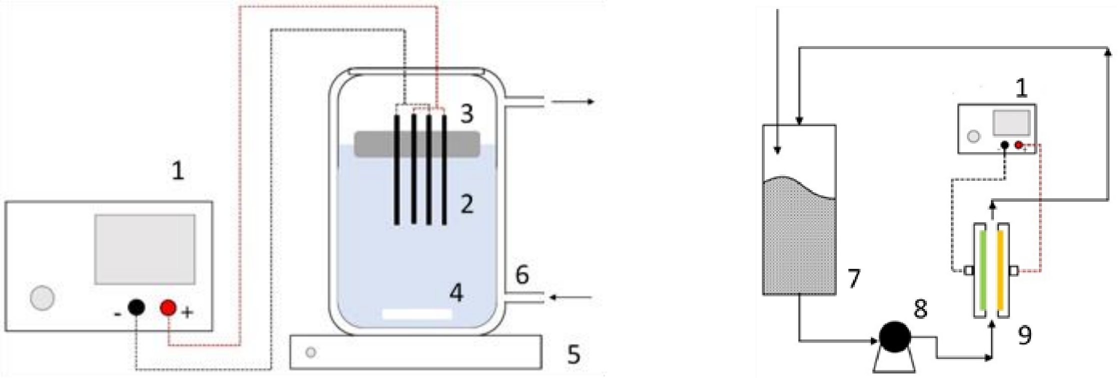

a) b)

**Figure V.1. (a) Batch and (b) flow cell electrocoagulation systems. (1-DC power supply, 2-Electrodes (2 anodes + 2 cathodes, 3-Floater, 4-Magnetic stirrer, 5-Stir plate, 6-Double wall for water recirculation, 7-Reservatory, 8-Pump, 9-Electrochemical flow cell).**

The concentration of 1.5 g L$^{-1}$ of NaCl was added to both systems in order to promote higher conductivity to the synthetic solution and real effluent. The conductivity was measured using a Consort C863 measurer and the initial pH value was adjusted between 3 and 9, using NaOH 3 M or $H_2SO_4$ 2 M whenever necessary. This parameter was followed (HANNA pH meter) but not adjusted during the treatment time. Samples were periodically withdrawn and immediately centrifuged at 4000 rpm (Hettich Zentrifugen – Rotofix 32A) and filtered with glass microfibres filters (VWR), particle retention of 1.2 µm, for further analysis.

### V.2.3 ANALYTICAL TECHNIQUES

The efficiency of the process was determined by UV-vis and chemical oxygen demand (COD) analysis. Colour removal was assessed by monitoring the decrease of the maximum absorbance of the Reactive Black 5 solution ($\lambda_{max.}$=597 nm) and the real dye effluent ($\lambda_{max.}$=574 nm) over time using an UV-vis spectrophotometer T60 PG Instruments (batch experiments) or Analytikjena SPECORD 210 PLUS (flow experiments). The percentage of decolourisation was estimated by the Equation (V.1):

$$\text{Colour removal (\%)} = \frac{(\text{Abs}_0 - \text{Abs}_t)}{\text{Abs}_0} \times 100 \tag{V.1}$$

where $\text{Abs}_0$ and $\text{Abs}_t$ correspond to the average absorbance at the beginning of the reaction and after an electrolysis time t, respectively.

COD was evaluated by the closed reflux procedure according to Standard Methods (5250D) [27]. In this technique, samples were digested in a thermal reactor (Eco 25, VELP Scientifica) at 150 °C during 120 min and then the absorbance was measured in a photometer (Photolab S6, WTW). The calibration curve was prepared using standard solutions of potassium hydrogen phthalate ($C_8H_5KO_4$) with COD values within the range 0–100 $\text{mgO}_2\ \text{L}^{-1}$ or 0–1200 $\text{mgO}_2\ \text{L}^{-1}$, being the absorbance measured at 445 or 605 nm, respectively. Analytical determinations were accomplished at least in duplicate to minimise experimental errors and the maximum deviations were 10 or 8 %, for colour and COD removal, respectively.

The energy consumption (EC) per volume of treated effluent was determined in terms of kWh $m^{-3}$ according to Equation (V.2):

$$\text{EC}(\text{kWh m}^{-3}) = \frac{\text{E}_{\text{cell}}\ \text{I t}}{\text{V}} \tag{V.2}$$

where $E_{cell}$ corresponds to the average potential difference of the cell (V), I is the current intensity applied (A), t expresses the electrolysis time (h) and V is the solution volume (L).

## V.3 RESULTS AND DISCUSSION

### V.3.1 BATCH STIRRED SYSTEM

#### V.3.1.1 Effect of stirring rate

The stirring rate provided to reaction systems allows to maintain the homogeneity of the process, avoiding the formation of a gradient of concentration inside the reactor. This operating condition plays a significant role for the transport in the solution of the electrogenerated ions. Thus, the effect of the stirring rate on the performance of EC experiments was evaluated for treating 100 mg $L^{-1}$ of RB5 at 300 and 800 rpm by applying 4 mA $cm^{-2}$ at $pH_0$ 6 and NaCl concentration of 1.5 g $L^{-1}$, and considering an electrode distance of about 5 mm. Figure V.2 shows colour and COD (see inset in Figure V.2) removals, as a function of time. As can be observed, similar behaviour was attained at 300 and 800 rpm for colour and COD removals. However, it is important to indicate that, there was a slight increase of around 7 % in the decolourisation of solution when 800 rpm was used as stirring rate. This behaviour can be related to the fact that raising the stirring rate, the mobility of the electrogenerated ions is also intensified, leading to a positive effect on the mass transfer [28,29], which results in a higher colour removal. After 240 min of EC process, 85.6 % and 90.2 % of colour were removed at 300 and 800 rpm, respectively. Nevertheless, a modest improvement for the organic load reduction is achieved at 800 rpm, reaching 39.8 % after 90 min.

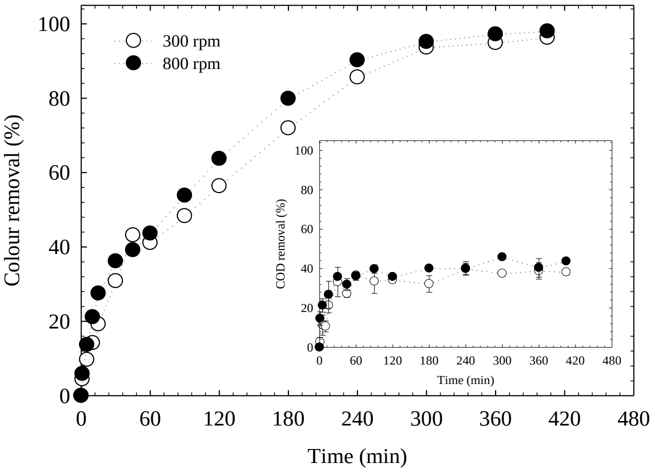

**Figure V.2. Effect of the stirring speed on colour removal over time. Inset: Effect of the stirring speed on COD removal over time. Operating conditions: batch system, current density=4 mA cm$^{-2}$, pH$_0$=6, 100 mg L$^{-1}$ of Reactive Black 5 and Al anode.**

### V.3.1.2 Effect of current density

The efficiency of the EC process can be affected by the current density (*j*) applied to the system, since it determines the amount of coagulant dissolved from the electrodes into the liquid. Also, the size and growth of the flocs as well as the hydrogen bubbles production rate are parameters that can be influenced by *j* [30]. For this reason, the effect of this parameter was evaluated at two different *j*, 4 and 16 mA cm$^{-2}$ for treating 100 mg L$^{-1}$ of RB5, keeping constant the other operating conditions: pH$_0$ 6, 800 rpm, distance between electrodes of 5 mm and NaCl concentration of 1.5 g L$^{-1}$. Figure V.3 displays the colour depletion of RB5 over time, showing that 97.1 % of colour removal was achieved after 90 min by applying 16 mA cm$^{-2}$. Conversely, 360 min are necessary to achieve similar decolourisation percentage when lower *j* is applied. This means that an increase in *j* promotes a high dissolution of the Al anodes (Equation (V.3)), which led to a higher number of metal hydroxide flocs [28,31] (Equation (V.4)) contributing, in this way, to a higher colour removal efficiency.

$$\mathrm{Al} \rightarrow \mathrm{Al}^{3+} + 3\mathrm{e}^{-} \qquad \textbf{(V.3)}$$

$$\mathrm{Al}^{3+} + 3\mathrm{H_2O} \rightarrow \mathrm{Al(OH)_3} + 3\mathrm{H}^{+} \qquad \textbf{(V.4)}$$

Furthermore, the presence of $\mathrm{Cl}^{-}$ ions can lead to increase the dissolution rate of the Al anodes due to the corrosion phenomena, then, when *j* is increased, the rate of the flocs, due to the introduction of NaCl in the system, can lead to the electrogeneration of active chlorine species. Also, with the *j* increase, their formation will improve as well as the efficiency of the process.

Regarding the COD removal (inset of Figure V.3), no significant differences were observed at both current densities. After 120 min of electrolysis, 40 % of COD removal was achieved, at both current conditions. This result indicates that the colour is rapidly removed because chromophore group at dye structure is fragmented but the organic matter is not completely eliminated due to the formation of other intermediates that are difficult to be removed.

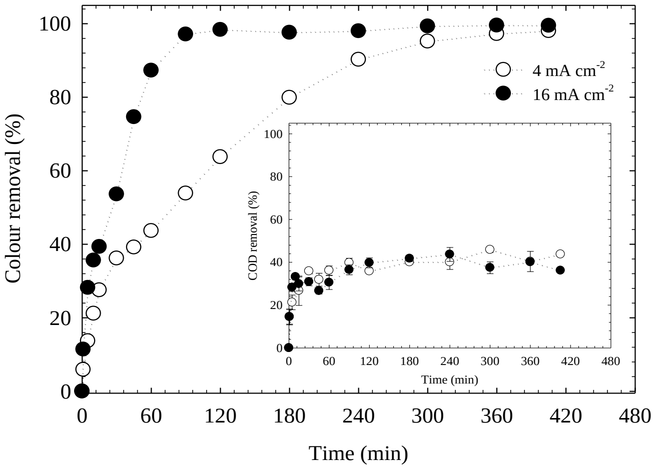

**Figure V.3. Effect of the current density on colour removal over time. Inset: Effect of the current density on COD removal over time. Operating conditions: batch system, stirring speed=800 rpm, $\mathrm{pH_0}$=6, 100 mg $\mathrm{L^{-1}}$ of Reactive Black 5 and Al anode.**

### V.3.1.3 Effect of initial pH

The pH of the effluent is an important operating parameter, since metal ions, at a suitable pH values can form wide ranges of coagulated species and metal hydroxides that precipitate and adsorb dissolved contaminants or destabilise and aggregate suspended particles. For that reason, this parameter was assessed at three different initial values, $\mathrm{pH_0}$ 3, 6 (raw effluent pH) and 9, which were adjusted with $\mathrm{H_2SO_4}$ or NaOH. During these experiments, the other operating conditions were maintained constant: stirring rate=800 rpm, current density=16 A $\mathrm{cm^{-2}}$, distance between electrodes=5 mm and [NaCl]=1.5 g $\mathrm{L^{-1}}$. Figure V.4 displays the colour removal, as a function of time, for treating 100 mg $\mathrm{L^{-1}}$ of RB5. As can be observed, a rapid decolourisation was achieved for $\mathrm{pH_0}$ 3 (91.8 %) after 5 min of treatment, followed by a steady drop until 30 min (68.5 %). After this time, colour removal rose gradually until

98.2 % (90 min) and remained almost constant thereafter. Meanwhile, the experiments at $pH_0$ 6 and 9 revealed similar removal trends over time, attaining colour depletions around 97 %, after 90 min of reaction. The inset of Figure V.4a shows that organic load decreased under different pH conditions. At $pH_0$ 3, a fast COD elimination (71.2 %) is attained after 10 min, corroborating the results obtained about the colour removal. According to the *Pourbaix* diagram [32], when the aluminium is in the presence of acidic solutions, the dissolution of the electrode material to the liquid is more intense, allowing greater availability of $Al^{3+}$ ions (Equation (V.3)) to generate $Al(OH)_3$ flocs (Equation (V.4)), which having their minimum solubility in the range of pH 5–6 and their predominant precipitation will occur near pH 6, where they tend to aggregate and remove pollutants from the liquid medium (see inset of Fig. 4a and Fig. 4b). This situation can be due to the fact that the various positively charged hydrolysis species $(\mathrm{Al(OH)^{2+}, Al(OH)_2^{+}, Al_2(OH)_2^{4+}, Al_6(OH)_{15}^{3+}, Al_7(OH)_{17}^{4+},\ Al_8(OH)_{20}^{7+},\ Al_{13}O_4(OH)_{24}^{7+},\ Al_{13}(OH)_{34}^{5+}})$ [33], normally present at $pH < 6$ (Figure V.4b), can adsorb the pollutants into the surface since they have opposite charges [34], promoting the destabilisation of the stable colloidal particles. This phenomenon is commonly called as charge neutralisation [35]. However, between 10–45 min of electrolysis, COD removal decreased to 29.7 %. This may occur because at $pH > 6$, the hydroxide ions present in the liquid medium compete with the organic pollutant for metal adsorption sites, promoting the restabilisation of the particles and thus the release of coloured compounds to the liquid medium. Moreover, after this time, there was probably a high coagulant dose in the medium that led to an increase in the removal up to 48.1 % at 60 min of treatment.

Although, the tests at $pH_0$ 6 and 9 also had a drop in COD removal at 45 min of electrolysis, no rapid decrease was observed when compared to that observed at $pH_0$ 3. At the end of the process, the highest COD removal (inset of Figure V.4a) was attained at $pH_0$ 9 (50.9 %), followed by $pH_0$ 3 (47.8 %) and $pH_0$ 6 (40.1 %). For the experiment with $pH_0$ 6, the initial phase corresponds to the lower dissolution of the electrode [32]. For this reason, the process of formation of hydroxide flocs in solution to aggregate pollutants is reduced, leading to lower efficiency of the EC process, as a function of COD removal.

As it can be observed in Figure V.4b, the medium pH increased for the tests with $pH_0$ 3 and $pH_0$ 6 due to the electrolysis of water molecules at the cathode which promotes their dissociation into hydrogen bubbles and hydroxyl ions, and consequently, causing an increase on the pH conditions of the medium. In the case of $pH_0$ 9, in the early phase of treatment, its value decreased to 8, probably due to the formation of aluminate $(\mathrm{Al(OH)_4^-})$ that it is an alkalinity consumer [36,37]. During the EC process with $pH_0$ 6, the solution rose to a pH 7–8, which is considered the ideal range to be used in biological processes or even directly discharged , not needing pH adjustment. Therefore, this $pH_0$ was selected for the subsequent experiments.

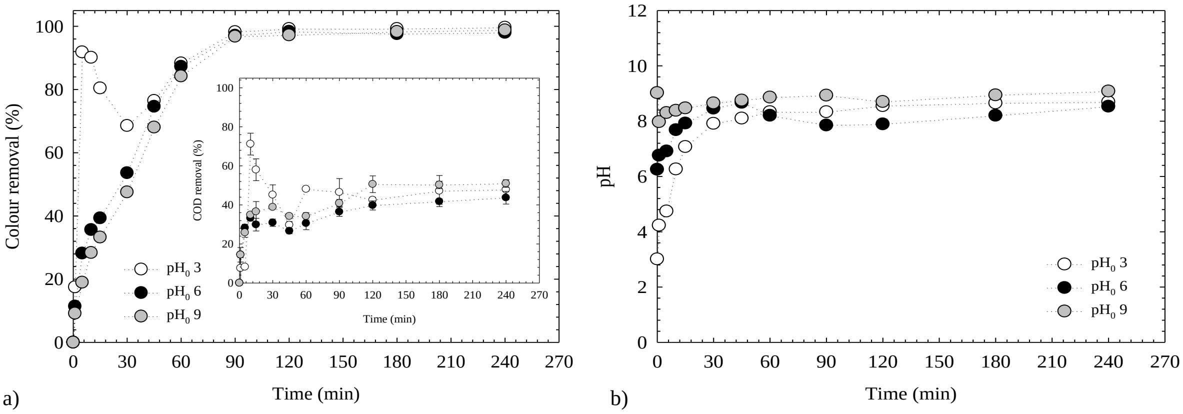

**Figure V.4. Effect of the initial pH on (a) colour removal and (b) pH medium over time. Inset (a): Effect of the initial pH on COD removal over time. Operating conditions: batch system, stirring speed=800 rpm, current density=16 mA cm$^{-2}$, Al anode and 100 mg L$^{-1}$ of Reactive Black 5.**

### V.3.1.4 Effect of dye concentration

EC process of three concentrations of RB5 (50, 100 and 200 mg L$^{-1}$) were studied by applying 16 mA cm$^{-2}$, at pH$_0$ 6, 5 mm of electrode distance and NaCl concentration of 1.5 g L$^{-1}$. Figure V.5a displays the colour removal over time. As it can be observed, there is a significant decolourisation efficiency (97.1–97.6 %) during the first 90 min of electrolysis when 50 and 100 mg L$^{-1}$ of dye were used as initial concentration. In the case of 200 mg L$^{-1}$ of RB5, 180 min of electrolysis were spent to attain 94.2 % of colour removal. Regarding COD removal (inset of Figure V.5a), the efficiency was dependent on the initial dye concentration. In fact, the test with 50 mg L$^{-1}$ of dye had a sharply depletion of 54.7 % after 10 min. By using 100 mg L$^{-1}$, 33.2 % of COD removal was achieved, whereas the assay using 200 mg L$^{-1}$ achieved only 22.7 % of depuration after 15 min. It is important to remark that, at higher concentrations (100 and 200 mg L$^{-1}$), longer electrolysis times were necessary to achieve 35 % of organic matter removals. This result indicates that the removal efficiency of a contaminant decreases with the increase of its initial concentration for the same current density, as already stated by Khandegar and Saroha [30]. This may be due to the fact that, for the same *j*, there is the same amount of Al$^{3+}$ electrogenerated, and consequently an equal amount of Al(OH)$_3$ is formed, and it is not enough amount to aggregate and sediment the organic dye molecules of the pollutant in excess, when the concentration of the RB5 is increased [6,21,38]. Therefore, 100 mg L$^{-1}$ of dye was chosen to continue the experiments, because after 90 min a satisfactory colour removal (97.1 %) was attained in the same line of 50 mg L$^{-1}$ (97.6 %), as can be observed in Figure V.5b.

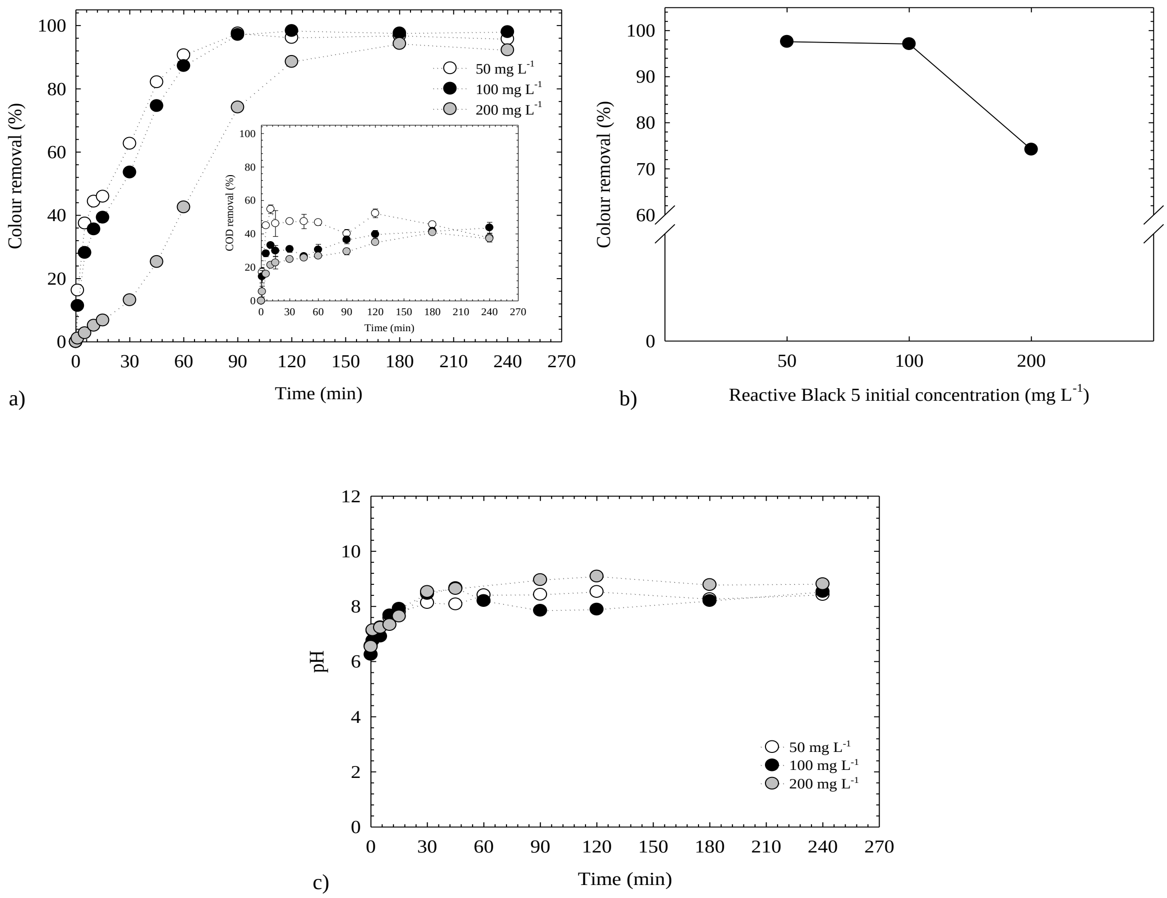

**Figure V.5. (a) Effect of the initial concentration of Reactive Black 5 on colour removal over time. (b) Colour removal profile at different initial Reactive Black 5 concentrations at 90 min of reaction. (c) Effect of the initial concentration of Reactive Black 5 on pH medium over time. Inset (a): Effect of the initial concentration of the pollutant on COD removal over time. Operating conditions: batch system, stirring speed=800 rpm, current density=16 mA cm$^{-2}$, Al anode and pH$_0$=6.**

### V.3.1.5 Effect of the nature of the anode material on the treatment of the synthetic and real effluent

The nature of the electrode determines the pollutant degradation mechanisms [39]. Thus, the efficiency of the system was evaluated with two different anode materials, aluminium (Al) and zinc (Zn), on the treatment of the synthetic and the real effluents. The experiments were performed in a monopolar mode at 800 rpm by applying 16 mA cm$^{-2}$ at the raw pH of the effluents. As it can be observed in Table V.2, the main features of the studied wastewaters are different. In fact, the absorbance of the real effluent (RE) is 9 times inferior to the synthetic effluent (SE). For this reason, the decolourisation of the real effluent (Figure V.6a) was quickly attained after 5 min of treatment, achieving 90.5 % and 69.8 % at Al and Zn anodes, respectively. At 180 min, these same experiments reached 96.5 % and 95.1 %, respectively. In the case of EC process of the synthetic effluent with Al anode, colour removal was gradually increased over time, achieving 97.1 % after 90 min of treatment, while the experiment with Zn, 67.3 % of decolourisation was achieved at the end of the process.

Regarding the organic matter removal, in terms of COD, for treating real and synthetic effluents by using Al and Zn electrodes, showed significant differences. When real effluent was treated by EC approach with Zn, 44.8 % of COD removal was reached while a 41.7 % was achieved at Al electrodes, after 90 min of treatment (Figure V.6b). In the case of the simulated effluent, Al anodes led to 36.5 % of removal, while 30.6 % with Zn was attained. According to the results, sacrificial Zn electrodes are more efficient for a real application. The final COD values are within or very close to the limits of discharge to the environment, for Zn and Al electrodes, respectively.

Comparing the treatment trend of both effluents by EC process with Zn, it seems that the evolution of pH of the medium at real effluent (Figure V.6c) was rapidly reached (pH > 8.6) favouring the substantial precipitation of $Zn(OH)_2$ flocs [32], and consequently, the removal was partially limited. Meanwhile, the pH conditions of the synthetic effluent (pH between 5 and 7) promote a low dissolution of the electrode in the form of $Zn^{2+}$ into the solution (Equation (V.5)). As a result, the formation of zinc hydroxide flocs in solution, by the reaction of $Zn^{2+}$ species with the hydroxyl anion formed at the cathode (Equation (V.6)), is reduced, leading to a low efficacy of the EC process.

$$\mathrm{Zn} \rightarrow \mathrm{Zn}^{2+} + 2\mathrm{e}^- \qquad \textbf{(V.5)}$$

$$\mathrm{Zn}^{2+} + 2\mathrm{OH}^- \rightarrow \mathrm{Zn(OH)}_2 \qquad \textbf{(V.6)}$$

In the meantime, among the tests with Al electrodes there were no significant differences in terms of COD removal (Figure V.6b). This may be justified by the fact that both experiments rapidly achieve the same suitable pH value for the formation of $Al(OH)_3$. Usually, these generated flocs have large surface area, being advantageous for a rapid adsorption of soluble organic compounds and trapping of colloidal particles.

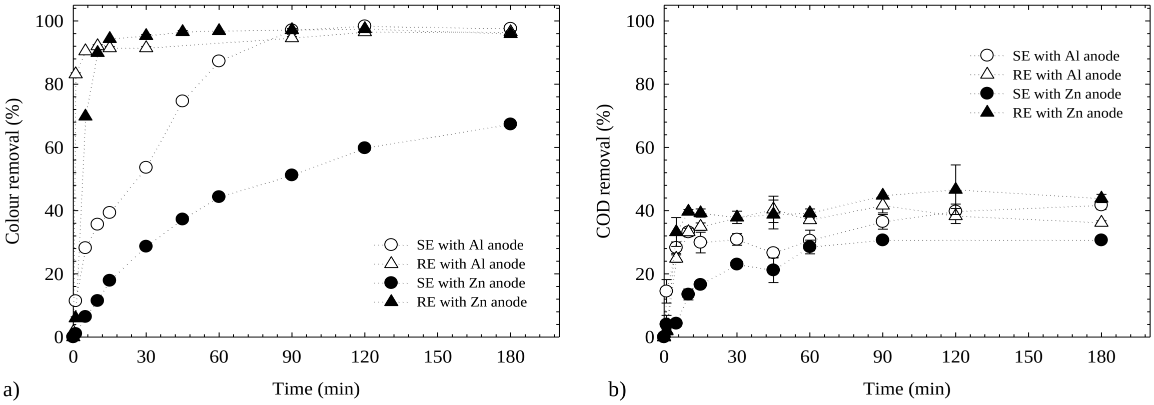

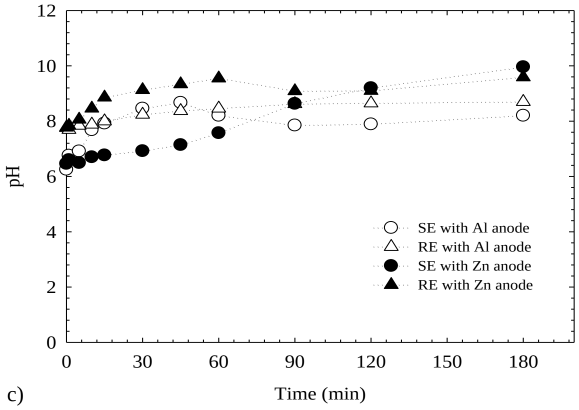

**Figure V.6. Effect of the nature of the anode material on (a) colour and (b) COD removal, as well as on pH medium over time, using a synthetic and a real effluents. Operating conditions: batch system, stirring speed=800 rpm, current density=16 mA cm$^{-2}$, pH$_0$=6 and 100 mg L$^{-1}$ of Reactive Black 5 (for synthetic effluent).**

## V.3.2 RECIRCULATION FLOW SYSTEM

Experiments in a recirculation flow system (FS) were also conducted in order to evaluate the effect of the different operating conditions including *j*, initial pH and the initial concentration of the pollutant on the efficiency of colour removal of RB5. These experiments will also be compared to those performed in the batch system (BS) with magnetic stirring.

### V.3.2.1 Effect of current density

The first parameter that was tested was the *j* at 4 and 16 mA cm$^{-2}$, using a pH$_0$ 6 and 100 mg L$^{-1}$ of RB5. Figure V.7 shows the colour removal as a function of the EC time and as it can be observed, in the first 5 min of operation, the efficiency on the colour decay for the flow system was similar (∼62 %) regardless the applied *j*. However, the colour removal efficiency was enhanced as a function of electrolysis time, achieving 94.8 % after 90 min and 97.6 % after 240 min by applying 16 mA cm$^{-2}$, while for lower *j* (4 mA cm$^{-2}$), decolourisation was about 80 % after 45 min of treatment, remaining constant until the end of the process. Another feature is that, after passing 0.5 Ah L$^{-1}$ of electrical charge, the colour removal was similar for both experiments (see inset of Figure V.7). However, higher removal is achieved when higher electrical charge was passed; then, it is possible when 16 mA cm$^{-2}$ is applied. This situation can be explained by a higher dissolution of the anode and thus, a higher quantity of flocs is formed to remove the pollutant, as the *j* raise [40]. By comparing electrocoagulation systems, batch and flow cells, in Fig. 7, the former achieved higher removal efficiency than that obtained at the latter. This can be due to the mass transport conditions in solution, which are favoured at flow system, allowing that a suitable mix is promoted between the electrogenerated coagulant and the pollutants present in the solution, improving the coagulation efficiency [41].

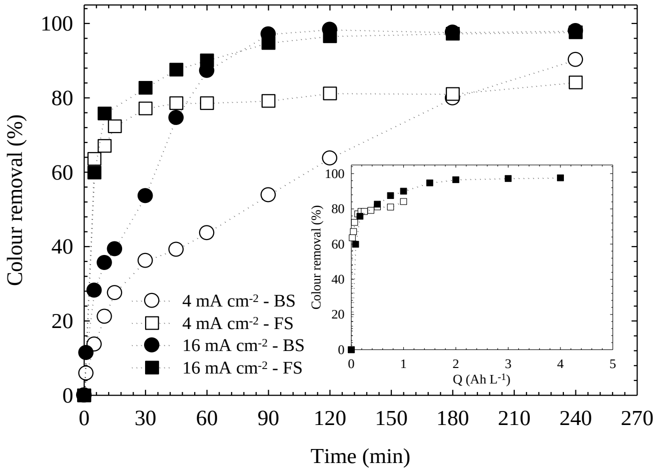

**Figure V.7. Effect of the current density on colour removal over time, for batch and flow systems. Inset: Colour removal as a function of the applied charge at different current densities for the flow system. Operating conditions: $pH_0$=6, 100 mg $L^{-1}$ of Reactive Black 5, stirring speed=800 rpm (batch system) and flow rate=160 L $h^{-1}$ (flow system).**

### V.3.2.2 Effect of initial pH

The initial pH was evaluated at three different values (3, 6 and 9), and compared for the two EC systems (Figure V.8) by applying 16 mA $cm^{-2}$. As can be observed, at $pH_0$=3 (Figure V.8a), both profiles follow a similar trend, achieving after 5 min of treatment, 91.8 % and 98 % of colour removal for batch and flow systems, respectively. After that time, a fall in colour decay occurred until 30 min of depuration. For the flow scheme, less 60 min were needed to achieve almost complete colour removal with respect to the efficacy of the batch arrangement. This decay can be explained as referred to batch system, in subsection V.3.1.3. Additionally, the difference in the removal rate for the two systems, in achieving again removals > 95%, can be justified due to the different pH evolution of the aquatic medium over time as shown in the inset of Fig. 8a, since this parameter determines the aluminium speciation in solution [21]. In the experiments at $pH_0$ 6 (Figure V.8b) and 9 (Figure V.8c), it is possible to observe that in the early stages of treatment, the colour removal rates for the flow systems are faster than those achieved at batch system. Probably, it is because of the flow system favours the mass transport conditions (better mixture between the coagulant and the dye).

In addition, when the pH is higher than 9, the $\mathrm{Al(OH)_4^-}$ anion is formed at the expense of the $Al(OH)_3$ (Equation (V.7)), diminishing the capacity of decolourisation, as already stated by other authors [21,37,42].

$$\mathrm{Al(OH)_3 + OH^- \leftrightarrow AlOH_4^-} \qquad \textbf{(V.7)}$$

In this study, it seems that the generation of $\mathrm{Al(OH)_4^-}$ begins to be more intense from pH 8, maintaining the efficacy of the process, but decreasing the colour rate. This can be observed for the batch systems, the liquid medium was above pH 8, during a short period of time for the experiment at $pH_0$=6 and during all the elapsed time for the assay at $pH_0$=9.

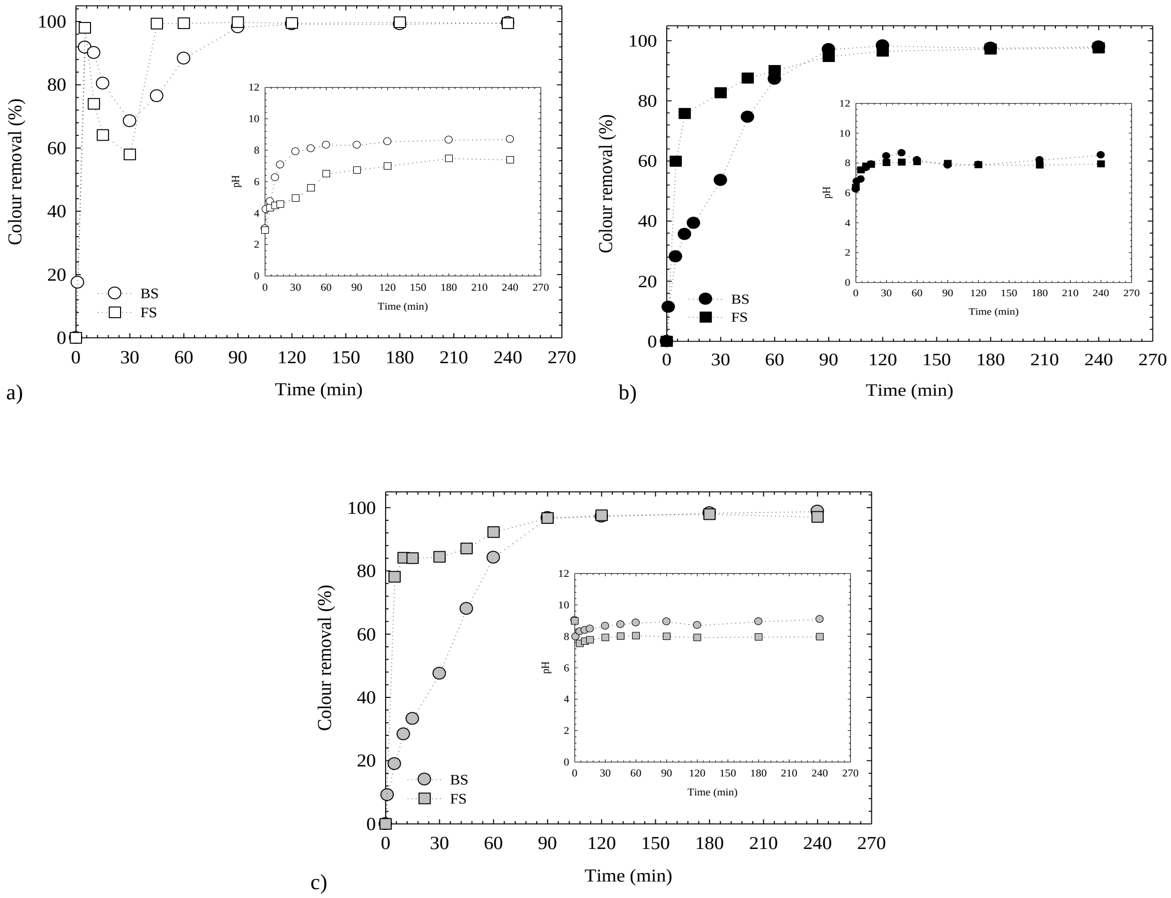
a) b) c)

**Figure V.8. Effect of the $pH_0$ at (a) 3, (b) 6 and (c) 9 on colour removal over time, for batch and flow systems. Insets: Evolution of pH medium over time. Operating conditions: current density=16 mA $cm^{-2}$, 100 mg $L^{-1}$ of Reactive Black 5, stirring speed=800 rpm (batch system) and flow rate=160 L $h^{-1}$ (flow system).**

### V.3.2.3 Effect of initial concentration of the dye

The effect of the initial RB5 concentration was evaluated in the range from 50 to 200 mg $L^{-1}$ (Figure V.9) for both systems by applying 16 mA $cm^{-2}$. Figure V.9a represents the colour removal over time for the experiments with 50 mg $L^{-1}$ of the initial dye concentration by using flow and batch systems. As can be observed, in the first 5 min of depuration, 68.9 % of colour removal was achieved by using flow cell, remaining almost constant up to 60 min. Under similar conditions, the colour decay for the batch system had a high increase, reaching 90.7 %, while a similar value is achieved after 120 min of treatment when flow configuration is used. For the assays at initial concentrations of 100 and 200 mg $L^{-1}$ of the RB5 (Figure V.9b and Figure V.9c), it is possible to observe that more efficient colour removal is achieved (100 mg $L^{-1}$–90.1 % and 200 mg $L^{-1}$–53.7 %) up to 60 min of treatment by using flow system. Afterwards, the removal values were very similar between batch and flow configurations until the end of the process.

Regarding the flow system (Figure V.9), an increase on the initial dye concentration (from 50 to 200 mg $L^{-1}$) results in a decrease on the removal efficiency (68.9–41.7 %) after 5 min of purification. Conversely, a rapid decolourisation for the experiment with a dye initial concentration of 100 mg $L^{-1}$ is observed, followed by those with 50 and 200 mg $L^{-1}$. This result demonstrates that the EC process provided very good results for all the studied initial concentrations because the removal was always higher than 90 % at the end of the treatment. In addition, it is worth mentioning that when the initial RB5 concentrations are lower (50–100 mg $L^{-1}$), the better is the colour decay rate, since for high initial dye concentrations, probably the adsorption capacity of metallic hydroxide flocs is not enough, as already stated by Sengil and Özacar [34] and Merzouk *et al.* [42].

These results show that even though for the initial reaction times the removal efficiencies measured in the flow system presents higher values, it is always possible to reach the same final degradation for the two reactors settings, with longer times for the batch system. This circumstance arises from the different operation modes and the way liquid samples are taken out from the EC systems. For the flow configuration, the liquid mixture is done through its external recirculation and samples are withdrawn at the outlet of the cell before its junction to the remaining liquid in the reservoir, not representing the conditions of the whole solution. Nevertheless, in final stages of the process, when maximum degradations are reached and recirculation promotes a good mixture, the conditions in the system will be about the same in any point of it. Conversely, in the batch reactor, the mixture of the system is carried out with a magnetic stirrer ensuring its total homogenization and thus, the effluent may have a uniform concentration throughout the process. For this reason, even at the initial times, the measured parameter values will represent the whole mixture in the bulk. Finally, similar removals are obtained for both systems at the end of the process because the effluents are equally mixed.

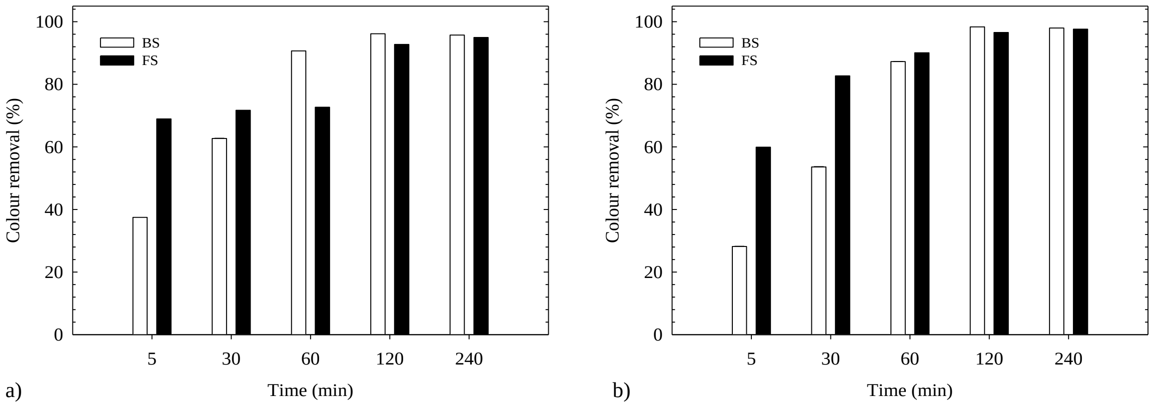

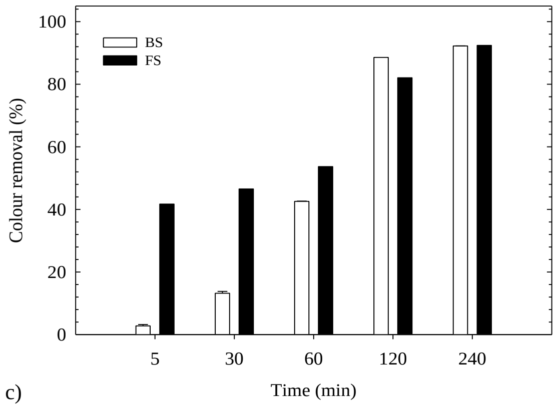

**Figure V.9. Effect of the initial Reactive Black 5 concentrations, (a) 50, (b) 100 and (c) 200 mg L$^{-1}$, on colour removal over time, for batch and flow systems. Operating conditions: current density=16 mA cm$^{-2}$, pH$_0$=6, stirring speed=800 rpm (batch system) and flow rate=160 L h$^{-1}$ (flow system).**

### V.3.2.4 Energy consumption

Taking into account the best operating conditions obtained for both EC systems (current density=16 mA cm$^{-2}$, pH$_0$=6 and [RB5]$_0$=100 mg L$^{-1}$), the energy consumption was determined since it is an important factor in EC process. This parameter was evaluated at two different colour removals (~76 % and ~97 %), once it is observed throughout the study that both EC systems have different removal rates in the early stages of the process, but higher colour removal occurs simultaneously. A colour decay of 76 % is reached in shorter times (10 min) using the flow system with lower power consumption (2 kWh m$^{-3}$), as indicated in the Figure V.10. Besides, more than 35 min were necessary at the batch configuration to achieve the same removal and consequently, it consumed 2.5-folds more of energy (5 kWh m$^{-3}$). Nevertheless, both systems spent the same treatment time to reach 97 % of removal, but lower energy consumption for the batch system (14 kWh m$^{-3}$) was needed.

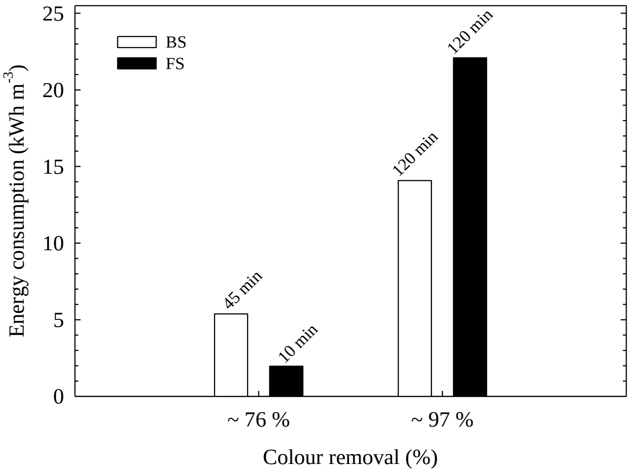

**Figure V.10. Energy consumption as a function of colour removal for batch and flow systems, at their respective time of treatment. Operating conditions: current density=16 mA cm$^{-2}$, pH$_0$=6, 100 mg L$^{-1}$ of Reactive Black 5, stirring speed=800 rpm (batch system) and flow rate=160 L h$^{-1}$ (flow system).**

## V.4 CONCLUSIONS

The elimination of the RB5 dye from aqueous solutions was performed by using Al anodes in –batch and –recirculation flow electrocoagulation systems. The effect of some operating conditions was tested and optimised. The current density, the nature of the anode and the dye concentration parameters had a strong effect on the process followed by a sparingly impact of the initial pH and the stirring rate. The operating conditions that led to the optimum results for both systems were: current density of 16 mA $cm^{-2}$, $pH_0$ of 6 and the initial concentration of the dye of 100 mg $L^{-1}$, Al anodes (and 800 rpm for the batch-stirred reactor). According to these parameters, using the batch-stirred EC system, after 45 and 120 min of operation, the colour decay increased from 76 % to 97 %, consuming 5 and 14 kWh $m^{-3}$, respectively. Regarding the recirculation flow EC system, only 10 min were necessary to achieve the 76 % of colour removal with 2 kWh $m^{-3}$; while to attain 97 % of decolourisation, 22 kW $m^{-3}$ of energy was consumed. The removal results greatly depend on how the liquid mixture is done. An actual textile effluent was also treated by applying Al or Zn anodes in the batch-stirred system, being obtained final satisfactory results in order to its discharge in aquatic medium.

In short, the EC process using these two systems seems to be a promising treatment to wastewaters containing dyes.

## ACKNOWLEDGMENTS

The authors, Ana S. Fajardo and Rui C. Martins gratefully acknowledge the Fundação para a Ciência e Tecnologia, for financial support under the Doc grant (SFRH/BD/87318/2012) and the IFCT 2014 programme (IF/00215/2014) with financing from the European Social Fund and the Human Potential Operational Programme, respectively. Financial support from National Council for Scientific and Technological Development (CNPq – 446846/2014-7 Brazil) is gratefully acknowledged.

Filzinc company, Oiã – Potugal, is also acknowledged for providing zinc electrodes.

## REFERENCES

[1] Brillas E, Martínez-Huitle CA (2015) Decontamination of wastewaters containing synthetic organic dyes by electrochemical methods. An up dated review. Appl. Catal. B. Environ. 166–167: 603–643.

[2] Mollah MYA, Schennach R, Parga JR, Cocke DL (2001) Electrocoagulation (EC)-science and applications. J. Hazard. Mater. B84: 29–41.

[3] Mollah MYA, Morkovsky P, Gomes JAG, Kesmez M, Parga J, Cocke DL (2004) Fundamentals, present and future perspectives of electrocoagulation. J. Hazard. Mater. B114: 199–210.

[4] Barrera-Díaz C, Bilyeu C, Roa G, Bernal-Martinez L (2011) Physicochemical aspects of electrocoagulation. Sep. Purif. Rev. 40 (1): 1–24.

[5] UN UT, Koparal AS, Ogutveren UB (2009) Electrocoagulation of vegetable oil refinery wastewater using aluminum electrodes. J. Environ. Manage. 90: 428–433.

[6] Daneshvar N, Sorkhabi HA, Kasiri MB (2004) Decolorization of dye solution containing Acid Red 14 by electrocoagulation with a comparative investigation of different electrode connections. J. Hazard. Mater. B112: 55–62.

[7] Golder AK, Hridaya N, Samanta AN, Ray S (2005) Electrocoagulation of methylene blue and eosin yellowish using mild steel electrodes. J. Hazard. Mater. B127: 134–140.

[8] Daneshvar N, Khataee AR, Ghadim ARA, Rasoulifard MH (2007) Decolorization of C.I. Acid Yellow 23 solution by electrocoagulation process: Investigation of operational parameters and evaluation of specific electrical energy consumption (SEEC). J. Hazard. Mater. 148: 566–572.

[9] Aleboyeh A, Daneshvar N, Kasiri MB (2008) Optimization of C.I. Acid Red 14 azo dye removal by electrocoagulation batch process with response surface methodology. Chem. Eng. Process. 47: 827–832.

[10] Zhang XD, Hao JD, Li WS, Jin HJ, Yang J, Huang QM, Lu DS, Xu HK (2009) Synergistic effect in treatment of C.I. Acid Red 2 by electrocoagulation and electrooxidation, J. Hazard. Mater. 170: 883–887.

[11] Durango-Usuga P, Guzmán-Duque F, Mosteo R, Vazquez MV, Peñuela G, Torres-Palma RA (2010) Experimental design approach applied to the elimination of crystal violet in water by electrocoagulation with Fe or Al electrodes. J. Hazard. Mater. 179: 120–126.

[12] Patel UD, Ruparelia JP, Patel M (2011) Electrocoagulation treatment of simulated floor-wash containing Reactive Black 5 using iron sacrificial anode. J. Hazard. Mater. 197: 128–136.

[13] Olad A, Amani-Ghadim AR, Dorraji MSS, Rasoulifard MR (2010) Removal of the alphazurine FG dye from simulated solution by electrocoagulation. Clean 38: 401–408.

[14] Pajootan E, Arami M, Mahmoodi NM (2012) Binary system dye removal by electrocoagulation from synthetic and real colored wastewaters. J. Taiwan Inst. Chem. Eng. 43: 282–290.

[15] Taheri M, Moghaddam MRA, Arami M (2012) Optimization of Acid Black 172 decolorization by electrocoagulation using response surface methodology. Iran. J. Environ. Health Sci. Eng. 9: 23–30.

[16] Wei M-C, Wang K-S, Huang C-L, Chiang C-W, Chang T-J, Lee S-S, Chang S-H (2012) Improvement of textile dye removal by electrocoagulation with low-cost steel wool cathode reactor. Chem. Eng. J. 192: 37–44.

[17] Amani-Ghadim AR, Olad A, Aber S, Ashassi-Sorkhabi H (2013) Comparison of organic dyes removal mechanism in electrocoagulation process using iron and aluminum anodes. Environ. Prog. Susain. Energy 32: 547–556.

[18] Ghernaout D, Al-Ghonamy AI, Messaoudene NA, Aichouni M, Naceur MW, Benchelighem FZ, Boucherit A (2015) Electrocoagulation of Direct Brown 2 (DB) and BF Cibacete Blue (CB) Using Aluminum Electrodes. Sep. Sci. Technol. 50(9): 1413–1420.

[19] Vidal J, Villegas L, Peralta-Hernández JM, González RS (2016) Removal of Acid Black 194 dye from water by electrocoagulation with aluminum anode. J. Environ. Sci. Health A. 51(4): 289–296.

[20] Kobya M, Demirbas E, Akyol A (2009) Electrochemical treatment and operating cost analysis of textile wastewater using sacrificial iron electrodes. Water Sci. Techn. 60(9): 2261–2270.

[21] Aoudj S, Khelifa A, Drouiche N, Hecini M, Hamitouche H (2010) Electrocoagulation process applied to wastewater containing dyes from textile industry. Chem. Eng. Process. 49: 1176–1182.

[22] Cañizares P, Martínez F, Jiménez C, Lobato J, Rodrigo MA (2006) Coagulation and Electrocoagulation of Wastes Polluted with Dyes. Environ. Sci. Technol. 40: 6418–6424.

[23] Zongo I, Maiga AH, Wéthé J, Valentin G, Leclerc J-P, Paternottea G, Lapicque F (2009) Electrocoagulation for the treatment of textile wastewaters with Al or Fe electrodes: Compared variations of COD levels, turbidity and absorbance. J. Hazard. Mater. 169: 70–76.

[24] Un UT, Aytac E (2013) Electrocoagulation in a packed bed reactor-complete treatment of color and cod from real textile wastewater. J. Environ. Manage. 123: 113–119.

[25] Parsa JB, Vahidian HR, Soleymani AR, Abbasi M (2011) Removal of Acid Brown 14 in aqueous media by electrocoagulation: Optimization parameters and minimizing of energy consumption. Desalination 278: 295–302.

[26] Fajardo AS, Martins RC, Quinta-Ferreira RM (2014) Treatment of a Synthetic Phenolic Mixture by Electrocoagulation Using Al, Cu, Fe, Pb, and Zn as Anode Materials. Ind. Eng. Chem. Res. 53: 18339−1834.

[27] Greenberg A, Clesceri L, Eaton A (1992) Standard Methods for the Examination of Water and Wastewater. American Public Health Association, Washington DC.

[28] Can OT, Bayramoglu M, Kobya M (2003) Decolorization of Reactive Dye Solutions by Electrocoagulation Using Aluminum Electrode. Ind. Eng. Chem. Res. 42: 3391–3396.

[29] Naje AS, Chelliapan S, Zakaria Z, Abbas SA (2015) Enhancement of an Electrocoagulation Process for the Treatment of Textile Wastewater under Combined Electrical Connections Using Titanium Plates. Int. J. Electrochem. Sci. 10: 4495–4512.

[30] Khandegar V, Saroha A (2013) Electrocoagulation for the treatment of textile industry effluent. A review. J. Environ. Manage. 128: 949–963.

[31] Kabdaşlı I, Arslan-Alaton I, Ölmez-Hancı T, Tünay O (2012) Electrocoagulation applications for industrial wastewaters: a critical review. Environ. Technol. Rev. 1(1): 2–45.

[32] Pourbaix (1966) Atlas of electrochemical equilibria in aqueous solutions, first ed., Pergamon Press, Oxford.

[33] Lekhlif B, Oudrhiri L, Zidane F, Drogui P, Blais JF (2014), Study of the electrocoagulation of electroplating industry wastewaters charged by nickel (II) and chromium (VI). J. Mater. Environ. Sci. 5(1): 111–120.

[34] Şengil IA, Özacar M (2009) The decolorization of C.I. Reactive Black 5 in aqueous solution by electrocoagulation using sacrificial iron electrode. J. Hazard. Mater. 161: 1369–1376.

[35] Aygun A, Yilmaz T (2010) Improvement of Coagulation-Flocculation Process for Treatment of Detergent Wastewaters Using Coagulant Aids. Int. J. Chem. Environ. Eng. 1(2): 97–101.

[36] Chen X, Chen G, Yue PL (2000) Separation of pollutants from restaurant wastewater by electrocoagulation. Sep. Purif. Technol. 19: 65–76.

[37] Kobya M, Hiz H, Senturk E, Aydiner C, Demirbas E (2006) Treatment of potato chips manufacturing wastewater by electrocoagulation. Desalination. 190: 201–211.

[38] Modirshahla N, Behnajady MA, Kooshaiian S (2007) Investigation of the effect of different electrode connections on the removal efficiency of Tartrazine from aqueous solutions by electrocoagulation. Dyes Pigments 74: 249–257.

[39] Ghanbari F, Moradi M, Eslami A, Emamjomeh MM (2014) Electrocoagulation/Flotation of Textile Wastewater with Simultaneous Application of Aluminum and Iron as Anode. Environ. Process. 1(4): 47–457.

[40] Mollah MYA, Gomes JAG, Das KK, Cocke DL (2010) Electrochemical treatment of Orange II dye solution—Use of aluminum sacrificial electrodes and floc characterization. J. Hazard. Mater. 174: 851–858.

[41] Kobya M, Demirbas E, DedelAi A, Sensoy MT (2010) Treatment of rinse water from zinc phosphate coating by batch and continuous electrocoagulation processes. J. Hazard. Mater. 173: 326–334.

[42] Merzouk B, Gourich B, Sekki A, Madani K, Vial Ch, Barkaoui M (2009) Studies on the decolorization of textile dye wastewater by continuous electrocoagulation process. Chem. Eng. J. 149: 207–214.

# PART C. ELECTROCHEMICAL OXIDATION PROCESS

# VI. ELECTROCHEMICAL OXIDATION OF PHENOLIC WASTEWATERS USING A BATCH-STIRRED REACTOR WITH NaCl ELECTROLYTE AND Ti/RuO2 ANODES

AS Fajardo[a], HF Seca[a], RC Martins[a], VN Corceiro[b], IF Freitas[b], ME Quinta-Ferreira[b,c] and RM Quinta-Ferreira[a]

[a] CIEPQPF – Chemical Process Engineering and Forest Products Research Centre; GERST – Group on Environment, Reaction, Separation and Thermodynamics; Department of Chemical Engineering, Faculty of Sciences and Technology, University of Coimbra, Pólo II, Rua Sílvio Lima, 3030-790 Coimbra, Portugal.

[b] Department of Physics, University of Coimbra, 3004-516 Coimbra, Portugal.

[c] CNC- Center for Neuroscience and Cell Biology, University of Coimbra, 3004-504 Coimbra, Portugal.

*Submitted to Journal of Electroanalytical Chemistry*

## ABSTRACT

An electrochemical oxidation (EO) process with Ti/$RuO_2$ anodes was applied to treat phenolic wastewaters. In order to optimise the system, different operating conditions (nature and electrolyte concentration, current density and initial pH) were tested. The nature of the electrolyte and the current intensity greatly affected the process, while the concentration of the electrolyte as well as the initial pH had a sparingly impact. The optimum operating conditions attained, 10 g $L^{-1}$ of NaCl, 119 mA $cm^{-2}$ and initial pH 3.4, allowed the complete removal of the total phenolic content (TPh) and chemical oxygen demand (COD) when applied to a simulated phenolic mixture. No significant differences were revealed on the surface of the anode after the treatment by SEM analysis. Neuronal studies were performed to verify the impact of the synthetic phenolic effluent, before and after the EO treatment, in the formation of neuronal reactive oxygen species (ROS). The treated effluent had a milder effect, compared to the raw one, but neuronal activity became enhanced after its removal. Regarding the depuration of an undiluted real olive mill wastewater (OMW) the treatment, performed with the optimised parameters, achieved 100 % of TPh removal and 17.2 % of COD removal.

This study demonstrates that the EO treatment process carried out with Ti/$RuO_2$ anodes can be successfully applied to effluents with COD up to 1100 $mgO_2$ $L^{-1}$, ensuring that the legal limit values of

the wastewater to be discharged into the natural streams are achieved. In addition, this EO is also considered a satisfactory pre-treatment process to real wastewaters, since all phenolic content can be removed in 180 min.

## VI.1 INTRODUCTION

Water pollution and its scarcity affect millions of people, threatening the existence of humankind and constitute one of the most important environmental issues of the century. Hazardous and persistent contaminants are dangerous compounds, which appear in wastewater streams coming from industrial and agricultural activities [1–4]. The seasonally produced olive mill wastewaters (OMW) present high pollutants load and are toxic to the environment. These characteristics are mainly due to the presence of phenolic acids and polyphenols substances, which are biorecalcitrant compounds not able to be removed by biological treatment [5]. High levels of phenolic acids, that are also important antioxidants, may interfere with health. Therefore, finding a safe solution for the management of OMW, so that they do not affect human health, becomes imperative.

Advanced oxidation processes (AOPs) have been successfully applied to reduce the organic load and toxicity present in wastewaters, since they are based on the generation of powerful oxidising species (hydroxyl radicals, $^{\bullet}OH$) in solution, which are able to destroy organics up to their mineralisation. Electrochemical oxidation (EO) appears as an environmental friendly method, being easy to operate and control. This technology can achieve high efficiencies through two different mechanisms: direct and indirect anodic oxidation. In the former, pollutants are oxidised by direct charge transfer. On the other hand, in indirect oxidation, a strong oxidant can be electrochemically generated at the anode that will degrade contaminants in the bulk solution. As exemple, there is the generation of hydroxyl radicals $M(^{\bullet}OH)$ produced by the decomposition of water molecules on the surface of the anode (M) (Equation (VI.1)) [6].

$$\mathrm{M} + \mathrm{H_2O} \rightarrow \mathrm{M}(\,^{\bullet}\mathrm{OH}) + \mathrm{H}^+ + \mathrm{e}^- \qquad \textbf{(VI.1)}$$

In addition, NaCl is a common mediator added to the system, allowing the production of active chlorine species. The oxidation of the chloride ($\mathrm{Cl}^-$) ion on the surface of the anode leads to the generation of chlorine ($Cl_2$) (Equation (VI.2)), which is further hydrolysed being disproportionated to HClO (hypochlorous acid) and $\mathrm{Cl}^-$ (Equation (VI.3)). In the bulk solution, the HClO is in equilibrium with $\mathrm{OCl}^-$ with pKa=7.55 (Equation (VI.4)) [7–9].

$$2\,\mathrm{Cl}^- \rightarrow \mathrm{Cl}_{2(\mathrm{aq})} + 2\mathrm{e}^- \qquad \textbf{(VI.2)}$$

$$\mathrm{Cl}_{2(\mathrm{aq})} + \mathrm{H_2O} \rightarrow \mathrm{HClO} + \mathrm{Cl}^- + \mathrm{H}^+ \qquad \textbf{(VI.3)}$$

$$\mathrm{HClO} \rightleftarrows \mathrm{H}^+ + \mathrm{OCl}^- \qquad \textbf{(VI.4)}$$

Moreover, it should be taken into account that during the treatment process, both oxidation mechanisms, direct and indirect, may coexist [8].

Electrochemical oxidation has already been applied to the depuration of phenolic acids and OMW, through the employment of different anode materials. In general, the anodic materials with high $O_2$ overpotential are preferentially selected for the EO treatment. An example is the boron-doped diamond (BDD) anode [10–13], since it generates greater amounts of reactive M($^{\bullet}$OH) than other materials such as Pt and $PbO_2$. Nevertheless, the application of BDD for wastewaters depuration is limited by its high acquisition cost. Therefore, the study of other anode materials has been accomplished in order to identify more affordable electrodes as suitable alternatives to reduce initial investment and operational costs. This is the case of the dimensional stable anodes (DSA) [14–25], which have a strong interaction between their surface (M) and $^{\bullet}$OH radicals allowing the formation of superoxide MO (an oxide with higher oxidation state) according to Equation (VI.5). This situation occurs when higher oxidation sates are available for a metal oxide anode, above the standard potential of oxygen evolution ($E^0$=1.23 V *vs* SHE). The redox couple MO/M acts as mediator in the selective oxidation of the organic compounds (R) (Equation (VI.6)), which directly competes with the side reaction of $O_2$ evolution that results from the chemical decomposition of the higher oxide (Equation (VI.7)) [2].

$$\mathrm{M}(\,^{\bullet}\mathrm{OH}) \rightarrow \mathrm{MO} + \mathrm{H}^{+} + \mathrm{e}^{-} \qquad \textbf{(VI.5)}$$

$$\mathrm{MO} + \mathrm{R} \rightarrow \mathrm{M} + \mathrm{RO} \qquad \textbf{(VI.6)}$$

$$\mathrm{MO} \rightarrow \mathrm{M} + \frac{1}{2}\mathrm{O}_2 \qquad \textbf{(VI.7)}$$

DSA are titanium anodes coated with mixed metal oxide compositions comprising different elements such as iridium, ruthenium, platinum, rhodium or tantalum [26]. Different oxides such as $IrO_2$, $RuO_2$, $SnO_2$ have already been applied to the treatment of model aqueous solutions containing phenolic compounds typically found in OMW [14,27–31]. Only few studies have described the use of titanium based-alloys (Ti/$RuO_2$, Ti/$IrO_2$, Ti/Ti$RuO_2$, Ti/Pt, and Ti/Ta/Pt/Ir) to treat real OMW [18–25,32–34]. According to Chatzisymeon *et al.* [24] and Papastefanakis *et al.* [25], the Ti/$IrO_2$ and Ti/$RuO_2$ anodes exhibit good activity to the depuration of this kind of wastewaters. Although, these effluents have a complex composition, which may compromise the activity and stability of the electrodes, a significant reduction of total organic pollution (COD=5–71 %, TOC=20–67 %) and an interesting removal of colour (50–100 %), phenolic content (75–96 %) and ecotoxicity may be attained.

This work addresses the use of an EO process to remove a mixture of six phenolic compounds typically found in OMW by using Ti/$RuO_2$ anodes. These anodes, which have high electrocatalytic activity for $Cl_2$ evolution and are generally used in the chlor-alkali process [35] were tested for determining the combined optimal operating conditions, including the nature and concentration of the electrolyte, the applied current density and the inital pH. These parameters can affect treatment performance and energy consumption; thus the aim was to attain an efficient and cost-effective treatment. Surface changes in the anodes structure were evaluated through SEM analysis. In a new set of studies, performed in mammalian brain slices, the influence of the raw and treated synthetic effluents in neuronal activity was addressed. Moreover, the best operating conditions were applied to a real undiluted OMW in order to verify the possibility of application of the mentioned technology.

## VI.2 EXPERIMENTAL

### VI.2.1 SYNTHETIC AND REAL EFFLUENTS

Six phenolic acids, commonly found in OMW, were selected to prepare a simulated phenolic mixture [36] with a concentration of 100 mg $L^{-1}$ of each acid: 3,4,5-trimethoxybenzoic (Alfa Aescar, 99 %), 4-hydroxybenzoic (99 %, Alfa Aescar), gallic (98 %, Fluka), protocatechuic (97 %, Sigma), trans-cinnamic (99 %, Sigma) and veratric (99 %, Acros Organics). No further purification was applied to them before use. A real wastewater was collected from a mill located in the Extremadura region of Spain and the experiments were performed with the filtered effluent. The filtration step was necessary in order to avoid electrode plugging during electrolysis [30]. The main features of the synthetic and real wastewater are displayed in Table VI.1. Both effluents have an acidic character, high phenolic content and organic matter load (chemical oxygen demand–COD). According to the Portuguese Decree-Law 236/98 of 1st August, an effluent can be directly discharged into an aquatic medium if COD value is lower than 150 $mgO_2\ L^{-1}$.

**Table VI.1. Main characteristics of the synthetic and real effluents.**

| Characteristics | Synthetic effluent | Real effluent [37] |
|---|---|---|
| pH | 3.4±0.3 | 3.3±0.4 |
| Conductivity (mS $cm^{-1}$) | 0.14±0.01 | 5.94±0.03 |
| TPh (mgGA $L^{-1}$) | 323±7 | 740±9 |
| COD ($mgO_2\ L^{-1}$) | 1118±41 | 22650±1302 |

### VI.2.2 ELECTROCHEMICAL OXIDATION PROCEDURE

The oxidation process was performed in a Perspex batch-stirred reactor at atmospheric pressure [37]. $Ti/RuO_2$ material was used as anode and stainless steel (SS) as cathode, with an effective area of 21.1 $cm^2$. The electrodes were parallel to each other, with a distance of 10 mm, linked to a DC power supply HY3010 Kaise (I=1.2–2.5 A). In each experiment, the reactor was filled with 1 L of synthetic effluent or with real effluent, and samples were periodically withdrawn and centrifuged at 3500 rpm (Nahita 2655) for further analysis. The conductivity of the electrolyte was measured using a Consort C863 unit and different concentrations of NaCl (1.8–20 g $L^{-1}$) or $Na_2SO_4$ (4–20 g $L^{-1}$) salts were added to the synthetic effluent to promote higher conductivity to the solution (above 2.5 mS $cm^{-1}$). In the experiment with the real effluent, 5 g $L^{-1}$ of NaCl were introduced in the system, to work with the same conductivity as the one leading to the best degradation conditions for the synthetic effluent. The initial pH of the medium was varied between 3 and 9, using NaOH at 3 M or $H_2SO_4$ at 2 M whenever necessary. This parameter was followed using an HANNA pH meter but not adjusted during the treatment time.

Some experiments were randomly run in duplicate to ensure the reproducibility of the results.

### VI.2.3 ANALYTICAL TECHNIQUES

Samples were analysed for total phenolic content (TPh) using the colourimetric Folin Ciocalteau method, as described elsewhere [39], using a T60 PG Instruments spectrophotometer. TPh values are given in terms of equivalent mg $L^{-1}$ of gallic acid, since the calibration curve was prepared with standard samples of this substance. COD closed reflux analysis was performed based on the 5250D method of the Standard Methods [40]. However, in the COD evaluation, the concentration of $HgSO_4$ used in the digestion solution was increased so that the concentration of $Cl^-$ in the samples, higher than 2.0 g $L^{-1}$, did not interfere with the measurements [40–42].

The samples withdrawn were measured in duplicate to minimise experimental errors. Deviations between runs were always lower than 10 % and 8 % for TPh and COD determinations, respectively. The results shown in the figures throughout the manuscript, represent the average of the measurements, including their standard deviations.

Based on the measured COD values, the current efficiency (CE) for the electrochemical oxidation of pollutants was determined applying Equation (VI.8). Moreover, the energy consumption (EC) per volume of treated effluent was determined in terms of kWh $m^{-3}$ according to Equation (VI.9) [43].

$$\mathrm{CE}(\%) = \frac{(\mathrm{COD_0} - \mathrm{COD_t})\ \mathrm{F\ V}}{8\mathrm{It}} \times 100 \qquad \textbf{(VI.8)}$$

$$\mathrm{EC}(\mathrm{kWh\ m^{-3}}) = \frac{\mathrm{E_{cell}\ I\ t}}{\mathrm{V}} \qquad \textbf{(VI.9)}$$

where $COD_0$ corresponds to the initial chemical oxygen demand ($gO_2$ $L^{-1}$), $COD_t$ to the chemical oxygen demand ($gO_2$ $L^{-1}$) at time t, F to the Faraday constant (96487 C $mol^{-1}$), V to the volume of the solution (L), 8 to the equivalent mass of oxygen (g $eq^{-1}$), I to the current intensity (A), t to the electrolysis time (s for CE or h for EC) and $E_{cell}$ to the average potential difference of the cell (V).

### VI.2.4 SEM ANALYSIS

The morphological properties of the anodes, before and after use, were analysed by scanning electron microscopy (SEM) with a VEGA3 SBH–TESCAN equipment.

### VI.2.5 NEURONAL STUDIES

Brain slice studies were performed in transverse hippocampal slices (400 µm thick) obtained from female Wistar rats (31 weeks old). The animals were sacrificed by cervical dislocation and the hippocampi dissected rapidly from the brain that had been immersed in cooled (5–8 °C) artificial cerebrospinal fluid (ACSF). This medium contained (in mM): NaCl 124; KCl 3.5; $NaHCO_3$ 24; $NaH_2PO_4$ 1.25; $MgCl_2$ 2; $CaCl_2$ 2 and D-glucose 10 (all reagents from Sigma, Sintra, Portugal); pH 7.4. The six phenolic acids used in the synthetic mixture (100 mg $L^{-1}$ of each), and in some studies also NaCl (10 g $L^{-1}$), were added to ACSF. The effect of the treated medium that included NaCl (10 g $L^{-1}$) was investigated using a solution with pH 7.4, made by adding the ACSF compounds to it. The slices were then placed, for at least 1 h, in an oxygenated solution (95 % $O_2$, 5 % $CO_2$) prepared adding 20 µM of the cell-permeant ROS indicator $H_2$DCFDA (Life technologies, Carslband, CA) to the ACSF medium. After that period they were kept in oxygenated ACSF, being, for the experiments, transferred to the experimental chamber. Here they were perfused at 1.5–2 mL $min^{-1}$, with the oxygenated medium of interest that was kept at 30–32 °C.

The optical measurements were performed at the hippocampal mossy fiber synapses, from CA3 area, using a transfluorescence setup in a microscope (Zeiss Axioskop). This instrument contained a tungsten/halogen lamp (12 V, 100 W) and excitation and emission filters of 480 nm (10 nm bandwidth) and >500 nm (high-pass filter), respectively. The emitted light was collected through a water immersion lens (40x, N.A. 0.75) by a photodiode (Hammamatsu, 1 $mm^2$), connected to a current/voltage converter (I/V) with a 1 GΩ feedback resistance. The data were processed at 1.67 Hz using a 16 bit analog/digital converter (National Instruments) and analysed using the Signal Express$^{TM}$ software. The average value of each group of 100 consecutive data points was calculated and is represented in the graphs. To correct for autofluorescence, all average points from incubated slices were subtracted a value obtained from data of indicator-free slices. The corrected signals were normalised by the average of the baseline responses (first 10 points) and are presented as mean±s.e.m.

All experiments were carried out in accordance with the European Communities Council Directive. All efforts were made to minimise animal suffering and to use only the number of animals necessary to produce reliable scientific data.

# VI.3 RESULTS AND DISCUSSION

## VI.3.1 EFFECT OF THE NATURE OF THE SUPPORTING ELECTROLYTE

Solutions must have conductivity in order to accomplish electrochemical experiments. The nature and concentration of the supporting electrolyte normally affects the performance of EO process. Thus, comparative experiments were carried out in order to treat 1 L of a synthetic solution containing six phenolic acids (100 mg $L^{-1}$) at pH 3.4, by applying 57 mA $cm^{-2}$ at the $Ti/RuO_2$ anode with 10 g $L^{-1}$ of two electrolytes: NaCl or $Na_2SO_4$. The effect of the electroactive anions of the electrolyte is depicted in Figure VI.1. As can be observed, the wastewater phenolic content (Figure VI.1a) and COD removal (Figure VI.1b) increased over time. In fact, the results clearly demonstrate that the degradation rate depends on the supporting electrolyte used. The introduction of NaCl led to better degradation values (TPh removal=100 % and COD removal=64.4 %) than the ones achieved with $Na_2SO_4$ (TPh removal=30.4 % and COD removal=6.8 %). This behaviour may be related to the generation of diverse oxidising species when each salt is applied, which are able to react directly and differently with organic compounds during the electrolysis. When the sulfate salt was employed, $S_2O_8^{2-}$ species were electrogenerated. These species show low reaction rate with organic compounds. Giannis *et al*. [21] and Panizza and Cerisola [9] referred that this oxidant is efficiently generated only using anodes with high oxygen evolution overpotential, such as the non-active anodes as boron-doped diamond (BDD) or lead dioxide ($PbO_2$). On the contrary, the anodes used in this investigation are characterised by a low oxygen evolution overpotential. They are active anodes, promoting mainly the selective oxidation, partially degrading organic matter. Thus, it is expected that a low amount of these oxidants is produced justifying the negligible efficiency of $Na_2SO_4$ as an electrolyte in this system. The addition of chloride promoted the electrochemical formation of active chlorine species, such as $Cl_2$ (Equation (VI.2)), HClO (Equation (VI.3)) and $OCl^-$ (Equation (VI.4)) which are strong oxidising species [2], leading to the rapid elimination of colour and organic matter (in terms of COD) from the synthetic solution. According to Chiang *et al.* [44], among sulfate, nitrate and chloride electrolytes, the last one was the best for the electrochemical oxidation of refractory organic pollutants. The satisfactory results with NaCl, its low acquisition cost and relatively high solubility [23] have led to its choice for the following experiments.

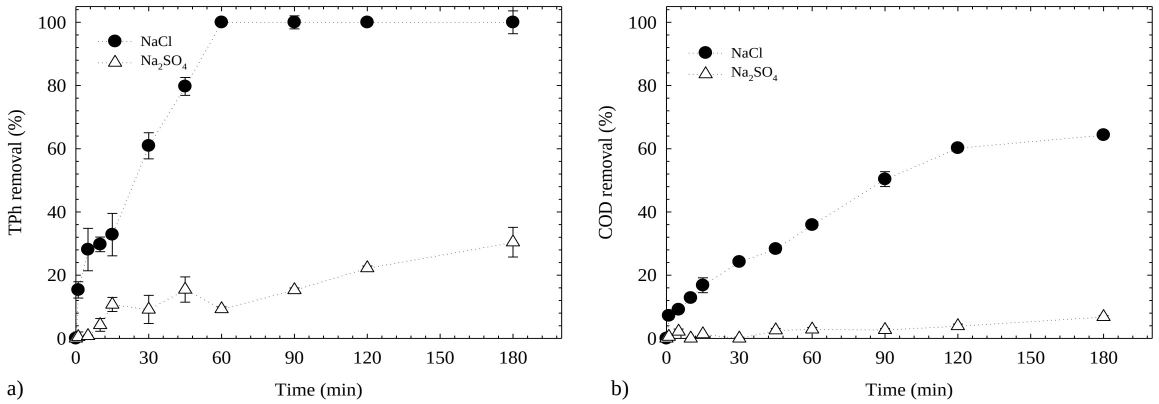

**Figure VI.1. Effect of the nature of the electrolyte on (a) TPh and (b) COD removal over time. Operating conditions: 100 mg $L^{-1}$ of synthetic phenolic solution, 10 g $L^{-1}$ of electrolyte, $pH_{initial}$=3.4, current density=57 mA $cm^{-2}$, distance between electrodes=1 cm, T=20 °C.**

### VI.3.2 EFFECT OF THE CONCENTRATION OF THE ELECTROLYTE

The effect of the concentration of NaCl was tested within the range of 1.8 and 20 g $L^{-1}$ for the removal of phenolic content and COD (Figure VI.2a and Figure VI.2b, respectively). Moreover, pH evolution over time was evaluated (Figure VI.2c). The tests were performed using 1 L of the phenolic synthetic solution (100 mg $L^{-1}$) at pH 3.4, by applying 57 mA $cm^{-2}$. As can be observed, an increase in NaCl concentration favoured a faster TPh removal over time. After 45 min all phenolic content was removed with 20 g $L^{-1}$ of NaCl, while > 90 % was removed with 1.8 g $L^{-1}$ after 180 min of treatment. Regarding COD, degradation values were lower than those obtained for TPh, suggesting that the elimination of phenolic acids leads to the formation of refractory intermediate compounds that still contribute to the significant final COD values. During the first 15 min, the degradation profiles were similar independently of the quantity of NaCl applied but, after this time, the profiles began to differentiate. At 60 min of oxidation, the COD removal was 21.9, 23.1, 31.9, 29.3, 35.9 and 37.7 % for 1.8, 4, 6, 8, 10 and 20 g $L^{-1}$, respectively. The process almost progressed as expected, i.e. the COD removal increased with the concentration of $Cl^{-}$. However, the treatment with 6 g $L^{-1}$ NaCl led to slightly higher removal than the one with 8 g $L^{-1}$. During the following hour, the COD removal was higher when 10 g $L^{-1}$ of electrolyte was used as can be seen in the inset of Figure VI.2b for 120 min, where a maximum removal value was achieved for this test. A similar behaviour was also detected by Bonfatti et *al*. [45]. At the end of the process, 180 min, the COD removal trend for the different electrolyte concentrations was the following: 6 g $L^{-1}$ (74.4 %) > 8 g $L^{-1}$ (69.3 %) > 20 g $L^{-1}$ (65.8 %) > 10 g $L^{-1}$ (64.4 %) > 4 g $L^{-1}$ (62.6 %) > 1.8 g $L^{-1}$ (52.5 %). The initial behaviour may indicate that at low NaCl concentrations there is a smaller amount of $Cl^{-}$ ions for promoting the generation of oxidants. Nevertheless, the electrochemical process using high electrolyte concentrations reach quickly an alkaline pH (Figure VI.2c), favouring the production of $ClO^{-}$ species. The concentration of these species may be limited by their anodic oxidation to $ClO_2^-$ ion (Equation (VI.10)) and their consecutive oxidation to $ClO_3^-$ and $ClO_4^-$ (Equations (VI.11) and (VI.12), respectively) [6], which are species with lower oxidation power, leading to a decrease in the process efficiency.

$$\mathrm{ClO^- + H_2O \rightarrow ClO_2^- + 2H^+ + 2e^-} \tag{VI.10}$$

$$\mathrm{ClO_2^- + H_2O \rightarrow ClO_3^- + 2H^+ + 2e^-} \tag{VI.11}$$

$$\mathrm{ClO_3^- + H_2O \rightarrow ClO_4^- + 2H^+ + 2e^-} \tag{VI.12}$$

In addition, the loss of $\mathrm{ClO^-}$ can also happen by its reduction to $\mathrm{Cl^-}$ ion at the cathode (Equation (VI.13)) and from reactions (Equations (VI.14)–(VI.16)) in the bulk solution [6].

$$\mathrm{ClO^- + H_2O + 2e^- \rightarrow Cl^- + 2OH^-} \tag{VI.13}$$

$$\mathrm{2HClO + ClO^- \rightarrow ClO_3^- + 2Cl^- + 2H^+} \tag{VI.14}$$

$$\mathrm{2ClO^- \rightarrow 2Cl^- + O_2} \tag{VI.15}$$

$$\mathrm{ClO^- + H_2 \rightarrow Cl^- + H_2O} \tag{VI.16}$$

The rates of the reactions 2 and 10–13 are normally related to the electrocatalyic activity of the anode, $\mathrm{Cl^-}$ concentration, salt cation, stirring mode, temperature and current density, whereas the waste reactions in the bulk solution are mainly dependent on the temperature of the system [6].

The concentration of 10 g $L^{-1}$ was then selected to continue the subsequent studies, because after 120 min of oxidation, a COD degradation of 60.2 % was achieved with 23.3 kWh $m^{-3}$ of energy consumed (from Equation (VI.9)), that is about half of the energy needed (47.1 kWh $m^{-3}$) with lower concentration and longer times (6 g $L^{-1}$ during 180 min). Moreover, the objective to increase current density was not possible to fulfil with low NaCl concentrations due to the solution low conductivity. It should be mentioned that various concentrations of $Na_2SO_4$ (4–20 g $L^{-1}$) were also tested, but an increase in the concentration was not reflected in an improvement in the COD removal. In fact, the degradation was practically the same regardless of the concentration used. In addition, the maximum TPh removal achieved was 30.4 % with 10 g $L^{-1}$, after 180 min. As aforementioned, the efficiency of the results obtained with $Na_2SO_4$ was always significantly lower than that of those obtained with NaCl.

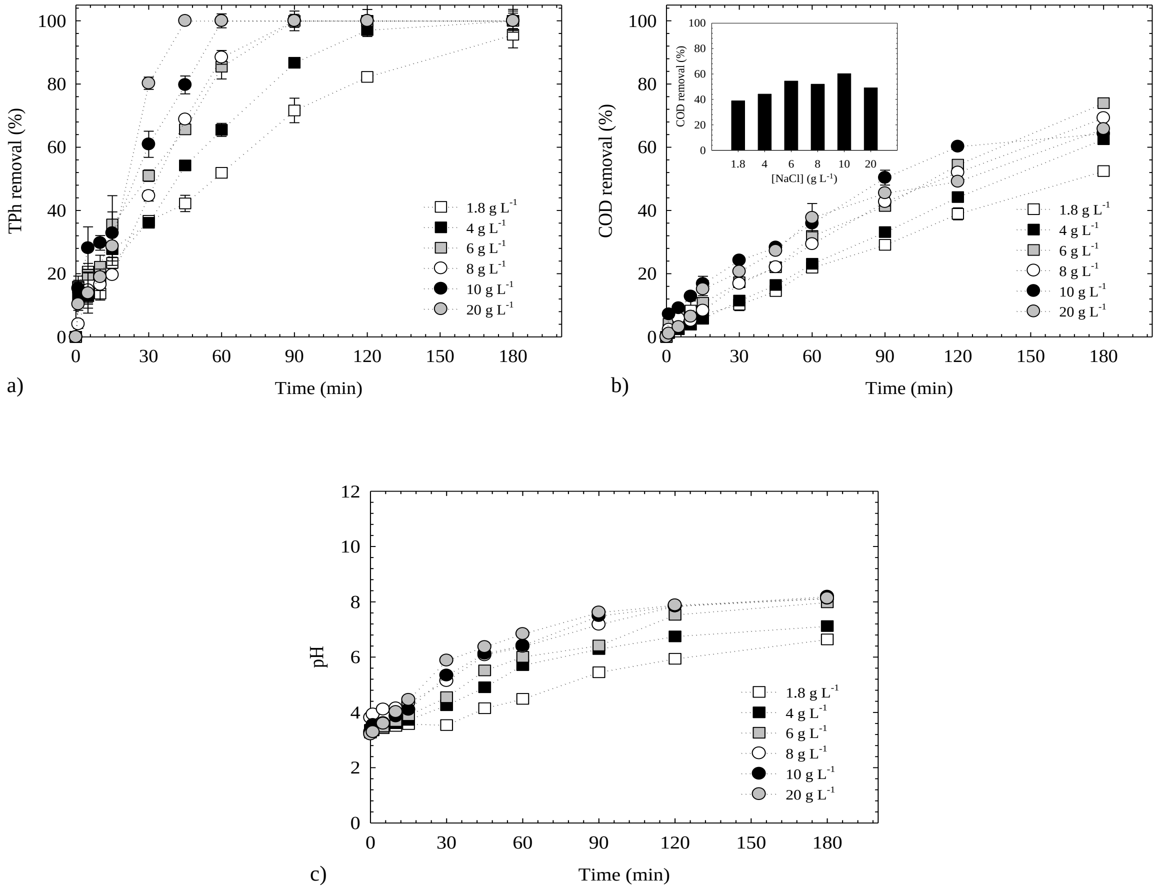

**Figure VI.2. Effect of the NaCl concentration on (a) TPh removal, (b) COD removal and (c) pH medium over time. Inset of Figure VI.2b: COD removal for the different NaCl concentrations after 120 min of treatment. Operating conditions: 100 mg L$^{-1}$ of synthetic phenolic solution, pH$_{initial}$=3.4, current density=57 mA cm$^{-2}$, distance between electrodes=1 cm, T=20 °C.**

### VI.3.3 EFFECT OF THE CURRENT DENSITY AND KINETIC STUDY

The current density is one of the most important parameters in electrochemical oxidation, since it reflects the driving-force in the migration of charge. Its influence was analysed in the range between 57 and 119 mA cm$^{-2}$ for the removal of the phenolic content and organic load over time (Figure VI.3a and Figure VI.3b, respectively) from the synthetic solution with 10 g L$^{-1}$ of NaCl at pH 3.4. The results show that the increase of the current density causes the enhancement of the rate of phenolic compounds and COD elimination. In Figure VI.3a, the experiment using 57 mA cm$^{-2}$ took 60 min to achieve complete TPh removal, while the tests with 95 and 119 mA cm$^{-2}$ had a similar trend with a sharp rise during the first 30 min, attaining 100 % of removal after 45 min of treatment. Regarding the COD analysis, the total removal was achieved after 180 min of oxidation in the experiment using 119 mA cm$^{-2}$, followed by the 95 mA cm$^{-2}$ with 90.1 % and at last 57 mA cm$^{-2}$ with 64.4 % of degradation. The COD decay exhibited an exponential behaviour for all the applied current densities demonstrating a pseudo first-order kinetic (Equation (VI.17)) for the electrochemical oxidation reaction [20,46].

$$-\frac{\mathrm{dCOD}}{\mathrm{dt}} = \mathrm{k_{app}COD} \qquad \textbf{(VI.17)}$$

which gives, after integration and linearisation (Equation (VI.18)),

$$\ln\left(\frac{\mathrm{COD_0}}{\mathrm{COD_t}}\right) = \mathrm{k_{app}t} \qquad \textbf{(VI.18)}$$

where, $\mathrm{COD_0}$ and $\mathrm{COD_t}$ correspond to the COD at the beginning of the experiment and at time t, respectively and $\mathrm{k_{app}}$ to the apparent pseudo first-order rate constant. Apparent kinetic constants for COD removal were estimated for the three different applied current densities by plotting $\ln(\mathrm{COD_0/COD_t})$ against time (Figure VI.3c). The following values were achieved $6.7\times10^{-3}$ $\mathrm{min^{-1}}$ ($R^2$=0.934), $1.2\times10^{-2}$ $\mathrm{min^{-1}}$ ($R^2$=0.994) and $1.7\times10^{-2}$ $\mathrm{min^{-1}}$ ($R^2$=0.982) for the applied current densities of 57 mA $\mathrm{cm^{-2}}$ (I=1.2 A), 95 mA $\mathrm{cm^{-2}}$ (I=2.0 A) and 119 mA $\mathrm{cm^{-2}}$ (I=2.5 A), respectively. The increase of the kinetic constants suggests that a great generation of $^{\bullet}$OH radicals is promoted as well as the electrogeneration of active chlorine, favouring the electrochemical oxidation of organic compounds, as a consequence of the increase of current densities [23,47]. Therefore, the current density of 119 mA $\mathrm{cm^{-2}}$ was selected for the subsequent experiments.

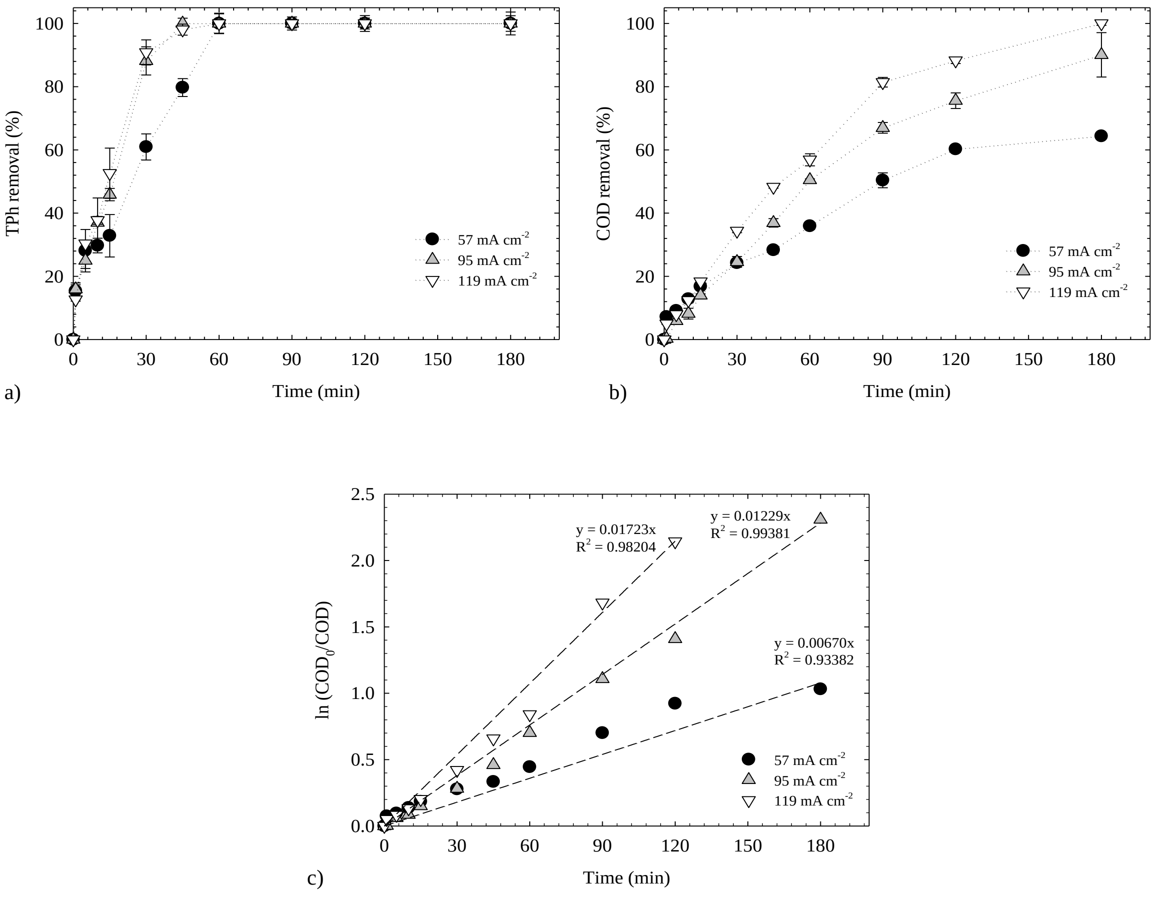

**Figure VI.3. Effect of the current density on (a) TPh removal and (b) COD removal over time. (c) Kinetic analysis assuming a pseudo-first-order reaction for COD removal at different current desnities.Operating conditions: 100 mg $\mathbf{L^{-1}}$ of synthetic phenolic solution, [NaCl]=10 g $\mathbf{L^{-1}}$, $\mathbf{pH_{initial}}$=3.4, distance between electrodes=1 cm, T=20 °C.**

### VI.3.4 EFFECT OF PH

As aforementioned, the pH of the solution is an essential parameter in indirect electrochemical oxidation, since the electrogeneration of certain oxidising species is dependent on the medium pH [6]. In the case of the formation of the active chlorine species, until pH 3.0, the main species is $Cl_{2\ (aq)}$, while the predominant one in the pH range 3–8 is HClO and for pH > 8 is $\mathrm{ClO^-}$. Thus, the system efficiency was evaluated for three different initial effluent pH values, pH 3.4, followed by pHs 7 and 9 that were adjusted with NaOH and $H_2SO_4$, whenever necessary. The other operating conditions were kept constant: 10 g $L^{-1}$ of NaCl and current density equal to 119 mA $cm^{-2}$. The timecourse of the corresponding removal efficiencies for TPh and COD are represented in Figure VI.4a and Figure VI.4b, respectively. As can be observed, the wastewater phenolic content was rapidly and completely removed in the first 30–60 min of treatment, regardless of the applied pH. Regarding COD depletion, similar removals were attained for pHs 7 and 9, within the 90 min of treatment (68.9–69.6 %, respectively). However, in the experiment with pH 3.4, at that time already 81.4 % of COD had been eliminated. At the end of the process, the highest COD removal (100 %) was attained for pH 3.4, followed by pH 7 (93.7 %) and at last pH 9 (82.5 %). As theoretically expected, the $\mathrm{Cl^-}$ mediated oxidation of the pollutants with the active chlorine species was more extended in acidic than in alkaline media due to the higher standard potentials of $Cl_{2\ (aq)}$ ($E^0\left(\mathrm{Cl_{2(aq)}/Cl^-}\right)$=1.36 *vs* SHE) and HClO ($E^0(\mathrm{HClO/Cl^-})$=1.49 *vs* SHE) than $\mathrm{ClO^-}$ ($E^0(\mathrm{ClO^-/Cl^-})$=0.89 *vs* SHE).

Figure VI.4c depicts the pH evolution for all experiments over time. As can be observed, the curve corresponding to initial pH 3.4 had a fast rise in the first 50 min, followed by a slower one. In the experiments, with initial pH 7 and 9, after the rapid increase observed during the first 10–15 min of treatment, the pH decayed during similar periods, rising again afterwards and more slowly in the final part of the reaction. The first increase may be associated to the reactions that occur at the cathode, since at this electrode, water molecules receive electrons and dissociate themselves into hydrogen ($\mathrm{H_2}$) bubbles and hydroxide ions ($\mathrm{OH^-}$) (Equation (VI.19)), causing pH increase [18,32].

$$\mathrm{2H_2O + 2e^- \rightarrow H_2 + 2OH^-} \qquad \textbf{(VI.19)}$$

The final pH of all the experiments was around 8.5, which is in the ideal range, according to the Portuguese Decree-Law 236/98 of 1st of August, to be directly discharged or even to be used in biological processes. Therefore, pH adjustment of the phenolic effluent for EO is not needed [48–50].

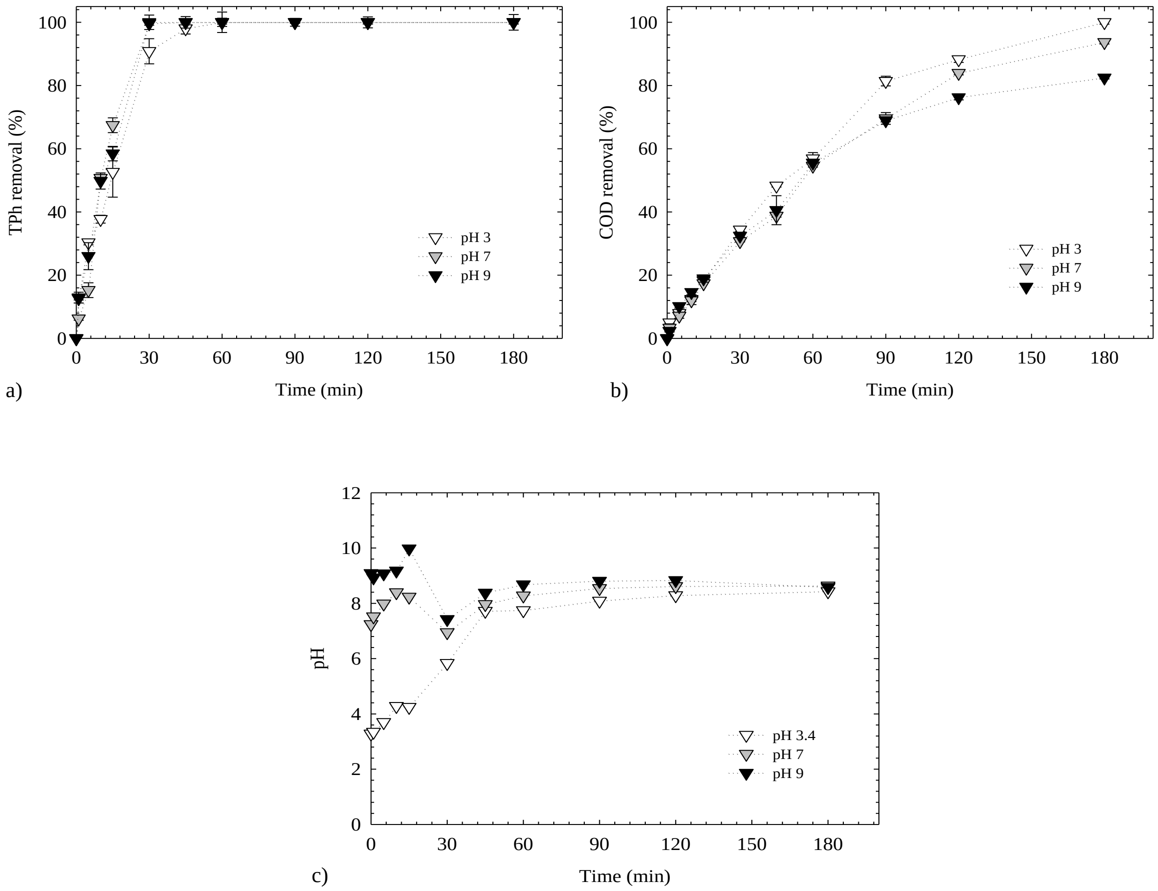

**Figure VI.4. Effect of the initial pH medium on (a) TPh removal, (b) COD removal and (c) pH medium over time. Operating conditions: 100 mg L$^{-1}$ of synthetic phenolic solution, [NaCl]=10 g L$^{-1}$, current density=119 mA cm$^{-2}$, distance between electrodes=1 cm, T=20 °C.**

### VI.3.5 MORPHOLOGICAL ANALYSIS OF THE Ti/RuO$_2$ ANODES

The morphology of the Ti/RuO$_2$ material was analysed by SEM at a magnification of 500× (Figure VI.5), before and after the use of the anodes in the EO process at the selected operating conditions (10 g L$^{-1}$ of NaCl, current density of 119 mA cm$^{-2}$ and initial raw pH 3.4). The unused anode (Figure VI.5a) shows microcracks on its surface, a usual feature of DSA, resulting from the sintering processes [51,52]. No significant differences were found in the same anode after the EO treatment (Figure VI.5b). This result suggests that the removal efficiency of the process can be maintained after several uses of these anodes.

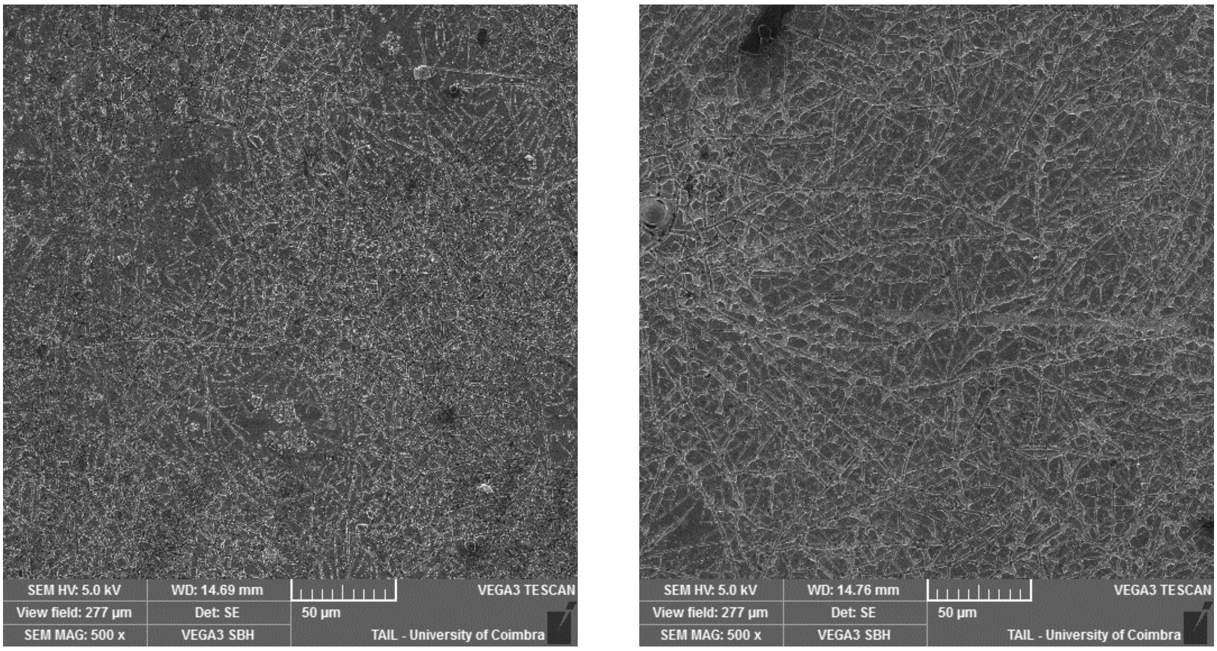
SEM HV: 5.0 kV
WD: 14.69 mm
VEGA3 TESCAN
View field: 277 μm
Det: SE
50 μm
SEM MAG: 500 x
VEGA3 SBH
TAIL - University of Coimbra
SEM HV: 5.0 kV
WD: 14.76 mm
VEGA3 TESCAN
View field: 277 μm
Det: SE
50 μm
SEM MAG: 500 x
VEGA3 SBH
TAIL - University of Coimbra

a) b)

**Figure VI.5. SEM photographs at 500× of the Ti/RuO$_2$ anode material, (a) before and (b) after EO treatment. Operating conditions: 100 mg L$^{-1}$ of synthetic phenolic solution, [NaCl]=10 g L$^{-1}$, pH$_{initial}$=3.4, current density=119 mA cm$^{-2}$, distance between electrodes=1 cm, T=20 °C.**

### VI.3.6 ENERGY CONSUMPTION AND CURRENT EFFICIENCY

Regarding industrial application, it was important to evaluate instantaneous current efficiency (CE–Equation (VI.8)) and also energy consumption (EC–Equation (VI.9)) as a function of COD removal (Figure VI.6), for the best operating conditions previously found: 10 g L$^{-1}$ of NaCl, current density of 119 mA cm$^{-2}$ and initial raw pH 3.4. As can be observed for the initial COD removal, the CE is about 127 % decreasing over time, while the energy consumption increased along the process treatment. This high current efficiency can be due to the presence of chloride ions that lead to an additional chemical oxidation process in the solution bulk [53,54]. For total COD removal, the CE value decreased to 44 % and EC increased to 115 kWh m$^{-3}$. This behaviour may be due to the reduction of organic load in the solution, being favoured the parasitic reaction of oxygen evolution; which means that Equation (VI.7) is preferred over Equation (VI.6).

Although, the treatment of the phenolic acids effluent with the Ti/RuO$_2$ anode is very effective, the energy consumption of the process is relatively high to be implemented in real context as solely one step. Nevertheless, this kind of depuration can be used as a pre-treatment [55]

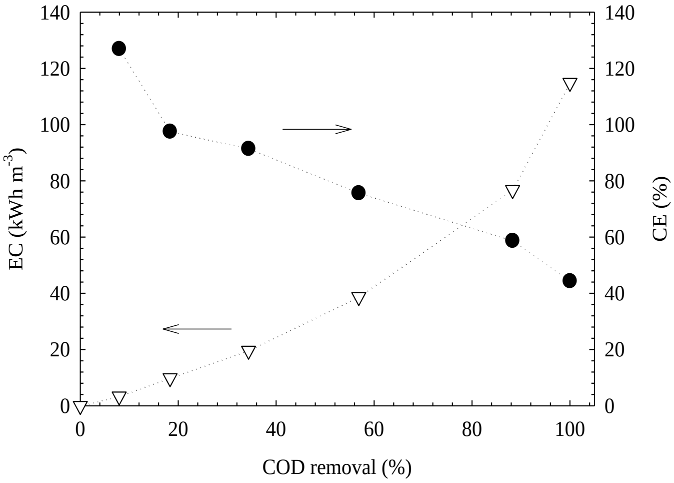

**Figure VI.6. Analysis of the energy consumption (EC) and current efficient (CE) over COD removal. Operating conditions: 100 mg $L^{-1}$ of synthetic phenolic solution, [NaCl]=10 g $L^{-1}$, $pH_{initial}$=3.4, current density=119 mA $cm^{-2}$, distance between electrodes=1 cm, T=20 °C.**

### VI.3.7 EFFECT OF THE SYNTHETIC PHENOLIC EFFLUENT IN NEURONAL ROS SIGNALS

In the EO treatment, 10 g $L^{-1}$ (equivalent to 171 mM) of NaCl were added to the pollutants mixture to increase its conductivity. In order to evaluate the effect of this effluent in neuronal ROS signals, brain slices were perfused with untreated solutions, both without and with that amount of the NaCl electrolyte (Figure VI.7a and Figure VI.7b, respectively). In the first case (Figure VI.7a), it can be observed that the signals decrease rapidly to lower values, almost linearly, and even more rapidly in the medium containing NaCl (Figure VI.7b).

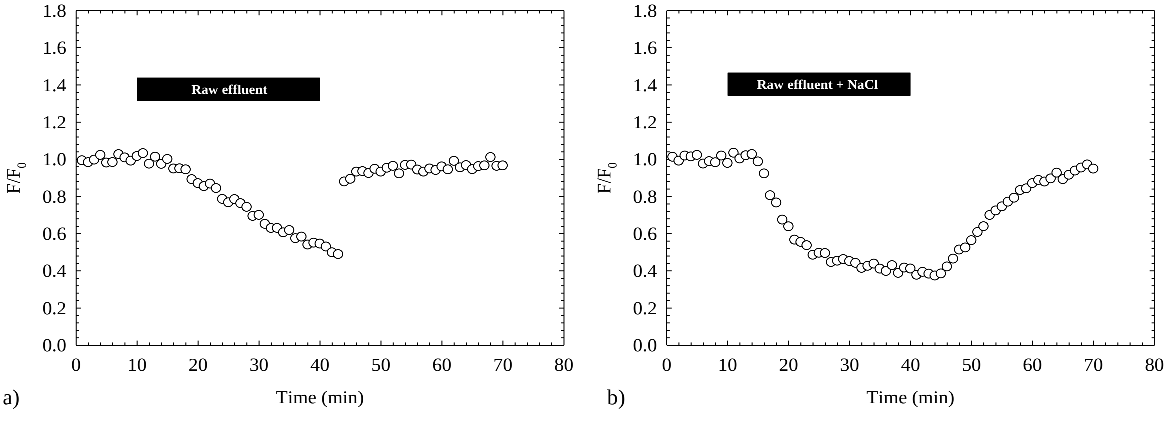

**Figure VI.7. ROS signals from brain slices evoked by the synthetic phenolic effluent. Effect of the phenolics mixture in ROS signals recorded in the normal and the pollutants media. The data were acquired using the fluorescent ROS indicator $H_2DCFDA$ (20 µM) and were normalised by the average of the first 10 responses. (a) ROS changes in the presence of the phenolics mixture, applied during the period indicated by the bar (30 min). (b) The pollutants mixture containing NaCl (171 mM) was applied during the period represented by the bar.**

Both signals were reversible upon washout of the effluent. The effect of the phenolic mixture in the ROS signals was significantly different after the EO treatment, since the depression had a smaller amplitude

(0.24±0.05, at 20–25 min) and was followed by a large potentiation upon washout (0.47±0.2 above baseline, at 65–70 min) (n=3), as shown in Figure VI.8. These signals, that include components from mitochondrial origin, are largely associated with synaptic activity since neurotransmitter release depends on the production of energy by that organelle [56]. The mentioned depressions are of the same type as those evoked by tetraethylammonium (TEA), in the same preparation, in another set of ROS studies (data not shown). This compound blocks voltage dependent potassium channels, eliciting long term potentiation (LTP), an intensely studied form of synaptic plasticity [57,58]. The depression is considered mediated by released zinc that activates presynaptic $K_{ATP}$ channels and inhibits voltage dependent calcium channels [59–62]. Thus, the results indicate that the applied effluents, both the untreated and the treated one, may interact with cellular processes similar to those activated following the application of TEA. The raw effluent caused a much larger depression than the treated one and, after its removal, the ROS signal recovered to the initial value, suggesting that the cells recovered normal function. The treated solution, caused a slower decay but was followed by a large potentiation and thus an altered physiological state.

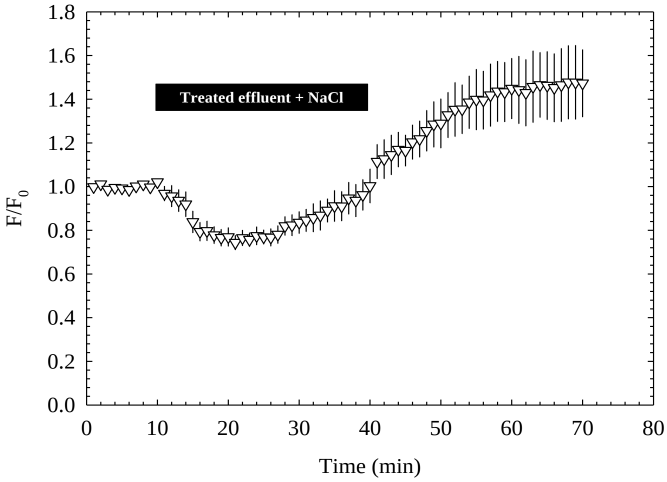

**Figure VI.8. Timecourse of ROS changes induced by the treated phenolic effluent. Normalised fluorescence data obtained from slices incubated with the ROS indicator $H_2DCFDA$ (20 µM). The bar indicates the period (30 min) of application of the treated medium, containing NaCl (171 mM), being the data represented as mean ± s.e.m (n=3).**

### VI.3.8 APPLICATION TO A REAL EFFLUENT

Once the operating parameters have been optimised for the synthetic effluent (NaCl electrolyte, current density of 119 mA $cm^{-2}$ and initial raw pH 3.4.), those conditions were applied to the depuration of a real OMW. In this experiment, only 5 g $L^{-1}$ of NaCl were added to the system in order to have the same conductivity as the simulated effluent (16.6 mS $cm^{-1}$). Figure VI.9a shows that the phenolic content can be completely removed after 180 min of treatment even though the removal rates are lower than those observed for the synthetic effluent probably due to the competition of other dissolved pollutants. However, at the same time, only 17.2 % of COD removal (Figure VI.9b) was achieved with an energy consumption of 162 kWh $m^{-3}$. This removal reveals that over time refractory intermediate non-phenolic compounds may have been formed and accounted as organic matter. As can be observed in Figure VI.9c, the timecourse of the pH medium for the real effluent was practically constant (pH=3.3–3.9). Thus, it could not provide as many oxidants as in the case of the synthetic effluent (pH=3.4–8.4), leading to a low removal of pollutants. In literature, some reports dealing with real OMW ($COD_{initial}$=28000–40000 $mgO_2\ L^{-1}$) treated by EO are presented but, normally the wastewater is diluted before use, applying an organic load similar to the common values (COD=300–1200 $mgO_2\ L^{-1}$) of synthetic solutions with phenolic values [18,24,25]. Thus, one can assume that the removal values obtained in this work are not so low, and that represent a satisfactory result for a real effluent, at least for TPh removal, after 180 min of reaction.

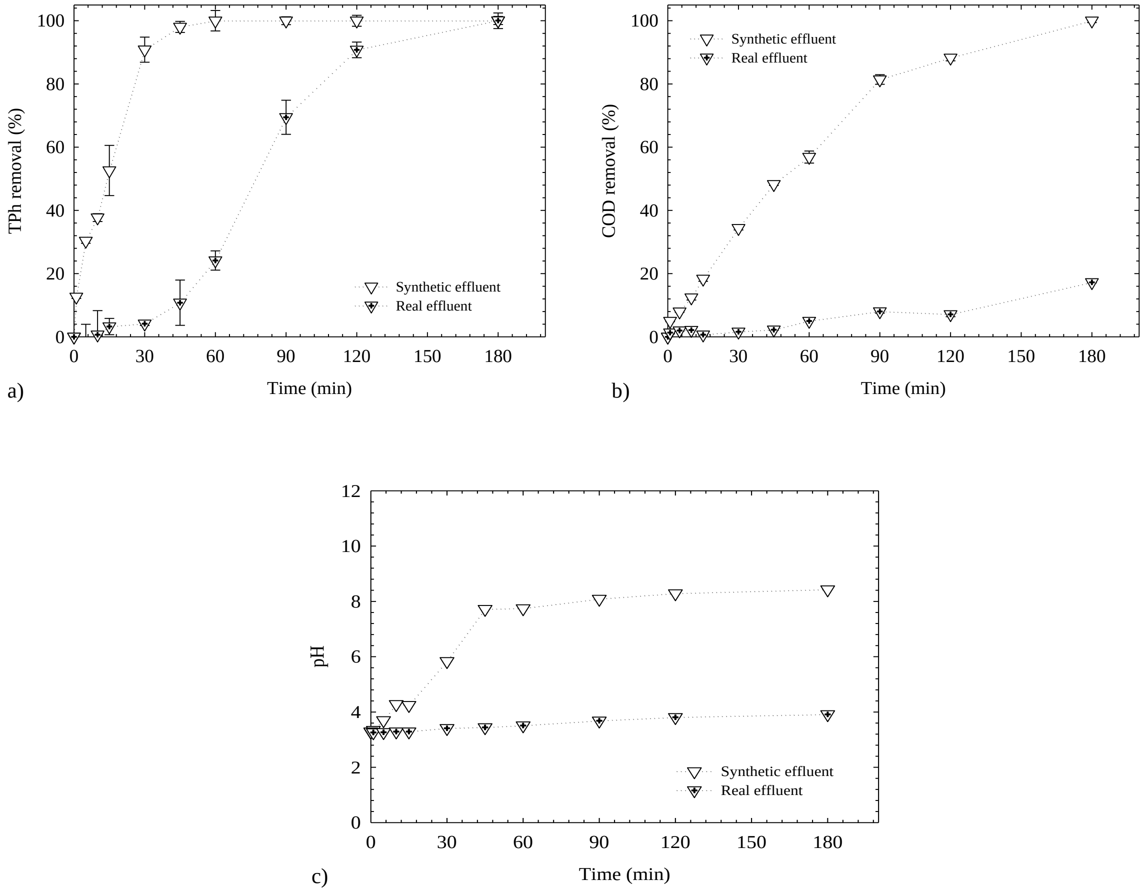

a)

b)

c)

**Figure VI.9. (a) TPh removal, (b) COD removal and (c) pH medium over time for the synthetic and real effluent at the best operating conditions: 100 mg $L^{-1}$ of synthetic phenolic solution, conductivity=16.6 mS $cm^{-1}$, pHinitial=3.4, current density=119 mA $cm^{-2}$, distance between electrodes=1 cm, T=20 °C.**

In addition, the visual observation of the samples showed that the blackish-brown colour of the real OMW turned to a yellowish colourisation over time, achieving, at the end of the process, an almost colourless solution (Figure VI.10). According to Belaid *et al.* [63], this behaviour can be explained by the action of the oxidants that were electrochemically generated which promoted the breakage of the double bonds in the conjugate chains of the aromatic compounds and discolouration via electrophilic cleavage of the chromophore groups.

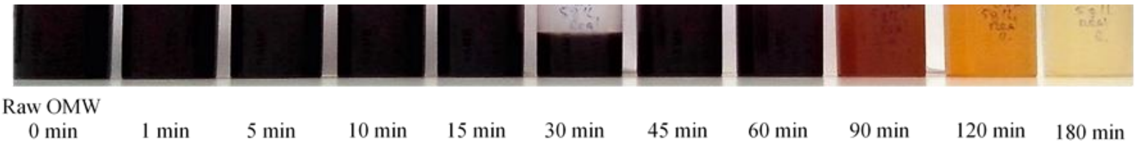

**Figure VI.10. Discoloration of the real OMW over time. Operating conditions: 100 mg $L^{-1}$ of synthetic phenolic solution, [NaCl]=5 g $L^{-1}$, $pH_{initial}$=3.4, current density=119 mA $cm^{-2}$, distance between electrodes=1 cm, T=20 °C.**

## VI.4 CONCLUSIONS

A phenolic synthetic effluent was depurated by an EO process with $Ti/RuO_2$ anodes. Different operating conditions were tested. The nature of electrolyte clearly affected the treatment process, and the increase in current density had a strong influence in TPh and COD removal. Regarding the concentration of the electrolyte and the initial pH, a sparingly impact in the system was observed. The best results for phenolic content and COD removal (100 %) were achieved with the following operating conditions: 10 g $L^{-1}$ of NaCl, 119 mA $cm^{-2}$ and pH 3.4. No significant morphological differences on the surface of $Ti/RuO_2$ anodes were observed before and after the EO process. In the neuronal studies, the untreated effluents without and with the electrolyte NaCl caused large depressions of the signals. However, both signals recovered to the initial values upon washout. With the treated effluent, the reduction was smaller than that observed with the corresponding raw medium containing the electrolyte and, following the effluent removal, the signal increased reaching a potentiated steady level. Considering that the treatment eliminated all phenolic compounds, the smaller depression and the large potentiation appearing after washout, may be due to the action of end products of the EO process. Applying the optimised parameters to the treatment of the real OMW, 100 % and 17.2 % of TPh and COD removal, respectively, were attained after 180 min of reaction with an energy consumption of 162 kWh $m^{-3}$.

The electrochemical process is optimised if the initial organic matter load (in terms of COD) at the beginning of the process is around 300–1200 $mgO_2$ $L^{-1}$, near the values of phenolic simulated effluents. Thus, the wastewater could be directly discharged into natural streams, since its analytical parameters stay within environmental legislation thresholds. This study additionally suggests that the EO process in question may be used as a pre-treatment for real OMW, since all phenolic content was removed after 180 min of treatment.

## ACKNOWLEDGMENTS

The authors, Ana S. Fajardo and Rui C. Martins gratefully acknowledge the Fundação para a Ciência e Tecnologia, for financial support under the Doc grant (SFRH/BD/87318/2012) and the IFCT 2014 programme (IF/00215/2014) with funding from the European Social Fund and the Human Potential Operational Programme, respectively.

Access to TAIL-UC facility funded under QREN-Mais Centro Project ICT/2009/02/012/1890 is gratefully acknowledged. The Biophysics group thanks the Centre for Neuroscience and Cell Biology, University of Coimbra, Coimbra, Portugal, for providing the rat brains. This work was funded by strategic project UID/NEU/04539/2013.

Ana S. Fajardo also acknowledge Dr. Sergi Garcia-Segura for fruitful discussions on advanced electrochemical processes.

## REFERENCES

[1] Inglezakis VJ, Poulopoulos SG (2006) Adsorption, Ion Exchange and Catalysis: Design of Operations and Environmental Applications, Elsevier, 1–28.

[2] Martínez-Huitle CA, Ferro S (2006) Electrochemical oxidation of organic pollutants for the wastewater treatment: direct and indirect processe. Chem. Soc. Rev. 35: 1324–1340.

[3] Britto JM, Rangel MC (2008) Processos avançados de oxidação de compostos fenólicos em efluentes industriais. Quím. Nova 31: 114–122.

[4] Särkkä H, Bhatnagar A, Sillanpää M (2015) Recent developments of electro-oxidation in water treatment – A review. J. Electroanal. Chem. 754: 46–56.

[5] Paraskeva P, Diamadopoulos E (2006) Technologies for olive mill wastewater (OMW) treatment: a review. J. Chem. Technol. Biotechnol. 81: 1475–1485.

[6] Brillas E, Martínez-Huitle CA (2015) Decontamination of wastewaters containing synthetic organic dyes by electrochemical methods. An up dated review. Appl. Catal. B: Environ. 166–167: 603–643.

[7] Szpyrkowicz L, Kaul SN, Neti RN, Satyanarayanb S (2005) Influence of anode material on electrochemical oxidation for the treatment of tannery wastewater. Water Res. 39: 1601–1613.

[8] Anglada A, Urtiaga A, Ortiz I (2009) Contributions of electrochemical oxidation to waste-water treatment: fundamentals and review of applications. J. Chem. Technol. Biotechnol. 84: 1747–1755.

[9] Panizza M, Cerisola G (2009) Direct and Mediated Anodic Oxidation of Organic Pollutants. Chem. Rev. 109: 6541–6569.

[10] Iniesta J, Michaud PA, Panizza M, Cerisola G, Aldaz A, Comninellis Ch (2001) Electrochemical oxidation of phenol at boron-doped diamond electrode. Electrochim. Acta 46: 3573–3578.

[11] Chen X, Chen G, Gao F, Yue PL (2003) High-Performance Ti/BDD Electrodes for Pollutant Oxidation. Environ. Sci. Technol. 37: 5021–5026.

[12] Cañizares P, Martínez L, Paz R, Sáez C, Lobato J, Rodrigo MA (2006) Treatment of Fenton-refractory olive oil mil wastes by electrochemical oxidation with boron-doped diamond anodes. J. Chem. Technol. Biotechnol. 81: 1331–1337.

[13] Cañizares P, Lobato J, Paz R, Rodrigo MA, Sáez C (2007) Advanced oxidation processes for the treatment of olive-oil mills wastewater. Chemosphere 67: 832–838.

[14] Comninellis Ch, Pulgarin C (1993) Electrochemical oxidation of phenol for wastewater treatment using $SnO_2$ anodes. J. Appl. Electrochem. 23: 108–112.

[15] Boudenne JL, Cerclier O, Galéa J, Van der Vlist E (1996) Electrochemical oxidation of aqueous phenol at a carbon black slurry electrode. Appl. Catal. A: Gen. 143: 185–202.

[16] Tahar NB, Savall A (1999) A comparison of different lead dioxide coated electrodes for the electrochemical destruction of phenol. J. New Mat. Electrochem. Sys. 2: 19–26.

[17] Chen X, Chen G, Yue PL (2003) Anodic oxidation of dyes at novel Ti/B-diamond electrodes. Chem. Eng. Sci. 58: 95–1001.

[18] Gotsi M, Kalogerakis N, Psillakis E, Samaras P, Mantzavinos D (2005) Electrochemical oxidation of olive oil mill wastewaters. Water Res. 39: 4177–4187.

[19] Belaid C, Kallel M, Khadhraou M, Lalleve G, Elleuch B, Fauvarque JF (2006) Electrochemical treatment of olive mill wastewaters: Removal of phenolic compounds and decolourization. J. App. Electrochem. 36: 1175–1182.

[20] Panizza M, Cerisola G (2006) Olive mill wastewater treatment by anodic oxidation with parallel plate electrodes. Water Res. 40: 1179–1184.

[21] Giannis A, Kalaitzakis M, Diamadopoulos E (2007) Electrochemical treatment of olive mill wastewater J. Chem. Technol. Biotechnol. 82: 663–671.

[22] Kotta E, Kalogerakis N, Mantzavinos D (2007) The effect of solids on the electrochemical treatment of olive mill effluents. J. Chem. Technol. Biotechnol. 82: 504–511.

[23] Un UT, Altay U, Koparal AS, Ogutveren UB (2008) Complete treatment of olive mill wastewaters by electrooxidation. Chem. Eng. J. 139: 445–452.

[24] Chatzisymeon E, Dimou A, Mantzavinos D, Katsaounis A (2009) Electrochemical oxidation of model compounds and olive mill wastewater over DSA electrodes: 1. The case of Ti/$IrO_2$ anode. J. Hazard. Mater. 167: 268–274.

[25] Papastefanakis N, Mantzavinos D, Katsaounis A (2010) DSA electrochemical treatment of olive mill wastewater on Ti/$RuO_2$ anode. J. Appl. Electrochem. 40: 729–737.

[26] Comninellis Ch, Vercesi G.P (1991) Characterization of DSA-type oxygen evolving electrodes: choice of a coating. J. Appl. Electrochem. 21: 335–345.

[27] Comninellis Ch, Nerini A (1995) Anodic oxidation of phenol in the presence of NaCl for wastewater treatment J. Appl. Electrochem. 25: 23–28.

[28] Longhi P, Vodopivec B. Fiori G (2001) Electrochemical treatment of olive oil mill wastewater Ann. Chim. 91: 169–174.

[29] Saracco G, Solarino L, Specchia V, Maja M (2001) Electrolytic abatement of biorefractory organics by combining bulk and electrode oxidation processes. Chem. Eng. Sci. 56: 1571–1578.

[30] Menini R, Henuset YM, Fournier J (2005) Electrochemical oxidation of phenolic compounds using a flow-through electrolyser with porous solid electrodes. J. Appl. Electrochem. 35: 625–631.

[31] Polcaro AM, Vacca A, Mascia M, Palmas S, Ferrara F, Ruiz J (2008) Selective oxidation of phenolic compounds at BDD and DSA anodes. J. Environ. Eng. Manage. 18(3): 213–220.

[32] Israilides CJ, Vlyssides AG, Mourafeti VN, Karvouni G (1997) Olive oil wastewater treatment with the use of an electrolysis system Bioresour. Technol. 61: 163–170.

[33] Gonçalves MR, Marques IP, Correia JP (2012) Electrochemical mineralization of anaerobically digested olive mill wastewater. Water Res. 46: 4217–4225.

[34] Patoni M, Passadis T, Kalogerakis N (2010) Electrolytic Pretreatment of Olive Mill Wastewater (OMW) for Methane to Hydrogen Production. Separ. Sci. Technol. 45 (11): 1529–1537.

[35] Kumar S, Singh S, Srivastava VC (2015) Electro-oxidation of nitrophenol by ruthenium oxide coated titanium electrode: Parametric, kinetic and mechanistic study. Chem. Eng. J. 263: 135–143.

[36] Balice V, Cera O (1984) Acid phenolic fraction of the olive vegetation water determined by a gas chromatographic method. Grasas y Aceites 35 (5): 178–180.

[37] Fajardo AS, Rodrigues RF, RC Martins, LM Castro, RM Quinta-Ferreira (2015) Phenolic wastewaters treatment by electrocoagulation process using Zn anode. Chem. Eng. J. 275: 331–341.

[38] Fajardo AS, Martins RC, Quinta-Ferreira RM (2014) Treatment of a Synthetic Phenolic Mixture by Electrocoagulation Using Al, Cu, Fe, Pb, and Zn as Anode Materials. Ind. Eng. Chem. Res. 53: 18339−18345.

[39] Silva A, Nouli E, Xekoukoulotakis N, Mantzavinos D (2007) Effect of key operating parameters on phenols degradation during $H_2O_2$-assisted $TiO_2$ photocatalytic treatment of simulated and actual olive mill wastewaters. Appl. Catal. B. 73: 11–22.

[40] Greenberg A, Clesceri L, Eaton A (1992) Standard Methods for the Examination of Water and Wastewater, 18th ed., American Public Health Association. Washington DC.

[41] Freire DDC, Sant'Anna Jr. (1998) A proposed method modification for the determination of COD in saline wastewaters Environ. Technol. 19: 1243–1247.

[42] Mahvi AH, Bazrafshan E, Jahed GhR (2005) Evaluation of COD Determination by ISO 6060 Method Comparing with Standard Method (5220 B). Pak. J. Biol. Sci. 8(6): 892–894.

[43] Araújo CKC, Oliveira GR, Fernandes NS, Zanta CLPS, Castro SSL, da Silva DR, Martínez-Huitle CA (2014) Electrochemical removal of synthetic textile dyes from aqueous solutions using Ti/Pt anode: role of dye structure. Environ. Sci. Pollut. Res. 21: 9777–9784.

[44] Chiang LC, Chang JE, Tseng SC (1997) Electrochemical oxidation pretreatment of refractory organic pollutants. Water Sci. Technol. 36(2–3): 123–130.

[45] Bonfatti F, De Battisti A, Ferro S, Lodi G, Osti S (2000) Anodic mineralization of organic substrates in chloride-containing aqueous media. Electrochim. Acta 46: 305–314.

[46] Panizza M, Cerisola G, (2009) Electrochemical degradation of gallic acid on a BDD anode Chemosphere 77: 1060–1064.

[47] Garcia-Segura S, Keller J, Brillas E, Radjenovic J (2015) Removal of organic contaminants from secondary effluent by anodic oxidation with a boron-doped diamond anode as tertiary treatment J. Hazard. Mater. 283: 551–557.

[48] Chiang LC, Chang JE, Wen TC (1995) Indirect oxidation effect in electrochemical oxidation treatment of landfill leachate. Wat. Res. 29(2): 671–678.

[49] Rajkumar D, Palanivelu K (2003) Electrochemical degradation of cresols for wastewater treatment. Ind. Eng. Chem. Res. 42(9): 1833–1839.

[50] Rajkumar D, Palanivelu K (2004) Electrochemical treatment of industrial wastewater. J. Hazard. Mater. 113(1–3):123–129.

[51] Zayas T, Picazo M, Morales U, Torres E, Salgado L (2015) Effectiveness of Ti/$RuO_2$ and Ti/RuIrCo(40%:40%:20%)Ox Anodes for Electrochemical Treatment of Paper Industry Wastewater. Int. J. Electrochem. Sci. 10: 7840 – 7853.

[52] Santos TES, Silva RS, Meneses CT, Martínez-Huitle CA, Eguiluz KIB, Salazar-Banda GR (2016) Unexpected Enhancement of Electrocatalytic Nature of Ti/$(RuO_2)x-(Sb_2O_5)y$ Anodes Prepared by the Ionic Liquid-Thermal Decomposition Method. Ind. Eng. Chem. Res. 55: 3182−3187.

[53] Aquino JM, Rocha-Filho RC, Ruotolo LAM, Bocchi N, Biaggio SR (2014) Electrochemical degradation of a real textile wastewater using β-$PbO_2$ and DSA® anodes. Chem. Eng. J. 251: 138–145.

[54] Coledam DAC, Aquino JM, Rocha-Filho RC, Bocchi N, Biaggio S (2014) Influence of chloride-mediated oxidation on the electrochemical degradation of the Direct Black 22 dye using boron-doped diamond and β-$PbO_2$ anodes. Quím. Nova 37: 1312–1317.

[55] Elaoud SC, Panizza M, Cerisola G, Mhiri T (2011) Electrochemical degradation of sinapinic acid on a BDD anode. Desalination 272: 148–153.

[56] Kasischke KA, Vishwasrao HD, Fisher PJ, Zipfel WR, Webb WW ( 2004) Neural activity triggers neuronal oxidative metabolism followed by astrocytic glycolysis. Science 305: 99–103.

[57] Nicoll RA, Schmitz D (2005) Synaptic plasticity at hippocampal mossy fibre synapses. Nat. Rev. Neurosci. 6: 863–876.

[58] Suzuki E, Okada T (2009) TEA-induced long-term potentiation at hippocampal mossy fiber-CA3 synapses: Characteristics of its induction and expression. Brain Res. 1247: 21–27.

[59] Smart TG, Xie X, Krishek BJ (1994) Modulation of inhibitory and excitatory amino acid receptor ion channels by zinc. Prog. Neurobiol. 42: 393–341.

[60] Bancila V, Nikonenko I, Dunant Y, Bloc A (2004) Zinc inhibits glutamate release via activation of pre-synaptic KATP channels and reduces ischaemic damage in rat hippocampus. J. Neurochem. 90: 1243–1250.

[61] Frederickson CJ, Koh JY, Bush AI (2005) The neurobiology of zinc in health and disease. Nat. Rev. Neurosci. 6(6): 449–462.

[62] Matias CM, Saggau P, Quinta-Ferreira ME (2010) Blockade of presynaptic K ATP channels reduces the zinc-mediated posttetanic depression at hippocampal mossy fiber synapses. Brain Res. 320: 22–27.

[63] Belaid C, Khadraoui M, Mseddi S, Kallel M, Elleuch B, Fauvarque JF (2013) Electrochemical treatment of olive mill wastewater: Treatment extent and effluent phenolic compounds monitoring using some uncommon analytical tools J. Environ. Sci. 25(1): 220–230.

# VII. PHENOLIC WASTEWATERS DEPURATION BY ELECTROCHEMICAL OXIDATION PROCESS USING Ti/IrO$_2$ ANODES

AS Fajardo[a], HF Seca[a], RC Martins[a], VN Corceiro[b], JP Veira[b], ME Quinta-Ferreira[b,c] and RM Quinta-Ferreira[a]

[a] CIEPQPF – Chemical Process Engineering and Forest Products Research Centre; GERST – Group on Environment, Reaction, Separation and Thermodynamics; Department of Chemical Engineering, Faculty of Sciences and Technology, University of Coimbra, Pólo II, Rua Sílvio Lima, 3030-790 Coimbra, Portugal.

[b] Department of Physics, University of Coimbra, 3004-516 Coimbra, Portugal.

[c] CNC - Centre for Neuroscience and Cell Biology, University of Coimbra, 3004-504 Coimbra, Portugal.

*Submitted to Environmental Science and Pollution Research*

## ABSTRACT

The electrochemical oxidation (EO) of phenolic wastewaters mimicking olive oil mill effluents was carried out in a batch stirring-reactor using Ti/IrO$_2$ anodes, varying the nature (NaCl and Na$_2$SO$_4$) and electrolyte concentration (1.8–20 g L$^{-1}$), current density (57–119 mA cm$^{-2}$) and initial pH (3.4–9). Phenolic content (TPh) and chemical oxygen demand (COD) removals were monitored as a function of applied charge and over time. The nature of the electrolyte greatly affected the efficiency of the system, followed by the influence of the current density. The NaCl concentration and the initial pH influenced the process in a lesser extent. The best operating conditions achieved were 10 g L$^{-1}$ of NaCl, current density of 119 mA cm$^{-2}$ and initial pH of 3.4. These parameters led to 100 and 84.8 % of TPh and COD removal, respectively. Under these conditions, some differences were observed by SEM on the surface of the anode after treatment. To study the potential toxicity of the synthetic effluent in neuronal activity, this mixture was applied to rat brain slices prior to and after EO. The results indicate that although the treated effluent causes a smaller depression of the neuronal reactive oxygen species (ROS) signal than the untreated one, it leads to a potentiation instead of recovery, upon washout. Furthermore, the purification of a real olive mill wastewater (OMW), with the organic load of the synthetic effluent, using

the same optimised operating conditions, achieved total phenolic compounds abatement and 62.8 % of COD removal.

This study demonstrates the applicability of this EO as a pre-treatment process of a real effluent, in order to achieve the legal limit values to be discharged into natural streams regarding its organic load.

## VII.1 INTRODUCTION

Recently, electrochemical processes demonstrated to be attractive alternatives to the conventional pathways to treat effluents containing toxic and/or refractory organic compounds [1–3]. Among these processes arose the electrochemical oxidation (EO), an advanced oxidation process (AOP) which involves in-situ electrogeneration of strong oxidants, allowing a better efficiency in the removal of organic compounds when compared to analogous techniques, such as ozonation and Fenton's processes [4–6]. The required equipment and operations are in general simple and inexpensive; nonetheless various considerations must be taken into account to optimise efficiency, such as reactor configuration and experimental conditions (nature of the electrode material, current density, flow dynamic regime, pH and presence of mediators) [7,8]. This technique is versatile and robust because it allows dealing with several pollutants and treat diverse volumes of wastewaters Additionally, the reaction can be easily completed in short times by cutting off the energy and has a rapid start over when an operation problem occurs [4,5]. EO does not need high temperature and pressure like incineration and supercritical oxidation systems. Moreover, it is amenable to automation since the electrical variables are simple to use for data acquisition, process automation and control. However, the main disadvantage of this process consist of its high operating cost due to the high energy consumption [4,5,9].

The elimination of pollutants by EO may follow two different mechanisms. The first one is the direct anodic oxidation, where the contaminants are diffused from the bulk solution to the anode surface, being destroyed there by direct charge transfer. In the second mechanism, indirect reaction, a mediator is introduced and an oxidant is electrochemically generated to carry out the oxidation in the liquid. Both pathways may coexist during oxidation.

The use of chloride ions has already been widely studied as a mediator to test the performance of EO [4], since their addition enhances pollutants removal efficiency because of the electrogeneration of active chlorine. In addition, the presence of these ions in many wastewaters and natural waters make the participation of active chlorine predictable [10]. The oxidation of the chloride $(\mathrm{Cl}^-)$ ion on the surface of the anode leads to the generation of chlorine ($Cl_2$) (Equation (VII.1)), which is further hydrolysed being disproportionated to HClO (hypochlorous acid) and $\mathrm{Cl}^-$ (Equation (VII.2)). In the bulk solution, the HClO is in equilibrium with $\mathrm{OCl}^-$ with pKa=7.55 (Equation (VII.3)) [5,11,12].

$$2\ \mathrm{Cl^-} \rightarrow \mathrm{Cl_{2(aq)}} + 2\mathrm{e^-} \qquad \textbf{(VII.1)}$$

$$\mathrm{Cl_{2(aq)}} + \mathrm{H_2O} \rightarrow \mathrm{HClO} + \mathrm{Cl^-} + \mathrm{H^+} \qquad \textbf{(VII.2)}$$

$$\mathrm{HClO} \rightleftarrows \mathrm{H^+} + \mathrm{OCl^-} \qquad \textbf{(VII.3)}$$

Some researchers have demonstrated that the effect of NaCl as mediator significantly depends on the anodic material [13,14]. Great attention has been given to dimensionally stable anodes (DSA) due to their stability and oxidation ability. Metal and mixed-metal oxide electrodes as $RuO_2$ and $IrO_2$ have largely been applied to the chloralkali industry due to their catalytic efficiency [15]. These electrodes are widely used in environmental electrochemistry because of their low cost, easiness of preparation, excellent mechanical stability, long service lifetime and reasonable electrocatalytic activity [1,12,16–18]. Comparing these two anode materials, $IrO_2$ and $RuO_2$, the former one is especially remarkable since it reveals high corrosion resistance and it is only slightly inferior to $RuO_2$ in terms of electrocatalysis performance. In addition, it is recognised as a good electrocatalyst for the oxidation of organic compounds due to the formation of adsorbed hydroxyl radicals (Equation (VII.4)) [19].

$$\mathrm{IrO_2} + \mathrm{H_2O} \rightarrow \mathrm{IrO_2}(\ ^{\bullet}\mathrm{OH}) + \mathrm{H^+} + \mathrm{e^-} \qquad \textbf{(VII.4)}$$

Some works have already used the $Ti/RuO_2$ and $Ti/IrO_2$ anode materials to treat phenolic compounds normally present in the seasonally produced olive mill wastewaters (OMW). These substances present high pollutant load and are toxic to the environment [20]. Moreover, they are biorecalcitrant, not being able to be removed by biological treatment.

Polcaro *et al.* [21] studied the selectivity oxidation of the phenolic fraction from solutions containing organic matter (glucose) at boron doped diamond (BDD) and $Ti/RuO_2$ anodes. Both materials showed to perform selective processes with different operating conditions. For instance, a good selectivity of the electrochemical system could be attained with low current densities and high mixing rates at BDD anodes. In addition, a fast and selective removal is achieved at $Ti/RuO_2$ anode at low mixing rates, high current densities and a chloride concentration between 1.0–2.5 g $L^{-1}$. Other authors [22] also tested the $Ti/RuO_2$ anode but focused on a treatment without any previous or post-process to depurate this kind of wastewaters. The best operating conditions (135 mA $cm^{-2}$, 2 M NaCl, 0.028 $m^3\ h^{-1}$ and 40 °C) led to almost complete removal of COD, phenolic content, turbidity and oil-grease concentration with an energy consumption involving 0.88 € $kg_{COD\ removed}^{-1}$. $Ti/RuO_2$ and $Ti/IrO_2$ anodes present good activity for the treatment of OMW, allowing the reduction of pollutants and the removal of turbidity and toxicity [23]. When both these DSAs were applied to an anaerobically digested OMW, $Ti/RuO_2$ led to almost complete removal of COD, phenols and colour. Although not providing as high removals as the previous electrode, the $Ti/IrO_2$ may be considered useful in the selective depuration of phenolic wastewaters prior to a biological treatment. The stability and the activity of $Ti/IrO_2$ anode was followed by Chatzisymeon *et al.* [24], realising that these parameters depend on current densities applied for oxygen evolution and on the type of compound to be oxidised.

The main objective of this work was to analyse the effect of that anode material on the depuration of a synthetic mixture of six phenolic acids usually present in OMW. The assessment of its activity is given in terms of total phenolic content (TPh) and chemical oxygen demand (COD) removal, taking into account different operating conditions, such as the nature/concentration of the electrolyte, current density and initial pH. After achieving the best operating conditions, the morphology of the anode was analysed before and after use. The possible application of such technology to depurate a real OMW was then evaluated. In recent years diseases of the central nervous system, that are affecting a growing number of people limiting their everyday life, are one of the main focus of biomedical research. In particular, synaptic activity and its major property, plasticity, that is involved in cellular learning [25], may be highly affected by pollutants of industrial origin. These include phenolic acids, present in large amounts in OMW that may interfere with the production of neuronal reactive oxygen species (ROS) and cause cellular degeneration [26–28]. For these reasons another aim of the work was to study the impact of the synthetic phenolic effluent in synaptic ROS formation. To the best of our knowledge, this kind of analysis was never performed for EO systems.

## VII.2 EXPERIMENTAL

### VII.2.1 SYNTHETIC AND REAL EFFLUENT

The synthetic effluent was prepared using a concentration of 100 mg L$^{-1}$ of each phenolic acid (3,4-dihydroxybenzoic, 3,4-dimethoxybenzoic, 3,4,5-trihydroxybenzoic, 3,4,5-trimethoxybenzoic, 4-hydroxybenzoic, trans-3-phenylacrylic) normally found in OMW [29]. The phenolic compounds structure and characteristics are collected in Table VII.1.

**Table VII.1. Characteristics and chemical structure of phenolic acids.**

| IUPAC name | Common name | M (g mol$^{-1}$) | Chemical structure |
|---|---|---|---|
| 3,4-dihydroxybenzoic acid | Protocatechuic acid | 154.12 | 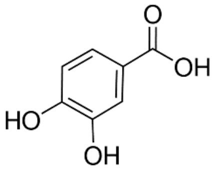 |
| 3,4-dimethoxybenzoic acid | Veratric acid | 182.17 | 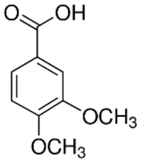 |
| 3,4,5-trihydroxybenzoic acid | Gallic acid | 170.12 | 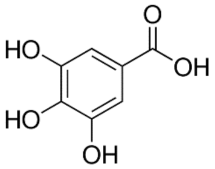 |
| 3,4,5-trimethoxybenzoic acid | Trimethylgallic acid | 212.20 | 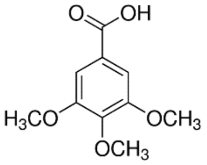 |
| 4-hydroxybenzoic acid | - | 138.12 | 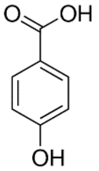 |
| trans-3-phenylacrylic acid | trans-cinnamic acid | 148.16 | 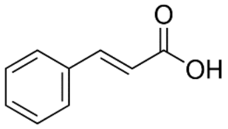 |

A real olive mill wastewater (OMW) was obtained from a mill located in the Extremadura region of Spain. The stream presented a dark brownish colour and a strong olive smell. The main characteristics of the effluents applied in the study are depicted in Table 2. Both wastewaters, synthetic and real, have an acidic character with low conductivity < 2.50 mS cm$^{-1}$ [30]. The high content of phenolic acids, determined as TPh (323–384 mgGA L$^{-1}$), is representative of this kind of wastewaters, being one of the key parameters to be reduced by the treatment, as well as the amount of organic matter (1118–6530 mgO$_2$ L$^{-1}$) expressed by the chemical oxygen demand (COD). According to the Portuguese Decree-Law 236/98 of 1st August, a wastewater only can be discharged into a natural stream if COD values are lower than 150 mgO$_2$ L$^{-1}$. Moreover, a high amount of solids in the real OMW (2574±181 and 3562±34 mg L$^{-1}$ in total suspended solids–TSS and total dissolved solids–TDS, respectively) was determined. The OMW was filtered using a sequence of three sieves Retsch (297, 210 and 105 mm) and filter paper of 45 µm in order to reduce the solids, achieving 5832±63 mgO$_2$ L$^{-1}$ and 352±35 mgGA L$^{-1}$ of initial COD and TPh values, respectively. To compare the removal efficiency of the EO process for the synthetic and real effluents, the filtered OMW was diluted 6 times with distilled water in order to achieve an initial

COD value similar to the simulated effluent, obtaining 1004±7 $mgO_2\ L^{-1}$ and 77±9 $mgGA\ L^{-1}$ of initial COD and TPh values, respectively.

**Table VII.2. Main characteristics of the synthetic and real effluents.**

| Characteristics | Synthetic effluent | Real effluent (before filtration) | Real effluent (after filtration) |
|---|---|---|---|
| pH | 3.4±0.3 | 4.3±0.1 | 4.3±0.1 |
| Conductivity (mS $cm^{-1}$) | 0.14±0.01 | 1.59±0.01 | 1.53±0.01 |
| TPh (mgGA $L^{-1}$) | 323±7 | 384±35 | 352±35 |
| COD ($mgO_2\ L^{-1}$) | 1118±41 | 6530±11 | 5832±63 |
| TSS (mg $L^{-1}$) | - | 2574±181 | - |
| TDS (mg $L^{-1}$) | - | 3562±34 | - |

### VII.2.2 ELECTROCHEMICAL OXIDATION (EO) PROCEDURE

EO was carried out in a lab-scale monocompartimental batch-stirred reactor of Perspex at atmospheric pressure and thermostated at 20 °C [31]. At the beginning of each experiment, the reactor was charged with 1 L of synthetic effluent or with real effluent. The $Ti/IrO_2$ material worked as anode and the stainless steel (SS) as cathode with an effective area of 21.1 $cm^2$ ($4.0 \times 2.5 \times 0.1$ cm). The electrodes were placed in parallel with a gap distance of 1 cm, linked to a DC power supply HY3010 Kaise (I=1.2–2.5 A). Samples were periodically withdrawn and centrifuged at 3500 rpm (Nahita 2655) for further analysis. NaCl and $Na_2SO_4$ were individually used as electrolytes in order to promote higher conductivity to the synthetic solution. This parameter was measured using a Consort C863 instrument. The initial pH of the synthetic solution was modified between 3.4 and 9, using NaOH at 3 M or $H_2SO_4$ at 2 M, whenever required. In addition, pH medium was followed during the treatment time by a HANNA pH meter, but not corrected. Some experiments were randomly run in duplicate to ensure the reproducibility of the results.

### VII.2.3 ANALYTICAL TECHNIQUES

Total phenolic content (TPh) was measured in terms of gallic acid (mgGA $L^{-1}$) using a T60 PG Instruments spectrophotometer at 765 nm by the colourimetric Folin Ciocalteau method, as described elsewhere [32]. Chemical oxygen demand (COD) was analysed by the closed reflux method (5250D) using potassium dichromate as oxidant [33]. The samples collected during the experiments were digested in a thermal reactor (Eco 25, VELP Scientifica) at 150 °C during 120 min and then, the absorbance was measured at 605 nm in a photometer (Photolab S6, WTW). The calibration curve was prepared using standard solutions of potassium hydrogenphthalate ($C_8H_5KO_4$) with COD values within the range 0–1200 $mgO_2\ L^{-1}$. Total dissolved solids (TDS) and total suspended solids (TSS) were carried out according to the Standard Methods (method 2540C and 2540D, respectively) [33]. Analytical determinations were accomplished at least in duplicate to minimise experimental errors and the maximum deviations were 10, 8, 5 and 5 %, for TPh, COD, TDS and TSS, respectively.

The energy consumption (EC) per volume of treated effluent was determined in terms of kWh $m^{-3}$ according to Equation (VII.5) [34]. Moreover, based on the amount of COD removed, current efficiency (CE) for the electrochemical oxidation of pollutants was determined by Equation (VII.6).

$$\mathrm{EC(kWh\ m^{-3})} = \frac{\mathrm{E_{cell}\ I\ t}}{\mathrm{V}} \tag{VII.5}$$

$$\mathrm{CE(\%)} = \frac{(\mathrm{COD_0} - \mathrm{COD_t})\ \mathrm{F\ V}}{8\mathrm{It}} \times 100 \tag{VII.6}$$

where $E_{cell}$ corresponds to the average potential difference of the cell (V), I to current intensity (A), t to the electrolysis time (h for EC or s for CE), V to the solution volume (L), $COD_0$ to the initial chemical oxygen demand ($gO_2$ L), $COD_t$ to the chemical oxygen demand ($gO_2$ L) at time t, F to the Faraday constant (96487 C $mol^{-1}$) and 8 to the equivalent mass of oxygen (g $eq^{-1}$).

### VII.2.4 MORPHOLOGICAL CHARACTERISATION OF THE ANODE

The morphological properties of the anode were analysed before and after use by SEM (scanning electron microscopy) at 500× magnification with a VEGA3 SBH–TESCAN equipment.

### VII.2.5 DETECTION OF REACTIVE OXYGEN SPECIES (ROS) SIGNALS FROM BRAIN SLICES

The biological preparation consisted of hippocampal slices from 31 weeks old female Wistar rats. The animals were sacrificed by cervical dislocation and after dissecting the hippocampus from the cooled brain, kept in artificial cerebrospinal fluid (ACSF), at 5–8 °C, the slices were cut transversely with a set of parallel, equally spaced (400 µm), blades. The ACSF medium had the following composition (in mM): NaCl 124; KCl 3.5; $NaHCO_3$ 24; $NaH_2PO_4$ 1.25; $MgCl_2$ 2; $CaCl_2$ 2 and D-glucose 10 (reagents from Sigma, Sintra, Portugal) at pH 7.4. The constituents of the synthetic effluent, with 10 g $L^{-1}$ of NaCl, equivalent to 171 mM, were added to the ACSF medium. For the studies with the treated medium, that included also NaCl (10 g $L^{-1}$), a solution with pH 7.4 was prepared adding the ACSF compounds to it. The slices were incubated, for 60 min, at room temperature, in a solution consisting of ACSF plus 20 µM of the permeant form of $H_2$DCFDA (Life technologies, Carlsband, CA), the ROS indicator used. After incubation the slices were transferred to the normal ACSF medium, kept also at room temperature, from where they were taken to the experimental chamber. Here, the perfusion solution was maintained at 30–32 ºC and circulated at 1.5–2 mL $min^{-1}$. All media bathing the slices were continuously oxygenated (95 % $O_2$, 5 % $CO_2$). The optical data, obtained in the presence of ACSF or a pollutant medium, were acquired at the mossy fiber synapses from hippocampal CA3 area, through a fluorescence microscope (Zeiss Axioskop). Transfluorescence measurements were made using a tungsten/halogen light source (12 V, 100 W), a narrow band (10 nm) interference excitation filter (480 nm) and a high-pass emission filter (> 500 nm). Emitted light was detected by a silicon photodiode (Hammamatsu, 1 $mm^2$) after being collected by a water immersion lens (40×, N.A. 0.75). The signal from the photodiode, after passing through an I/V converter (with 1 GΩ feedback resistance) entered a 16 bits analog/digital converter (National Instruments), being processed at 1.67 Hz and displayed using the Signal ExpressTM software. The data were corrected subtracting the autofluorescence component, estimated from non-incubated slices, and normalized by the average of the first 10 baseline responses, being presented as mean ± s.e.m.

All experiments were carried out in accordance with the European Communities Council Directive (2010/63/UE). All efforts were made to minimise animal suffering and to use only the number of animals necessary to produce reliable scientific data.

## VII.3 RESULTS AND DISCUSSION

### VII.3.1 EFFECT OF THE NATURE AND CONCENTRATION OF THE SUPPORTING ELECTROLYTES

Two different electrolytes, NaCl and $Na_2SO_4$ at 10 g $L^{-1}$, were separately studied in order to test their effect in terms of TPh and COD removal (Figure VII.1) for the depuration of 1 L of a simulated phenolic solution at pH 3.4, by applying 57 mA $cm^{-2}$ using the Ti/$IrO_2$ anode.

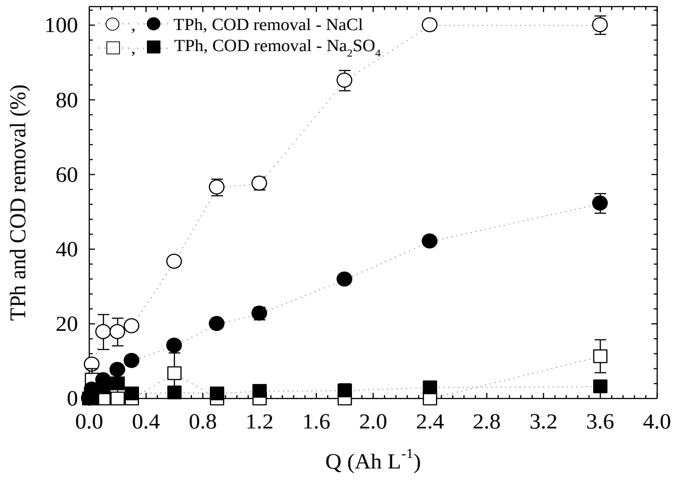

**Figure VII.1. Effect of the nature of electrolytes on TPh and COD removal as a function of the applied charge. Operating conditions: 100 mg $L^{-1}$ of synthetic phenolic solution, 10 g $L^{-1}$ of electrolyte, $pH_{initial}$=3.4, current density=57 mA $cm^{-2}$, distance between electrodes=1 cm, T=20 °C.**

As can be observed, for an applied charge of 3.6 Ah $L^{-1}$, corresponding to 180 min of treatment, a complete phenolic degradation is achieved with the utilisation of the NaCl salt, while with the $Na_2SO_4$ electrolyte, only 11.3 % is removed. Regarding COD, the maximum abatement, 52.2 %, was reached with NaCl, having the addition of $Na_2SO_4$, almost no effect on the removal of organic matter. The results indicate that the TPh removal rate is higher than that of COD. This behaviour is due to the break of phenolic acids molecules that are generally easily degradable into more recalcitrant compounds which may be difficult to remove during the oxidation process. In addition, these tests clearly show that the nature of the electrolyte significantly affects the performance of the process, since the electrogenerated species from each salt are not the same, thus promoting different oxidant routes to react with organic compounds during the treatment process, as also pointed out by Giraldo *et al.* [35]. The kind of anode material used will also influence how efficiently the oxidants are generated. For instance, the generation of the persulfate oxidant ($S_2O_8^{2-}$) is favoured when anodes with high oxygen evolution overpotential (boron doped-diamond or $PbO_2$) are used, while the electrode materials based on platinum or on a mixture of metal oxides, such as $IrO_2$, $RuO_2$ or $TiO_2$, are the most employed for the in situ generation of active chlorine species (Equations (VII.1)–(VII.3)) [12]. These active anodes mainly favour the selective oxidation, which leads to the partial degradation of organic matter (R), Equation (VII.7) and Equation (VII.8) [4,14,36].

$$IrO_2(\,^{\bullet}OH) \rightarrow IrO_3 + H^+ + e^- \qquad \textbf{(VII.7)}$$

$$IrO_3 + R \rightarrow IrO_2 + RO \qquad \textbf{(VII.8)}$$

Different amounts of NaCl (1.8–20 g $L^{-1}$) were used in order to evaluate its effect on electrochemical assays. Figure VII.2a represents the removal of phenolic content as a function of the applied charge. As can be observed, TPh removal rises with the increase of the supporting electrolyte concentration. The experiments with 1.8 g $L^{-1}$, 4 g $L^{-1}$ and 6 g $L^{-1}$ followed close removal values up to 1.8 Ah $L^{-1}$ of applied charge (COD removal=56.1–61.7 %), while for the tests with 10 and 20 g $L^{-1}$, this charge corresponded to the degradation of 85.1 and 100 %, respectively. At the end of the process (3.6 Ah $L^{-1}$), every experiment achieved total removal, except one, the test with 1.8 g $L^{-1}$ of NaCl (73.7 %). This situation might be due to the insufficient formation of oxidants to eliminate the phenolic content. Figure VII.2b reveals that the organic load decreased with all NaCl concentrations studied and the profiles were quite analogous along with the applied charge. At 3.6 Ah $L^{-1}$, the highest COD removal obtained was with 10 g $L^{-1}$ (52.2 %) followed by 6 g $L^{-1}$ (51.8 %), 4 g $L^{-1}$ (47.6 %), 20 g $L^{-1}$ (45.4 %) and 1.8 g $L^{-1}$ (39.7 %). As can be noticed, the electrochemical process is negatively affected by the presence of high concentrations of $Cl^-$ ions ([NaCl] >10 g $L^{-1}$). At the experiment with 20 g $L^{-1}$, an alkaline pH medium (inset of Figure VII.2b) can be rapidly achieved allowing the formation of $ClO^-$. The concentration of these species can be diminished by their anodic oxidation to $ClO_2^-$ ion and their consecutive oxidation to chlorates ($ClO_3^-$) and perchlorates ($ClO_4^-$) [37–40]. The probable formation of these chlorinated organic intermediates and final compounds, which can be more hazardous than the initial components, may hinder the application of EO, thus, requiring control on the amount of electrolyte added.

Another interesting feature is the energy consumption achieved by each trial. As can be observed in Figure VII.2c, although EC decreases when more salt is added to the system from 1.8 to 10 g $L^{-1}$, higher COD removals are obtained, which is beneficial for the process operation costs. Indeed, as shown in Figure VII.2d, higher conductivity is promoted in the system, leading to the decrease of the resistance in the medium (which implies a lower potential difference–Figure VII.2e), diminishing EC and enhancing the degradation of the organics. Moreover, for similar final EC values (35.9–38.8 kWh $m^{-3}$, Figure VII.2c), it was found that a higher COD removal was obtained for the 10 g $L^{-1}$ experiment (52.2 %) than with the introduction of greater amounts of salt, 20 g $L^{-1}$ with 45.4 % of removal. Additionally, comparing the final COD decay of the assays with 6 and 10 g $L^{-1}$, they were quite similar, but using the higher NaCl concentration led to an energy consumption 1.2 times smaller. Therefore, the concentration of 10 g $L^{-1}$ of NaCl was chosen to continue the experiments.

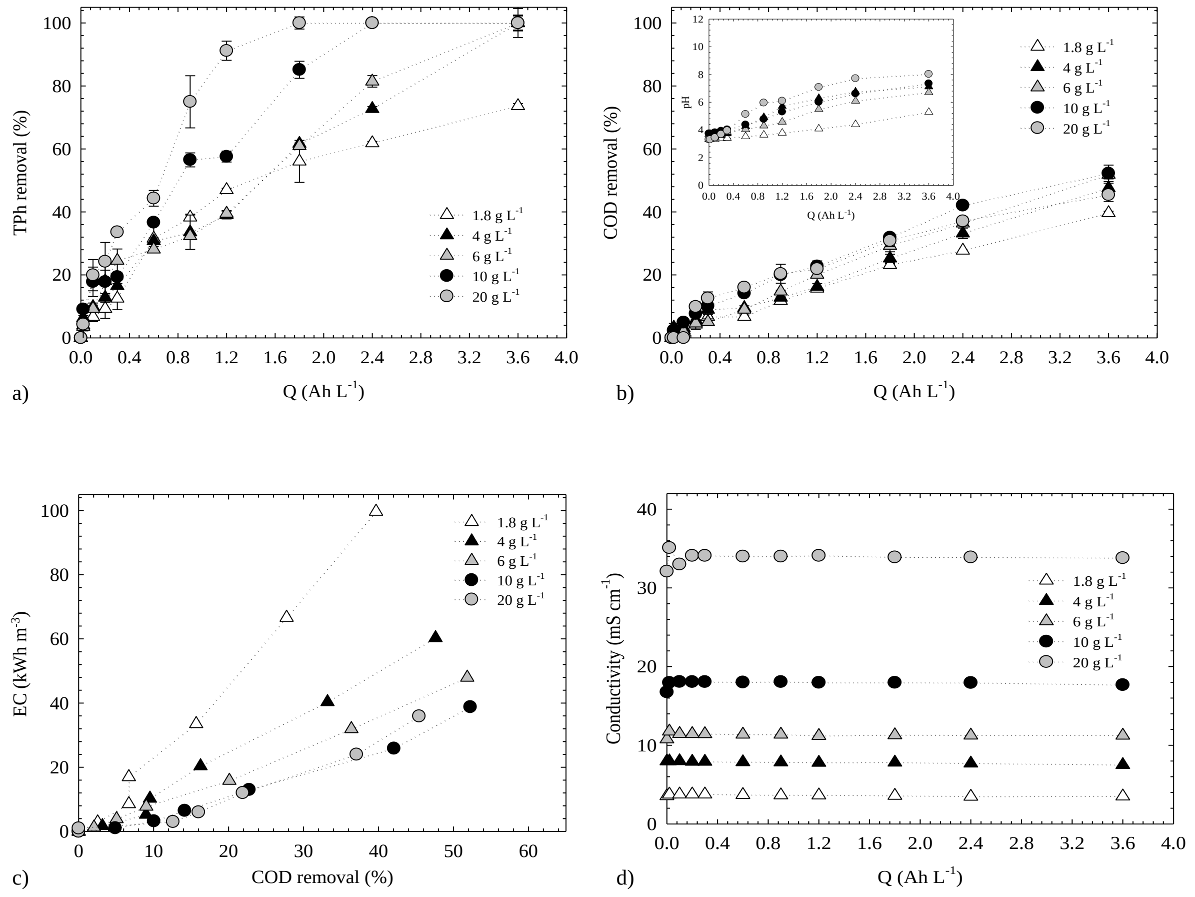

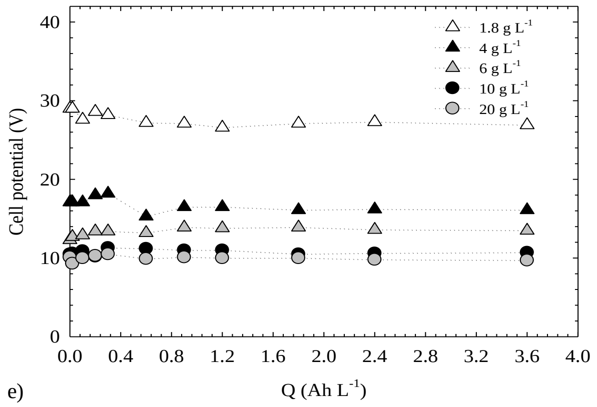

**Figure VII.2. Effect of the NaCl concentration on (a) TPh removal, (b) COD removal, (c) energy consumption, (d) conductivity and (e) cell potential. (a), (b), (d) and (e) as a function of the applied charge and (c) over COD removal. Inset of Figure VII.2: Evolution of pH medium at different NaCl concentrations. Operating conditions: 100 mg $L^{-1}$ of synthetic phenolic solution, $pH_{initial}$=3.4, current density=57 mA $cm^{-2}$, distance between electrodes=1 cm, T=20 °C.**

## VII.3.2 EFFECT OF CURRENT DENSITY

The effect of the current density was analysed between 57 and 119 mA $cm^{-2}$ at pH 3.4, with a distance between electrodes of 1 cm and NaCl concentration of 10 g $L^{-1}$. Figure VII.3a represents the TPh removal as a function of the applied charge and as can be observed, phenolic content decay improved with the increase of the applied charge, regardless the applied current density. Complete TPh removal was achieved between 2.4 and 3 Ah $L^{-1}$ for all the experiments. Analysing the timecourse of the results (Figure VII.3b), it can be seen that there is a significant decrease of TPh (100 % removal) during the first 60 min of oxidation with 119 mA $cm^{-2}$, followed by 95 mA $cm^{-2}$ after 90 min. In the case of the experiment with 57 mA $cm^{-2}$ double time (120 min) was needed to obtain a similar removal value. This means that the application of a fixed charge to achieve a certain TPh abatement, can be made either with high current densities with low treatment times or vice versa. Furthermore, the experiment with 57 mA $cm^{-2}$ until 3.6 Ah $L^{-1}$ of applied charge seems to have slightly higher COD removal values (Figure VII.3c) than the other assays even though its efficiency begins to decrease after 2.4 Ah $L^{-1}$. Moreover, Figure VII.3d, which displays the decay timecourse of organic compounds, shows that in this case the maximum COD removal reached after 180 min (≈ 52.2 %) can be attained with much lower times for higher current densities. Indeed, for 119 mA $cm^{-2}$ only 90 min are enough to get the same efficiency, being then possible to conclude that by doubling the current density, only half of the time is necessary to achieve the same COD removal. Also, at the end of the EO process, the highest COD removal was 84.8 % at 119 mA $cm^{-2}$.Thus, this current density was then selected to carry on the subsequent studies.

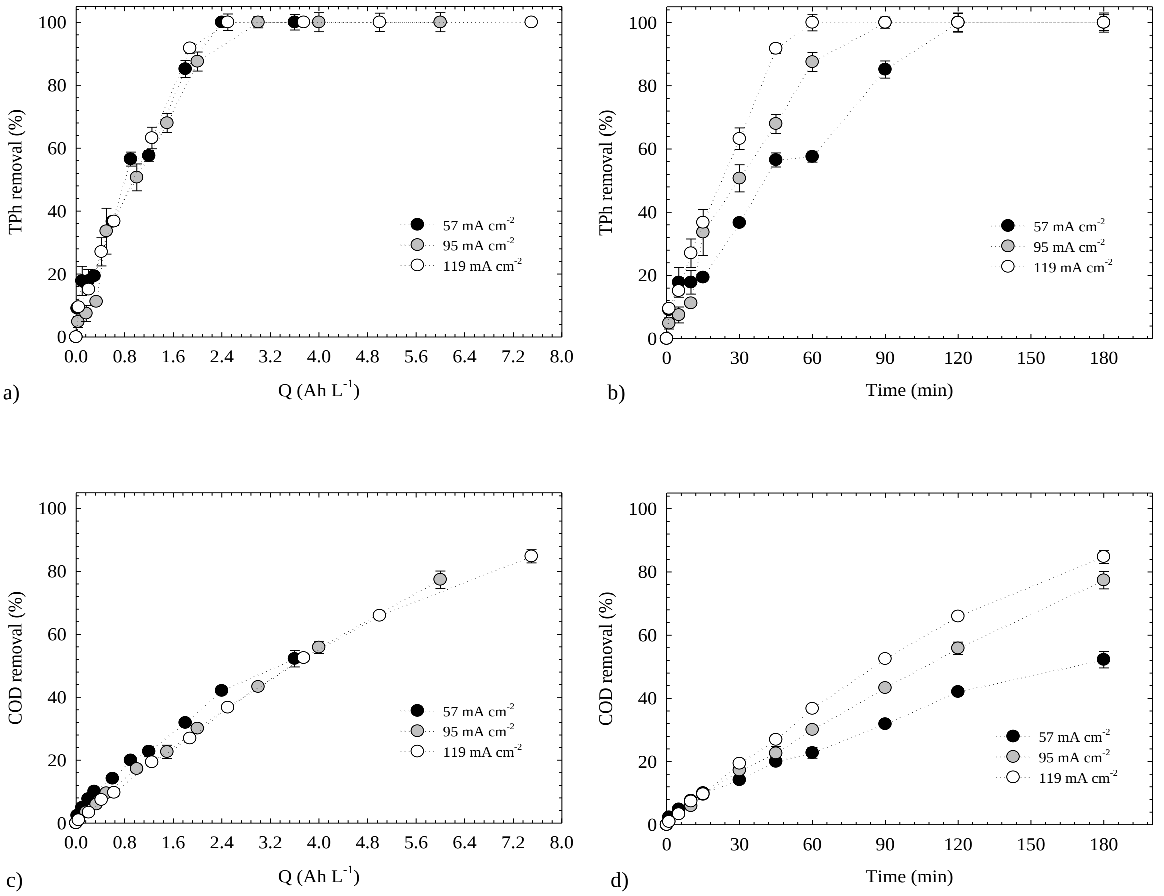

**Figure VII.3. Effect of the current density on (a,b) TPh removal and (c,d) COD removal as a function of the applied charge (a,c) and over time (b,d). Operating conditions: 100 mg L$^{-1}$ of synthetic phenolic solution, [NaCl]=10 g L$^{-1}$, pH$_{initial}$=3.4, distance between electrodes=1 cm, T=20 °C.**

### VII.3.3 EFFECT OF INITIAL PH

The pH of solutions plays an important role in indirect electrochemical oxidation, since the electrogeneration of specific oxidising species strongly depends on this parameter. For that reason, the effect of the initial pH value (pH$_0$) has been investigated in the range 3.4 – 9 at 119 mA cm$^{-2}$ with 10 g L$^{-1}$ of NaCl (Figure VII.4). The results demonstrate that the acidic conditions led to higher TPh and COD abatements (Figure VII.4a and Figure VII.4b, respectively) than neutral or alkaline media. This result is remarkable because most studies conducted in the presence of NaCl are performed at alkaline pH to minimise the reduction of efficiency due to chlorine free evaporation [8,39]. At pH$_0$ 7 and 9, complete phenolic content degradation (Figure VII.4a) was obtained after 5 Ah L$^{-1}$ applied charge (120 min of treatment), while only 2.4 Ah L$^{-1}$ (60 min of oxidation) were required when operating at pH$_0$ 3.4. At this latter pH$_0$, 84.8 % of COD was removed with 7.5 Ah L$^{-1}$ of applied charge, while for the same amount of charge, the experiments at pH 7 and 9 achieved 64.1 % and 62.1 %, respectively (Figure VII.4b). In fact, depending on the pH of the medium, different distributions of aqueous chlorine species may be obtained [41]. Generally, until pH 3, the main generated specie is $Cl_{2\,(aq)}$, while in the pH range of 3–8 is HClO and for pH > 8 is $ClO^{-}$. Then, the oxidation of organics mediated by the active chlorine species is faster in acidic than in alkaline media due to the higher standard potential of $Cl_{2\,(aq)}$ ($E^0$=1.36 *vs* SHE) and HClO ($E^0$=1.49 *vs* SHE) than that of $ClO^-$ ($E^0$=0.89 *vs* SHE). Moreover, it can be observed in the inset of Figure VII.4b that the highest current efficiency, 37.6 %, occurs for the experiment with pH 3.4. This means, however, that the most part of the energy consumed is not totally used to oxidise the organic compounds but is also used in parasitic reactions as oxygen and chlorine evolution.

Figure VII.4c displays the pH evolution as a function of applied charge. As can be observed, the pH of the solutions changed during the oxidation process. Particularly, in the experiments with initial pH of 3.4 and 7, this parameter increased up to 8.3 and 8.6, respectively. Meanwhile, at initial pH 9, a small pH change was observed throughout the experiment, ending with a pH of 8.8. Similar behaviour was described by Rajkumar *et al.* [42] and Scialdone *et al.* [8] during the electrochemical oxidation of organics in the presence of chlorides. In addition, the rise of pH during the delivery of charge may be explained by the reactions that occur at the cathode since, at this electrode, water molecules receive electrons and dissociate themselves into hydrogen ($H_2$) gas and hydroxide ions ($OH^-$) (Equation (VII.9)), causing a pH increase [43,44].

$$2H_2O + 2e^- \rightarrow H_2 + 2OH^- \tag{VII.9}$$

As aforementioned, the final pH of the experiments was around 8.3 and 8.8. Rajkumar *et al.* [42] tried to justify the final pH values by the formation of bicarbonate buffer, since the hydroxide ions ($OH^-$) may react with the carbon dioxide generated during pollutants oxidation, leading to the buffer formation. This final pH range is within the legal limits for wastewater discharge both in sewage and natural water courses, according to the Portuguese Decree-Law 236/98 of 1st of August. As a result, the pH adjustment over the electrochemical oxidation process is not necessary.

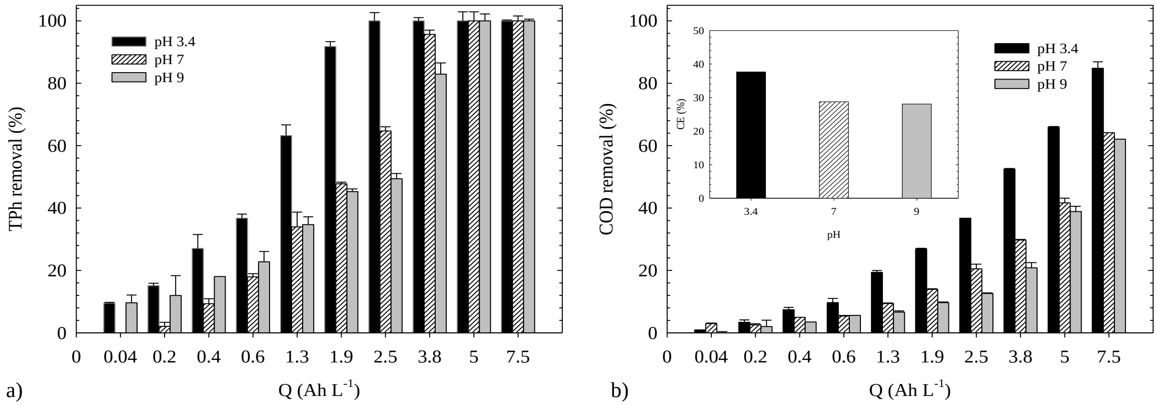

a)

b)

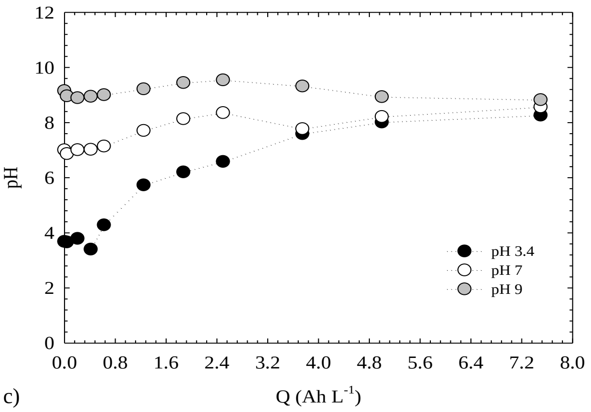

**Figure VII.4. Effect of the initial pH medium on (a) TPh removal, (b) COD removal and (c) pH medium evolution as function of the applied charge. Inset of Figure VII.4b: Current efficiency at 7.5 Ah $L^{-1}$ for the different initial pH mediums. Operating conditions: 100 mg $L^{-1}$ of synthetic phenolic solution, [NaCl]=10 g $L^{-1}$, current density=119 mA $cm^{-2}$, distance between electrodes=1 cm, T=20 °C.**

### VII.3.4 Ti/$IrO_2$ ANODE MORPHOLOGY

The morphology of the Ti/$IrO_2$ material was analysed by SEM at a magnification of 500× (Figure VII.5), before and after its use in the EO process at the selected operating conditions (10 g $L^{-1}$ of NaCl, current density of 119 mA $cm^{-2}$ and initial raw pH 3.4). The unused anode (Figure VII.5a) showed a surface with a porous mud [45,46]. After the EO treatment, the same anode presented some irregularities on its surface (Figure VII.5b). This modification suggests that the surface of the anode is eroded.

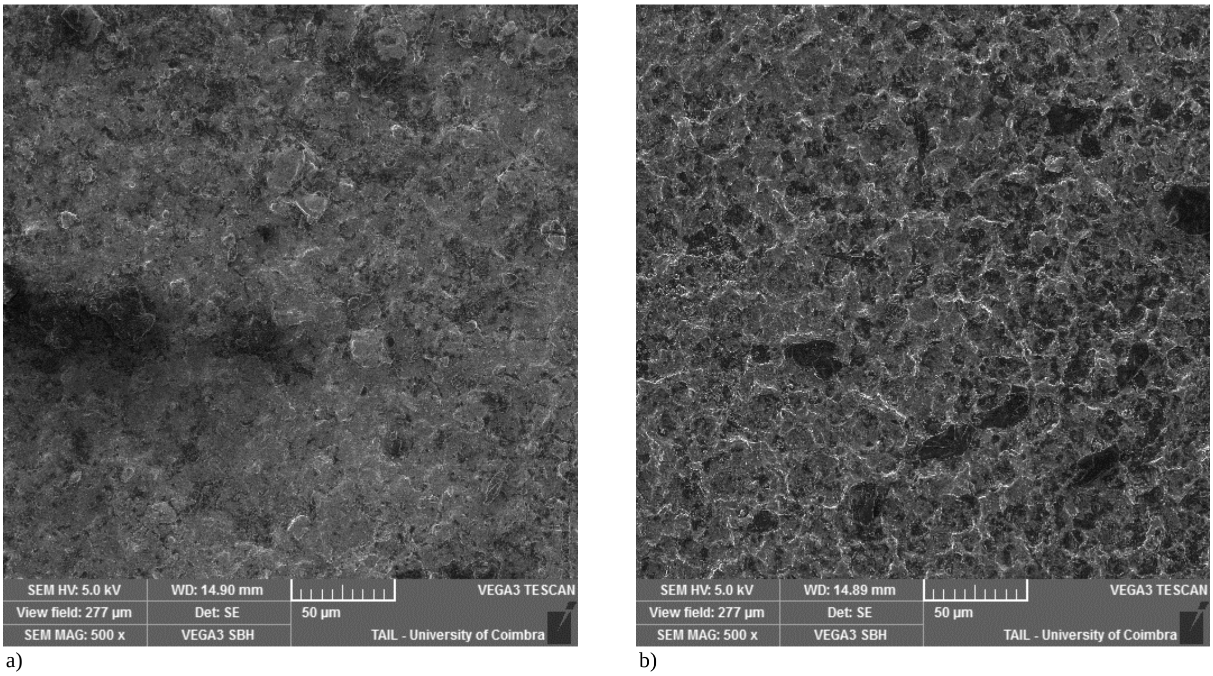
SEM HV: 5.0 kV
WD: 14.90 mm
VEGA3 TESCAN
View field: 277 μm
Det: SE
50 μm
SEM MAG: 500 x
VEGA3 SBH
TAIL - University of Coimbra
SEM HV: 5.0 kV
WD: 14.89 mm
VEGA3 TESCAN
View field: 277 μm
Det: SE
50 μm
SEM MAG: 500 x
VEGA3 SBH
TAIL - University of Coimbra

a) b)

**Figure VII.5. SEM photographs at 500× of the Ti/$IrO_2$ anode material, (a) before and (b) after EO treatment. Operating conditions: 100 mg $L^{-1}$ of synthetic phenolic solution, [NaCl]=10 g $L^{-1}$, $pH_{initial}$=3.4, current density=119 mA $cm^{-2}$, distance between electrodes=1 cm, T=20 °C.**

### VII.3.5 IMPACT OF THE PHENOLIC EFFLUENTS IN NEURONAL ROS ACTIVITY

The efficiency of the EO treatment was evaluated in brain slices. After 10 min in the control (ACSF) solution, the slices were perfused for 30 min with the untreated or treated effluent. This was then removed and the normal medium was circulated again, for the same period.

Figure VII.6 shows the timecourse of normalised fluorescence changes evoked by the treated effluent. After an initial rapid decay towards a minimum (0.67±0.05, at 15–20 min, n=3), the signal recovered reaching the baseline approximately 10 min after washout. It continued to increase and became stable (1.26±0.06, at 65–70 min, n=3) at the end of the new period in ACSF. The amplitude of the depression observed in the untreated and treated media were quite different as can be seen in the inset of Figure VII.6. Thus, in the presence of the raw effluent, the changes were larger and the signal recovered, reaching the initial value at the end of the following control period. As for the treated effluent, a large potentiation was observed during this control period. These results show that before treatment the phenolic mixture caused a pronounced decrease in the synaptic ROS signal that recovered completely upon returning to the control medium (ACSF). After treatment the depression was smaller but following the removal of the effluent, the signal reached a high level above baseline. With respect to the depression, a signal reduction was also evoked, in the same preparation and using the same ROS indicator, by the voltage dependent potassium channel blocker tetraethylammoniun (TEA) (data not shown). It is considered that the membrane depolarisation evoked by TEA leads to a sequence of events including glutamate and zinc co-release, the activation of $K_{ATP}$ channels and inhibition of voltage dependent calcium channels by zinc, causing the depression [47–51]. Thus, the phenolic mixture used may interfere with similar cellular pathways as those activated following the potassium channels blockade by TEA. Those pathways are likely to involve mitochondrial reactions triggered by the TEA-evoked membrane depolarisation. This causes calcium entry to the presynaptic terminal, that is necessary for providing the energy required for vesicle fusion and neurotransmission.

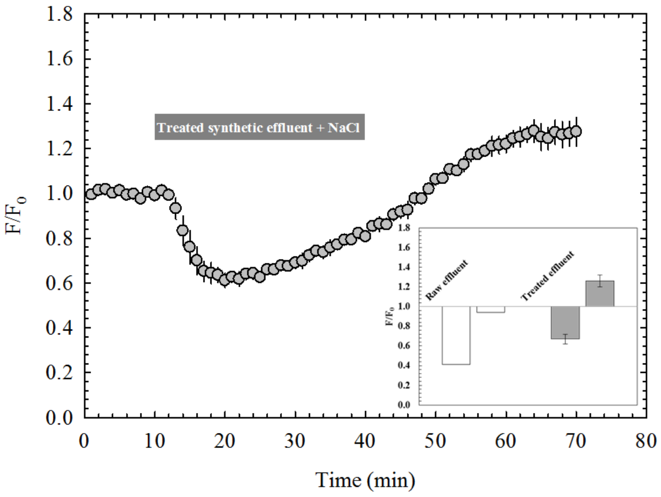

**Figure VII.6. Neuronal ROS signals evoked by the synthetic effluent plus NaCl. The points indicate the normalised amplitude of fluorescence signals recorded with the ROS indicator $H_2$DCFDA (20 µM), in the absence and presence (period indicated by the bar) of the treated effluent. Inset: The white bars represent the normalised amplitude of the depression in the presence of the raw effluent (left bar) and of the signal at the end of the washout period (right bar). The grey bars represent the equivalent data obtained for the treated effluent. The data were acquired using the ROS indicator $H_2$DCFDA (20 µM) and are represented as the mean ± s.e.m (n=3) for the treated effluent.**

## VII.3.6 APPLICATION TO A REAL EFFLUENT

The previously optimised operating parameters for a synthetic OMW, i.e., 10 g $L^{-1}$ of NaCl, current density of 119 mA $cm^{-2}$ and raw pH were tested in an electrochemical treatment of an effluent with the same initial COD charge ($COD_0$=1004±7 mg$O_2$ $L^{-1}$) obtained from a real wastewater. An experiment with the effluent without dilution ($COD_0$=5832±63 mg$O_2$ $L^{-1}$) was also carried out for comparison purposes. As can be observed in Figure VII.7a, the real diluted effluent, with lower initial TPh value (77 mgGA $L^{-1}$), needed lesser applied charge (1.3 Ah $L^{-1}$) than the synthetic one, while the undiluted real effluent requires a higher value (7.5 Ah $L^{-1}$) to achieve total phenolic removal. In addition, the inset of Figure VII.7a also demonstrates that the test with the diluted real wastewater achieved quicker the pH for the generation of active chlorine than the simulated effluent, promoting the faster removal of phenolic compounds. According to Figure VII.7b, after 7.5 Ah $L^{-1}$ of charge is applied (180 min) the final COD removal (62.8 %) for the experiment with the real diluted effluent was 22 % lower than the value obtained for the synthetic mixture.This means that the high complexity of the real effluent must be bear in mind [24], since some scavenger species may be in solution inhibiting the action of the oxidants. Under the same conditions, the COD decay for the assay with the undiluted effluent did not go beyond 16.5 %, because of the higher concentration of organic matter in the beginning of the treatment and possible potentiation of the scavenging behaviour. There was an interesting phenomenon in this last experiment, in which the COD seems to increase during the initial stage of the reaction. This might have occurred due to oxidative polymerisation of certain compounds such as phenols and tannins normally present in real OMW, as already observed in other studies conducted by Khoufi *et al.* [52], Gotsi *et al.* [44] and Papastefanakis *et al.* [23]. Additionally, in a lesser extent, the dissolution of the unfiltered solids during the EO could also be accounted as organic matter as also pointed out by Kotta *et al.* [53].

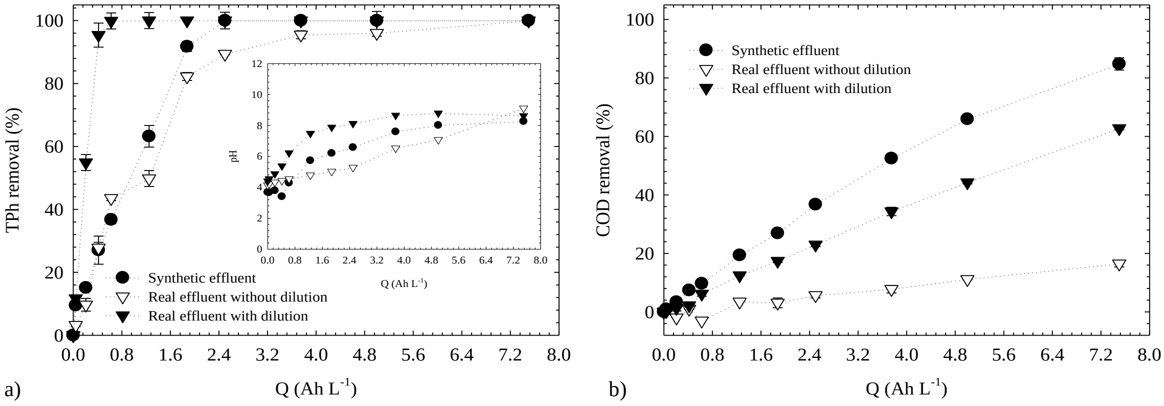

**Figure VII.7. (a) TPh removal and (b) COD removal as function of the applied charge. Inset of Fig. 7a: Evolution of pH medium over the applied charge. Operating conditions: 10 g L$^{-1}$ of NaCl, current density=119 mA cm$^{-2}$, raw pH, distance between electrodes=1 cm, T=20 °C.**

The decolourisation of the undiluted and diluted real OMW can be observed by naked eye over time and as a function of the applied charge in Figure VII.8. The colour decay in those two experiments is consistent with the results obtained for TPh removal (Figure VII.7a), suggesting that the phenolic content present in the actual wastewater is largely responsible for its brownish dark colour [23].

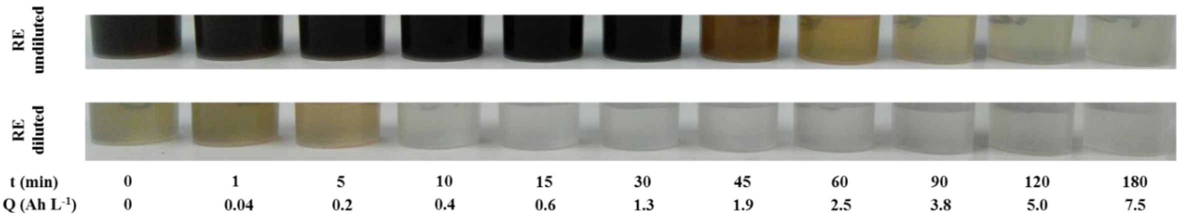
RE undiluted
RE diluted
t (min) 0 1 5 10 15 30 45 60 90 120 180
Q (Ah L$^{-1}$) 0 0.04 0.2 0.4 0.6 1.3 1.9 2.5 3.8 5.0 7.5

**Figure VII.8. Discolouration of the undiluted and diluted real effluents (RE) over time and as a function of the applied charge. Operating conditions: 10 g L$^{-1}$ of NaCl, current density=119 mA cm$^{-2}$, raw pH, distance between electrodes=1 cm, T=20 °C.**

At the end of the process (7.5 Ah L$^{-1}$ and 180 min), the energy consumptions achieved for the simulated effluent and for the undiluted or diluted real OMW tests were 135.8 and126.7 or 107.0 kWh m$^{-3}$, respectively. These values are within the range obtained by Panizza and Cerisola [16], who have also tested the treatment of OMW by anodic oxidation using another anode material, the Ti/TiRuO$_2$.

Regarding the optimised operating conditions used, the phenolic compounds and colour can be completely removed. Nevertheless, since the standards to the effluent be discharged in natural streams was not accomplished to ensure a concentration of organic pollutants (COD) below a value of 150 mgO$_2$ L$^{-1}$, this electrochemical process can be envisaged as a pre-treatment system.

## VII.4 CONCLUSIONS

The electrochemical oxidation of synthetic phenolic wastewaters was successfully attained with Ti/$IrO_2$ anodes in the presence of chloride ions. The best operating conditions were 10 g $L^{-1}$ of NaCl, 119 mA $cm^{-2}$ of current density and initial pH of 3.4, which allowed 100 and 84.8 % of TPh and COD removal, respectively. This initial pH increased over time to neutral-alkaline conditions, which is an interesting feature for a possible industrial application of this EO process. During the tests, it was notable the effect of the nature of different electrolytes in process efficiency. Regarding NaCl concentrations and initial pH, a sparingly effect in the system was achieved by these parameters. The current density had a strong influence on phenolic compounds and organic matter removal over time. Considering the morphological characteristics obtained by SEM, some changes occurred on the surface of the anode after the EO treatment. The ROS studies performed in brain slices show clear differences of the impact of the untreated and treated effluents in neuronal activity. The smaller depression, observed with the treated medium, suggests that if phenolic compounds were completely removed after the treatment, as the previous results indicate, then other compounds may have been formed during the treatment that account for it. These may also be responsible for the enhancement of the signal, upon washout of the effluent.

When the optimised operating conditions were applied to a real OMW, complete TPh removal was achieved and 16.5 or 62.8 % of COD removals were attained, with the undiluted or diluted effluent, respectively. This means that EO is an efficient method to remove phenolic content, while it can also be used as a pre-treatment of subsequent degradation processes to attain the legal limits of organic load (in terms of COD) to be discharged in natural streams.

## ACKNOWLEDGMENTS

The authors, Ana S. Fajardo and Rui C. Martins gratefully acknowledge the Fundação para a Ciência e Tecnologia, for financial support under the Doc grant (SFRH/BD/87318/2012) and the IFCT 2014 programme (IF/00215/2014) with funding from the European Social Fund and the Human Potential Operational Programme, respectively.

The Biophysics group thanks the Centre for Neuroscience and Cell Biology, University of Coimbra, Coimbra, Portugal, for providing the rat brains. This work was funded by strategic project UID/NEU/04539/2013.

## REFERENCES

[1] Comninellis Ch (1994) Electrocatalysis in the electrochemical conversion/combustion of organic pollutants for waste water treatment. Electrochim. Acta 39 (11-12): 1857–1862.

[2] Comninellis Ch, Pulgarin C (1993) Electrochemical oxidation of phenol for wastewater treatment using $SnO_2$ anodes. J. Appl. Electrochem. 23: 108–112.

[3] Rajeshwar K, Ibanez JG (1997) Environmental Electrochemistry: Fundamentals and Applications in Pollution Sensors and Abatement. Elsevier Science & Technology Books.

[4] Martínez-Huitle CA, Ferro S (2006) Electrochemical oxidation of organic pollutants for the wastewater treatment: direct and indirect processes. Chem. Soc. Rev. 35: 1324–1340.

[5] Anglada A, Urtiaga A, Ortiz I (2009) Contributions of electrochemical oxidation to waste-water treatment: fundamentals and review of applications. J. Chem. Technol. Biotechnol. 84: 1747–1755.

[6] Cañizares P, Paz R, Sáez C, Rodrigo MA (2009) Costs of the electrochemical oxidation of wastewaters: A comparison with ozonation and Fenton oxidation processes. J. Environ. Manage. 90: 410–420.

[7] Jüttner K, Galla U, Schmieder H (2000) Electrochemical approaches to environmental problems in the process industry. Electrochim. Acta 45: 2575–2594.

[8] Scialdone O, Randazzo S, Galia A, Silvestri G (2009) Electrochemical oxidation of organics in water: Role of operative parameters in the absence and in the presence of NaCl. Water. Res. 43: 2260–2272.

[9] Panizza M, Cerisola G (2009a) Electrochemical degradation of gallic acid on a BDD anode. Chemosphere 77: 1060–1064.

[10] Martínez-Huitle CA, Ferro S, De Battisti A (2005) Electrochemical Incineration in the Presence of Halides. Electrochem. Solid-State. Lett. 8 (11): D35–D39.

[11] Szpyrkowicz L, Kaul SN, Neti RN, Satyanarayanb S (2005) Influence of anode material on electrochemical oxidation for the treatment of tannery wastewater. Water. Res. 39: 1601–1613.

[12] Panizza M, Cerisola G (2009b) Direct and Mediated Anodic Oxidation of Organic Pollutants. Chem. Rev. 109: 6541–6569.

[13] Chiang L-C, Chang J-E, Wen T-C (1995) Indirect oxidation effect in electrochemical oxidation treatment of landfill leachate. Water. Res. 29 (2): 671–678.

[14] Comninellis Ch, Nerini A (1995) Anodic oxidation of phenol in the presence of NaCl for wastewater treatment. J. Appl. Electrochem. 25: 23–28.

[15] Karlsson RKB, Cornell A (2016) Selectivity between Oxygen and Chlorine Evolution in the ChlorAlkali and Chlorate Processes. Chem. Rev. 116: 2982–3028.

[16] Panizza M, Cerisola G (2006) Olive mill wastewater treatment by anodic oxidation with parallel plate electrodes. Water. Res. 40: 1179–1184.

[17] Fierro S, Comninellis Ch (2010) Kinetic study of formic acid oxidation on Ti/$IrO_2$ electrodes prepared using the spin coating deposition technique. Electrochim. Acta. 55: 7067–7073.

[18] Fierro S, Kapałka A, Comninellis Ch (2010) Electrochemical comparison between $IrO_2$ prepared by thermal treatment of iridium metal and $IrO_2$ prepared by thermal decomposition of $H_2IrCl_6$ solution. Electrochem. Commun. 12: 172–174.

[19] Borbón B, Oropeza-Guzman MT, Brillas E, Sirés I (2014) Sequential electrochemical treatment of dairy wastewater using aluminum and DSA-type anodes. Environ. Sci. Pollut. Res. 21: 8573–8584.

[20] Víctor-Ortega MD, Ochando-Pulido JM, Airado-Rodríguez D, Martínez-Férez A (2016) Experimental design for optimization of olive mill wastewater final purification with Dowex Marathon C and Amberlite IRA-67 ion exchange resins. J. Ind. Eng. Chem. 34: 224–232.

[21] Polcaro AM, Vacca A, Mascia M, Palmas S, Ferrara F, Ruiz JR (2008) Selective oxidation of phenolic compounds at BDD and DSA anodes. J. Environ. Eng. Manage. 18(3): 213–220.

[22] Un UT, Altay U, Koparal AS, Ogutveren UB (2008) Complete treatment of olive mill wastewaters by electrooxidation. Chem. Eng. J. 139: 445–452.

[23] Papastefanakis N, Mantzavinos D, Katsaounis A (2010) DSA electrochemical treatment of olive mill wastewater on Ti/$RuO_2$ anode. J. Appl Electrochem 40: 729–737.

[24] Chatzisymeon E, Dimou A, Mantzavinos D, Katsaounis A (2009) Electrochemical oxidation of model compounds and olive mill wastewater over DSA electrodes: 1. The case of Ti/$IrO_2$ anode. J. Hazard. Mater. 167: 268–274.

[25] Nicoll RA, Schmitz D (2005) Synaptic plasticity at hippocampal mossy fibre synapses. Nat .Rev. Neurosci. 6: 863–876.

[26] Valencia A, Morán J (2004) Reactive oxygen species induce different cell death mechanisms in cultured neurons. Free. Radic. Biol. Med. 36: 1112–1125.

[27] Pereira DM, Valentão P, Pereira JA, Andrade PB (2009) Phenolics: From Chemistry to Biology. Molecules 14: 2202–2211.

[28] Uttara B, Singh AV, Zamboni P, Mahajan RT (2009) Oxidative Stress and Neurodegenerative Diseases: A Review of Upstream and Downstream Antioxidant Therapeutic Options. Curr. Neuropharmacol. 7: 65–74.

[29] Balice V, Cera O (1984) Acid phenolic fraction of the olive vegetation water determined by a gas chromatographic method. Grasas y Aceites 35 (5): 178–180.

[30] Esplugas S, Contreras S, Ollis D (2004) Engineering aspects of the integration of chemical and biological oxidation: simple mechanistic models for the oxidation treatment. J. Environ. Eng. 130(9): 967–974.

[31] Fajardo AS, Martins RC, Quinta-Ferreira RM (2014) Treatment of a Synthetic Phenolic Mixture by Electrocoagulation Using Al, Cu, Fe, Pb, and Zn as Anode Materials. Ind. Eng. Chem. Res. 53: 18339−18345.

[32] Silva A, Nouli E, Xekoukoulotakis N, Mantzavinos D (2007) Effect of key operating parameters on phenols degradation during H2O2-assisted $TiO_2$ photocatalytic treatment of simulated and actual olive mill wastewaters. Appl. Catal. B. 73: 11–22.

[33] Greenberg A, Clesceri L, Eaton A (1992) Standard Methods for the Examination of Water and Wastewater. American Public Health Association, Washington DC.

[34] Araújo CKC, Oliveira GR, Fernandes NS, Zanta CLPS, Castro SSL, da Silva DR, Martínez-Huitle CA (2014) Electrochemical removal of synthetic textile dyes from aqueous solutions using Ti/Pt anode: role of dye structure. Environ. Sci. Pollut. Res. 21: 9777–9784.

[35] Giraldo AL, Erazo-Erazo ED, Flórez-Acosta OA, Serna-Galvis EA, Torres-Palma RA (2015) Degradation of the antibiotic oxacillin in water by anodic oxidation with Ti/$IrO_2$ anodes: Evaluation of degradation routes, organic by-products and effects of water matrix components. Chem. Eng. J. 279: 103–114.

[36] Panizza M, Martínez-Huitle CA (2013) Role of electrode materials for the anodic oxidation of a real landfill leachate–Comparison between Ti–Ru–Sn ternary oxide, PbO2 and boron-doped diamond anode. Chemosphere 90: 1455–1460.

[37] Bonfatti F, De Battisti A, Ferro S, Lodi G, Osti S (2000) Anodic mineralization of organic substrates in chloride-containing aqueous media. Electrochim. Acta 46: 305–314.

[38] Brillas E, Martínez-Huitle CA (2015) Decontamination of wastewaters containing synthetic organic dyes by electrochemical methods. An up dated review. Appl. Catal. B 166–167: 603–643.

[39] Garcia-Segura S, Keller J, Brillas E, Radjenovic J (2015) Removal of organic contaminants from secondary effluent by anodic oxidation with a boron-doped diamond anode as tertiary treatment. J. Hazard. Mater. 283: 551–557.

[40] Radjenovic J, Sedlak DL (2015) Challenges and opportunities for electrochemical processes as next-generation technologies for the treatment of contaminated water. Environ. Sci. Technol. 49: 11292–11302.

[41] Deborde M, von Gunten U (2008) Reactions of chlorine with inorganic and organic compounds during water treatment—Kinetics and mechanisms: A critical review. Water. Res. 42: 13–51.

[42] Rajkumar D, Kim JG, Palanivelu K (2005) Indirect Electrochemical Oxidation of Phenol in the Presence of Chloride for Wastewater Treatment. Chem. Eng. Technol. 28: 98–105.

[43] Israilides CJ, Vlyssides AG, Mourafeti VN, Karvouni G (1997) Olive oil wastewater treatment with the use of an electrolysis system. Bioresour. Technol. 61: 163–170.

[44] Gotsi M, Kalogerakis N, Psillakis E, Samaras P, Mantzavinos D (2005) Electrochemical oxidation of olive oil mill wastewaters. Water. Res. 39: 4177–4187.

[45] Kawaguchi K, Haarberg GM, Morimitsu M (2010) Nano-Architecture on the Mud-Cracked Surface of IrO$_2$-Ta$_2$O$_5$ Binary System. ECS. Transactions. 25 (33): 67–73.

[46] Felix C, Maiyalagan T, Pasupathi S, Bladergroen B, Linkov V (2012) Synthesis, Characterisation and Evaluation of IrO$_2$ Based Binary Metal Oxide Electrocatalysts for Oxygen Evolution Reaction. Int. J. Electrochem. Sci. 7: 12064–12077.

[47] Smart TG, Xie X, Krishek BJ (1994) Modulation of inhibitory and excitatory amino acid receptor ion channels by zinc. Prog. Neurobiol. 42: 393–341.

[48] Bancila V, Nikonenko I, Dunant Y, Bloc A (2004) Zinc inhibits glutamate release via activation of pre-synaptic KATP channels and reduces ischaemic damage in rat hippocampus. J. Neurochem. 90: 1243–1250.

[49] Frederickson CJ, Koh JY, Bush AI (2005) The neurobiology of zinc in health and disease. Nat. Rev. Neurosci. 6 (6): 449–462.

[50] Suzuki E, Okada T (2009) TEA-induced long-term potentiation at hippocampal mossy fiber-CA3 synapses: Characteristics of its induction and expression. Brain. Res. 1247: 21–27.

[51] Matias CM, Saggau P, Quinta-Ferreira ME (2010) Blockade of presynaptic K ATP channels reduces the zinc-mediated posttetanic depression at hippocampal mossy fiber synapses. Brain Res. 320: 22–27.

[52] Khoufi S, Aouissaoui H, Penninckx M, Sayadi S (2004) Application of electro-Fenton oxidation for the detoxification of olive mill wastewater phenolic compounds. Water. Sci. Technol.49:97–102.

[53] Kotta E, Kalogerakis N, Mantzavinos D (2007) The effect of solids on the electrochemical treatment of olive mill effluents. J. Chem. Technol. Biotechnol. 82: 504–511.

# VIII. TREATMENT OF AMARANTH DYE IN AQUEOUS SOLUTION BY USING ONE CELL OR TWO CELLS IN SERIES WITH ACTIVE AND NON-ACTIVE ANODES

AS Fajardo[a,b], RC Martins[a], CA Martínez-Huitle[b] and RM Quinta-Ferreira[a]

[a] CIEPQPF – Centro de Investigação em Engenharia dos Processos Químicos e dos Produtos da Floresta, GERST – Group on Environment, Reaction, Separation and Thermodynamics, Department of Chemical Engineering, Faculty of Sciences and Technology, University of Coimbra, Pólo II, Rua Sílvio Lima, 3030-790 Coimbra, Portugal.

[b] LEAA – Laboratório de Eletroquímica Ambiental e Aplicada, Institute of Chemistry, Federal University of Rio Grande do Norte, Av. Senador Salgado Filho 3000, Lagoa Nova, CEP 59072-970 Natal, RN, Brazil.

*Electrochimica Acta 210 (2016) 96–104*

## ABSTRACT

The anodic oxidation of Amaranth dye has been studied by electrochemical measurements (cyclic voltammetry and polarisation curves) and bulk electrolysis employing a single or two cells in a serial mode system using active and non-active anodes (Ti/$IrO_2$-$Ta_2O_5$ and Nb/BDD) as electrode materials. The results of electrochemical measurements showed that, Nb/BDD had a significant oxidation power to mineralise Amaranth dye when compared to Ti/$IrO_2$-$Ta_2O_5$ anode. Single cells were tested at different current densities (30, 60 and 80 mA cm$^{-2}$). At Nb/BDD anode, total colour elimination and 49.1 % of COD removal were achieved by applying 30 mA cm$^{-2}$ after 60 min of treatment. Conversely, 98.5 % of colour removal and 43.2 % of COD decay were accomplished at 60 mA cm$^{-2}$ with Ti/$IrO_2$-$Ta_2O_5$ electrode, after 360 min of electrolysis time. Supported on the obtained results with single cells, a system in a serial mode was further evaluated for the first time. The arrangement with Ti/$IrO_2$-$Ta_2O_5$ electrode at 30 mA cm$^{-2}$ in the first cell followed by Nb/BDD anode at 30 mA cm$^{-2}$ revealed the most interesting results. Complete decolourisation and 75.1 % of COD abatement were achieved after 60 min with lower energy requirements of about 25.4 kWh m$^{-3}$ (0.2 kWh gCOD$^{-1}$). This study demonstrates the potential of a serial system to be applied as a wastewater pre-treatment approach.

## VIII.1 INTRODUCTION

Azo dyes are synthetic substances characterised by the presence of one or various –N=N– chromophore groups on their structure. These compounds, due to their unique properties such as brilliant shades, relative low cost and simple manufacture, are mainly used in textile and food industries (approximately 60–70 % of dyes employed worldwide) [1]. These substances when disposed together with the generated industrial effluents lead to the colourisation of the aquatic systems, obstructing the light penetration and the oxygen solubility, thus affecting the aquatic life [2]. Currently, food additives (including azo dyes) are also considered as emergent pollutants because of their impact on human health and environment. Indeed, serious risks may arise from the toxicity and the carcinogenicity character of the dye, as well as the potential mutagenicity of the breakdown products formed during the chromophore groups cleavage, in particular the aromatic amines [3,4]. Therefore, the demand for adequate treatments to remove this kind of dyes from water systems and wastewaters becomes imperative.

In this regard, even though physical-chemical techniques including adsorption, coagulation-flocculation and membrane separation may enable the decolourisation of dyeing wastewaters [5], the production of large amounts of sludge, the remaining high content of dissolved solids in the effluent and the high cost of maintenance are not attractive features for applying these methods [6]. Additionally, no significant removal efficiencies were achieved when the use of biological treatment is proposed because dyes contain different functional groups that make them more recalcitrant and biologically stable [5]. Thus, advanced oxidation processes (AOPs) emerge as an alternative due to their efficiency in oxidising a wide variety of organic contaminants by the in-situ generation of highly oxidative species, mainly hydroxyl radicals ($^{\bullet}$OH). Among the AOPs, electrochemical advanced oxidation processes (EAOPs) have currently received great attention for the remediation of toxic and biorefractory organic pollutants [1,7,8]. These technologies allow to mineralise the organic matter by mediated oxidation with $^{\bullet}$OH generated in-situ at the anode surface at high current, promoting complete combustion of most organics to $CO_2$, inorganic ions and water [9]. The most common EAOP is anodic oxidation (AO), in which water is oxidised to $O_2$ at an anode (M) with high $O_2$-overpotential to generate, physically or chemically, adsorbed hydroxyl radical M ($^{\bullet}$OH) as intermediate (Reaction (VIII.1)) [10,11].

$$\mathrm{M} + \mathrm{H_2O} \rightarrow \mathrm{M}(\,^{\bullet}\mathrm{OH}) \qquad \textbf{(VIII.1)}$$

Meanwhile, for an indirect AO, other stronger oxidants can be produced, such as peroxodisulphate from the AO of bisulphate (or sulphate) or active chlorine species from direct oxidation of chloride ion, favouring the oxidation of organics [9,12]. Based on the existing literature [1,2,7,9,11], the efficacy of the direct and indirect AO depends on the configuration of the system, and it can be affected by the current density, the type of the electrolyte and the electrodes used. Various synthetic dyes solutions (Acid Orange II, Acid Red 211, Alizarin Blue Black B, Indigo Carmine, Malachite Green, Methyl Orange, Procion Blue, Reactive Black 5, Remazol Red, Rhodamine B) and real textile effluents have been treated under different current densities (3.1–60 mA $cm^{-2}$), temperatures (25–60 °C), flow rates (60–720 L $h^{-1}$) or electrolytes leading to efficient treatments (colour and COD removals > 90 %) at reasonable operating costs [1,13–16]. Among the anodes tested, boron-doped diamond (BDD) electrodes are preferred because their weak BDD-$^{\bullet}$OH interaction and greater $O_2$ overpotential endorses the generation of higher amounts of reactive physisorbed BDD($^{\bullet}$OH) radicals that mineralise more effectively dyestuff effluents than other anodes as Pt and $PbO_2$ [13–23]. Nonetheless, DSA electrodes, such as $Sb_2O_5$-doped Ti/$RuO_2$-$ZrO_2$, Ti/Pt, Ti/Pt-SnSb, Ti-Pt/b-$PbO_2$ and Ti/$SnO_2$-Sb-Pt [20,24–26], are still satisfactory selections due to the BDD material acquisition cost and its higher energy consumption.

On the other hand, the electrochemical reactor is also an essential key on AO performance and special attention should be given to its design/configuration in order to achieve high pollutants removal as well as high current efficiencies for the desired reaction [27,28]. A wide range of different electrochemical systems have been applied to the treatment of dyeing wastewaters, ranging from traditional plate-in-tank configurations [24] up to more sophisticated designs, for example, flow cells with parallel electrodes [19,24,27], flow plants with a three-phase three-dimensional electrode [29], a bipolar trickle tower reactor [30] as well as flow electrochemical reactors in series [27] including microfluidic cells [31].

In this frame, a good design of electrochemical reactors and a good selection of the anodes allow the optimisation of the mass transport coefficient for a maximum current efficiency with higher removal efficiencies. Therefore, in this study is proposed the use of an AO approach to remove dyes from aqueous solutions by employing single cells and two cells in a serial mode and combining the electrocatalytic properties of active and non-active anodes (Ti/$IrO_2$-$Ta_2O_5$ and BDD, respectively). The influence of anode material, current density and electrochemical cell arrangement on the removal of colour and organic matter (in terms of chemical oxygen demand (COD)) of dye wastewater is the main objective of this investigation. Amaranth dye was chosen as model organic pollutant because it is a dark red and water soluble monoazo substance commonly used by Brazilian food industries [32].

## VIII.2 EXPERIMENTAL

### VIII.2.1 SYNTHETIC EFFLUENT

The synthetic effluent encompasses 100 mg $L^{-1}$ of Amaranth dye (Figure VIII.1) (Cotia Foods S.A.) which was dissolved into a solution containing 20 g $L^{-1}$ of $Na_2SO_4$ (Anidrol). This effluent is a neutral solution (pH 6.4±1.8) with an amount of organic matter expressed by a chemical oxygen demand (COD) of 140.7±5.4 $mgO_2$ $L^{-1}$. No further purification was applied to reagents before use.

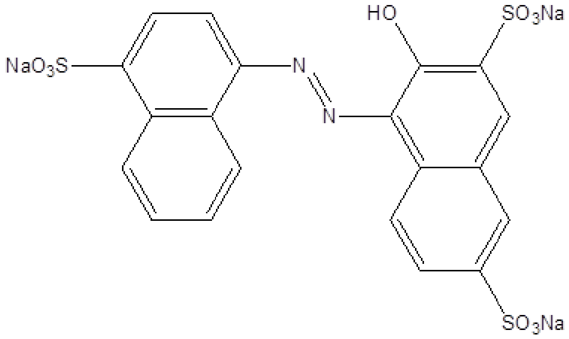

**Figure VIII.1. Amaranth dye structure.**

### VIII.2.2 ELECTROCHEMICAL MEASUREMENT

Cyclic voltammetry (CV) was carried out at room temperature (25 °C) in a conventional three-electrode cell using a computer controlled Metrohm AUTOLAB potentiostat model PGSTAT302N. Nb/BDD and Ti/$IrO_2$-$Ta_2O_5$ were used as working electrodes, an Ag/AgCl electrode as reference and Pt wire as the counter electrode. The exposed area of the working electrodes was 1 $cm^2$. Nb/BDD and Ti/$IrO_2$-$Ta_2O_5$ electrodes were subjected to repetitive cyclic voltammetry from 0.0 to +3.5 V (ten cycles each) at the scan rate of 100 mV $s^{-1}$ in a blank solution of 20 g $L^{-1}$ of $Na_2SO_4$ and in the presence of the synthetic dye solution. Quasi-steady polarisation curves were carried out at a scan rate of 5 mV $s^{-1}$ and with a 2.44 mV step potential, in the same solutions aforementioned and measurements were performed between 0.0 and +3.5 V.

### VIII.2.3 ELECTROCHEMICAL SYSTEM AND PROCEDURE

Bulk electrolyses of Amaranth dye solution were performed in two kinds of electrochemical systems: one single cell and two single cells in a serial mode [27] during 360 min and 120 min at 25 °C, respectively. In each experiment, the reservoir was filled with 1 L of the model solution and it was recirculated through the electrolytic cells with parallel electrodes by a pump at 250 L $h^{-1}$. The anode and cathode disks, both with 63.6 $cm^2$ of geometric area, were placed at 1.2 cm of distance. A power supply (MINIPA MPL–3305 M) was employed for applying current density ($j$) values of 30, 60 and 80 mA $cm^2$ to evaluate the influence of this control parameter. Nb/BDD and Ti/$IrO_2$-$Ta_2O_5$ electrodes were used as anodes and Ti as cathode. The anodes were supplied by METAKEM GmbH (Germany) and Industrie De Nora Elettrodi (Italy), respectively. Nb/BDD anode was polarised during 30 min with 1 L of 0.1 M $H_2SO_4$ solution at 30 mA $cm^{-2}$ to remove any kind of impurity from its surface. Samples were periodically withdrawn for further analysis. pH (HANNA pH meter), as well as conductivity were parameters followed over time.

### VIII.2.4 ANALYTICAL TECHNIQUES

In order to determine the process efficiency, UV-vis, chemical oxygen demand (COD) and High-Performance Liquid Chromatography (HPLC) analysis were performed. The colour removal was monitored by using the spectrophotometer Shimadzu UV 1800, while COD was analysed by the closed reflux procedure, according to Standard Methods (5250D) [33], with a thermo-reactor and a photometer from HANNA Instruments (HI 839800 and HI 83099, respectively). The concentration of the synthetic effluent was followed by a Finnigan Surveyor Plus HPLC system. 20 µL were injected of each one of the samples via an autosampler (Surveyor Autosampler Plus). The mobile phase, consisting of 60 % of ultrapure water, 30 % of acetonitrile and 10 % of methanol, was pumped at a flow rate of 0.5 mL $min^{-1}$ through a C18 column at 30 °C, and the detection was performed at 524 nm in the Finnigan Surveyor PDA Plus Detector.

## VIII.3 RESULTS AND DISCUSSION

### VIII.3.1 CYCLIC VOLTAMMETRY (CV) AND POLARISATION CURVES

Prior to bulk oxidations and on the basis of the electrocatalytic nature of each one of the electrodes used, electrochemical measurements were carried out (cyclic voltammetry and polarisation curves) in the absence (20 g $L^{-1}$ of $Na_2SO_4$) and in the presence of the model organic compound (100 mg $L^{-1}$). Figure VIII.2a shows the cyclic voltammograms for background electrolyte and for Amaranth-containing electrolyte at Ti/$IrO_2$-$Ta_2O_5$ anode, recorded with a scan rate of 100 mV $s^{-1}$. As can be observed, a typical voltammetric profile of metal oxide surface was achieved [34,35] in absence of organic compound in solution (Figure VIII.2a, black curve). The shape in the CV with not well-defined peaks can be understood in terms of a large heterogeneity in the surface site and superposition of the redox processes for the transition lower metal oxide/higher metal oxide [34,35]. Also, the oxygen evolution started at about +1.3 V *vs* Ag/AgCl, confirming that Ti/$IrO_2$-$Ta_2O_5$ has lower oxygen evolution overpotential. When a known amount of Amaranth was added in solution (100 mg $L^{-1}$), a very broad peak at +0.7 V *vs* Ag/AgCl was registered (Figure VIII.2a, grey dashed curve). This indicates that Amaranth dye is directly oxidised by electron transfer on the Ti/$IrO_2$-$Ta_2O_5$ anode in the region before oxygen evolution reaction (o.e.r.), at lower $j$ than 20 mA $cm^{-2}$. It is also interesting to observe that the current at the o.e.r. is shifted to more negative potentials and increased (inset in Figure VIII.2a). This may point out that Amaranth dye oxidation is also due to water decomposition intermediates, mainly $^{\bullet}OH$ (Reaction (VIII.2)), which are only available in conditions of oxygen evolution, rather than direct electron transfer from the substrate.

$$2H_2O \rightarrow 2\ {}^{\bullet}OH + 2H^+ + 2e^- \qquad \textbf{(VIII.2)}$$

Voltammetric curves obtained with Nb/BDD in 20 g L$^{-1}$ of $Na_2SO_4$ (Figure VIII.2b) presented the typical behaviour of synthetic diamond layer [36,37]. In the presence of $Na_2SO_4$, the potential where oxygen evolution starts is about +2.3 V *vs* Ag/AgCl meaning that this electrode has higher oxygen evolution overpotential than that registered at Ti/$IrO_2$-$Ta_2O_5$, highlighting its better electrocatalyst character for anode oxidation [34]. During the voltammetric cycles, in the solution containing Amaranth (100 mg L$^{-1}$) a slight anodic peak at approximately +1.7 V *vs* Ag/AgCl was observed (inset in Figure VIII.2b), corresponding to direct oxidation of Amaranth dye on BDD surface. However, this peak did not rise as the number of cycles increased, indicating that the organic compound is rapidly oxidised by the $^{\bullet}OH$ produced. Nevertheless, this behaviour can be also due to the formation of a passivation layer that might have inhibited the electron tunnelling between the anodic surface and the water molecules or to the partial deactivation of the BDD surface which are competitively occupied by the organic molecule [38].

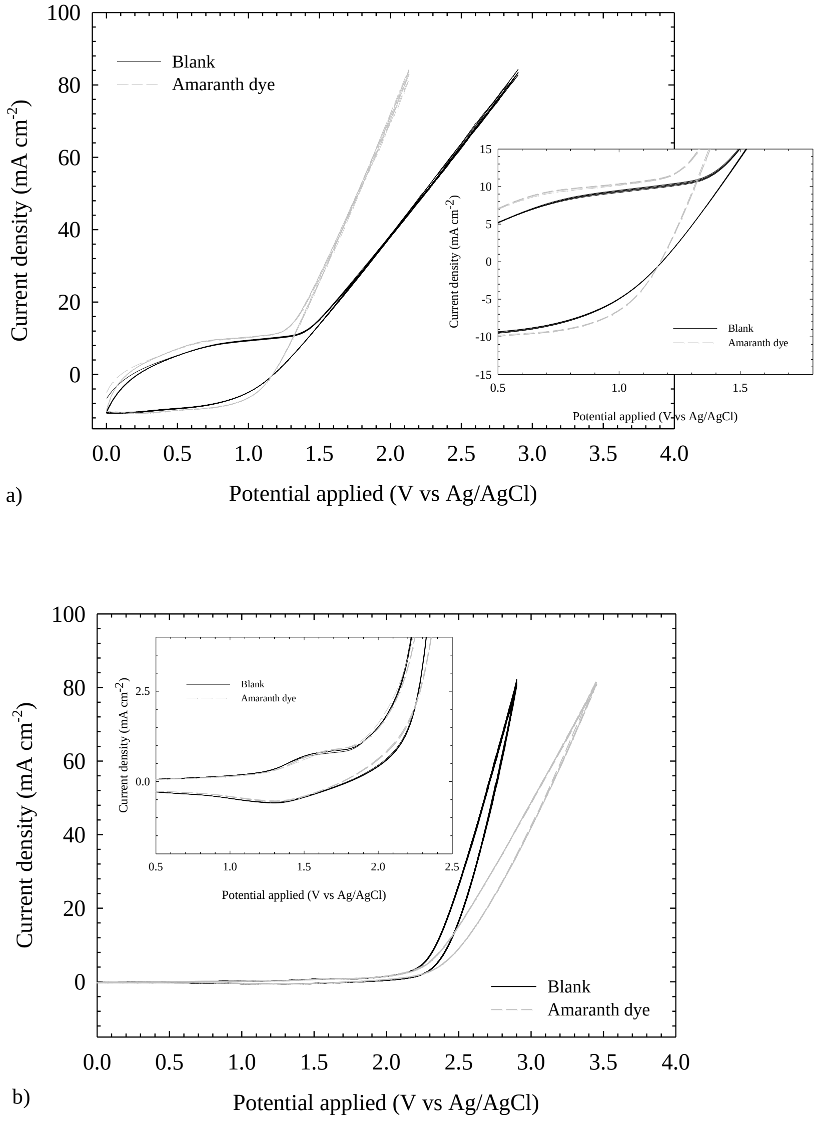

**Figure VIII.2. Cyclic voltammograms of the (a) Ti/$IrO_2$-$Ta_2O_5$ and (b) Nb/BDD anodes in 20 g L$^{-1}$ of $Na_2SO_4$, without (full line) and with 100 mg L$^{-1}$ of Amaranth dye (dashed line); scan potential from 0.0 to 3.0 V and scan rate 100 mV s$^{-1}$ (10 voltammetric cycles). Insets: Zoom to the cyclic voltammograms (a) and (b), respectively.**

Based on the effect of supporting electrolyte and Amaranth dye in the cyclic voltammetric measurements, a new set of experiments was performed to increase the understanding of dye oxidation by involving the participation of oxygen reactive species, like hydroxyl radicals. To address it, the results obtained by voltammetric profiles were compared to the polarisation curves under similar experimental conditions. Figure VIII.3 shows linear polarisation curves for both anode materials at scan rate of 100 mV $s^{-1}$. The curves (Figure VIII.3a and VI.3b, black curves) are very different and show that oxygen evolution potential increases to +1.3 V and +2.3 V *vs* Ag/AgCl for Ti/$IrO_2$-$Ta_2O_5$ and Nb/BDD, respectively. This means that Ti/$IrO_2$-$Ta_2O_5$ has low oxygen evolution overpotential and consequently is a good electrocatalyst for the o.e.r. in respect to Nb/BDD [34]. This behaviour is in accordance with the voltammetric study (Figure VIII.2).

As it can be also observed from Figure VIII.3, Ti/$IrO_2$-$Ta_2O_5$ and Nb/BDD electrodes have showed different electrochemical behaviour in presence of Amaranth (100 mg $L^{-1}$) in solution by anodic polarisation (grey dashed curves). In the case of Ti/$IrO_2$-$Ta_2O_5$, Amaranth oxidation occurs in the potential range close to water discharge at lower *j* than 20 mA $cm^{-2}$, which indicates that direct oxidation by electron transfer may be attained (Figure VIII.3a, dashed curve) [34,35]. Meanwhile, at higher *j* (more than 20 mA $cm^{-2}$), the Amaranth oxidation occurs in concomitance with o.e.r. Conversely, potentiodynamic experiments indicated that Nb/BDD material presents higher oxygen overpotential [34], which implies that this anode is a better electrocatalyst for pollutants oxidation (Figure VIII.3b, dashed curve). Then, the Amaranth dye oxidation is promoted via hydroxyl radicals electrogenerated from water discharge [39] in competition with o.e.r., favouring a more efficient elimination of dye from solution, as already commented at voltammetric analysis (Figure VIII.2b).

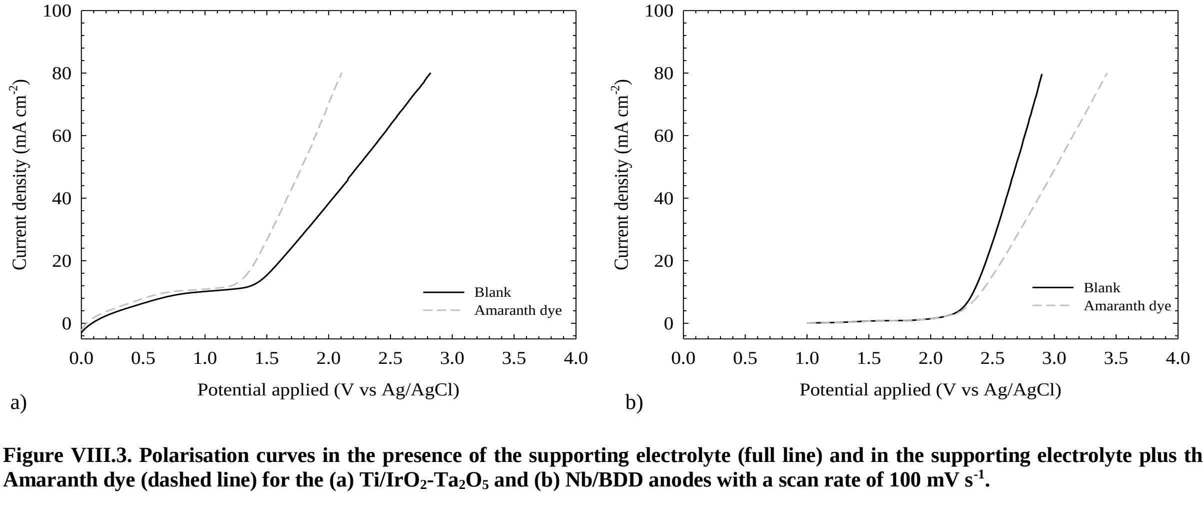

**Figure VIII.3. Polarisation curves in the presence of the supporting electrolyte (full line) and in the supporting electrolyte plus the Amaranth dye (dashed line) for the (a) Ti/$IrO_2$-$Ta_2O_5$ and (b) Nb/BDD anodes with a scan rate of 100 mV $s^{-1}$.**

### VIII.3.2 SINGLE CELL – EFFECT OF THE TYPE OF ANODE AND CURRENT DENSITY

Bulk experiments performed by using a single cell system allowed to evaluate the performance of each anode material as well as the effect of *j*.

The colourisation of the effluent is one of the most important characteristics that must be accounted by the industries using dyes before discharging the effluent into the aquatic systems due to aesthetic and environmental problems. For those reasons, a single cell with two different anodes (Nb/BDD and $Ti/IrO_2$-$Ta_2O_5$) was tested at different *j* values (30, 60 and 80 mA $cm^{-2}$) in order to degrade the Amaranth dye solution. The peak of maximum absorption of this solution appeared in the visible light region at 524 nm, which is associated with the chromophore group of $-\mathrm{N}=\mathrm{N}-$ present on the chemical structure of the dye. Weaker bands at 270 between 350 nm are related to $\pi \rightarrow \pi^*$ transitions in the conjugated aromatic systems [32,40]. Regardless the anode used and *j* applied, the band of absorbance continuously decreased over time (data not shown). In this way, the percentage of decolourisation of the Amaranth dye solution was determined by the Equation (VIII.3).

$$\mathrm{Colour\ removal} = \left(\frac{\mathrm{Abs_0} - \mathrm{Abs_t}}{\mathrm{Abs_0}}\right) \times 100 \tag{VIII.3}$$

where $\mathrm{Abs_0}$ and $\mathrm{Abs_t}$ correspond to the average absorbance at the beginning of the reaction and after an electrolysis time t, respectively.

Figure VIII.4a shows the evolution of the colour removal, as a function of the treatment time for the $Ti/IrO_2$-$Ta_2O_5$ and Nb/BDD anodes at 30, 60 and 80 mA $cm^{-2}$. As it can be observed, satisfactory colour removals were achieved for both anodic materials. However, the decolourisation rate strongly depended on the nature of the electrode used [9]. In fact, the maximum colour removal achieved with $Ti/IrO_2$-$Ta_2O_5$ electrode at 30 mA $cm^{-2}$ was 91.8 % after 360 min. Conversely, the colour was completely eliminated with Nb/BDD anode in about 30 min, at the same *j*. Moreover, *j* is known to be an important controlling parameter in AO because it allows to module the generation and accumulation of oxidants on the anodes surface as well as the distribution of the electrochemical reactions [9]. An increase on the applied *j* enhanced the reaction rate for both materials. This effect was significantly pronounced for the Nb/BDD anode since total disappearance of colour occurred after 15 min (60 mA $cm^{-2}$) of electrolysis while that at lower *j* (30 mA $cm^{-2}$), decolourisation was achieved after 30 min. This result indicates that, when *j* is increased, there are more $^{\bullet}OH$ radicals available to attack the chromophore groups of the dye, fragmenting them to other more simple organic compounds.

As aforementioned, the colour is an important feature to be taken into account, but this parameter is not indicative of the mineralisation of the dye. Therefore, organic matter elimination, in terms of COD, must be monitored before the discharge of the effluent into water bodies to achieve the legal limits according to environmental laws.

Figure VIII.4b showed that the COD elimination rates were less remarked than those observed for the colour removal. At Nb/BDD anode, a rapid COD removal was attained (49.1 %) in the first 60 min by applying 30 mA $cm^{-2}$, and later on, 80 % of COD was reduced after 360 min of electrolysis. Conversely, a decrease on the organic matter removal was observed when *j* is increased. In fact, 50.5 % and 21.5 %

were reached when 60 and 80 mA cm$^{-2}$ were used during 360 min of treatment. These results clearly indicate that, increasing current density, a higher charge consumed for complete mineralisation is needed because during the electrochemical process a relative greater amount of radical $^{\bullet}$OH is wasted in parasite non-oxidising reactions such as oxygen evolution. This behaviour is in agreement with the polarisation curves (Figure VIII.3) where at lower *j* (below 30 mA cm$^{-2}$), efficient production of hydroxyl radicals promotes the oxidation of Amaranth dye in solution, but at higher *j* (above 30 mA cm$^{-2}$), oxidation of dye by hydroxyl radicals is in competition with o.e.r.

In order to further investigate the effects of colour and COD removals, the concentration of the Amaranth dye was monitored by HPLC during the bulk experiments by using a single cell with Nb/BDD (Figure VIII.4c). As can be observed, after 60 min of AO treatment, it was noticeable the high efficiency of the process for removing completely the concentration of the Amaranth in solution. These figures support the results obtained for the complete colour removal (Figure VIII.4a) by using this anode material. However, when the Amaranth dye is rapidly eliminated, it is transformed into more simpler compounds which are not efficiently mineralised at BDD electrode [41,42]; favouring secondary reactions (such as o.e.r.) and diminishing the COD decay efficiency (see Figure VIII.4b).

At Ti/IrO$_2$-Ta$_2$O$_5$ anode (Figure VIII.4b), COD removals were about 8 %, 43.2 % and 27.9 % by applying 30, 60 and 80 mA cm$^{-2}$, respectively, after 360 min of treatment. In this case, the low COD removal using Ti/IrO$_2$-Ta$_2$O$_5$ electrode at 30 mA cm$^{-2}$ was due to the direct oxidation of Amaranth on its surface [39], favouring the formation of a passivation film as well as the intermediates formed during electrolysis that are difficult to be oxidised [14,43,44]. Meanwhile, at 60 mA cm$^{-2}$, a more significant concentration of hydroxyl radicals is produced, promoting an increase on the Amaranth degradation. However, at higher *j* (80 mA cm$^{-2}$), the oxidation occurs in concomitance with the o.e.r., limiting the efficiency of the elimination of dye in solution. These results are in agreement with the behaviour observed at potentiodynamic measurements (Figure VIII.2a) for Ti/IrO$_2$-Ta$_2$O$_5$ anode in the absence and in the presence of the organic compound. The lower COD removal indicates that, despite the degradation of the dye attained, there is a subsequent formation of more refractory intermediates that contribute to still-significant final COD values.

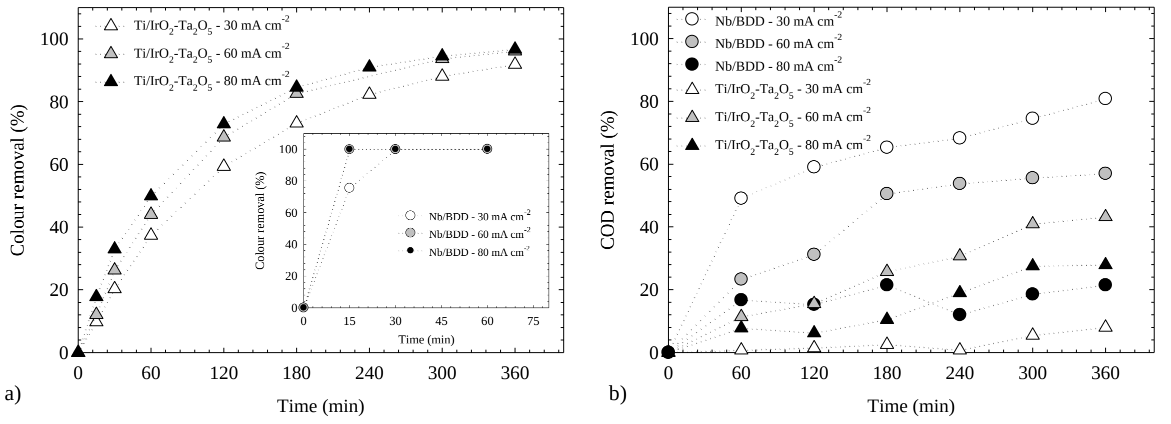

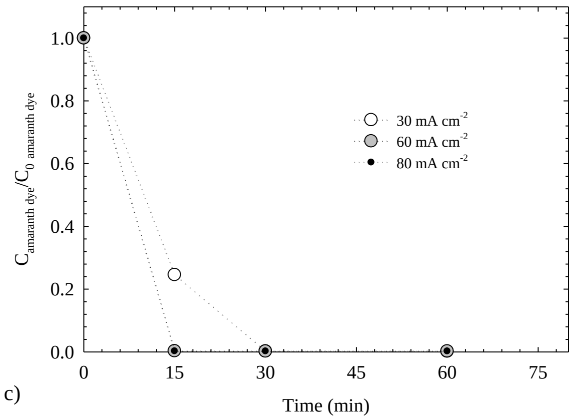

**Figure VIII.4. Oxidation of the Amaranth dye using a single cell. Effect of the anode material and current density on (a) colour removal over time for Ti/IrO$_2$-Ta$_2$O$_5$ anode, inset: colour removal over time for Nb/BDD anode; (b) COD removal and (c) decay of the normalised dye concentration. Operating conditions: 100 mg L$^{-1}$ of Amaranth dye, 20 g L$^{-1}$ of Na$_2$SO$_4$, current density=30, 60 and 80 mA cm$^{-2}$, T=25 °C.**

Generally speaking, when comparing the removal efficiencies obtained with both electrode materials, Nb/BDD showed high superiority to oxidise Amaranth effluent than the Ti/IrO$_2$-Ta$_2$O$_5$ anode. This performance is mainly due to the nature of the electrode: Ti/IrO$_2$-Ta$_2$O$_5$ is considered an active anode in which $^{\bullet}$OH radicals are chemically adsorbed, thus presenting lower reactivity favouring the pollutants electrochemical conversion instead their mineralisation. In its turn, Nb/BDD is the ideal non-active electrode, where $^{\bullet}$OH radicals are physically adsorbed showing strong oxidant power to promote the complete mineralisation of organic pollutants.

In this context, a new electrochemical cell arrangement, a serial configuration was proposed for increasing the efficiency of elimination of organic pollutants.

### VIII.3.3 TWO CELLS IN SERIES – EFFECT OF THE CELL ASSEMBLY AND THE CURRENT DENSITY

In a serial mode system, two different positions with two cells were tested: Ti/IrO$_2$-Ta$_2$O$_5$+Nb/BDD and Nb/BDD+Ti/IrO$_2$-Ta$_2$O$_5$. In addition, four different arrangements of *j* were evaluated (30+30, 60+60, 30+60 and 60+30 mA cm$^{-2}$). It is important to specify that the designation of the electrochemical cell system informs that, for example the first single cell contains the Ti/IrO$_2$-Ta$_2$O$_5$ anode while the second single cell contains the Nb/BDD electrode or viceversa. The same strategy was used to designate the current density.

The colour removal, as a function of electrolysis time, for both cells in a serial mode, Ti/IrO$_2$-Ta$_2$O$_5$+Nb/BDD and Nb/BDD+Ti/IrO$_2$-Ta$_2$O$_5$, was depicted in Figure VIII.5a and Figure VIII.5b, respectively. As can be observed, complete decolourisation was accomplished at short electrolysis times, ranging from 15 to 60 min. Results clearly demonstrate the effectiveness of the two cells in a serial mode, in terms of colour removal and electrolysis time, when compared to the single systems. This is due to the synergetic effects obtained by the recirculation of the Amaranth dye effluent through the two compartments. Nb/BDD anode in the first cell promotes a rapid breaking of the chromophore group, increasing the colour removal efficiency in the second single cell with the active electrode (Ti/$IrO_2$-$Ta_2O_5$). Additionally, an increase on the applied *j* improves the decolourisation rate at Nb/BDD anode, being consistent with the results obtained for the individual cells. The decay of the concentration of dye was also evaluated (Figure VIII.5c and Figure VIII.5d) and it is faster by applying 30+60 and 60+60 mA $cm^{-2}$ for Ti/$IrO_2$-$Ta_2O_5$+Nb/BDD and 60+30 and 60+60 mA $cm^{-2}$ for Nb/BDD+Ti/$IrO_2$-$Ta_2O_5$, respectively. This effect is completely consistent with the colour removals reported in Figure VIII.5a and Figure VIII.5b.

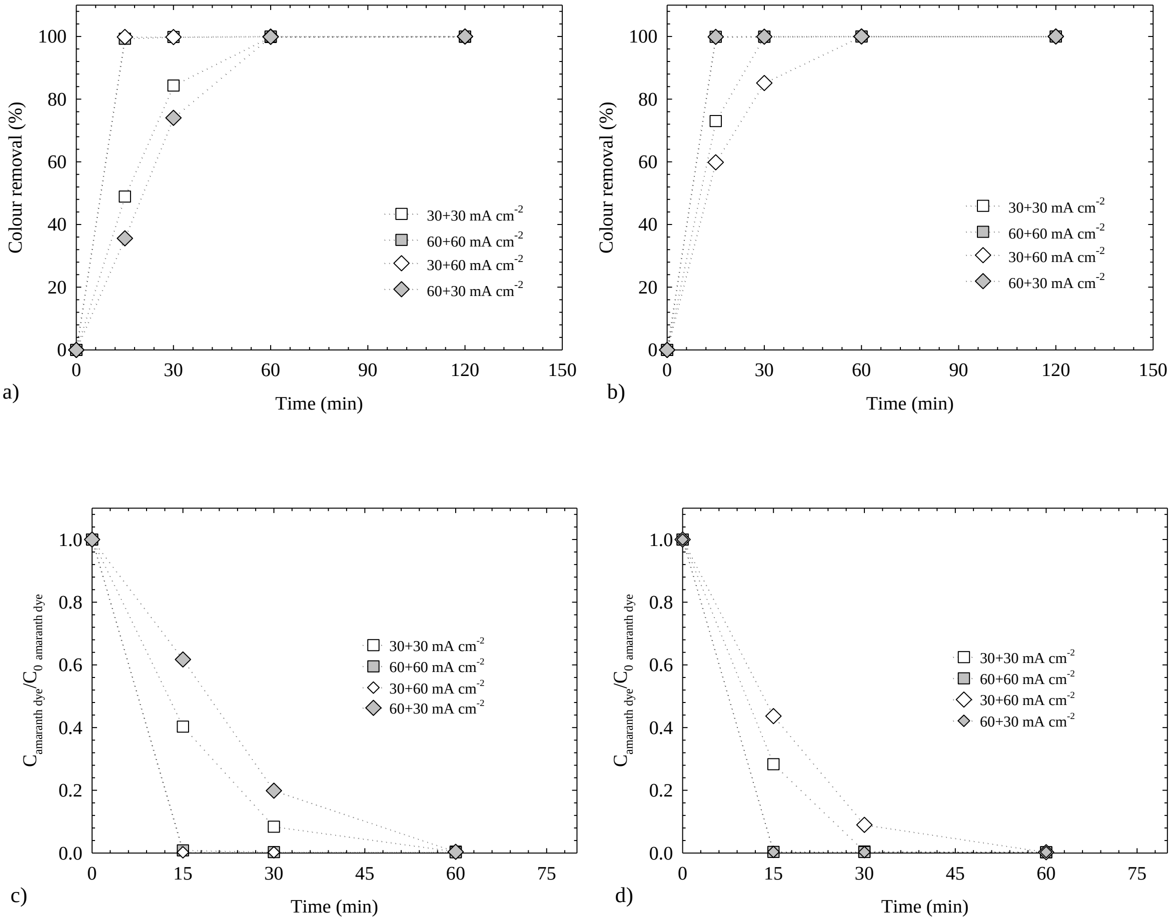

**Figure VIII.5. Oxidation of the Amaranth dye using two cells in a serial mode. Effect of current density on colour removal and decay of the normalised dye concentration over time for Ti/$IrO_2$-$Ta_2O_5$+Nb/BDD (a and c) and Nb/BDD+Ti/$IrO_2$-$Ta_2O_5$ (b and d) arrangements. Operating conditions: 100 mg $L^{-1}$ of Amaranth dye, 20 g $L^{-1}$ of $Na_2SO_4$, current density=30 and 60 mA $cm^{-2}$, T=25 °C.**

Although the colour and dye removal results are important, the abatement of COD led to more interesting outcomes. The use of the two cells in a serial mode allowed to achieve high COD removal values (Figure VIII.6), depending on the cell combinations, with respect to the results achieved when a single cell was used.

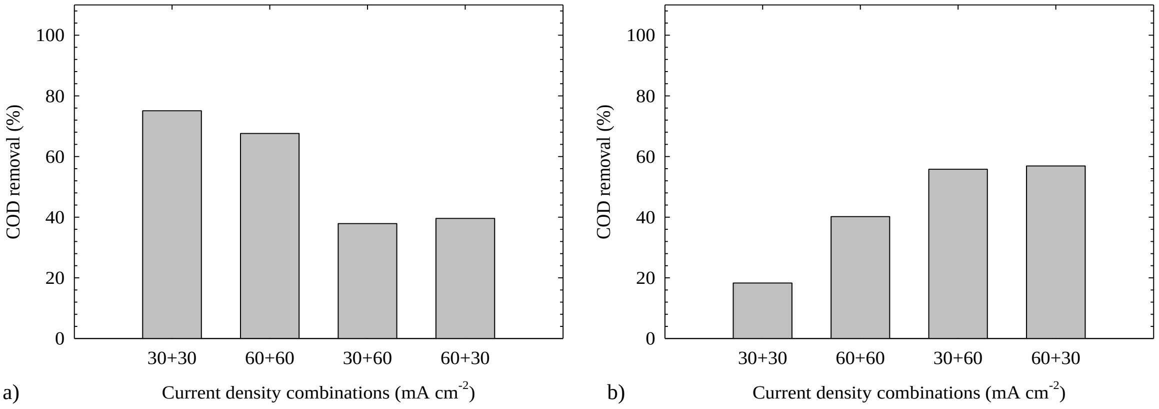

**Figure VIII.6. Oxidation of the Amaranth dye using two cells in a serial mode. Effect of current density on COD removal after 60 min of treatment for (a) Ti/$IrO_2$-$Ta_2O_5$+Nb/BDD and (b) Nb/BDD+Ti/$IrO_2$-$Ta_2O_5$ arrangements. Operating conditions: 100 mg $L^{-1}$ of Amaranth dye, 20 g $L^{-1}$ of $Na_2SO_4$, current density=30 and 60 mA $cm^{-2}$, T=25 °C.**

For example, using two cells with Ti/$IrO_2$-$Ta_2O_5$+Nb/BDD anodes by applying 30 mA $cm^{-2}$ at each one of the cells (Figure VIII.6a), the COD abatement increased from 49.1 % (with solely Nb/BDD at 30 mA $cm^{-2}$) to 75.1 %. At 60+60 mA $cm^{-2}$, for the same arrangement, a slight decrease on the COD removal (down to 67.6 %) was observed. These results are due to the electrochemical conversion of Amaranth in some by-products in the first cell with Ti/$IrO_2$-$Ta_2O_5$ that can be mineralised by Nb/BDD in the second cell. These figures are in agreement with the results obtained by using single cells, where at 30 mA $cm^{-2}$ with BDD, higher removal of COD was achieved, while the organic load reduction increases when *j* increases from 30 to 60 mA $cm^{-2}$ with Ti/$IrO_2$-$Ta_2O_5$ (Figure VIII.6b). For this reason, when serial mode configuration was used, efficient organic matter was removed. Moreover, when 60 mA $cm^{-2}$ is applied to Nb/BDD anode, the o.e.r. is enhanced, consequently decreasing the AO efficacy. When different current densities were applied to each cell, a synergetic effect was not achieved since the removals just reached 37.9–39.6 %.

Different trends were obtained when the above-mentioned experiments were performed using the serial mode arrangement with Nb/BDD+Ti/$IrO_2$-$Ta_2O_5$ electrodes (Figure VIII.6b). Lower COD removals were achieved, when the same current density for each one of the cells was applied, about 18.3 % and 40.2 % for 30+30 and 60+60 mA $cm^{-2}$, respectively. In the first case, this behaviour may be due to the promotion of the electrochemical conversion of Amaranth dye in aromatic compounds that can be adsorbed on the anodic surface of active and non-active electrodes at lower *j*, favouring a partial passivation. For an increase of the *j* values, an improvement on COD removal was observed, even if no more than 40 % degradation was reached. Efficiency was, however, enhanced when enough amount of $^{\bullet}$OH radicals was produced with Nb/BDD anode at 30 or 60 mA $cm^{-2}$ to promote a more efficient mineralisation of Amaranth but accumulating aliphatic acids that are difficult to be eliminated at both anodes.

From an industrial point of view, it is interesting to evaluate the COD removal according to the specific electrical charge, Q, passed for one and two cells systems. As an example, Figure VIII.7 compares the efficiency for Q=3.8 Ah $L^{-1}$, at 30 and 60 mA $cm^{-2}$. Results demonstrated that regardless the *j* used, the Nb/BDD anode material always promoted higher COD removals than Ti/$IrO_2$-$Ta_2O_5$ electrode, even when differences are attenuated for *j*=60 mA $cm^{-2}$ due to a removal increase for Ti/$IrO_2$-$Ta_2O_5$ and a decrease for Nb/BDD. When COD abatements were compared for one and two cells arrangements, it was possible to observe that the performance of the process was improved under suitable operating conditions at the serial mode system. Single cell with Ti/$IrO_2$-$Ta_2O_5$ anode led to lower degradation values (1.4–11.4 %). On the other hand, the experiment with Nb/BDD achieved 59 % at 30 mA $cm^{-2}$ (in 120 min), while the Ti/$IrO_2$-$Ta_2O_5$+Nb/BDD arrangement at 30+30 mA $cm^{-2}$ removed about 75.1 % in 60 min. These results indicated that, the sequence of the cells affect the efficiency of the process due to the high variety of compounds that can be formed in each one of the cells during the degradation of the Amaranth dye and through their recirculation over the system.

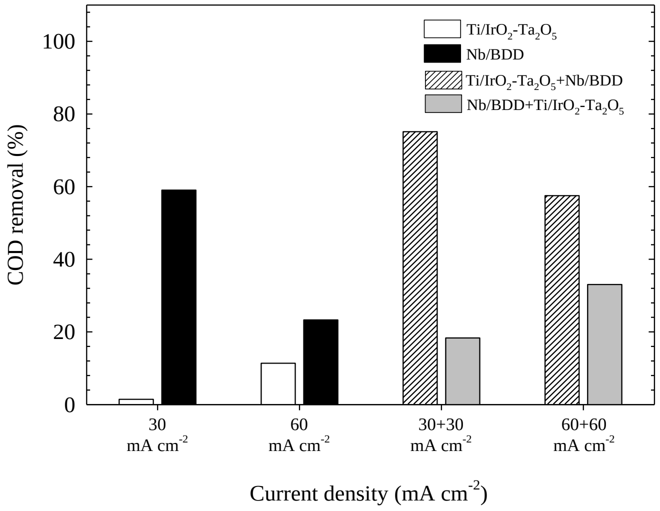

**Figure VIII.7. Effect of the current density and system configuration on COD abatement at single cells (Ti/$IrO_2$-$Ta_2O_5$ and Nb/BDD) and two cells in a serial mode (Ti/$IrO_2$-$Ta_2O_5$+Nb/BDD and Nb/BDD+Ti/$IrO_2$-$Ta_2O_5$) at a specific electric charge of 3.8 Ah $L^{-1}$. Operating conditions: 100 mg $L^{-1}$ of Amaranth dye, 20 g $L^{-1}$ of $Na_2SO_4$, current density=30 and 60 mA $cm^{-2}$, T=25 °C.**

### VIII.3.4 ENERGY CONSUMPTION

An essential parameter to be taken into account to lessen economic and environmental impacts is the electrical energy consumption (EC). This variable may be determined in terms of kWh $m^{-3}$ (Equation (VIII.4)) or kWh $gCOD^{-1}$ (Equation (VIII.5)) [1]:

$$\text{Energy consumption (kWh m}^{-3}\text{)} = \frac{E_{\text{cell}} It}{1000\ V} \qquad \textbf{(VIII.4)}$$

$$\text{Energy consumption (kWh gCOD}^{-1}\text{)} = \frac{E_{\text{cell}} It}{1000^2\ \Delta\text{COD}\ V} \qquad \textbf{(VIII.5)}$$

where $E_{cell}$ corresponds to the average potential difference of the cell (V), I to the current intensity (A), t to the electrolysis time (h), ΔCOD to the experimental abatement of COD ($gO_2$ $L^{-1}$) and V to the solution volume ($m^3$).

Figure VIII.8a represents the values of EC estimated in terms of kWh $m^{-3}$, after 60 min of treatment, for single cells at 30, 60 and 80 mA $cm^{-2}$. As can be observed, for both anode materials, the energy consumption values rose, as the applied *j* increased, since the cell potentials were also enhanced (Table VIII.1). On the contrary, COD removal values decrease for the experiments with Nb/BDD.

In addition, Figure VIII.8b displays the EC estimations in terms of kWh $m^{-3}$ for the cells in a serial mode. The values obtained with these new configuration system seem higher (25.4–72.6 kWh $m^{-3}$) when compared to the single cell systems alone (11.4–60.9 kWh $m^{-3}$). However, the energy spent by the cells in a serial mode is quite similar or slightly lower (depending on the cell position) than if the treatment was performed by the sum of the two individual cells (Table VIII.1).

Although at industrial level, energy consumption in terms of kWh $m^{-3}$ is more significant to calculate the process cost, this study also took into consideration the energy that is necessary to remove the organic matter (g of COD (Table VIII.1)). As can be verified, the cells in a serial mode required less/similar energy to remove the organic matter. For example, using Ti/$IrO_2$-$Ta_2O_5$+Nb/BDD combination at 30+30 mA $cm^{-2}$ instead of Nb/BDD at 30 mA $cm^{-2}$, the COD removal increased from 49.1 to 75.1 % with an EC of 0.2 kWh $gCOD^{-1}$ for both systems. Moreover, this cell system in a serial mode allowed 9.6 % of current efficiency to degrade the pollutant.

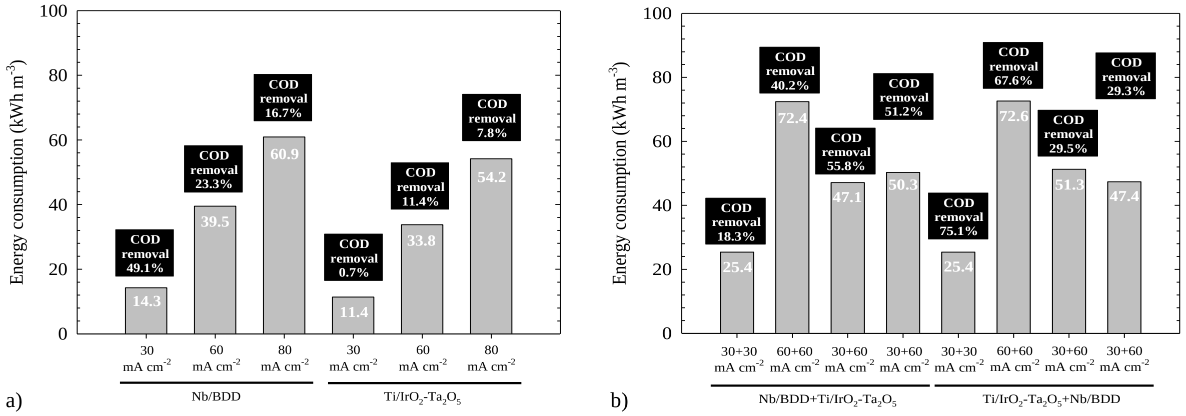

**Figure VIII.8. Effect of the arrangement of the cells on energy consumption (kWh $m^{-3}$) for the (a) single cell and the (b) two cells in a serial mode during 60 min of treatment. Operating conditions: 100 mg $L^{-1}$ of Amaranth dye, 20 g $L^{-1}$ of $Na_2SO_4$, current density=30, 60 and 80 mA $cm^{-2}$, T=25 °C.**

**Table VIII.1. Cell potentials and respective energy consumption for different applied current densities using one (cell 1) or two cells (cell 1 and 2) in a serial mode, after 60 min of treatment. Sum of the individual COD removals and energy consumptions of the single cells for 60 min of electrolysis time.**

| **Electrochemical system** | **$E_{cell\ 1}$ (V)** | **$E_{cell\ 2}$ (V)** | **Energy consumption (kWh $m^{-3}$)** | **Energy consumption (kWh $gCOD^{-1}$)** |
|---|---|---|---|---|
| Nb/BDD | | | | |
| 30 mA $cm^{-2}$ | 7.5 | - | 14.3 | 0.2 |
| 60 mA $cm^{-2}$ | 10.4 | - | 39.5 | 1.2 |
| 80 mA $cm^{-2}$ | 12.0 | - | 60.9 | 2.7 |
| Ti/$IrO_2$-$Ta_2O_5$ | | | | |
| 30 mA $cm^{-2}$ | 6.0 | - | 11.4 | 11.4 |
| 60 mA $cm^{-2}$ | 8.9 | - | 33.8 | 2.3 |
| 80 mA $cm^{-2}$ | 10.7 | - | 54.2 | 5.4 |
| Nb/BDD+Ti/$IrO_2$-$Ta_2O_5$ | | | | |
| 30+30 mA $cm^{-2}$ | 7.5 | 5.8 | 25.4 | 1.0 |
| 60+60 mA $cm^{-2}$ | 10.4 | 8.6 | 72.4 | 1.3 |
| 30+60 mA $cm^{-2}$ | 7.4 | 8.7 | 47.1 | 0.6 |
| 60+30 mA $cm^{-2}$ | 10.4 | 5.6 | 50.3 | 0.7 |
| Ti/$IrO_2$-$Ta_2O_5$+Nb/BDD | | | | |
| 30+30 mA $cm^{-2}$ | 5.8 | 7.5 | 25.4 | 0.2 |
| 60+60 mA $cm^{-2}$ | 8.5 | 10.6 | 72.6 | 0.7 |
| 30+60 mA $cm^{-2}$ | 5.7 | 10.6 | 51.3 | 1.2 |
| 60+30 mA $cm^{-2}$ | 8.7 | 7.4 | 47.4 | 1.1 |

| **Sum of single cells** | **COD removal (%)** | **Energy consumption (kWh $m^{-3}$)** | **Energy consumption (kWh $gCOD^{-1}$)** |
|---|---|---|---|
| Nb/BDD 30 mA $cm^{-2}$ + Ti/$IrO_2$-$Ta_2O_5$ 30 mA $cm^{-2}$ | 49.8 | 25.7 | 11.6 |
| Nb/BDD 60 mA $cm^{-2}$ + Ti/$IrO_2$-$Ta_2O_5$ 60 mA $cm^{-2}$ | 34.7 | 73.3 | 3.5 |
| Nb/BDD 30 mA $cm^{-2}$ + Ti/$IrO_2$-$Ta_2O_5$ 60 mA $cm^{-2}$ | 56.9 | 48.0 | 2.5 |
| Nb/BDD 60 mA $cm^{-2}$ + Ti/$IrO_2$-$Ta_2O_5$ 30 mA $cm^{-2}$ | 24.0 | 50.9 | 12.6 |

These results clearly demonstrate that the dual combination, once again depending on the active and non-active anode position, is an interesting reactor arrangement to be implemented as a pre-treatment for the degradation of organic dyes with higher removal efficiencies and consequently, lower energy consumptions.

## VIII.4 CONCLUSIONS

The depuration of a synthetic wastewater containing Amaranth dye was investigated in an AO process using one or two cells in a serial mode with active and non-active anodes. The treatment of the dye using single cells was strongly affected by the type of the anode materials, since it determines how easily the $^{\bullet}OH$ radicals are delivered to the system and how these oxidant species react with the organic pollutants, promoting their elimination. Also, the process efficiency depended on the current density. For a single electrochemical cell, complete colour removal and 49.1 % of organic load was eliminated (in terms of COD) with energy consumption of 14.3 kWh $m^{-3}$ (0.2 kWh $gCOD^{-1}$), after 60 min of treatment with Nb/BDD at 30 mA $cm^{-2}$.

In the case of the two cells in a serial mode, depending on its arrangement, this system showed to be more efficient in colour and COD removal with less energy consumption than the sum of the individual cells. The Ti/$IrO_2$-$Ta_2O_5$+Nb/BDD combination at 30+30 mA $cm^{-2}$, after 60 min of reaction, achieved the optimum efficiency results, with 100 % and 75.1 % of colour and COD removals, respectively; with 25.4 kWh $m^{-3}$ (0.2 kWh $gCOD^{-1}$) of energy consumed. Therefore, this dual arrangement seems to be an interesting set-up to be applied as a pre-treatment of this kind of wastewaters.

Finally, it is important to remark that, with regard to cells in series, many commercial models are now available in the market. Nevertheless, single cells or the stacking of single cells are mainly used for electrosynthesis (production of chlorine, chlorate, etc.). Conversely, the research of the AO for environmental application has not reported enough studies about the use of cells in a serial mode or stack cells in lab-scale; for this reason, this work proposal is not new but it opens an innovative application to scale-up the electrochemical technologies for wastewater treatment.

## ACKNOWLEDGMENTS

AS Fajardo and RC Martins gratefully acknowledge the Fundação para a Ciência e Tecnologia, for financial support under the Doc grant (SFRH/BD/87318/2012) and the IFCT 2014 programme (IF/00215/2014) with financing from the European Social Fund and the Human Potential Operational Programme, respectively.

Financial support from National Council for Scientific and Technological Development (CNPq – 446846/2014-7 Brazil) is gratefully acknowledged.

AS Fajardo also acknowledge the LEAA group in the Institute of Chemistry at Federal University of Rio Grande do Norte for providing the laboratory and the necessary conditions to perform this work, as well as Dr. Professor João Fernandes de Sousa from the Department of Chemical Engineering of the same university, who put the HPLC equipment available to run the samples.

## REFERENCES

[1] Brillas E, Martínez-Huitle CA (2015) Decontamination of wastewaters containing synthetic organic dyes by electrochemical methods. An up dated review. Appl. Catal. B: Environ. 166–167: 603–643.

[2] Oturan MA, Aaron JJ (2014) Advanced oxidation processes in water/wastewater treatment: principles and applications. A review. Crit. Rev. Env. Sci. Technol. 44: 2577–2641.

[3] Garcia-Segura S, Centellas F, Arias C, Garrido JA, Rodríguez RM, Cabot PL, Brillas E (2011) Comparative decolorization of monoazo, diazo and triazo dyes by electro-Fenton Process. Electrochim. Acta 58: 303–311.

[4] Solanki K, Subramanian S, Basu S (2013) Microbial fuel cells for azo dye treatment with electricity generation: A review. Bioresour. Technol. 131: 564–571.

[5] Forgacs E, Cserháti T, Oros G (2004) Removal of synthetic dyes from wastewaters: a review. Environ. Int. 30: 953–971.

[6] Erkurt HA (2010) Biodegradation of Azo Dyes, in: Erkurt HA (Ed.), The Handbook of Environmental Chemistry, 09, Springer, Berlin, 1–210.

[7] Sirés I, Brillas E, Oturan MA, Rodrigo MA, Panizza M (2014) Electrochemical advanced oxidation processes: today and tomorrow. A review. Environ. Sci. Pollut. Res. 21: 8336–8367.

[8] Barrera-Diaz C, Canizares P, Fernandez FJ, Natividad R, Rodrigo MA (2014) Electrochemical Advanced Oxidation Processes: An Overview of the Current Applications to Actual Industrial Effluents. J. Mex. Chem. Soc. 58: 256–275.

[9] Martínez-Huitle CA, Rodrigo MA, Sirés I, Scialdone O (2015) Single and Coupled Electrochemical Processes and Reactors for the Abatement of Organic Water Pollutants: A Critical Review. Chem. Rev. 115: 13362–13407.

[10] Panizza M, Cerisola G (2008) Removal of colour and COD from wastewater containing acid blue 22 by electrochemical oxidation. J. Hazard. Mater. 153: 83–88.

[11] Panizza M, Cerisola G (2009) Direct and mediated anodic oxidation of organic pollutants. Chem. Rev. 109: 6541–6569.

[12] Marselli B, García-Gómez J, Michaud P-A, Rodrigo MA, Comninellis C (2003) Electrogeneration of hydroxyl radicals on boron-doped diamond electrodes. J. Electrochem. Soc. 150: D79–D83.

[13] Martínez-Huitle C.A, Santos EV, DM Araújo, Panizza M (2012) Applicability of diamond electrode/anode to the electrochemical treatment of a real textile effluent. J. Electroanal. Chem. 674: 103–107.

[14] Ramírez C, Saldaña A, Hernández B, Acero R, Guerra R, Garcia-Segura S, Brillas E, Peralta-Hernández JM (2013) Electrochemical oxidation of methyl Orange azo dye at pilot flow plant using BDD technology. J. Ind. Eng. Chem. 19: 571–579.

[15] Guenfoud F, Mokhtari M, Akrout H (2014) Electrochemical degradation of malachite green with BDD electrodes: Effect of electrochemical parameters. Diam. Relat. Mater. 46: 8–14.

[16] Palma-Goyes RE, Vazquez-Arenas J, Torres-Palma RA, Ostos C, Ferraro F, González I (2015) The abatement of indigo carmine using active chlorine electrogenerated on ternary $Sb_2O_5$-doped Ti/$RuO_2$-$ZrO_2$ anodes in a filter-press FM01-LC reactor. Electrochim. Acta 174: 735–744.

[17] Abdessamad N, Akrout H, Hamdaoui G, K Elghniji, Ksibi M, Bousselm L (2013) Evaluation of the efficiency of monopolar and bipolar BDD electrodes for electrochemical oxidation of anthraquinone textile synthetic effluent for reuse. Chemosphere 93: 1309–1316.

[18] Vasconcelos VM, Ponce-de-León C, Nava JL, Lanza MRV (2015) Electrochemical degradation of RB-5 dye by anodic oxidation, electro-Fenton and by combining anodic oxidation-electro-Fenton in a filter-press flow cell. J. Electroanal. Chem. 765: 179–187.

[19] Zhang C, Wang J, Murakami T, Fujishima A, Fu D, Gu Z (2010) Influence of cations during Orange-II degradation on boron-doped diamond electrode. J. Electroanal. Chem. 638: 91–98.

[20] Aquino JM, Pereira GF, Rocha-Filho RC, Bocchi N, Biaggio SR (2011) Electrochemical degradation of a real textile effluent using boron-doped diamond or b-$PbO_2$ as anode. J. Hazard. Mater. 192: 1275–1282.

[21] Zhang C, Liu L, Li W, Wua J, Rong F, Fu D (2014) Electrochemical degradation of Acid Orange II dye with boron-doped diamond electrode: Role of operating parameters in the absence and in the presence of NaCl. J. Electroanal. Chem. 726: 77–83.

[22] Araújo DM, Sáez C, Martínez-Huitle CA, Cañizares P, Rodrigo MA (2015) Influence of mediated processes on the removal of Rhodamine with conductive-diamond electrochemical oxidation. Appl. Catal. B: Environ. 166–167: 454–459.

[23] Uranga-Flores A, Rosa-Júarez C, Gutierrez-Granados S, Moura DC, Martínez-Huitle CA, Peralta Hernández JM (2015) Electrochemical promotion of strong oxidants to degrade Acid Red 211: Effect of supporting electrolytes. J. Electroanal. Chem. 738: 84–91.

[24] Basha CA, Sendhil J, Selvakumar KV, Muniswaran PKA, Lee CW (2012) Electrochemical degradation of textile dyeing industry effluent in batch and flow reactor systems. Desalination 285: 188–197.

[25] del Río AI, Fernández J, Molina J, Bonastre J, Cases F (2011) Electrochemical treatment of a synthetic wastewater containing a sulphonated azo dye. Determination of phthalenesulphonic compounds produced as main byproducts. Desalination 273: 428–435.

[26] del Río AI, Benimeli MJ, Molina J, Bonastre J, Cases F (2012) Electrochemical Treatment of C.I. Reactive Black 5 Solutions on Stabilized Doped Ti/$SnO_2$ Electrodes. Int. J. Electrochem. Sci. 7: 13074–13092.

[27] Ferreira MB, Rocha JHB, Melo JV, Martinez-Huitle CA, Alfaro MAQ (2013) Use of a Dual Arrangement of Flow Cells for Electrochemical Decontamination of Aqueous Solutions Containing Synthetic Dyes. Electrocatal. 4: 274–282.

[28] Trinidad P, Walsh F (1998) Conversion expressions for electrochemical reactors which operate under mass transport controlled reaction conditions, Part I: Batch Reactor, PFR and CSTR. Int. J. Eng. 14: 431–441.

[29] Xiong Y, Strunk PJ, Xia H, Zhu X, Karlsson HT (2001) Treatment of dye wastewater containing acid orange II using a cell with three-phase three-dimensional electrode. Water Res. 35(17): 4226–4230.

[30] Yavuz Y, Shahbazi R (2012) Anodic oxidation of Reactive Black 5 dye using boron doped diamond anodes in a bipolar trickle tower reactor. Sep. Purif. Technol. 85: 130–136.

[31] Sabatino S, Galia A, Scialdone O (2016) Electrochemical Abatement of Organic Pollutants in Continuous-Reaction Systems through the Assembly of Microfluidic Cells in Series. ChemElectroChem 3: 83–90.

[32] Barros WRP, Franco PC, Steter JR, Rocha RS, Lanza MRV (2014) Electro-Fenton degradation of the food dye amaranth using a gas diffusion electrode modified with cobalt (II) phthalocyanine. J. Electroanal. Chem. 722–723: 46–53.

[33] Greenberg A, Clesceri L, Eaton A (1992) Standard Methods for the Examination of Water and Wastewater, 18th ed., American Public Health Association, Washington DC.

[34] Panizza M, Cerisola G (2007) Electrocatalytic materials for the electrochemical oxidation of synthetic dyes. Appl. Catal. B: Environ. 75: 95–101.

[35] Labiadh L, Barbucci A, Cerisola G, Gadri A, Ammar S, Panizza M (2015) Role of anode material on the electrochemical oxidation of methyl orange. J. Solid State Electrochem. 19: 3177–3183.

[36] Garcia-Segura S, Santos EV, Martínez-Huitle CA (2015) Role of $sp^3/sp^2$ ratio on the electrocatalytic properties of boron-doped diamond electrodes: A mini review. Electrochem. Commun. 59: 52–55.

[37] Panizza M, Cerisola G (2005) Application of diamond electrodes to electrochemical processes. Electrochim. Acta 51: 191–199.

[38] Scialdone O, Galia A, Guarisco C (2013) Electrochemical Oxidation of Carboxylic Acids in Water at Boron-Doped Diamond (BDD) Anodes in the Range of Potential of Oxygen Evolution: Detection Measurements and Studies on the Reaction Mechanism. Electrocatal. 4: 290–301.

[39] Rocha JHB, Gomes MMS, Santos EV, Moura ECM, Silva DR, Quiroz MA, Martínez-Huitle CA (2014) Electrochemical degradation of Novacron Yellow C-RG using boron-doped diamond and platinum anodes: Direct and Indirect oxidation. Electrochim. Acta 140: 419–426.

[40] Florenza X, Solano AMS, Centellas F, CA Martínez-Huitle, Brillas E, Garcia-Segura S (2014) Degradation of the azo dye Acid Red 1 by anodic oxidation and indirect electrochemical processes based on Fenton's reaction chemistry. Relationship between decolorization, mineralization and products. Electrochim. Acta 142: 276–288.

[41] Martínez-Huitle CA, Ferro S, De Battisti A (2004) Electrochemical incineration of oxalic acid. Role of electrode material. Electrochim. Acta 49: 4027–4034.

[42] Martínez-Huitle CA, S Ferro, De Battisti A (2005) Electrochemical incineration of oxalic acid: Reactivity and engineering parameters. J. Appl. Electrochem. 35: 1087–1093.

[43] Isarain-Chávez E, de la Rosa C, Godínez, Brillas E, Peralta-Hernández JM (2014) Comparative study of electrochemical water treatment processes for a tannery wastewater effluent. J. Electroanal. Chem. 713: 62–69.

[44] Moreira FC, Garcia-Segura S, Vilar VJP, Boaventura RAR, Brillas E (2013) Decolorization and mineralization of Sunset Yellow FCF azo dye by anodic oxidation, electro-Fenton UVA photoelectro-Fenton and solar photoelectron-Fenton processes. Appl. Catal. B: Environ. 142–143: 877–890.

# IX. ELECTROCHEMICAL ABATEMENT OF AMARANTH DYE SOLUTIONS USING INDIVIDUAL OR AN ASSEMBLING OF FLOW CELLS WITH Ti/Pt AND Ti/Pt-SnSb ANODES

AS Fajardo[a,b], RC Martins[a], DR Silva[b], RM Quinta-Ferreira[a] and CA Martínez-Huitle[b]

[a] CIEPQPF – Centro de Investigação em Engenharia dos Processos Químicos e dos Produtos da Floresta; GERST – Group on Environment, Reaction, Separation and Thermodynamics; Department of Chemical Engineering, Faculty of Sciences and Technology, University of Coimbra, Pólo II, Rua Sílvio Lima, 3030-790 Coimbra, Portugal.

[b] LEAA – Laboratório de Eletroquímica Ambiental e Aplicada; Institute of Chemistry, Federal University of Rio Grande do Norte, Lagoa Nova, CEP 59078-970 Natal, RN, Brazil.

*Submitted to Separation and Purification Technology*

## ABSTRACT

Electrochemical measurements and bulk electrolysis using individual or an assembling of flow cells in series were performed to study the anodic oxidation of amaranth dye solutions with Ti/Pt and Ti/Pt-SnSb anodes. Polarisation curves demonstrated that Ti/Pt-SnSb has high electroactivity to eliminate the pollutant. Bulk electrolysis with this material, at 30 mA cm$^{-2}$, removed 97.5 % and 70.3 % of colour and COD, consuming 71.6 kWh m$^{-3}$ of energy. Two cell configurations led to higher removal rates. Additionally, experiments combining Ti/Pt-SnSb and Nb/BDD materials were performed to clarify the effect of non-active anodes in the system. Assembling cells revealed to be an interesting pre-treatment to degrade organic compounds. The suitable system choice will be dependent on the final target COD value, the reaction time and the energy consumption.

## IX.1 INTRODUCTION

Water pollution by synthetic dyes remains an important ecological issue due to their large worldwide production estimated over $7\times10^5$ tons per year. Natural streams contamination and aesthetic constrains encourage the scientific community to search novel strategies to adequately treat industrial effluents [1]. Nevertheless, traditional technologies have demonstrated to be ineffective for removing these pollutants from water and wastewaters. In this context, a wide variety of advanced oxidation processes (AOPs) has been studied for environment protection [2,3]. Among these technologies, the electrochemical advanced oxidation process (EAOP) has received great attention for the elimination of a broad-range of organic contaminants in the last years [4]. The most popular EAOP is the electrochemical oxidation (EO) that consists either in oxidation of pollutants by electrons transfer to the electrode surface (direct anodic oxidation) and/or mediated oxidation with electrogenerated hydroxyl radicals ($^{\bullet}$OH) formed from water discharge at the anode surface (M) (Equation (IX.1)) [1].

$$\mathrm{M + H_2O \rightarrow M(\,^{\bullet}OH) + H^+ + e^-} \qquad \textbf{(IX.1)}$$

The activity of the $^{\bullet}$OH radicals is strongly related to their interaction with the electrode surface M, which can be in the form of chemisorbed "active oxygen" (oxygen in the lattice of a metal oxide (MO) anode) (Equation (IX.2)) or physically adsorbed "active oxygen" (free hydroxyl radical M($^{\bullet}$OH)) [5,6].

$$\mathrm{M(\,^{\bullet}OH) \rightarrow MO + H^+ + e^-} \qquad \textbf{(IX.2)}$$

When active anodes such as $IrO_2$ or Pt are used, the $^{\bullet}$OH radicals are converted to chemisorbed $IrO_3$ and PtO species, respectively, favouring partial conversion of the contaminants (R) (Equations (IX.3) and (IX.4)) [7,8].

$$\mathrm{R + IrO_3 \rightarrow IrO_2 + RO} \qquad \textbf{(IX.3)}$$

$$\mathrm{R + PtO \rightarrow Pt + RO} \qquad \textbf{(IX.4)}$$

Generally, Equation (IX.2) and Equation (IX.3) are in in competition with the side reaction of oxygen evolution (Equation (IX.5)), which is due to the chemical decomposition of the higher oxide.

$$\mathrm{MO \rightarrow M + \frac{1}{2}O_2} \qquad \textbf{(IX.5)}$$

Meanwhile, the use of non-active anodes such as boron doped diamond (BDD) promotes the generation of high amounts of physisorbed BDD($^{\bullet}$OH) characterised by a weak electrode–hydroxyl radical interaction resulting in a high ability to mineralise the compounds to $CO_2$, $H_2O$ and inorganic ions (Equation (IX.6)). This reaction competes with the parasitic reaction of the oxygen evolution (Equation (IX.7)) without any participation of the anode surface [9–13].

$$\mathrm{R + BDD(\,^{\bullet}OH) \rightarrow BDD + m\,CO_2 + nH_2O + H^+ + \ e^-} \qquad \textbf{(IX.6)}$$

$$\mathrm{BDD(\,^{\bullet}OH) \rightarrow BDD + \frac{1}{2}O_2 + H^+ + e^-} \qquad \textbf{(IX.7)}$$

The lab scale experiments with BDD anodes led to significant efficiencies regarding the degradation of dyes. However, the viability of these electrodes for industrial application is not well established due to their high cost [14–16]. For this reason, the choice of anode materials becomes a noteworthy issue in order to reduce the energy consumption and consequently, the operation costs; converting this process in a more attractive alternative than chemical treatments. As a result, electrocatalytic materials prepared by a thin conducting layer of metal oxide or mixed metal-oxides in a Ti base metal, commonly named as DSA (dimensional stable anodes), have been also tested for the treatment of dyes by EO, obtaining encouraging results. Simulated synthetic dyes wastewaters containing Acid Red 73 [17], Acid Orange 7 [18], Methyl Orange [19], Methyl Red [20], Reactive Orange 4 [21], Reactive Red 2 [22], Reactive Red 120 [23], Reactive Red 195 [24] and Reactive Violet 5 [25] have been depolluted with anodes such as Ti/$SnO_2$-Sb, Ti/Antimony-doped tin oxide nanoparticles, Ti/$RuO_2$-Pt, $TiRuSnO_2$, Ti/$Ru_{0.3}Ti_{0.7}O_2$, Ti/$SnO_2$-Pt-Sb, Ti/$Bi_2O_3$, Ti/$IrO_2$-$RuO_2$, Ti/$SnO_2$-Sb/$PbO_2$ and Ti/RuOx/$MnO_x$. Conversely, real wastewaters have been treated in a lesser extent with DSA electrodes like Ti/RuOx-TiOx [26], Ti-Pt/β-$PbO_2$ and Ti/$Ti_{0.7}Ru_{0.3}O_2$ [27].

According to the literature, the Ti/Pt, a less expensive electrode than diamond films, has demonstrated to be effective on colour removal of dyes with moderate removal values of the organic matter (COD removal=5–90 %, TOC removal=17–82 %) and energy consumption around 6–61 kWh $m^{-3}$ [20,28–30].

Therefore, the present study proposes the use of two commercial anode materials, the Ti/Pt and the Ti/Pt-SnSb for the electrochemical abatement of a dye in an aqueous solution by using one flow cell or an assembling of electrochemical flow cells in series. The main objectives of the work were to analyse the effect of the nature of the electrode materials by potentiodynamic measurements and bulk electrolysis. In the former case, the catalytic activity of these electrodes was explored; while the efficacy of EO process was tested by using single and two flow cells in a serial mode in order to evaluate favourable arrangement combinations and current densities on colour and COD removals as well as on energy consumption. Additionally, tests were performed with an assembling of electrochemical flow cells in series with Ti/Pt-SnSb and Nb/BDD materials to verify the effect of the combination of non-active anodes in the system. Amaranth dye (AM) was the selected pollutant model because it has been classified as an endocrine disruptor which causes negative effects in animal and human health [31]. Additionally, even if the dye is not carcinogenic, the reductive cleavage of the azo bonds produces amines that are known to be cancer-causing [32,33].

# IX.2 MATERIAL AND METHODS

## IX.2.1 SYNTHETIC SOLUTION

The dye solution model was prepared by dissolving 100 mg of AM dye (Cotia Foods S. A.) in 1 L of distilled water containing 20 g $L^{-1}$ of $Na_2SO_4$ (Anidrol) as background electrolyte since this salt appears in many dyestuff wastewaters and it allows good electrical conductivity. No further purification was conducted to reagents before use. The dye structure and characteristics are displayed in Table IX.1. In addition, the synthetic effluent encompasses an initial pH value of 5.6±1.1, conductivity of 228.4±0.8 µS $cm^{-1}$ and an amount of organic matter expressed by chemical oxygen demand (COD) of 134.5±15.4 $mgO_2$ $L^{-1}$.

**Table IX.1. Chemical structure and characteristics of the Amaranth dye.**

| Chemical structure | $\lambda_{max}$ (nm) | M (g $mol^{-1}$) | Common name | Colour Index name |
|---|---|---|---|---|
| 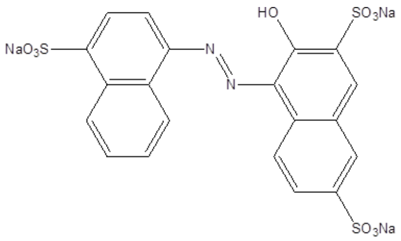 | 524 | 604.5 | Amaranth dye | Food Red 9<br>Acid Red 27 |

## IX.2.2 ELECTROCHEMICAL MEASUREMENTS

Linear polarisation and cyclic voltammetry analysis were performed at room temperature (25 °C) with a Metrohm AUTOLAB potentiostat model PGSTAT302N. The three-electrode cell was constituted by a Ag/AgCl (KCl 3 mol $L^{-1}$) as reference electrode, Pt wire as the counter electrode and Ti/Pt and Ti/Pt-SnSb materials as working electrodes with an exposed geometric area of 1 $cm^2$. The working electrodes were subjected to repetitive cycles from 0 to 3.0 V (ten cycles each) at the scan rate of 100 mV $s^{-1}$, by using cyclic voltammetry, in 20 g $L^{-1}$ of $Na_2SO_4$ as supporting electrolyte as well as in a solution containing the AM dye. Quasi-steady polarisation curves were carried out at a scan rate of 100 mV $s^{-1}$ and with a 2.44 mV step potential, under similar above experimental conditions.

## IX.2.3 ELECTROCHEMICAL SYSTEM

EO experiments were performed by using systems with an individual flow cell or by an assembling of electrochemical flow cells in series under galvanostatic conditions with a MINIPA MPL-3305M power supply. Ti/Pt and Ti/Pt-SnSb electrode materials were supplied by Industrie De Nora Elettrodi (Italy) and used as anodes, while Ti was employed as cathode. Some tests were also performed with Nb/BDD as anode, and it was supplied by METAKEM GmbH (Germany). All electrodes had a disk format with an electroactive area of 63.6 cm$^2$. Anodes and cathodes were placed in parallel with an inter-electrode gap of 1.2 cm. In each experiment, the reservoir was filled with 1 L of the synthetic solution and recirculated through the system by a centrifugal pump working at 250 L h$^{-1}$. The oxidation was conducted at mild conditions of pressure and temperature to study the effect of the applied current density (*j*) of 30, 60 and 80 mA cm$^{-2}$.

### IX.2.4 ANALYTICAL TECHNIQUES

The colour removal was assessed by monitoring the decrease of the maximum absorbance of AM solution ($\lambda_{max.}$=524 nm) over time using an UV-vis spectrophotometer Analytikjena SPECORD 210 PLUS. The percentage of decolourisation of the dye solution was estimated by the Equation (IX.8):

$$\text{Colour removal (\%)} = \frac{(\text{Abs}_0 - \text{Abs}_\text{t})}{\text{Abs}_0} \times 100 \tag{IX.8}$$

where $\text{Abs}_0$ and $\text{Abs}_\text{t}$ correspond to the average absorbance at the beginning of the reaction and after an electrolysis time t, respectively.

The chemical oxygen demand (COD) was determined according to the *Standard Methods (5250D)* [34] through the use of HANNA Instruments equipment, where the COD kits (HI93754B-25) were mixed with the samples, and after that, these were digested in the thermal reactor HI 839800. COD values were directly given by the photometer HI 83099. The current efficiency (CE) for the EO of the pollutant was estimated from the COD experimental values by Equation (IX.9) [1].

$$\text{CE(\%)} = \frac{(\text{COD}_0 - \text{COD}_\text{t})\ \text{F V}}{8\text{It}} \times 100 \tag{IX.9}$$

where $\text{COD}_0$ and $\text{COD}_\text{t}$ corresponds to chemical oxygen demands at time t=0 and time t, respectively ($\text{gO}_2$ L$^{-1}$), F to the Faraday constant (96487 C mol$^{-1}$), V to the solution volume (L), I is the current intensity applied (A), 8 is the oxygen equivalent mass ($\text{g}_{\text{equiv.}}{}^{-1}$) and t express the electrolysis time (s). Furthermore, the energy consumption (EC) per volume of treated effluent was determined in terms of kWh m$^{-3}$ according to Equation (IX.10) [29]:

$$\text{EC(kWh m}^{-3}) = \frac{\text{E}_\text{cell}\ \text{I t}}{\text{V}} \tag{IX.10}$$

where $\text{E}_\text{cell}$ corresponds to the average potential difference of the cell (V), *t* expresses the electrolysis time (h) and V is the solution volume (L).

# IX.3 RESULTS AND DISCUSSION

## IX.3.1 CYCLIC VOLTAMMETRY AND POLARISATION CURVES

Prior to electrochemical oxidations and on the basis of the introductory considerations regarding the electrocatalytic nature of each one of the electrodes employed, electrochemical measurements were performed using cyclic voltammetry and polarisation curves. Both analysis were carried out using as background the electrolyte solution containing 20 g L$^{-1}$ of $Na_2SO_4$, with and without the model pollutant (100 mg L$^{-1}$). Figure IX.1a represents the cyclic voltammograms for the Ti/Pt material obtained at the previous referred conditions and recorded at a scan rate of 100 mV s$^{-1}$. As can be seen on Ti/Pt anode, no redox peak was obtained with blank $Na_2SO_4$ solution showing that the anode is non-active in the selected scanning region (Figure IX.1a, grey dashed curve) [17]. The oxygen evolution started at about +1.5 V *vs* Ag/AgCl, demonstrating that this electrode has low oxygen evolution overpotential. The addition of the AM (100 mg L$^{-1}$) to the electrolyte showed a slight increase about +1.0 V *vs* Ag/AgCl, in the region before oxygen evolution reaction (o.e.r.) (Figure IX.1a, solid black curve) respect to the curve obtained in absence of AM in solution (Figure IX.1a, grey dashed curve). This may indicate that direct electron transfer process occurred between the dye molecules and the electrode, at lower applied current densities, demonstrating that a partial absorption on the active sites of the platinum surface by organic molecules may occur [24]. In fact, in the region after o.e.r., a significant decrease on the $j$ is observed due to a partial deactivation of the active sites on the Ti/Pt surface, limiting an efficient decomposition of the supporting electrolyte [19].

The voltammogram obtained with Ti/Pt-SnSb in 20 g L$^{-1}$ of $Na_2SO_4$ (Figure IX.1b, grey dashed curve) showed that the oxygen evolution started at about +1.7 V *vs* Ag/AgCl revealing that this electrode has a slightly higher oxygen evolution overpotential when compared to the Ti/Pt anode. As can be observed form inset in Figure IX.1b (black solid curve), no noteworthy differences were observed at voltammogram obtained in presence of 100 mg L$^{-1}$ of AM dye in respect to the supporting electrolyte (Figure IX.1b, grey dashed curve), in the region before o.e.r. (ranging from +0.5 to +1.3 V *vs* Ag/AgCl). In addition, a significant increase in $j$ is attained in the region of supporting electrolyte decomposition when AM is present in the solution. This behaviour shows that the oxidation of the dye may involve intermediates generated from water decomposition, mainly $^{\bullet}OH$ radicals (Equation (IX.11)) that are only available in conditions of oxygen evolution [19].

$$2H_2O \rightarrow 2\ ^{\bullet}OH + 2H^+ + 2e^- \qquad \textbf{(IX.11)}$$

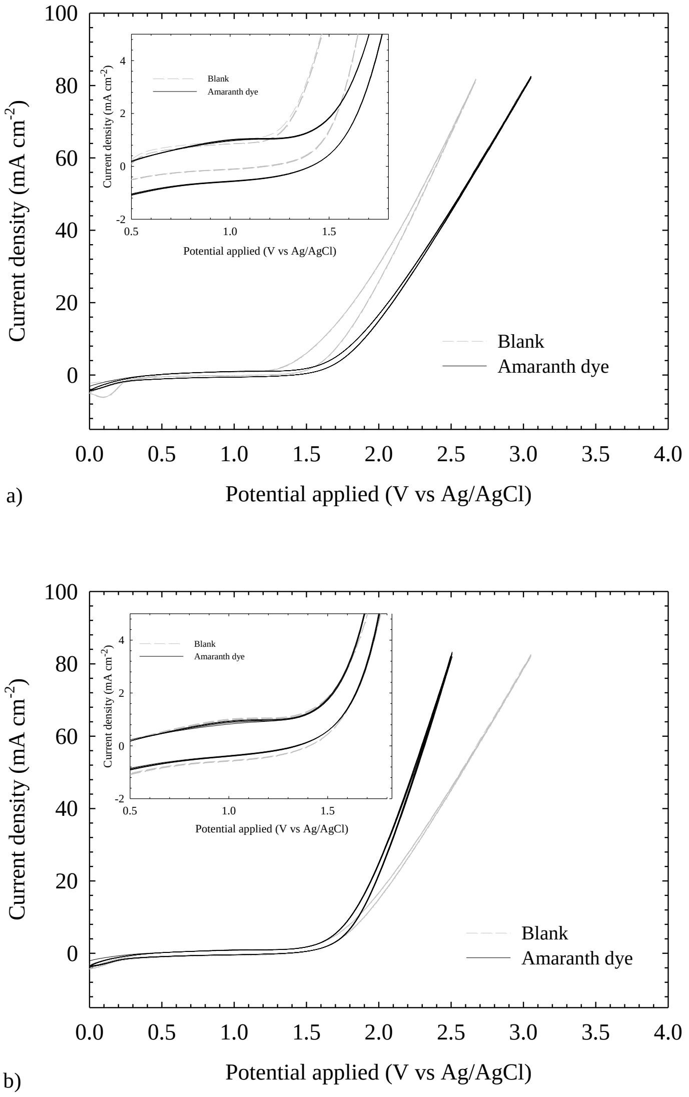

**Figure IX.1. Cyclic voltammograms of the Ti/Pt (a) and Ti/Pt-SnSb (b) anodes in 20 g $L^{-1}$ de $Na_2SO_4$, without (full line) and with 100 mg $L^{-1}$ of amaranth dye (dashed line); scan potential from 0.0 to 3.0 V and scan rate 100 mV $s^{-1}$ (10 voltammetric cycles). Insets: Zoom to the cyclic voltammograms (a) and (b), respectively.**

Figure IX.2 represents linear polarisation curves of Ti/Pt and Ti/Pt-SnSb electrodes recorded at scan rate of 100 mV $s^{-1}$ in 20 g $L^{-1}$ of $Na_2SO_4$ in absence and in presence of AM dye in solution. As can be observed, the two grey dashed curves (Figure IX.2a and Figure IX.2b) are different and show that oxygen evolution potential increased from +1.5 to +1.7 V *vs* Ag/AgCl for Ti/Pt and Ti/Pt-SnSb, respectively. This behaviour suggests that Ti/Pt material is a better electrocatalyst for the o.e.r, when compared to Ti/Pt-SnSb since it has low oxygen evolution overpotential, as supported by the cyclic voltammograms in Figure IX.1.

The oxidation of 100 mg $L^{-1}$ of AM dye is represented by the solid black curves (Figure IX.2a and Figure IX.2b) at both electrocatalytic materials. In the case of Ti/Pt, AM is directly oxidised at the electrode surface when the current density is above 15–20 mA $cm^{-2}$. Meanwhile, at higher *j* (> 20 mA $cm^{-2}$), the current density at a given potential in the region of supporting electrolyte decomposition decreased, meaning the inhibition for the oxygen evolution reaction as a consequence of a partial deactivation of the active sites on the electrode surface, limiting the EO of AM. Conversely, at Ti/Pt-SnSb anode, the participation •OH radicals electrogenerated from water discharge in concomitance with o.e.r. is achieved at higher *j* (> 20 mA cm$^{-2}$). These figures, at both anodes, are in agreement with the results obtained at voltammetric curves (see, Figure IX.1).

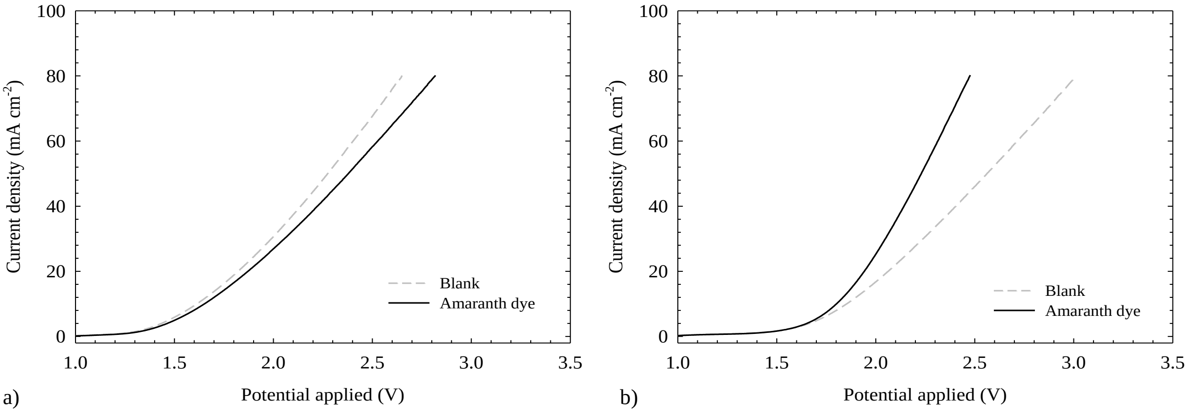

**Figure IX.2. Polarisation curves in the presence of the supporting electrolyte (full line) and in the supporting electrolyte plus the AM dye (dashed line) for the Ti/Pt (a) and Ti/Pt-SnSb (b) anodes with a scan rate of 100 mV s$^{-1}$.**

### IX.3.2 BULK ELECTROLYSIS

The degradation of the AM (100 mg L$^{-1}$) was performed by bulk electrolysis using Ti/Pt and Ti/Pt-SnSb anodes. Firstly, experiments with single flow cells were conducted in order to evaluate the performance of each one of the anode materials. Then, tests with assembling of electrochemical flow cells were accomplished. The efficacy of the oxidation process was followed by colour decay, COD removal, current efficiency and energy consumption.

#### IX.3.2.1 Single flow cells

Figure IX.3a and Figure IX.3b show the effect of the current density, *j*, on colour decay during the EO of the synthetic dye at 25 °C, using Ti/Pt and Ti/Pt-SnSb anodes, respectively. In all experiments, the colour removal was almost totally achieved independently of the *j* used. This behaviour was established from the visible spectra of the AM dye (inset Figure IX.3a and Figure IX.3b) for each anode, where the bands of absorbance decreased over time by applying 30 mA cm$^{-2}$, meaning colour reduction. The peak of maximum absorption occurred in the visible light region at 524 nm which is directly related to the colour of the solution due to the chromophore group of –N=N– present in the structure of the dye. The intensity of this peak continuously diminished resulting in 97.5–99.4 % of colour decay after 360 min of treatment. Weaker peaks that arose between 270 and 350 nm are commonly related to aromatic rings and also disappeared over time. These outcomes may indicate that in the initial treatment stage there are mechanisms promoting the dye oxidation to more simple organic compounds (aromatic or aliphatic intermediates) via the breaking of the chromophore group or even its mineralisation into $CO_2$ and $H_2O$ [19,35,36].

Furthermore, when an increase on the *j* was attained, a slight improvement was achieved on colour removal rate for both anodes (Figure IX.3a and Figure IX.3b). This behaviour suggests that the dye degradation occurs by direct anodic oxidation and by its reaction with $^{\bullet}OH$ radicals electrogenerated on the surface of the electrode (indirect oxidation) [28]. As long as *j* rises more radicals may become available to attack the chromophore group of the dye, fragmenting it and yielding other more simple organic compounds.

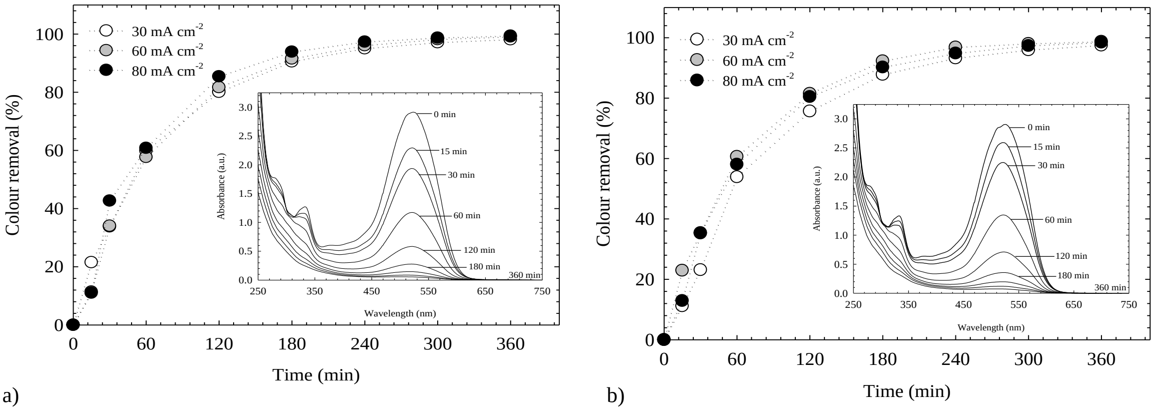

a) b)

**Figure IX.3. Effect of the current density on colour removal over time with Ti/Pt (a) and Ti/Pt-SnSb (b) anodes. Insets: Absorbance band evolution over time by employing Ti/Pt (a) and Ti/Pt-SnSb (b) electrodes at 30 mA cm$^{-2}$. Operating conditions: Individual flow cell, 100 mg L$^{-1}$ of amaranth dye, 20 g L$^{-1}$ of $Na_2SO_4$, flow rate=250 L h$^{-1}$, T=25 °C.**

Figure IX.4 displays COD removal as a function of time for Ti/Pt and Ti/Pt-SnSb anodes by applying different *j*. Contrary to colour removal, lower COD removal efficiencies were achieved. This behaviour suggests that the oxidation of the dye occurs by its fragmentation (elimination of the chromophore group as a first stage of the process) to different by-products which are more difficult to be degraded or by favouring secondary reactions, such as o.e.r. In the former case, oxidation intermediates can favour the growth of an adherent passivating film on the anode surface that poisoned the electrode, resulting in a low COD depletion and the rapid decrease of the reaction rate, and consequently, decreasing the current efficiency. If the oxidation intermediates are aliphatic acids, these are quite stable against further attack at these electrodes, limiting the efficacy of the EO approach. Meanwhile, when secondary reactions are favoured, great part of the current applied during the process is spent on undesired reactions, decreasing the current efficiency. Another important feature that can be observed from Figure IX.4 is that, lower organic matter was removed at Ti/Pt than those achieved for Ti/Pt-SnSb at different *j*.

In Figure IX.4a, a COD removal rise is reached, when an increase in *j* is attained from 30 to 60 mA cm$^{-2}$ (from 18.5 % to 46 %, respectively) at Ti/Pt electrode. Conversely, at higher *j* (80 mA cm$^{-2}$), the efficiency on the COD removal decreases significantly, up to 5.4 %. These figures mean that the parasitic reactions that auto-consumed $^{\bullet}$OH radicals are favoured over the EO of dye, such as the $O_2$ evolution, as shown by the potentiodynamic measurements in Figure IX.2a [28,29]. Additionally, the rapid conversion of AM dye to by-products at 30 and 60 mA $cm^{-2}$ decreases the electrode activity. This can be due to deposition of aromatic polymeric products on the electrode surfaces, limiting its oxidation power efficacy [28,30,35]. The last assumption is supported by the electrochemical measurements (cyclic voltammetry and polarisation curves, see Figure IX.1a and Figure IX.2a) where, at these *j* values, when the dye was added to the solution, the current density at a given potential in the region of supporting electrolyte decomposition decreased, meaning the inhibition for the o.e.r. due to the partial deactivation of the active sites on the Ti/Pt surface. However, at 60 mA $cm^{-2}$, there is probably a high generation of $^{\bullet}$OH radicals (Equation (IX.12)) and persulfate species (resulting from the oxidation of the electrolyte–Equation (IX.12)) [8] that favours the increase of AM degradation.

$$2SO_4^{2-} \rightarrow S_2O_8^{2-} + 2e^- \qquad \textbf{(IX.12)}$$

Concerning to the Ti/Pt-SnSb anode (Figure IX.4b), organic matter removal (in terms of COD) had a steady rose over time as well as this elimination improved in respect to the figures obtained with Ti/Pt. In fact, COD abatement was about 70.3 %, 55.1 % and 27.5 % at Ti/Pt-SnSb electrode by applying 30, 60 and 80 mA $cm^{-2}$, respectively; obtaining modest values of current efficiency (Figure IX.4b, inset) with the increase in *j*. This behaviour may be due to the enhancement of the o.e.r. during the EO at high values of current density, restraining the oxidation of organic compounds. Furthermore, this statement is in accordance with the polarisation curves (Figure IX.2b) where the oxidation of AM dye was firstly achieved than the electrolyte, at lower *j* (below 30 mA $cm^{-2}$), suggesting that an efficient production of $^{\bullet}$OH radicals improves the oxidation of AM dye in solution, while at higher *j* (above 30 mA $cm^{-2}$), the mediated oxidation via $^{\bullet}$OH radicals is in competition with o.e.r.

From the insets in the Figure IX.4a and Figure IX.4b, it has been observed that modest current efficiencies (4.4–0.4 %) were obtained by using Ti/Pt-SnSb electrode. Nevertheless, when Ti/Pt anode was employed, less than 1 % of current efficiency was achieved (0.1–0.9 %) by applying different *j*. It is important to note that, in the latter case, when an increase in *j* is attained from 30 to 60 mA $cm^{-2}$, current efficiency goes from 0.8 % to 0.9 %. After that, at 80 mA $cm^{-2}$, the efficiency decreases significantly, up to 0.1 %. This is probably due to the $O_2$ evolution at higher *j* (see, potentiodynamic measurements reported in the Figure IX.2a). Likewise, Ti/Pt is considered an active anode in which $^{\bullet}$OH radicals are chemically adsorbed, thus presenting lower reactivity and favouring the electrochemical conversion of the pollutant instead of its total mineralisation. Meanwhile, Ti/Pt-SnSb anode showed a partially non-active character due to the fact that on its surface, the electrogenerated $^{\bullet}$OH are weakly adsorbed and consequently, more reactive than those produced on Ti/Pt surface, promoting the complete mineralisation of the dye to $CO_2$, $H_2O$ and inorganic species [1]. Therefore, these results showed that the intensification of the COD removal and the average of current efficiency are affected by the nature of the electrode as well as current density.

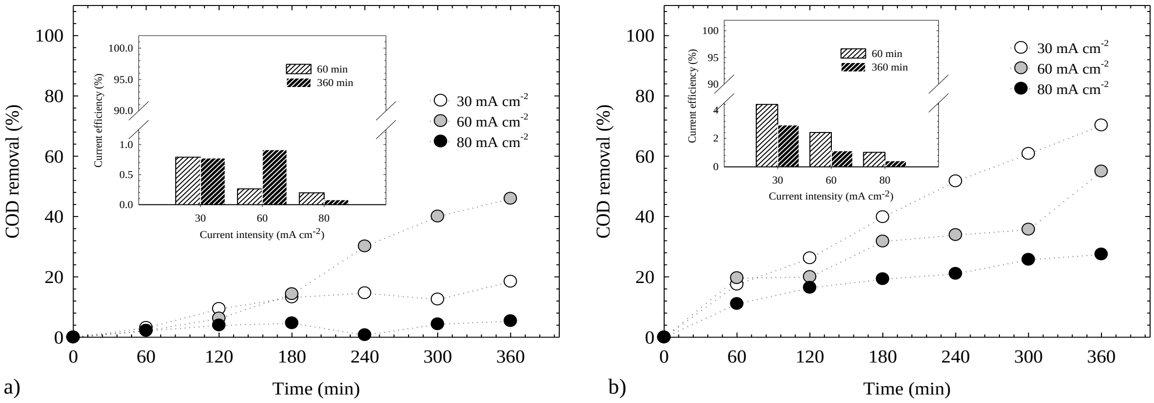

**Figure IX.4. Effect of the applied current density on COD removal over time with Ti/Pt (a) and Ti/Pt-SnSb (b) anodes. Insets: Comparison of the current efficiency in each current density for the Ti/Pt (a) and Ti/Pt-SnSb (b) electrodes. Operating conditions: Individual flow cell, 100 mg $L^{-1}$ of amaranth dye, 20 g $L^{-1}$ of $Na_2SO_4$, flow rate=250 L $h^{-1}$, T=25 °C, current densities=30, 60 and 80 mA $cm^{-2}$.**

Moreover, the estimation of the energy consumption (EC) is also an important parameter for industrial purposes. Thus, these values were estimated and reported in Table IX.2 for both electrodes after 360 min of treatment. As can be observed, an increase on the *j*, intensified significantly the energy consumption. This behaviour is also related to the energy that is mostly consumed by side reactions such as o.e.r. when higher *j* are used [28,37,38].

**Table IX.2. Energy consumption (kWh $m^{-3}$) for different applied current density (*j*) after 360 min of electrolysis using the single flow cells with Ti/Pt and Ti/Pt–SnSb.**

| **Single flow cell** | **Energy consumption (kWh $m^{-3}$)** | | |
|---|---|---|---|
| | ***j*=30 mA $cm^{-2}$** | ***j*=60 mA $cm^{-2}$** | ***j*=80 mA $cm^{-2}$** |
| Ti/Pt | 78.2 | 219.3 | 354.1 |
| Ti/Pt-SnSb | 71.6 | 206.6 | 314.8 |

Regarding the results obtained for each single flow cell, a new system arrangement - electrochemical cells in series was explored in order to intensify the efficiency of organic pollutants elimination and reduce the energy requirements. In this new configuration, values of 30 and 60 mA $cm^{-2}$ were considered to be applied because when higher *j* was employed (*j*=80 mA $cm^{-2}$), the efficiency of the treatment decreased meaningfully.

### IX.3.2.2 Electrochemical cells in series

In order to enhance the oxidation rate of pollutants, electrochemical cells in a serial mode were tested by using two different electrode combinations, Ti/Pt+Ti/Pt-SnSb and Ti/Pt-SnSb+Ti/Pt. The current densities used were 30+30 mA cm$^{-2}$, 60+60 mA cm$^{-2}$, 30+60 mA cm$^{-2}$ and 60+30 mA cm$^{-2}$ where the first *j* is applied to the first cell while the second value is imposed to the follow electrochemical cell.

Figure IX.5a and Figure IX.5b present the colour removal over time for the electrochemical cells in series (Ti/Pt+Ti/Pt-SnSb and Ti/Pt-SnSb+Ti/Pt, respectively) by applying the four different *j* combinations. Results clearly showed that, colour decay was completely achieved in short times, independently of the electrode and *j* arrangement. As can be observed from the insets of Figure IX.5a and Figure IX.5b, at 30+30 mA cm$^{-2}$, the absorbance was reduced satisfactorily after 180 min of treatment, 96.7 % and 97.1 %, respectively. A similar trend was attained for the other experimental combinations (data not shown). All configurations with electrochemical cells in a serial mode allowed almost complete colour removal in less time (about 180 min less) than when single flow cell systems were used (Figure IX.3). This behaviour reveals that the recirculation of the pollutant by the two cells enhances the efficiency of the process when compared to the previous cases where just one cell was used.

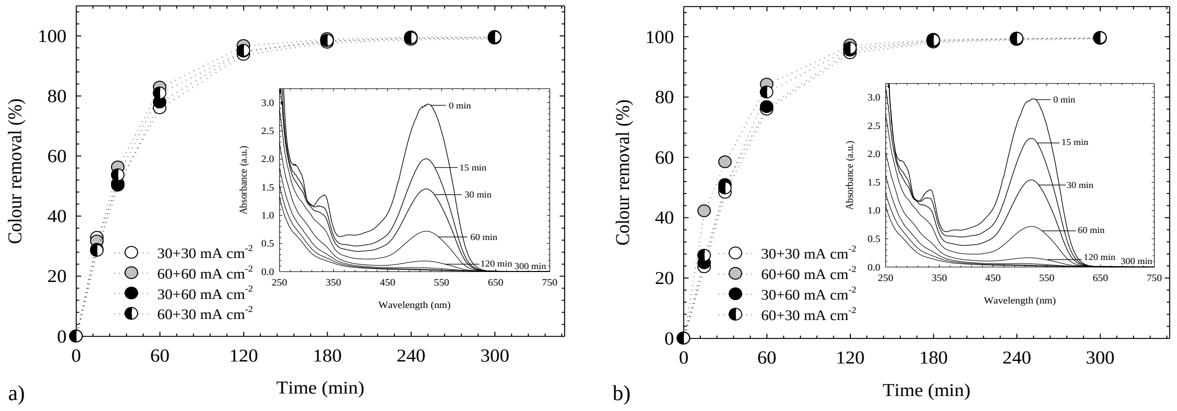

**Figure IX.5. Effect of the applied current density on colour removal over time with Ti/Pt+Ti/Pt-SnSb (a) and Ti/Pt-SnSb+Ti/Pt (b) anodes. Insets: Absorbance band evolution over time by employing Ti/Pt+Ti/Pt-SnSb (a) and Ti/Pt-SnSb+Ti/Pt (b) electrodes at 30+30 mA cm$^{-2}$. Operating conditions: Assembling of flow cells in series, 100 mg L$^{-1}$ of amaranth dye, 20 g L$^{-1}$ of $Na_2SO_4$, flow rate=250 L h$^{-1}$, T=25 °C.**

Considering the removal of organic matter (Figure IX.6a), the electrochemical cells in serial mode with Ti/Pt+Ti/Pt-SnSb at 60+60 mA cm$^{-2}$ led to the highest COD removal (≈74 %) after 300 min of reaction followed by 60+30 mA cm$^{-2}$, 30+30 mA cm$^{-2}$ and 30+60 mA cm$^{-2}$ with 43.6 %, 42.1 % and 38.1 %, respectively. By the results for single cell with Ti/Pt at 30 mA cm$^{-2}$, it was stated that may have occurred the passivation of the anode. Nevertheless, the degradation of the AM dye was significantly intensified (42.1 % of COD removal) through the use of the Ti/Pt+Ti/Pt-SnSb set at 30+30 mA cm$^{-2}$, avoiding partially the deactivation of the anode surface. Conversely, with Ti/Pt-SnSb+Ti/Pt anodes at 30+30 mA cm$^{-2}$ (Figure IX.6b), 21.8 % of COD removal was obtained after 300 min of treatment. This behaviour is probably due to a poor removal of dye at Ti/Pt-SnSb anode surface, generating by-products that are difficult to be subsequently eliminated by Ti/Pt electrode. In addition, this set at 60+30 mA cm$^{-2}$ led to a steadily COD removal (45.4 %) up to 120 min, remaining almost constant thereafter.

Generally speaking, COD removal efficiencies, at the end of the electrolysis, for both serial cells combinations were mostly superior to those obtained when single cells were used. Then, the results clearly demonstrated that the EO approach is enhanced in both compartments with different electrocatalytic materials at the same/different current densities with recirculation, favouring a variety of mechanisms during the this process.

Further than the colour and COD depuration, energetic consumption is also an important parameter to be analysed. Insets of Figure IX.6 represent the energy consumption (EC) and COD removal values obtained after 300 min of reaction time, for the four current densities combinations. As can be observed, EC rose as the *j* increased (30+30 mA cm$^{-2}$ to 60+60 mA cm$^{-2}$). In the inset of Figure IX.6a, the highest organic matter removal with Ti/Pt+Ti/Pt-SnSb (73.7 %) corresponded to the highest energy consumption with 304.3 kWh m$^{-3}$ by applying 60 mA cm$^{-2}$ to both cells. At this current density, the Ti/Pt anode promotes the electrogeneration of $^{\bullet}$OH radicals and persulfate species to oxidise the AM dye, increasing COD decay, while at Ti/Pt-SnSb, the by-products formed in the first cell were more easily removed. Conversely, the combinations 30+30 mA cm$^{-2}$, 30+60 mA cm$^{-2}$ and 60+30 mA cm$^{-2}$ led to similar COD removals (38.1–43.6 %), requiring different energy consumptions, whereas the combination of *j* at 30+30 mA cm$^{-2}$ attained the lowest energy consumption of 110.9 kWh m$^{-3}$.

In the case of the electrochemical cells in a serial mode with Ti/Pt-SnSb+Ti/Pt electrodes (inset of Figure IX.6b), highest COD removals were achieved at 60+30 mA cm$^{-2}$ (51.1 %) and 30+60 mA cm$^{-2}$ (47.5 %) with 207.3 and 209.9 kWh m$^{-3}$, respectively. Meanwhile, the *j* combination of 30+30 and 60+60 mA cm$^{-2}$ accomplished lower COD removals of about 21.8 % and 36.7 % with distinct energy requirements of 113 and 303.3 kWh m$^{-3}$, respectively.

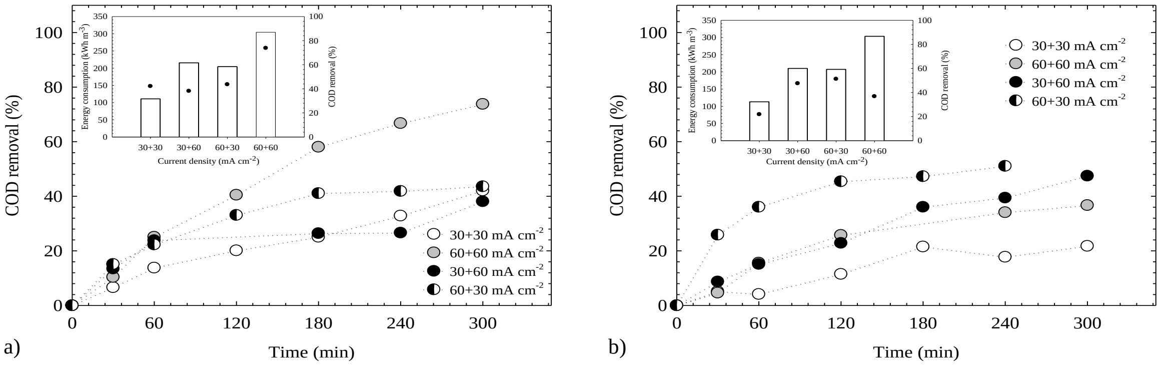

**Figure IX.6. Effect of the applied current density on COD removal over time with Ti/Pt+Ti/Pt-SnSb (a) and Ti/Pt-SnSb+Ti/Pt (b) anodes. Inset: Effect of the combinations of current density in energy consumption at the final COD removal values (black circles) after 300 min of treatment time with Ti/Pt+Ti/Pt-SnSb (a) and Ti/Pt-SnSb+Ti/Pt (b) anodes. Operating conditions: Assembling of flow cells in series, 100 mg L$^{-1}$ of amaranth dye, 20 g L$^{-1}$ of Na$_2$SO$_4$, flow rate=250 L h$^{-1}$, T=25 °C, current densities=30+30, 60+60, 30+60 and 60+30 mA cm$^{-2}$.**

### IX.3.2.3 Effect of electrochemical arrangements (single or assembling of cells in series) in energy consumption

Figure IX.7 represents the energy consumption for the electrochemical treatment of the AM dye necessary to remove approximately 90 % of the pollutant colour by using single electrochemical flow cells and electrochemical cells in a serial mode. Almost all single flow cells experiments attained this removal value until 180 min of electrolysis, except the one with Ti/Pt-SnSb at 30 mA cm$^{-2}$ which took 240 min. In the case of the electrochemical cells in series, it was attained after 120 min for every trial.

Comparing the energy requirements between electrochemical cells in serial mode and single flow cells (Figure IX.7), the power consumption for the former ones seems analogous or even higher (44.9–124.9 kWh m$^{-3}$) than those obtained by using single arrangements (39.2–110.9 kWh m$^{-3}$). However, when the energy required by assembling electrochemical cells in series is compared to the sum of energy consumed by each cell separately, it is possible to conclude that the cells in series spent lower electrical energy, obtaining in several cases, higher COD removals than those achieved at single flow cell arrangements. The obtained energy consumption values are in accordance to those referred in literature by Brillas and Matínez-Huitle [1], 1.1–163 kWh m$^{-3}$. Regarding industrial sources, the energy cost is 0.12 € kWh$^{-1}$. Thus, the treatment cost may vary between 4.7–13.3 € m$^{-3}$ for individual cells, 5.4–15.0 € m$^{-3}$ for the assembling of two cells in series and 10.4–25.8 € m$^{-3}$ for the sum of individual cells.

Another important remark is that, although the energy consumption for the individual cells seems to depend on the applied *j* rather than on the nature of the electrode; this last parameter strongly affects the COD removals. Furthermore, the energy consumption for the electrochemical cells in a serial mode was also similar between pairs of experiments, independently of the order of the anodes in the system since the same *j* was maintained for each material type. For example, the energy consumption for the tests Ti/Pt+Ti/Pt-SnSb (30+60 mA cm$^{-2}$) and Ti/Pt-SnSb+Ti-Pt (60+30 mA cm$^{-2}$) were 88.3 and 84.6 kWh m$^{-3}$, respectively (Figure IX.7c and Figure IX.7d). Therefore, the most suitable arrangement choice will depend on the COD value to be achieved, the electrolysis time and the energy consumption. For example, at 240 min the cell with Ti/Pt-SnSb anode at 30 mA cm$^{-2}$ reached 51.7 % of COD removal consuming 47.9 kWh m$^{-3}$, while the system with Ti/Pt-SnSb+Ti/Pt (60+30 mA cm$^{-2}$) can remove 45.4 % of COD in 120 min with 84.6 kWh m$^{-3}$.

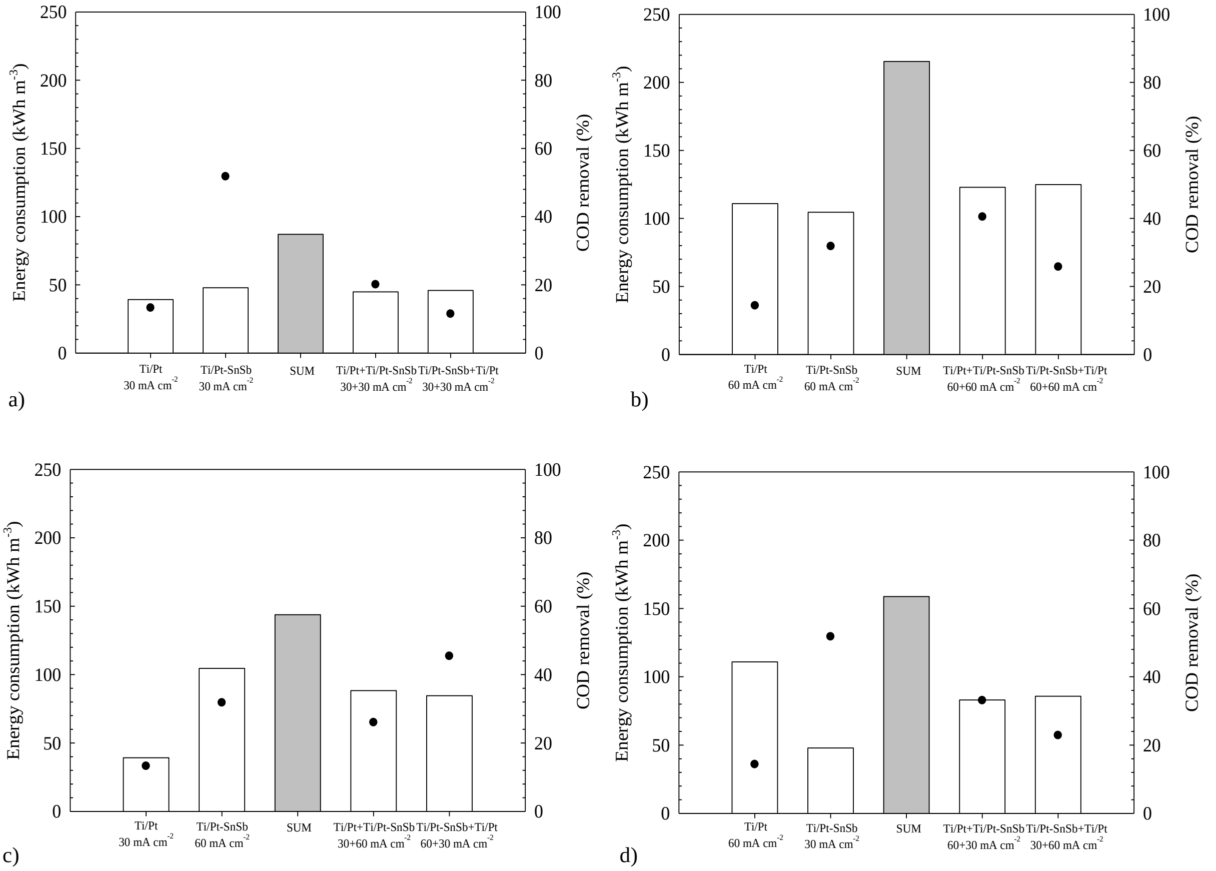

**Figure IX.7. Energy consumption to achieve approximately 90 % of colour removal using single and an assembling of electrochemical flow cells in series, and respectively COD removal values (black circles). (a) Ti/Pt at 30 mA cm$^{-2}$ and Ti/Pt-SnSb at 30 mA cm$^{-2}$, (b) Ti/Pt at 60 mA cm$^{-2}$ and Ti/Pt-SnSb at 60 mA cm$^{-2}$, (c) Ti/Pt at 30 mA cm$^{-2}$ and Ti/Pt-SnSb at 60 mA cm$^{-2}$ and (c) Ti/Pt at 60 mA cm$^{-2}$ and Ti/Pt-SnSb at 30 mA cm$^{-2}$. SUM corresponds to the sum of energy consumption applying both single flow cells. Operating conditions: Individual flow cell and an assembling of flow cells in series, 100 mg L$^{-1}$ of amaranth dye, 20 g L$^{-1}$ of $Na_2SO_4$, flow rate=250 L h$^{-1}$, T=25 °C, current densities=30 and 60 mA cm$^{-2}$.**

### IX.3.3 EFFECT OF THE NON-ACTIVE ANODE IN AN ASSEMBLING OF FLOW CELLS IN SERIES

As low/moderate COD removals were achieved by using electrochemical cells in a serial mode with Ti/Pt and Ti/Pt-SnSb anodes, new sets of experiments were performed with a non-active anode, the boron doped-diamond (Nb/BDD), in order to improve the electrochemical abatement and the efficiency of the process. In addition, bearing in mind the COD removals previously obtained with Ti/Pt and Ti/Pt-SnSb electrodes in single flow cells, the best performances were obtained with Ti/Pt-SnSb anode; thus this material was selected to be part of the new cell arrays in a serial mode (Ti/Pt-SnSb+Nb/BDD and Nb/BDD+Ti/Pt-SnSb).

Figure IX.8 displays colour removal over time for both arrangements at four different *j* combinations 30+30 mA cm$^{-2}$, 60+60 mA cm$^{-2}$, 30+60 mA cm$^{-2}$ and 60+30 mA cm$^{-2}$. As can be observed, the decolourisation was considerably improved when Nb/BDD material was included in the electrochemical cells in series, reducing significantly the electrolysis time. Using cell arrays in a serial mode (Ti/Pt-SnSb+Nb/BDD and Nb/BDD+Ti/Pt-SnSb), colour decay was totally accomplished between 30 and 180 min, in both cases. The insets of Figure IX.8a and Figure IX.8b illustrate the fast disappearance of the absorbance band, which is related to the chromophore group, for the experiments at 30+30 mA cm$^{-2}$ with Ti/Pt-SnSb+Nb/BDD and Nb/BDD+Ti/Pt-SnSb anodes, respectively. In these serial combinations of cells, it seems that when Nb/BDD anode is used at 60 mA cm$^{-2}$, it promotes a rapid cleavage of the chromophore group, intensifying the efficiency of the colour removal, while the cell with Ti/Pt-SnSb electrocatalytic material acts as a polishing step of wastewater, finalising the elimination of discolouration treatment. The improvement on the colour removal with arrays in a serial mode is consistent with the results obtained for the individual cells using BDD anode because an increase in the applied *j* improves the decolourisation rate (data not shown).

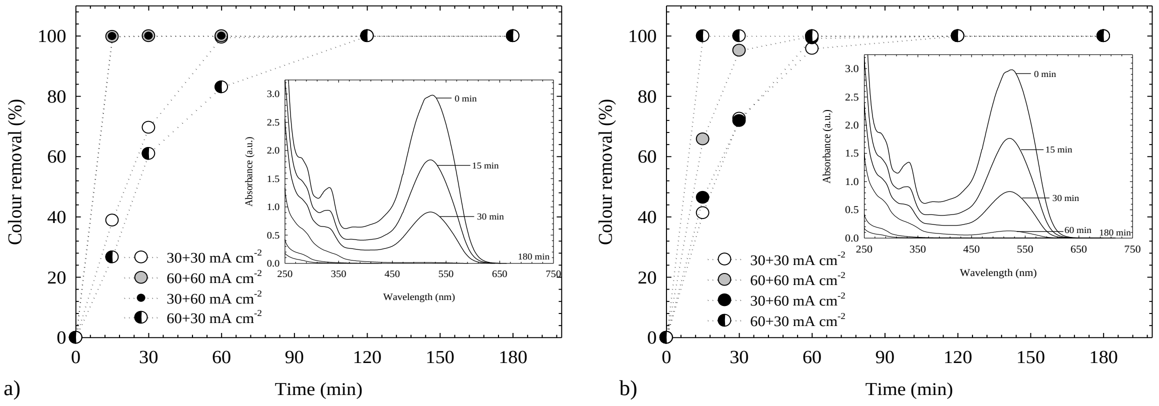

**Figure IX.8. Effect of the applied current density on colour removal over time with Ti/Pt-SnSb+Nb/BDD (a) and Nb/BDD+Ti/Pt-SnSb (b) anodes. Insets: Absorbance band evolution over time by employing Ti/Pt-SnSb+Nb/BDD (a) and Nb/BDD+Ti/Pt-SnSb (b) electrodes at 30+30 mA cm$^{-2}$. Operating conditions: Assembling of flow cells in series, 100 mg L$^{-1}$ of amaranth dye, 20 g L$^{-1}$ of $Na_2SO_4$, flow rate=250 L h$^{-1}$, T=25 °C.**

Figure IX.9 depicts the energy consumption (EC) and the time required to remove the maximum colour of the AM dye by using single (97.5–100 %) and arrays in a serial mode (100 %) systems. As can be observed, the electrolysis time for colour decay diminished with the use of BDD material, in single and serial arrangements. The energy consumption in single flow cells seems to depend on the nature of the electrode material as well as on the applied *j*, since the EC values achieved for Nb/BDD were lower (14.3–39.5 kWh m$^{-3}$) than those obtained for Ti/Pt-SnSb (71.6–206.6 kWh m$^{-3}$) during the AM dye degradation. While colour removal globally increased with *j*, in its turn, COD abatement was mainly more efficient for the experiments when 30 mA cm$^{-2}$ was applied by using single flow cells. This behaviour indicates that the electrical charge supplied is not efficiently employed for the degradation of organic matter but it is spent in parasitic reactions such as o.e.r.

In some cases when serial cell combinations were used, the EC also appeared to be higher than the ones attained for the individual ones. However, if both individual flow cells were used to achieve similar COD removals as the serial mode arrangement, higher energy requirements would be necessary. In fact, the power consumption required by electrochemical cells in serial mode are lower than those attained with the use of Ti/Pt-SnSb and Nb/BDD anodes (sum of EC for the use of electrochemical cells independently).

Another interesting feature observed from Figure IX.9 is that COD removal values of the serial combination with Ti/Pt-SnSb and Nb/BDD are higher when compared to ones of the previous serial mode arrangement by using Ti/Pt and Ti/Pt-SnSb anodes (see, Figure IX.7), in less electrolysis time. It is possible to observe in Figure IX.9a that similar COD removal values can be achieved at different electrolysis times. For the cells in series, the power consumption was quite comparable (78 kWh $m^{-3}$) or inferior (52.5 kWh $m^{-3}$) to the individual cell with Ti/Pt-SnSb (71.6 kWh $m^{-3}$). In the case of Ti/Pt-SnSb+Nb/BDD at 60+60 mA $cm^{-2}$ (Figure IX.9), after 30 min of oxidation, a COD removal value of 55.1 % was achieved with an energy consumption of 37.3 kWh $m^{-3}$. This arrangement allowed the same or higher COD degradations when compared to the experiments involving single cells with Ti/Pt-SnSb at 60 mA $cm^{-2}$ (55 %) or Nb/BDD at 60 mA $cm^{-2}$ (23.3 %), respectively; but with a shorter oxidation time of 30 min. In Figure IX.9c, as can be seen, the assembling of electrochemical cells in series consumed low energy (≈ 26 kWh $m^{-3}$) if related to their respectively individual cell (Ti/Pt-SnSb at 30 mA $cm^{-2}$ and Nb/BDD at 60 mA $cm^{-2}$). In addition, it was also possible to verify that the test with Nb/BDD+Ti/Pt-SnSb at 60+30 mA $cm^{-2}$ attained 3/4 of the COD removal achieved by Ti/Pt-SnSb at 30 mA $cm^{-2}$ in just 30 min, rather than the 360 min required by the individual cell. Among the tests performed, the maximum COD depletion obtained was 74.4 % for the Nb/BDD+Ti/Pt-SnSb at 30+60 mA $cm^{-2}$ in 120 min of electrolysis with 96.8 kWh $m^{-3}$ of energy consumed (Figure IX.9d).

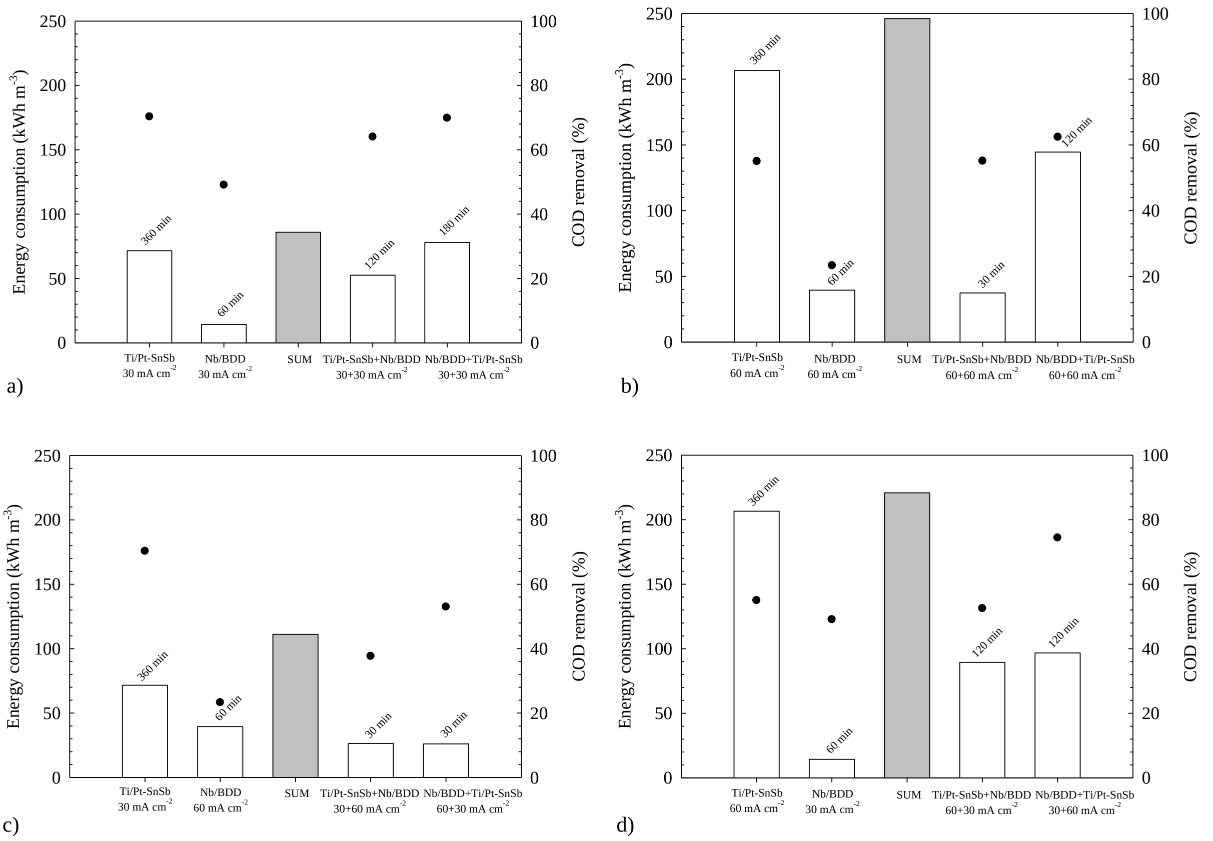

**Figure IX.9. Energy consumption to achieve the maximum colour removal (black circles) using single and an assembling of electrochemical flow cells in series. (a) Ti/Pt-SnSb at 30 mA $cm^{-2}$ and Nb/BDD at 30 mA $cm^{-2}$, (b) Ti/Pt-SnSb at 60 mA $cm^{-2}$ and Nb/BDD at 60 mA $cm^{-2}$, (c) Ti/Pt-SnSb at 30 mA $cm^{-2}$ and Nb/BDD at 60 mA $cm^{-2}$ and (c) Ti/Pt-SnSb at 60 mA $cm^{-2}$ and Nb/BDD at 30 mA $cm^{-2}$. SUM corresponds to the sum of energy consumption applying both single flow cells. Operating conditions: Individual flow cell and an assembling of flow cells in series, 100 mg $L^{-1}$ of amaranth dye, 20 g $L^{-1}$ of $Na_2SO_4$, flow rate=250 L $h^{-1}$, T=25 °C, current densities=30 and 60 mA $cm^{-2}$.**

These results clearly show that the use of Nb/BDD anode enhances the efficiency of the process. This might be due to its nature, since it is a non-active anode meaning that the generation of physisorbed BDD($^{\bullet}$OH) radicals characterised by a weak electrode–hydroxyl radical interaction results in high ability to completely mineralise the organic compounds. It should be stressed that the treatment cost using the assembling of cells in series varied between 3.1–17.4 € m$^{-3}$, while for the individual cells was 1.7–24.8 € m$^{-3}$, which would lead to that the sum of the individual cells varied between 0.3–29.5 € m$^{-3}$. Thus, generally speaking, the assembling of electrochemical cells can achieve lower operating costs when compared to the sum of the individual ones to reach the same COD degradation.

### *Final remarks*

The best performances of EO, in terms of COD removal and energy power, using an assembling of electrochemical flow cells in series are summarised in Table 3. As can be observed, the experiment with less electric power demand (26 kW m$^{-3}$) was the Nb/BDD+Ti/Pt-SnSb at 30+30 mA cm$^{-2}$ with a COD removal of 69.9 %. When power consumption was duplicated (52.2 kW m$^{-3}$) or even triplicated (74.7 kW m$^{-3}$), the removal of COD decreased 24–27 % for the Nb/BDD+Ti/Pt-SnSb at 60+30 mA cm$^{-2}$ and Ti/Pt-SnSb+Nb/BDD at 60+30 mA cm$^{-2}$ tests, respectively. This reduction in organic load decay is in accordance with the removals obtained with the increasing of *j* for individual cells of Nb/BDD and Ti/Pt-SnSb. In the case of Nb/BDD+Ti/Pt-SnSb at 60+30 mA cm$^{-2}$ trial, although there was a growth of 6 % in COD removal, this rise promoted an increase of 1.9 times the power consumption compared to the baseline experience. Regarding, the experiment with both active anodes, the lowest COD decay with 45.4 % removal was achieved by it.

It is noteworthy mentioning that tests using Nb/BDD at 30 mA cm$^{-2}$ in the first position of the serial mode allowed better removal efficiencies; while a higher *j* led to lower COD removals and higher energy consumption per hour. Therefore, the most appropriate experiment to treat solutions containing AM dye is Nb/BDD+Ti/Pt-SnSb at 30+30 mA cm$^{-2}$.

**Table IX.3. Summary of the best experiments of assembling of electrochemical flow cells in series according to electric power demand and COD removal.**

| **Electric power demand (kW m$^{-3}$)** | **COD removal (%)** | **Cell combination** | ***j* (mA cm$^{-2}$)** |
|---|---|---|---|
| 26 | 69.9 | Nb/BDD+Ti/Pt-SnSb | 30+30 |
| 42.3 | 45.4 | Ti/Pt-SnSb+Ti/Pt | 60+30 |
| 48.4 | 74.4 | Nb/BDD+Ti/Pt-SnSb | 30+60 |
| 52.2 | 53 | Nb/BDD+Ti/Pt-SnSb | 60+30 |
| 74.7 | 55.1 | Ti/Pt-SnSb+Nb/BDD | 60+60 |

## IX.4 CONCLUSIONS

The electrochemical depuration of the AM dye from a synthetic effluent was studied through the application of individual flow cells or an assembling of electrochemical flow cells in series employing active and non-active anodes.

The efficacy of the EO process was mainly affected by the nature of the anode since this parameter determines how easily the $^{\bullet}$OH radicals are generated, promoting the elimination of the organic compounds. In addition, the current density also influenced the process by controlling the quantity of electrogenerated radicals and the energy consumed. Among the experiments with single electrochemical flow cells with active anodes, the Ti/Pt-SnSb at 30 mA cm$^{-2}$ led to highest COD removal of 70.3 %, 97.5 % of colour removal and energy consumption of 71.6 kWh m$^{-3}$, after 360 min of reaction.

Regarding the electrochemical cells in a serial mode, complete colour removal was achieved in about 180 min less when compared to single flow cell systems. Furthermore, in serial combinations, the wastewater treatment was even affected by the order of anodes in the system as well as by the current densities applied to each one of the cells, leading to higher COD removals than in individual cells. The Nb/BDD+Ti/Pt-SnSb arrangement at 30 + 30 mA cm$^{-2}$, after 180 min of reaction, achieved the optimum combination of results, with 100 % and 69.9 % of colour and COD removals, respectively, as well as 78 kWh m$^{-3}$ of energy consumed. Therefore, this arrangement revealed to be an efficient alternative pre-treatment to the colour and COD removals of dye effluents. Although the main goal of this work was the use of cheaper anode materials for the treatment of wastewaters containing dyes, it was found that the use of Nb/BDD becomes attractive to reduce the time of the process, keeping it as an interesting material.

Finally, it is important to highlight that the electrochemical cells in series arrangements are still a new environmental application under study (this arrangement is mainly used in electro-synthesis [38]), therefore more experiments will be established in order to understand how the efficiency of the process can be improved and consequently, obtain a significant reduction on the treatment time and energy consumption.

## ACKNOWLEDGMENTS

The authors, Ana S. Fajardo and Rui C. Martins gratefully acknowledge the Fundação para a Ciência e Tecnologia, for financial support under the Doc grant (SFRH/BD/87318/2012) and the IFCT 2014 programme (IF/00215/2014) with financing from the European Social Fund and the Human Potential Operational Programme, respectively. Financial support from National Council for Scientific and Technological Development (CNPq–446846/2014-7 Brazil) is gratefully acknowledged.

## REFERENCES

[1] Brillas E, Martínez-Huitle CA (2015) Decontamination of wastewaters containing synthetic organic dyes by electrochemical methods. An up dated review. Appl. Catal. B: Environ. 166-167: 603–643.

[2] Robinson T, McMullan G, Marchant R, Nigam P (2001) Remediation of dyes in textile effluent: a critical review on current treatment technologies with a proposed alternative. Bioresour. Technol. 77: 247–255.

[3] Forgacs E, Cserháti T, G Oros (2004) Removal of synthetic dyes from wastewaters: a review. Environ. Int. 30: 953–971.

[4] Martínez-Huitle CA, Andrade LS (2011) Electrocatalysis in wastewater treatment: recent mechanism advances. Quim. Nova 34: 850–858.

[5] Anglada A, Urtiaga A, Ortiz I (2009) Contributions of electrochemical oxidation to waste-water treatment: fundamentals and review of applications. J. Chem. Technol. Biotechnol. 84: 1747–1755.

[6] Oturan MA, Aaron JJ (2014) Advanced Oxidation Processes in Water/Wastewater Treatment: Principles and Applications. A Review, Environ. Sci. Technol. 44 (23): 2577–2641.

[7] Fóti G, Gandini D, Comninellis C, Perret A, Haenni W(1999) Oxidation of organics by intermediates of water discharge on $IrO_2$ and synthetic diamond anodes Electrochem. Solid-State Lett. 2: 228–230.

[8] Panizza M, Cerisola G (2009) Electrochemical degradation of gallic acid on a BDD anode. Chemosphere 77: 1060–1064.

[9] Marselli B, Garcia-Gomez J, Michaud PA, Rodrigo MA, Comninellis C (2003) Electrogeneration of hydroxyl radicals on boron-doped diamond electrodes. J. Electrochem. Soc. 150: D79–D83.

[10] Fóti G, Comninellis C (2004) Electrochemical oxidation of organics on iridium oxide and synthetic diamond based electrodes, in: E. White, B.E. Conway, C.G. Vayenas, M.E. Gamboa-Adelco (Eds.), Modern Aspects of Electrochemistry, Springer US, New York, 87–130.

[11] Comninellis C, Kapalka A, Malato S, Parsons SA, Poulios I, Mantzavinos D (2008) Advanced oxidation processes for water treatment: advances and trends for R&D, J. Chem. Technol. Biotechnol. 83: 769–776.

[12] Cavalcanti EB, Garcia-Segura S, Centellas RF, Brillas E (2013) Electrochemical incineration of omeprazole in neutral aqueous medium using a platinum or boron-doped diamond anode: Degradation kinetics and oxidation products. Water Res. 47: 1803–1815.

[13] Antonin VS, Santos MC, Garcia-Segura S, Brillas E (2015) Electrochemical incineration of the antibiotic ciprofloxacin in sulfate medium and synthetic urine matrix, Water Res. 83: 31–41.

[14] Martínez-Huitle CA, Santos EV, Araújo DM, Panizza M (2012) Applicability of diamond electrode/anode to the electrochemical treatment of a real textile effluent, J. Electroanal. Chem. 674: 103–107.

[15] Bogdanowicz R, Fabiańska A, Golunski L, Sobaszek M, Gnyba M, Ryl J, Darowicki K, Ossowski T, Janssens SD, Haenen K, Siedlecka EM (2013) Influence of the boron doping level on the electrochemical oxidation of the azo dyes at Si/BDD thin film electrodes. Diam. Relat. Mat. 39: 82–88.

[16] Solano AMS, Araújo CKC, Melo JV, Peralta-Hernandez JM, Silva DR, Martínez-Huitle CA (2013) Decontamination of real textile industrial effluent by strong oxidant species electrogenerated on diamond electrode: viability and disadvantages of this electrochemical technology. Appl. Catal. B: Environ. 130-131: 112–120.

[17] Xu L, Song X (2015) A novel Ti/antimony-doped tin oxide nanoparticles electrode prepared by screen printing method and its application in electrochemical degradation of C.I. Acid Red 73. Electrochim. Acta 185: 6–16.

[18] Zhang F, Feng C, Li W, Cui J, (2014) Indirect Electrochemical Oxidation of Dye Wastewater Containing Acid Orange 7 Using Ti/$RuO_2$-Pt Electrode. Int. J. Electrochem. Sci. 9: 943–954.

[19] Labiadh L, Barbucci A, Cerisola G, Gadri A, Ammar S, Panizza M (2015) Role of anode material on the electrochemical oxidation of methyl orange, J. Solid State Electr. 19: 3177–3183.

[20] Tavares MG, Silva LVA, Solano AMS, Tonholo J, Martínez-Huitle CA, Zanta CLPS (2012) Electrochemical oxidation of Methyl Red using Ti/$Ru_{0.3}Ti_{0.7}O_2$ and Ti/Pt anodes Chem. Eng. J. 204-206: 141–150.

[21] Río AI, Molina J, Bonastre J, Cases F (2009) Study of the electrochemical oxidation and reduction of C.I. Reactive Orange 4 in sodium sulphate alkaline solutions J. Hazard. Mat. 172: 187–195.

[22] Petrović MM, Mitrović JZ, Antonijević MD, Matović B, Bojić DV, Bojić AL (2015) Synthesis and characterization of new Ti/$Bi_2O_3$ anode and its use for reactive dye degradation. Mat. Chem. Phys. 158: 31–37.

[23] Panakoulias T, Kalatzis P, Kalderis D and Katsaounis A (2010) Electrochemical degradation of Reactive Red 120 using DSA and BDD anodes. J. Appl. Electrochem. 40: 1759–1765.

[24] Song S, Fan J, He Z, Zhan L, Liu Z, Chen J, Xu X (2010) Electrochemical degradation of azo dye C.I. Reactive Red 195 by anodic oxidation on Ti/$SnO_2$–Sb/$PbO_2$ electrodes. Electrochim. Acta 55: 3606–3613.

[25] Sotgiu G, Tortora L, Petrucci E (2015) Influence of surface roughening of Titanium substrate in the electrochemical activity of Manganese oxide thin film electrode in anodic oxidation of dye-containing solutions. J. Appl. Electrochem. 45: 787–797.

[26] Basha CA, Sendhil J, Selvakumar KV, Muniswaran PKA, Lee CW (2012) Electrochemical degradation of textile dyeing industry effluent in batch and flow reactor systems. Desalination 285: 188–197.

[27] Aquino JM, Rocha-Filho RC, Ruotolo LAM, Bocchi N, Biaggio SR (2014) Electrochemical degradation of a real textile wastewater using β-$PbO_2$ and DSA® anodes. Chem. Eng. J. 251: 138–145.

[28] Oliveira GR, Fernandes NS, Melo JV, Silva DR, Urgeghe C, Martínez-Huitle CA (2011) Electrocatalytic properties of Ti-supported Pt for decolorizing and removing dye from synthetic textile wastewaters. Chem. Eng. J. 168: 208–2014.

[29] Araújo CKC, Oliveira GR, Fernandes NS, Zanta CLPS, Castro SSL, Silva DR, Martínez-Huitle CA (2014) Electrochemical removal of synthetic textile dyes from aqueous solutions using Ti/Pt anode: role of dye structure. Environ. Sci. Pollut. Res. 21: 9777–9784.

[30] Rocha JHB, Gomes MMS, Santos EV, Moura ECM, Silva DR, Quiroz MA, Martínez-Huitle CA (2014) Electrochemical degradation of Novacron Yellow C-RG using boron-doped diamond and platinum anodes: Direct and Indirect oxidation. Electrochim Acta 140: 419–426.

[31] European Food Safety Authority (2010) Panel on Food Additives and Nutrient Sources added to Food (ANS), Scientific Opinion on the reevaluation of Amaranth (E 123) as a food additive on request from the European Commission. EFSA J. 8(7): 1649.

[32] Barros WRP, Franco PC, Steter JR, Rocha RS, Lanza MRV (2014) Electro-Fenton degradation of the food dye amaranth using a gas diffusion electrode modified with cobalt (II) phthalocyanine. J. Electroanal. Chem. 722-723: 46–53.

[33] Barros WRP, Steter JR, Lanza MRV, Motheo AJ (2014) Degradation of amaranth dye in alkaline medium by ultrasonic cavitation coupled with electrochemical oxidation using a boron-doped diamond anode. Electrochim. Acta 143: 180–187.

[34] Greenberg A, Clesceri L, Eaton A (1992) Standard Methods for the Examination of Water and Wastewater. American Public Health Association, Washington DC.

[35] Panizza M, Cerisola G (2007) Electrocatalytic materials for the electrochemical oxidation of synthetic dyes. Appl. Catal. B: Environ. 75: 95–101.

[36] Aquino JM, Pereira GF, RC Rocha-Filho, Bocchi N, Biaggio SR (2011) Electrochemical degradation of a real textile effluent using boron-doped diamond or β-$PbO_2$ as anode. J. Hazard. Mater. 192: 1275–1282.

[37] Martínez-Huitle CA, Ferro S, De Battisti A Electrochemical incineration of oxalic acid. Role of electrode material. Electrochim. Acta 49: 4027–4034.

[38] Martínez-Huitle CA, Rodrigo MA, Sirés I, Scialdone O (2015) Single and Coupled Electrochemical Processes and Reactors for the Abatement of Organic Water Pollutants: A Critical Review. Chem. Rev. 115: 13362–13407.

# PART D. MAIN CONCLUSIONS AND FORTHCOMING WORK

# X. GENERAL OVERVIEW AND CONCLUDING REMARKS

The main objective of this research was to study the application of the electrocoagulation (ECG) and the electrochemical oxidation (EO) processes for the depuration of two distinct types of wastewaters, phenolic and dye (simulated or real). In order to accomplish efficient solutions, laboratory trials were designed and executed. The experiments performed were grouped in two main parts comprising the ECG and EO methodologies, being divided into case studies.

According to the ECG results, it is possible to highlight that the performance of the process greatly depends on the kind of the sacrificial anode material applied (Al, Cu, Fe, Pb and Zn) for the depuration of six phenolic acids typically found in olive mill wastewaters (OMW). Among the materials studied the Zn anode was found to provide the highest removal of TPh and COD. However, the treated solution still had low biodegradability and ecological impact, detected by bio-luminescence techniques, probably due to the formation of organochlorine species and metal leaching content.

Once Zn showed to be a suitable anode material for pre-treating wastewater through ECG, this process was optimised for a simulated phenolic mixture, by testing several operating conditions such as the pH, current density (*j*), distance between electrodes, nature of electrolyte and type of cathode (SS and Zn). The medium pH and the type of electrolyte were found to be the parameters that affected most the system, since the first one determines what species are formed in the bulk medium and the second one the amount of coagulant formed. The cathode material and *j* had a less pronounced effect, while that of the distance between electrodes was quite negligible in the studied range (0.5–2.0 cm). The anode performance was accessed by four fed-batch trials, exhibiting almost constant activity during the operation time. The optimum operating conditions achieved were initial pH of the effluent equal to 3.2, current density of 25 mA cm$^{-2}$, distance between electrodes of 1.0 cm, 1.5 g L$^{-1}$ of NaCl and SS as cathode, leading to 84.2 % and 40.3 % of TPh and COD removals, consuming 40 kWh m$^{-3}$. Those optimised conditions without NaCl addition were applied to the remediation of a filtered real OMW, leading to 72.3 % of TPh and 20.9 % of COD abatements with a consumption of 34 kWh m$^{-3}$. This study revealed the advantages of the ECG process as a pre-treatment of other methods, namely the EO, to ensure the legal limit values of the wastewaters to be discharged into the aquatic streams regarding their organic load. In addition, the results achieved for the degradation of the TPh of the OMW may be most likely generalised for other agro-effluents containing phenolic compounds.

The ECG technology has also been applied to the elimination of the Reactive Black 5 dye from aqueous solutions by the use of Al anodes in batch and recirculation flow systems. In both configurations, it was verified that the parameters that affected most the systems were the current density (*j*), the nature of the anode and the dye concentration, while the initial pH was less significant. The best results for both systems were achieved by the following operating conditions: *j* of 16 mA cm$^{-2}$, pH$_0$ of 6 and the initial concentration of the dye of 100 mg L$^{-1}$ (and 800 rpm for the batch-stirred reactor). In the first min of treatment, the recirculation flow ECG system led to higher decolourisation rates, whereas at the end of the electrolysis both configurations attend the same colour removal (97 %) with different energy consumptions (14 and 22 kWh $m^{-3}$ for batch and flow reactors, respectively). This conveyed that the performance of the systems depends on the way in which the liquid is mixed. An actual textile effluent was also treated by applying Al or Zn anodes in the batch-stirred system, having been obtained final satisfactory results for its discharge in aquatic media.

The experiments with ECG showed that the superiority of different electrode materials varies between different types of aqueous solutions being treated, meaning that this must always be determined case-specifically.

Regarding the application of the EO process to depurate phenolic wastewaters mimicking OMW, the use of Ti/$RuO_2$ and Ti/$IrO_2$ anode materials was addressed, being carried out in a batch-stirred reactor. The effect of the nature and electrolyte concentration (1.8–20 g $L^{-1}$ of NaCl or $Na_2SO_4$), current density (57–119 mA $cm^{-2}$) and initial pH (3.4–9) was tested. The nature of the electrolyte clearly affected the treatment process, and the increase in current density had a strong influence in TPh and COD removal, while the concentration of the electrolyte as well as the initial pH had a sparingly impact. The optimum operating conditions attained, 10 g $L^{-1}$ of NaCl, 119 mA $cm^{-2}$ and initial pH 3.4, allowed the complete removal of TPh for both anodes, while the COD abatement was 100 % and 84.8 % with Ti/$RuO_2$ and Ti/$IrO_2$ electrodes, respectively, after 180 min of reaction. The surface of the anodes was evaluated by SEM. In the case of Ti/$RuO_2$, its morphology was maintained after use, whereas some changes occurred on the surface of the iridium along the process. Neuronal studies were also performed before and after the EO treatment with both active anodes. The ROS analysis showed clear differences of the impact of the untreated and treated effluents in neuronal activity. The untreated effluents without and with the electrolyte NaCl caused large depressions of the ROS signal. However, both signals recovered to the initial values upon washout. The effluent treated using any of the anode had a milder effect, compared to the raw one, but the neuronal ROS activity became enhanced after the effluent's removal. Considering that the treatment eliminated all phenolic compounds, the smaller depression and the large potentiation appearing after washout, may be due to the action of end products of the EO process. Moreover, when those optimised parameters were applied to the depuration of an undiluted real OMW ($COD_0$=23 $gO_2$ $L^{-1}$ for the Ti/$RuO_2$ experiments or $COD_0$=6.5 $gO_2$ $L^{-1}$ for the Ti/$IrO_2$ experiments), a complete TPh removal was achieved and 17.2 % or 16.5 % of COD removals were attained with Ti/$RuO_2$ or Ti/$IrO_2$ anodes, respectively. The latter anode was also used to treat a diluted real OMW ($COD_0$=1.0 $gO_2$ $L^{-1}$), achieving 62.8 % of COD removal. These achievements demonstrate that the EO, with both anode materials, is an interesting process to eliminate TPh, while it can also be used as a pre-treatment of subsequent degradation methodologies to attain the legal limits of COD to be discharged in natural streams.

Concerning the dye wastewaters treatment, the performance of Ti/$IrO_2$-$Ta_2O_5$ and Nb/BDD anodes to degrade Amaranth dye has been tested by electrochemical measurements such as cyclic voltammetry and polarisation curves. The non-active anode had a substantial oxidation power to oxidise the dye compared to the active one. Moreover, bulk electrolysis employing one or two flow cells in series have been accomplished by varying current densities and/or the sequence of the cells of the serial mode. The kind of the anode applied to the system strongly influenced its efficiency, since it controls the way the generated $^{\bullet}OH$ radicals (chemisorbed or physisorbed) interact with the organic pollutants in the system. In addition, the current density showed to greatly affect the process depending on the type of the anode material. The optimum results achieved by individual cells were complete decolourisation and 49.1 % of COD removal by the Nb/BDD experiments at 30 mA $cm^{-2}$ after 60 min of treatment. In the case of Ti/$IrO_2$-$Ta_2O_5$ material were 98.5 % of colour and 43.2 % of COD removals after 360 min of electrolysis. The assays with cells in series revealed that, depending on the combination, their efficiency may be higher with less energy consumption than the sum of the individual cells. The arrangement Ti/$IrO_2$-$Ta_2O_5$+Nb/BDD at 30+30 mA $cm^{-2}$ led to the most interesting results, wherein 100 % and 75.1 % of colour and COD removals were obtained, after 60 min, consuming 25.4 kWh $m^{-3}$. Similar studies were performed with two active anodes, Ti/Pt and Ti/Pt-SnSb, in order to test their potential as cheaper anode materials for the treatment of wastewaters containing dyes. Polarisation curves showed that the latter material exhibited higher electroactivity to degrade the dye. This electrode applied to a single flow cell at 30 mA $cm^{-2}$ led to 97.5 % and 70.3 % of colour and COD removals, respectively, consuming 72 kWh $m^{-3}$ of energy after 360 min of treatment. Combining the two active anodes, a total colour removal was achieved 180 min earlier than when a single cell is used. Experiments relating Ti/Pt-SnSb and Nb/BDD anode materials were accomplished to clarify the effect of non-active anodes in the arrangement. The trial with Nb/BDD+Ti/Pt-SnSb at 30+30 mA $cm^{-2}$ reached the optimum combination of results, after 180 min of reaction, with 100 % and 69.9 % of colour and COD removals, respectively, as well as 78 kWh $m^{-3}$ of energy consumed.

The BDD material still is an attractive material in EO due to the high removals of pollutants achieved, but also in the reduction of electrolysis time. Among the tests with flow cells configuration in series, it seems that the combination Ti/$IrO_2$-$Ta_2O_5$+Nb/BDD at 30+30 mA $cm^{-2}$ leads to the most noteworthy solution to the purification of a synthetic solution containing the Amaranth dye.

Additionaly, the suitable system choice of an EO system will depend on the final target COD value, the reaction time and the energy consumption. Thus, taylor-made solutions must be designed for each particular effluent and final objectives. However, electrochemical processes show interesting versatile features that allow an easy adaptation of the operating conditions for specific cases.

# XI. SUGGESTIONS OF FORTHCOMING WORK

The results of the present study are important to understand the features of advanced electrochemical systems involving electrocoagulation and electrochemical oxidation processes for the treatment of liquid effluents addressed here through olive mill and dye wastewaters. Moreover, it should be kept in mind that research and work in this area is not over yet. The search for strategies with optimal removals and a good cost-efficiency ratio must be a constant attempt.

In order to achieve that goal:

- Real wastewaters should be applied more often instead of simulated model solutions to resemble as much as possible an actual treatment.
- The integration of the electrochemical technologies with biological processes may be required. Since the electrocoagulation (ECG) or electrochemical oxidation (EO) will allow the removal or degradation of the recalcitrant and toxic pollutants, enhancing their biodegradability and improving the performance of an inexpensive biological reactor. These integrated strategies may provide the most economical solution.
- Combining ECG and EO processes should be carried out for effluents that present a high amount of solids. The first step corresponding to the ECG will remove the solids that can enhance the efficiency of the subsequent EO.
- Other kind of integration to be tested could be ECG/EO with Advanced Oxidation Processes (AOPs). If the electrochemical processes do not allow to achieve the environmental laws to the discharge of the effluent, the AOPs such as ozonation and Fenton’s process can be used as a polish stage to eliminate the residual organic matter which may lead to treated water with quality for reuse.
- The use of renewable energy resources, namely sun light with photovoltaic cells, can be one way of reducing the cost of the electrochemical treatments, making the process more competitive.
- Improvement of the design of the flow cells systems presented in this work may also be a path to be futurally followed.
- Study and analysis of pilot and full scale systems in continuous mode will be demanding for final industrial applictions.
- Investigate the operating and investment costs associated with each of the electrochemical processes are surely one of the succeeding steps of these studies.

Regarding the specific processes addressed in this work the following issues should be complemented.

In ECG:

- evaluate the concentration of the coagulant over time;
- analyse the sludge produced during the treatment and determine what its future application will be;
- apply flow systems to the treatment of OMW.

In EO:

- prepare less expensive electrodes with high stability and activity that could replace the use of BDD;
- determine and monitor the intermediate compounds electrogenerated.

There is still much interesting work to be done in order to continue the promising development of ECG and EO processes to defeat the increasing pollution problems and to help to preserve the environment for the benefits of all living beings.